Agronomy Research

Established in 2003 by the Faculty of Agronomy, Estonian Agricultural University

Aims and Scope:
Agronomy Research is a peer-reviewed international Journal intended for publication of broad-spectrum original articles, reviews and short communications on actual problems of modern biosystems engineering incl. crop and animal science, genetics, economics, farm- and production engineering, environmental aspects, agro-ecology, renewable energy and bioenergy etc. in the temperate regions of the world.

***Agronomy Research* online:**
Agronomy Research is available online at: http://agronomy.emu.ee/

Acknowledgement to Referees:
The Editors of *Agronomy Research* would like to thank the many scientists who gave so generously of their time and expertise to referee papers submitted to the Journal.

Abstracted and indexed:
SCOPUS, CABI Full Paper and Thompson Scientific database: (Zoological Records, Biological Abstracts and Biosis Previews, AGRIS, ISPI, CAB Abstracts, AGRICOLA (NAL; USA), VINITI, INIST-PASCAL.)

Subscription information:
Estonian Grassland Society
St. Teaduse 4, 75501 Saku, ESTONIA
E-mail: heli.meripold@eria.ee

Journal Policies:
Estonian University of Life Sciences, Estonian Research Institute of Agriculture, Latvia University of Agriculture, Aleksandras Stulginskis University, Lithuanian Institute of Agriculture and Lithuanian Institute of Horticulture and Editors of *Agronomy Research* assume no responsibility for views, statements and opinions expressed by contributors. Any reference to a pesticide, fertiliser, cultivar or other commercial or proprietary product does not constitute a recommendation or an endorsement of its use by the author(s), their institution or any person connected with preparation, publication or distribution of this Journal.

ISSN 1406-894X

CONTENTS

I AGRICULTURAL ENGINEERING

Increase in tractor drawbar pull using special wheels

R. Abrahám[1], R. Majdan[1], T. Šima[2,*], J. Chrastina[1] and J. Tulík[1]

[1]Slovak University of Agriculture in Nitra, Faculty of Engineering, Department of Transport and Handling, Tr. A. Hlinku 2, 949 76 Nitra, Slovak Republic
[2]Slovak University of Agriculture in Nitra, Faculty of Engineering, Department of Machines and Production Systems, 949 76 Nitra, Slovak Republic;
*Correspondence: tomasko.sima@gmail.com

Abstract. The paper is aimed at the possibility of increasing in maximal drawbar pull of tractor working on the soil. The increasing in drawbar pull occurred due to a special wheels mounted on drive axle. The special wheels were equipped with auto-extensible blades and designed in Slovak university of agriculture in Nitra. The main advantage of the special wheels is the automatic extension of steel blades to increase the drawbar pull during a wheel slip and automatic return to the base position to allow the transport of tractor by the route. The testing operation points at the increase in drawbar pull resulting in decrease of wheel slip. A drawbar pull of tractor equipped with standard tires and special wheels was compared on the different soil moisture condition. The higher increasing in drawbar pull was measured during the tractor operation on the soil with higher moisture in comparison the soil with lower moisture level. In case of soil moisture 14% the increase in drawbar pull of tractor equipped with special wheels reached the value 17.2% in compare with standard tires. Using the special wheels on the same field with higher level of soil moisture 22% the increase in drawbar pull reached the value 36.1% in compare with standard tires.

Key words: tractor wheels, soil moisture, drawbar pull, wheel slip.

INTRODUCTION

The testing of tractors used in agriculture is continuously increasing because these machines directly influence the results of agricultural production. Agricultural tractors are losing a lot of energy by the slip of driving wheels. To reduce the tyre slip, tractors are loaded with a heavy weight, which increases the drawbar pull but excessively increases soil compaction and tyre wear on a hard surface (Semetko et al., 2004). Nowadays, diesel oil and petroleum products belong to the most used fuels. Unfortunately, fossil fuels are non-renewable and exhaustible sources of energy (Müllerová et al., 2012). The increase of tractor drawbar pull influences the fuel consumption and emissions of exhaust gases.

The drawbar pull, travel reduction (slip), and rolling resistance are the main criteria to describe the traction behaviour of off road vehicles. Besides the engine performance, the drawbar pull is influenced by the traction conditions such as soil and the tire parameters (Schreiber & Kutzbach, 2008).

The drawbar pull of tractor is influenced by various factors. Very significant parameter influencing the drawbar pull is a tire pressure. Noréus & Trigell (2008) realized the measurement of drawbar pull at various tire pressure. The test showed that the drawbar pull is vastly improved at lower tire pressure.

Dabrowsky et al. (2006) realized the tests of terrain vehicle equipped with different tire types. All-season tyres installed in a military truck provide slightly better traction for both terrain surfaces, at all three loading levels, or the differences between traction measures are not significant. Soil stress analysis showed that the difference between the two tread patterns is not significant. Generally, on soft surfaces all-season tyres performed no worse than snow tyres, while they are pronouncedly better for highway use.

Söhne (1968) & Sonnen (1969) compered two and four wheel drive for agricultural tractors. It was found that the tractor with four-wheel drive achieves better drawbar performance in compare tractor with rear wheel drive. It is concluded that as tractor power increases and as soil becomes weaker and less frictional, then the balance of advantage changes from two wheel to four wheel drive. The type of tires is the next important factor to increase the drawbar pull and influence tractive performance, as well as soil stresses under a vehicle. Soil compaction caused by agricultural machinery is important factor which affects soil infiltration rate (Krištof et al., 2010), carbon dioxide (Šima & Dubeňová, 2013) and nitrous oxide (Šima et al., 2013) flux from soils and therefore has significant environmental effect.

The results of a theoretical analysis reveal that, for a four-wheel-drive tractor to achieve the optimum tractive performance under a given operating condition, the thrust (or driving torque) distribution between the front and rear axles should be such that the slips of the front and rear tyres are equal. Field test data confirm the theoretical findings that, when the theoretical speed ratio is equal to 1, the efficiency of slip and tractive efficiency reach their respective peaks, the fuel consumption per unit drawbar power reaches a minimum, and the overall tractive performance is at an optimum (Wong et al., 1998).

Force interaction between tractor drive wheels and ground (soil, grass plot, route etc.) limits a maximum drawbar pull of wheels tractors. Mainly an atmospheric exposure such as rainfall or snow increases the ground moisture resulting in wheel slip and decrease of drawbar pull. In the past, various measures to increase the drawbar pull of wheel tractor have been implemented and published. Some measures are used in practice but many concepts were not successful. This paper presents a new method to increase the drawbar pull of wheel tractors. It is a device that is mounted on the drive wheels of the tractor. The device reduces wheel slip especially in poor traction conditions and thus increases the drawbar pull and also eliminates the undesirable effects of the wheels on the soil. The device could be also suitable for terrain, army or forest vehicles under poor traction conditions. The research presented in this paper is aimed at the increase of drawbar pull using the special wheels designed on Slovak agriculture university in Nitra

MATERIAL AND METHODS

To compare standard tires and special wheels the measurements of drawbar pull were realized on the same field at different soil moisture on October 2010 and 2012. In these years cucumbers were grown on the field. Remains of cucumber plants were taken away so the next to nothing covered the soil. There were a negligible amount of very small stones. The field was ready for autumn tillage. The difference soil moisture results in different rainfall in year 2010 and 2012. Tractor type Mini 070 was used to compare the standard tires and special wheel equipped with auto-extension steel blades. Tractor was braked by the second tractor during the measurement of drawbar pull. The maximum drawbar pull was reached at the 100% wheel slip.

Design of special wheels equipped with auto-extensible blades

Wheels equipped with auto-extensible blades have been developed at the Department of Transport and Handling for the rear driving wheels of a tractor MINI 070. Wheels equipped with auto-extensible blades were designed according to the work published by Sloboda et al. (2008). A big advantage is that they do not have to be removed from the tractor when passing on the road and also that they are automatically extended when the tractor driving wheels are slipping. Re-folding of driving blades occurs with the reverse movement of the tractor. The tractor needs not be equipped with additional load weights because they are replaced by wheels equipped with auto-extensible blades. Wheels equipped with auto-extensible blades are mounted to the wheel disc, and according to Fig. 1, they consist of the following parts.

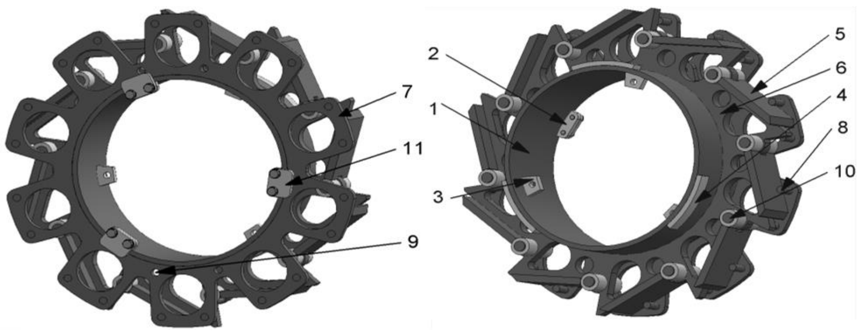

Figure 1. Wheels equipped with auto-extensible blades: 1 – support tube, 2 – locking tab, 3 – bracket fastening the mechanism to the wheel disc, 4 – spacer plates, 5 – blade, 6 – driving disc, 7 – blade control disc, 8 – guide pin, 9 – locking hole, 10 – blade pin, 11 – buffer plate.

A support tube (1) is a basic part of the whole mechanism. It enables the remaining parts of the whole mechanism to be attached to each other. On the support tube, there are welded three locking tabs (2), three brackets (3) by which the whole mechanism is connected to the tractor wheel, and a driving disc (6) containing blades (5) mounted by means of ten pins. On the support tube, there are also welded spacer plates (4) through which the mechanism position is centred with respect to the tractor wheel disc. After the driving disc (6), the support tube contains a freely rotating disc for the control of blades (7). The blade control disc contains on its circumference twenty pressed guide pins by means of which blades move into the extended and retracted positions. On the other side of the blade control disc, there are four locking holes (9) to fix the position of blades in the retracted position. Three buffer plates (11), attached by six screws to the locking tabs (2), fix the blade control disc on the support tube.

The measurement of drawbar pull

The drawbar pull measurement of the tractor type Mini 070 (Fig. 3) equipped with different wheels was performed by means of a tensometric force sensor marked as 150 EMS, as shown in Fig. 2. The force sensor is connected between the loading tractor T4K10 and the tractor type Mini 070 through a chain. A portable recording unit HMG 2020 (Hydac GmbH, Germany) was used to record electrical signals from the force sensor. A description of HMG 2020 is presented in the work published by Drabant et al. (2003). The tractor type Mini was set on the first gear (I gear) during the measurement.

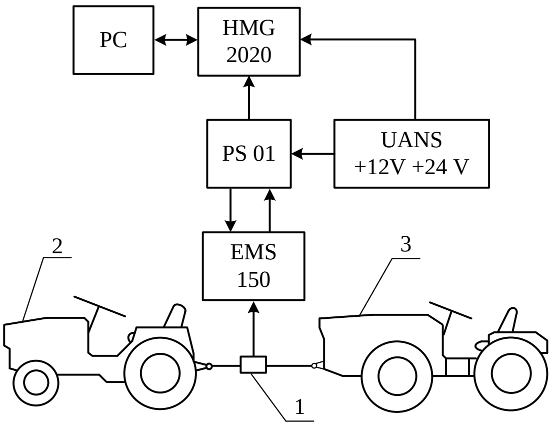

Figure 2. System for measurement of tractor drawbar pulls: 1 – force sensor EMS 150, 2 – tractor type Mini 070 equipped with different wheel types, 3 – loading tractor type T4K10, HMG 2020 – digital portable recording device, UANS – universal battery source, PC – personal computer, PS 01 – junction box.

Figure 3. The tractor type Mini 070 equiped with standard tires and special wheels.

Technical parameters and apecification of tractor type Mini 070 equiped with different wheels types and the tractor type T4K10 used to brake the first one are listed in Table 1 and 2.

The rear drive wheels of tractor type Mini 070 were equipped with tyres type TS 790 – 6.15/155 – 14 – 4PR, 2 pliesnylon + 1 plynylon and chemlon made by company Barum (Barum a. s. Czech republic).

Table 1. Specifications of the tractor type Mini 070

Year of manufacture	1989	
Construction weight	310 kg	
Driving speed at rated engine speed 3,600 rpm	1st gear	1.53 km h^{-1}
	2nd gear	2.72 km h^{-1}
	3rd gear	4.96 km h^{-1}
	4th gear	14.40 km h^{-1}
Clutch	Dry, single plate, with direct mechanical shutoff	
Engine	Petrol, four-stroke, air-cooled Briggs & Stratton	
	Number of cylinders	1
	Displacement	400 cm^3
	Max. performance / rotation speed	8 kW / 3,600 rpm

Table 2. Specifications of the tractor type T4K10

Year of manufacture	1966	
Construction weight	820 kg	
Engine	Two-stroke, air-cooled diesel	
	Number of cylinders	1
	Displacement	900 cm^3
	Max. performance	10 kW

Statistical proceeding of measured values

The measurements of drawbar pull were realized during the time 2.8 second. The sampling frequency 20 Hz was set on portable recording device to obtain the high precision results. Therefore the measured data-set consists of 56 values. The final mean value of drawbar pull was calculated from data file by using the 50 values. The first 6 values represent the increase in drawbar pull and therefore they didn't use to calculate mean value. The measurements of drawbar pull were replicated several times. Tractor was braked along the field length 100 m. In this paper the results from 3 measurements of drawbar pull are presented. During the drawbar pull measurement the data-set were obtained and statistical processed by use the mean value.

The mean value A of drawbar pull was calculated by using the arithmetic mean:

$$A = \frac{1}{n}\sum_{i=1}^{n} a_i \tag{1}$$

where: n – data-set extent; a_i – variable at the i index of a data-set, N.

The coefficient of variation Cv was used to express a measure of the dispersion of data points in a data series around the mean:

$$Cv = \frac{\sigma}{A} 100 \tag{2}$$

where: σ – standard deviation, N; A – mean, N.

Bulk weight ρ_w of soil was determined by using gravimetric method according to standard STN 72 1010:

$$\rho_w = \frac{m_1}{V} \tag{3}$$

where: m_1 – weight of soil volume, g; V – volume of soil, cm^3.

The soil moisture was calculated according to standard STN 46 5321 after drying at 105 °C:

$$w = \frac{m_1}{m_2} 100 \tag{4}$$

where m_2 – weight of soil after drying, g.

RESULTS AND DISCUSION

The measurement of drawbar pull was realized on the field with area approximately 2,000 m^2. The measurements were carried out on soil type chernozem. There were soil moisture $w = 22\%$ and average soil bulk density $\rho_w = 1.33$ g cm^{-3} in the year 2010. In the year 2012 the measurement were realized at soil moisture $w = 14\%$ and average soil bulk density $\rho_w = 1.51$ g cm^{-3}. The penetrometrical resistance was measured by mechanical penetrometer and shown in Fig. 4.

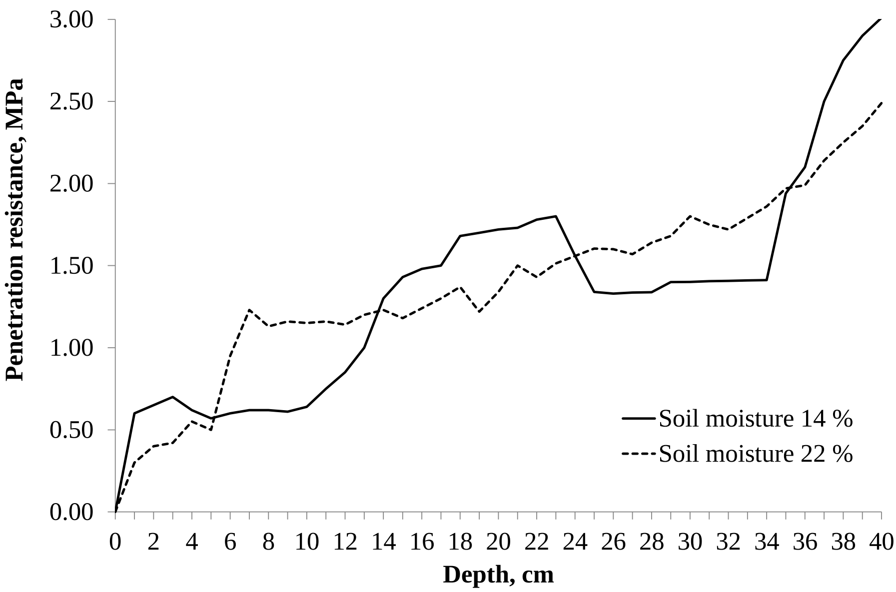

Figure 4. Penetrometrical resistance in the same field at diferent soil moisture.

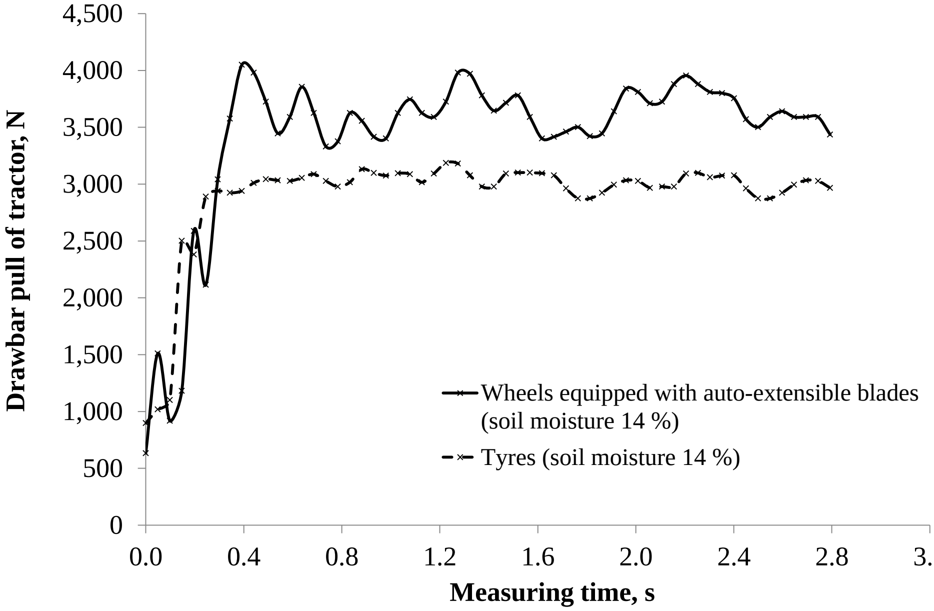

Figure 5. The comparison of special wheels and standard tyres on the basis of drawbar pull measured at soil moisture w = 14%.

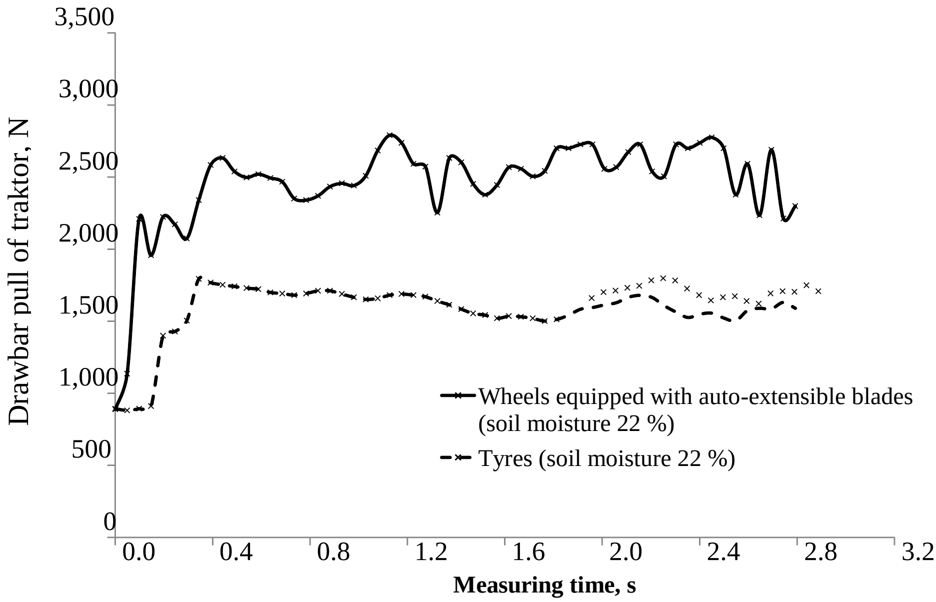

Figure 6. The comparison of special wheels and standard tyres on the basis of drawbar pull measured at soil moisture w = 22%.

The measurements of drawbar pull at soil moisture w = 14% and w = 22% shows the increase in drawbar pull due to the use of special wheels equipped with auto-extensible steel blades.

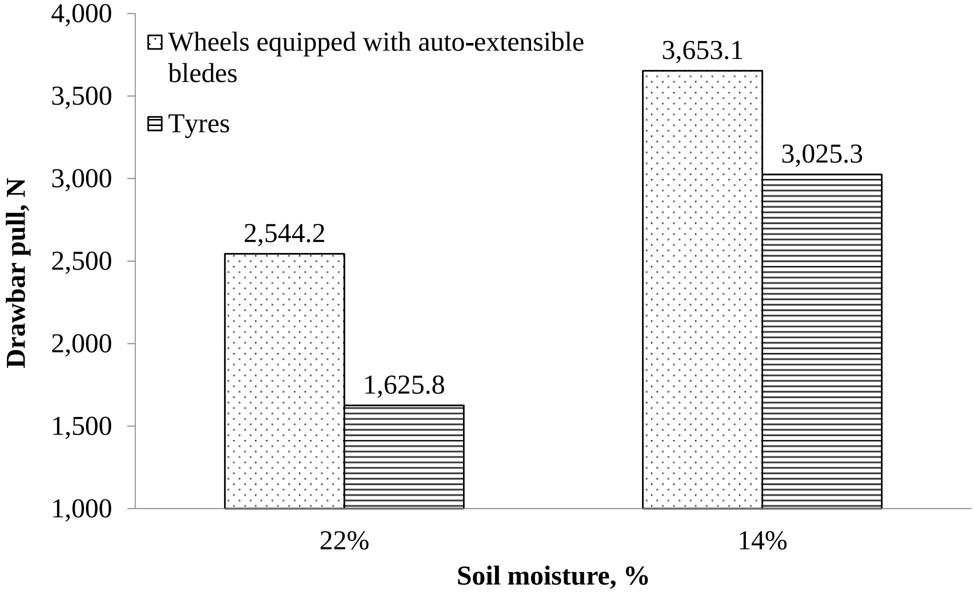

Figure 7. The final comparison of special wheels and tyres installed in tractor.

The measurements were realized on October in year 2010 and 2012 because the soil is prepared to autumn tillage in this time. Tillage is the one of the operation requiring the high drawbar pull of tractor. Fig. 5 and 6 shows the course of drawbar pull at different soil moistures. The measured data and mean of drawbar pull are listed in table 3. The final comparison of special wheels and tires is shown in Fig. 7. The results show that the increase of drawbar pull reached value 17.2% at the soil moisture w = 14% and 36.1% at soil moisture w = 22%. Therefore, at higher soil moisture the special wheels show the better properties in compare with standard tyres. The special wheels can be used to increase drawbar pull or eliminate the wheels slip and therefor reduce the fuel consumption and soil damage.

Table 3. The measured values and mean of drawbar pull

	Special wheels				Standard tyres			
Soil moisture	14%		22%		14%		22%	
The measured values of drawbar pull, N	3042.4	3591.0	2073.8	2445.0	2940.1	3100.9	1503.8	1520.0
	3576.0	3401.5	2340.0	2568.8	2923.7	3095.3	1793.8	1535.0
	4049.9	3416.4	2583.8	2557.5	2940.1	3077.0	1767.5	1531.3
	3980.0	3461.3	2632.5	2505.0	3011.3	2962.0	1752.5	1520.0
	3725.7	3501.2	2538.8	2542.5	3044.1	2874.4	1741.3	1501.3
	3446.4	3421.4	2497.5	2700.0	3033.2	2874.4	1730.0	1512.5
	3591.0	3446.4	2520.0	2700.0	3027.7	2923.7	1722.5	1542.5
	3855.3	3640.9	2493.8	2726.3	3055.1	2994.8	1700.0	1583.8
	3625.9	3840.4	2467.5	2726.3	3087.9	3033.2	1692.5	1595.0
	3331.7	3810.5	2351.3	2557.5	3027.7	3027.7	1681.3	1613.8
	3376.5	3710.7	2340.0	2568.8	2978.4	2967.5	1692.5	1628.8
	3625.9	3725.7	2370.0	2673.8	3016.7	2978.4	1711.3	1666.3
	3556.1	3880.3	2433.8	2726.3	3131.7	2978.4	1711.3	1680.0
	3416.4	3955.1	2456.3	2538.8	3098.5	3093.4	1688.8	1665.0
	3401.5	3880.3	2441.3	2505.0	3075.2	3098.2	1666.3	1608.8
	3625.9	3810.5	2508.8	2726.3	3095.8	3060.1	1651.3	1563.8
	3745.6	3800.5	2685.0	2700.0	3087.9	3075.3	1658.8	1526.3
	3625.9	3755.6	2790.0	2737.5	3016.7	3077.0	1681.3	1548.8
	3591.0	3571.1	2737.5	2775.0	3093.4	2962.0	1688.8	1556.3
	3725.7	3501.2	2591.3	2700.0	3186.5	2874.4	1681.3	1522.5
	3980.0	3591.0	2572.5	2377.5	3181.0	2874.4	1670.0	1503.8
	3970.1	3640.9	2253.8	2591.3	3077.0	2923.7	1640.0	1575.0
	3780.5	3591.0	2632.5	2235.0	2978.4	2994.8	1613.8	1590.0
	3645.9	3591.0	2602.5	2688.8	2978.4	3033.2	1583.8	1586.3
	3715.7	3591.0	2452.5	2212.5	3093.4	3027.7	1553.8	1631.3
Mean, N	3653.10		2544.19		3025.29		1625.76	
Cv, %	4.94		5.89		2.51		4.80	

CONCLUSION

The comparison of special wheels equipped with auto-extensible steel blades and standard tire was realized on the basis of drawbar pull measurement. The measurements were carried out in October in the year 2010 and 2012 on chernozem soil type in the same area of botanical gardens SPU The year 2010 was extremely dry while the year 2012 was an average year. The drawbar pull of small tractor type Mini 070 equipped with standard tyres and special wheels was measured at slip due to braking by using the second tractor type T4-K10. The special wheels can be used on larger tractors too. The main advantage of the special wheels is the easy using in case of tractor wheel slip. Backward driving after the field operation returns the special wheels to the base position for transportation on the route. In case of soil moisture 14% the increase in drawbar pull of tractor equipped with special wheels reached the value 17.2% in compare with standard tires. Using the special wheels on the same field with higher level of soil moisture 22% the increase in drawbar pull reached the value 36.1% in compare with standard tires.

ACKONWLEDGEMENTS. This contribution was realized under the agreement of solution of grant project VEGA 1/0857/12 'Reduction of unfavorable impacts of agricultural and transport machinery on environment'.

REFERENCES

Dąbrowski, J., Pytka, J., Tarkowski, P. & Zając, M. 2006, Advantages of all-season versus snow tyres for off-road traction and soil stresses. *Journal of Terramechanics* **43**(2), 163–175.

Drabant, Š., Tkáč, Z., Gonda, Ľ. & Bolla, M. 2003, The energy requirements of the no-till lawn drill. In *Acta mechanica Slovaca* **7**(3), 541–546.

Drabant, Š., Žikla, A., Petranský, I., Grman, I. & Jablonický, J. 2002, Strain-gauge measurement of a tractor body. *Acta technologica agriculturae* **5**(3), 68–74.

Krištof, K., Boďo, T. & Misiewicz, P. 2010. Influence of work implements on selected soil properties. *Technics in agrisector technologies 2010: proceedings of scientific works*, Nitra, november 2010. pp. 86–92.

Müllerová, D., Jablonický, J., Hujo, Ľ., Tkáč, Z., Kučera, M. & Kosiba, J. 2012, Measurement of operating parameters and emissions of tractor with diesel ol and biofuel. In TEAM. University Josip Juraj Strossmayer, Osijek-Baranja, pp. 299–302 (in Bulgaria).

Noréus, O. & Trigell, A. 2008, Measurement of terrain values and drawbar pull for six wheeled vehicle on sand. In*: 16th International Conference of the International Society for Terrain Vehicle Systems.* ISTVS, Turin, pp. 250–257 (in Italy).

Schreiber, M. & Kutzbach, H. 2008, Influence of soil and tire parameters on traction. *Research in Agricultural Engineering* **54**(2), 43–49.

Semetko, J., Janoško, I. & Pernis, P. 2004, Determination of power of multidrive vehicles. *Acta technologica agriculturae* **7**(1), 20–23.

Sloboda, A., Ferencey, V., Hlavňa, V. & Tkáč, Z. 2008. *Construction of tyres and crawlers vehicles.* Vienala, Košice, 552 pp. (in Slovak).

Sonnen, F.J. 1969. Drawbar performance of high-powered farm tractors with rear-wheel and four-wheel drive. *Journal of Terramechanics* **6**(1), 7–21.

Söhne, W. 1968, Four-wheel drive or rear-wheel drive for high power farm tractors. *Journal of Terramechanics* **5** (3), 9–28.

STN 46 5321 The measurement of soil moisture. 1969.

STN 72 1010 The statement of soil bulk density. 1989.

Šima, T. & Dubeňová, M. 2013. Effect of crop residues on CO_2 flux in the CTF system during soil tillage by a disc harrow Lemken Rubin 9. *Res. Agr. Eng.* **59**, Special Issue, 15–21.

Šima, T., Nozdrovický, L., Dubeňová, M., Krištof, K. & Krupička, J. 2013. Effect of crop residues on nitrous oxide flux in the controlled traffic farming system during the soil tillage by LEMKEN Rubin 9 disc harrow. *Agronomy Research* **11**, 103–110.

Wong, J.Y., McLaughlin, N.B., Knezevic, Z. & Burtt, S. 1998, Optimization of the tractive performance of four-wheel-drive tractors: Theoretical analysis and experimental substantiation. *Journal of Automobile Engineering* **212**(4), 285–297.

Agronomy Research **12**(1), 17–24, 2014

Light tractor simulator

J. Ahokas[1] and T. Jokiniemi[2]

Department of Agricultural Sciences, University of Helsinki, PL 28, 00014 Helsingin yliopisto, Finland; e-mail: [1]jukka.ahokas@helsinki.fi, [2]tapani.jokiniemi@helsinki.fi

Abstract. A tractor simulator was made for hard tillage work. The aim of the simulator was to have it in national language and that it is easy to use. There are tractor simulators available but they are mainly made for different conditions than we have and they are also in languages not common to our farmers. The simulator user can interactively experiment how working depth and – width, soil conditions, ballasting and driving speed effect on wheel slip, field capacity and fuel consumption l ha^{-1}. The simulator also shows how complicated a tractor – implement system is. Because the soil conditions and implement conditions are varying there can be large scatter in the results.

Key words: tractor, implement, field capacity, fuel efficiency.

INTRODUCTION

The purpose of the simulation was to demonstrate how tractor performance changes in heavy tillage work. With this simulator farmers and students can experiment how tractor size, implement size, working depth, driving gear, soil conditions and ballasting effect on fuel consumption, wheel slip and work rate.

There have been several tractor simulators available but these are focused on special subjects, for instance tyres (Al-Hamed et al., 1994) and ballasting (Evans et al., 1989). There are not many simulators available to simulate the tractor performance during heavy draft work. Grisso et al. (2007) made software, which selects either suitable implement for a tractor or a suitable tractor for an implement. The software is done with spreadsheet program and it calculates field capacity and fuel consumption in l ha^{-1}. Also it includes tyre inflation and ballast options. A simulator based on this can be downloaded at http://www.bae.ksu.edu/precisionag/index_files/Page832.htm (31.1.2014) and a Google Android Application is also available at Google Store.

Buckmaster & Beheshi Tabar (2013) made for educational purposes a spreadsheet program, where laboratory work and modelling allow virtual experimenting tractor-implement performance. Abdulrahman & Saad (2002) made a program, which calculates the performance of tractor-implement system. It was developed to use in farm machinery management and educational and research purposes. The program calculates the optimum field speed that matches to the pull of a tractor and shows the performance of the system.

The aim of this study was to develop a tool, where the user could interactively change the implement parameters and choose in this way the optimum parameters for the work. It also includes fuel consumption figures so that the user can see besides field capacity also fuel consumption l ha^{-1}. The program was done in Finnish language and also a translation in English and Estonian languages are available. The simulator was done with a spreadsheet program, and the aim was to keep the file size small and the interactivity high.

MATERIALS AND METHODS

Implement draft forces

The simulator was done only for heavy tillage work. In practice, if the size of the tractor and the implement are matched correctly, tillage is done with engine throttle set to full speed. Normally tractor engine performance measurement in tractor tests is only done with full speed and this information from test reports can be used in the simulation.

In heavy tillage the implement draft force depends on soil conditions, tillage depth, implement width and driving speed. The implement draft force was calculated with equation 1, where F_x is the draught force, S_i is a coefficient for the soil type, *A, B* and *C* are implement related coefficients and v is the driving speed (km h^{-1}), *t* is the working depth (m) and *b* (m) is the working width. This equation is widely used in implement draft and power calculations and it is given in standard ASAE D497 (ASAE D497). Also coefficient values can be found in the standard.

$$F_x = S_i \left(A + B \cdot v + C \cdot v^2 \right) \cdot t \cdot b \tag{1}$$

The coefficients used in the simulation can be found in table 1. The ploughing coefficients were taken from ASAE D497 standard. The S-tine coefficients are based on own experiments. ASAE D497 coefficients were not used for S-tine because they do not include working depth information. The S-tine harrow can have different options, such as levelling plates or roller. Also it has normally supporting wheels. For the calculations only supporting wheel resistance was included and value of 0.3 kN m^{-1} was used.

Table 1. Draft coefficients in ploughing and for one s-tine

Implement	*A* kN m^{-2}	*B* kN h $(m^2\ km)^{-1}$	*C* kN h^2 $(m^2\ km^2)^{-1}$	S^*
Moldboard plough (ASAE D497)	65.2	0	0.51	$S_1 = 1$ $S_2 = 0{,}7$ $S_1 = 45$
S-tine (single), organic soils	0.96	0.081	0	1
S-tine (single), loamy soils	0.86	0.347	0	1

* S_1 is fine clay soil, S_2 is medium texture loamy soils and S_3 is coarse texture sandy soil

It is assumed that S-tine harrow is pulled with horizontal force, which means that there is no weight transfer from the harrow to the tractor. Plough, on the other hand, may be mounted, semi-mounted or pulled. The amount of weight transfer depends on the plough condition, mounting type and so il resistance and only an estimate can be given. The simulation can be calculated with four different estimates from zero to 30% weight transfer from the plough on the tractor. For the plough weight transfer calculations it was assumed that a mounted reversible plough was in use. The weight of the plough and weight transfer is taken into account with this type of plough.

ASAE D497 standard states that the variation of the force can be quite high. For instance in ploughing it can be 50% from the calculated value depending on the implement type, condition and soil condition.

Tractor pulling force

The implement requires a pulling force from the tractor and also the tractor requires its own rolling force. The soil in the simulation was divided into three different categories, hard, normal and soft. The corresponding rolling resistance coefficients were 0.06 on hard soil, 0.1 on normal soil and 0.15 on soft soil (Renius, 1999). The traction coefficients depend on wheel slip and the values were taken from the values given by Renius, Fig. 1.

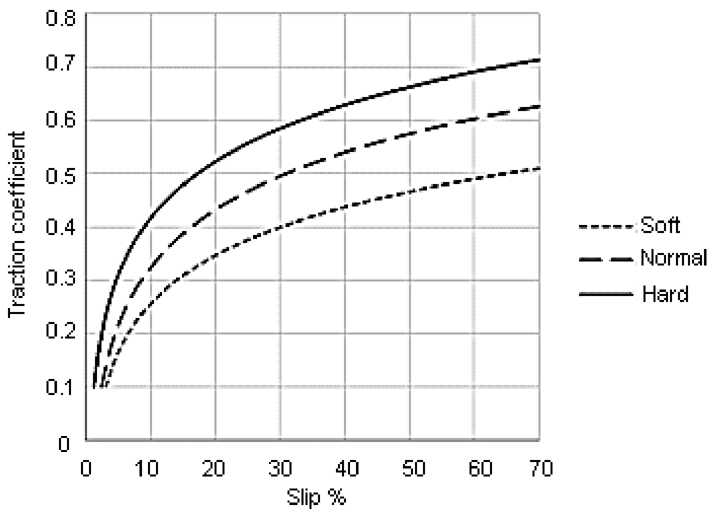

Figure 1. Coefficient of traction as a function of slip on three different soil types (Renius, 1999).

In the simulation we calculate first the necessary traction coefficient and from that we solve the wheel slip. This was done using an exponential equation 2, where *A* and *B* are soil dependant coefficients, which were calculated from Fig. 1 curves.

$$s = Ae^{B\mu} \quad (2)$$

The pulling force of a four wheel driven tractor is given in equation 3, where μ is the coefficient of traction, f is the coefficient of rolling resistance G is the weight of the tractor and α is the slope.

$$F_p = (\mu - f)G\cos\alpha \pm G\sin\alpha \quad (3)$$

In calculations we must first calculate the traction coefficient value, which means that we have to solve equation 3 for μ. After that we can calculate wheel slip with equation 2. In four wheel driven tractor we assume that traction of every wheel is about the same. The front and rear wheels are in agricultural tractors mechanically connected without differential between the axles. This means that we can consider the tractor as one traction unit and we do not have to calculate traction for each wheel independently.

Traction coefficient μ is the wheel traction force F_n divided by the wheel load R. Because we are handling tractor as one unit, traction coefficient can be determined with equation 4, where F_n is the sum of wheel traction forces (four wheel driven tractor) and G is the weight of the tractor.

$$\mu = \frac{F_n}{G} \tag{4}$$

F_n is the sum wheel traction forces and G is the weight of tractor. We must solve the wheel traction force F_n from this equation. With this force and wheel driving radius r we can calculate the torque of the driven axles and with the transmission gear ratio I we can calculate the engine torque T, equation 5.

$$T = F_n \cdot r \cdot i = \mu \cdot R \cdot r \cdot i \tag{5}$$

Extra ballast will increase the tractor weight and increase traction force, which in turn decreases wheel slip and improves performance. In four wheel driven tractors rear wheel or front weights act on the same way when front and rear wheel traction is assumed to be equal. For this reason the simulator needs only the total ballast amount regardless if it is on rear or front of the tractor.

Engine characteristics

When the needed engine torque is known (equation 5), we can calculate the engine operating point. For this we need the tractor power curve. These we can find in different tractor test reports. For instance OECD tractor test results can be found at http://www2.oecd.org/agr-coddb/index_en.asp, Nebraska test reports can be found at http://tractortestlab.unl.edu/testreports.htm and DLG test reports at http://www.dlg.org/tractors.html. Beside these some agricultural journals also publish their own test data. We need in minimum six data point from the power curve, Fig. 2 shows an example tractor power curve.

The operating point is found after we have calculated the engine torque. Example in Fig. 2 shows that if we need a torque of 350 Nm, the corresponding engine speed is 1,900 1 min^{-1} and the fuel consumption is 22 l h^{-1}. Also we can see that the power taken from the engine is 68 kW and the specific fuel consumption is 290 g $(kWh)^{-1}$.

In simulation the operating point falls in most cases between two measured points. Then the point is calculated from the adjacent measured points with linear interpolation.

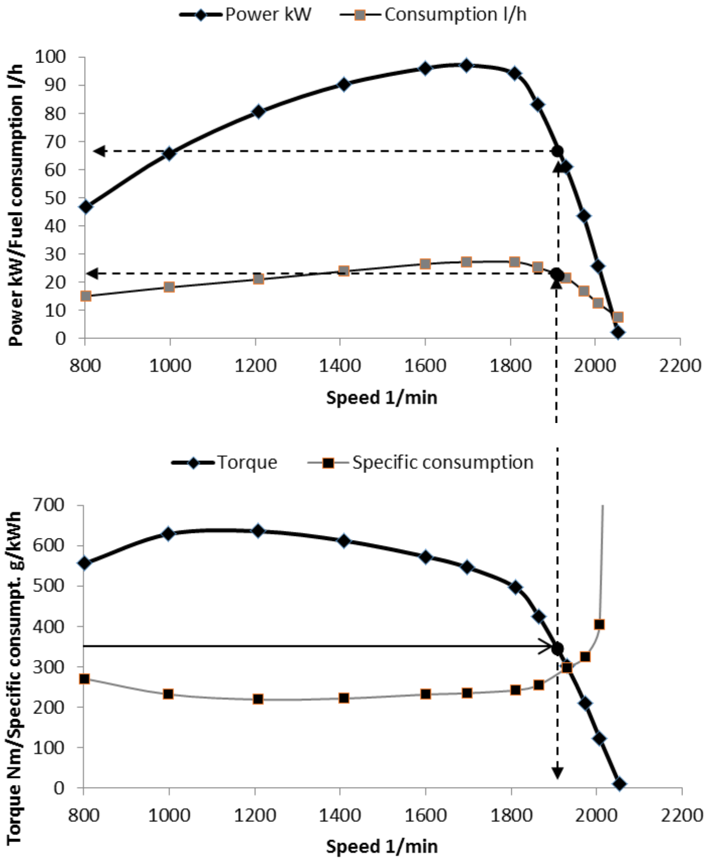

Figure 2. Example of tractor engine characteristics (Valtra T 140).

Work rate and work specific fuel consumption

The driving speed and fuel consumption q_l (l h^{1}) do not reveal how efficiently the work is done. The work rate can be calculated from the implement width and driving speed, equation 6.

$$q_A\left[ha\ h^{-1}\right] = \frac{v\left[km\,h^{-1}\right] \cdot b\left[m\right]}{10} \tag{6}$$

Fuel consumption per worked area q_f can now be calculated with equation 7.

$$q_f\left[l\ ha^{-1}\right] = \frac{q_l\left[l\ h^{-1}\right]}{q_A\left[ha\ h^{-1}\right]} \tag{7}$$

RESULTS

The simulator was done with Excel spreadsheet program. Besides spreadsheet calculations also user defined functions were used and they were done with visual basic. Fig. 3 shows the tractor information fill in form.

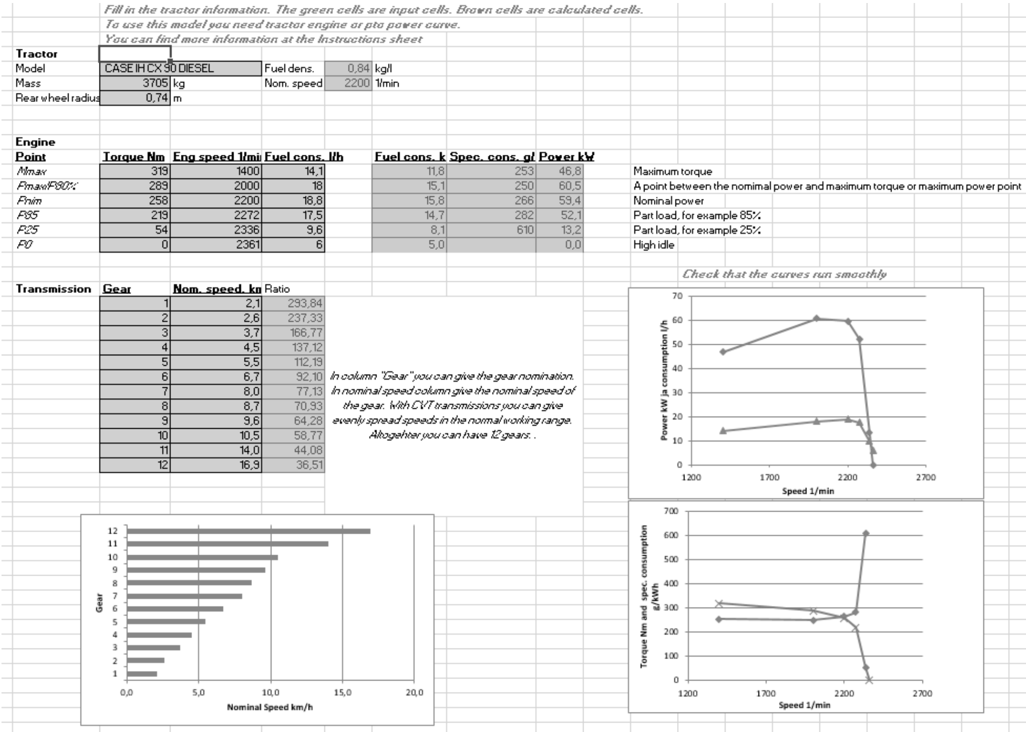

Fill in the tractor information. The green cells are input cells. Brown cells are calculated cells.
To use this model you need tractor engine or pto power curve.
You can find more information at the Instructions sheet

Tractor					
Model	CASE IH CX 90 DIESEL		Fuel dens.	0,84	kg/l
Mass	3705	kg	Nom. speed	2200	1/min
Rear wheel radius	0,74	m			

Engine

Point	Torque Nm	Eng speed 1/mi	Fuel cons. l/h	Fuel cons. k	Spec. cons. g/	Power kW	
Nmax	319	1400	14,1	11,8	253	46,8	Maximum torque
Pmax/P80%	289	2000	18	15,1	250	60,5	A point between the nomimal power and maximum torque or maximum power point
Pnim	258	2200	18,8	15,8	266	59,4	Nominal power
P85	219	2272	17,5	14,7	282	52,1	Part load, for example 85%
P25	54	2336	9,6	8,1	610	13,2	Part load, for example 25%
P0	0	2361	6	5,0		0,0	High idle

Check that the curves run smoothly

Transmission	Gear	Nom. speed. km	Ratio
	1	2,1	293,84
	2	2,6	237,33
	3	3,7	166,77
	4	4,5	137,12
	5	5,5	112,19
	6	6,7	92,10
	7	8,0	77,13
	8	8,7	70,93
	9	9,6	64,28
	10	10,5	58,77
	11	14,0	44,08
	12	16,9	36,51

In column "Gear" you can give the gear nomination. In nominal speed column give the nominal speed of the gear. With CVT transmissions you can give evenly spread speeds in the normal working range. Altogehter you can have 12 gears. .

Figure 3. Tractor information is given by filling in the green coloured cells.

When the tractor information is filled in it is possible to choose from the spreadsheet tab if ploughing or S-tine harrowing is simulated. Fig. 4 shows an example of simulation in ploughing. Different conditions can be tested by changing the plough, soil and tractor characteristics. If the tractor gear is improper and the engine stops, then a message is shown on the left side of the results. On the last column is shown the slip value importance. Normally 10–20% slip gives best traction efficiency. If slip exceeds 20% there is a danger of rut deformation on the field, which will destroy the soil structure.

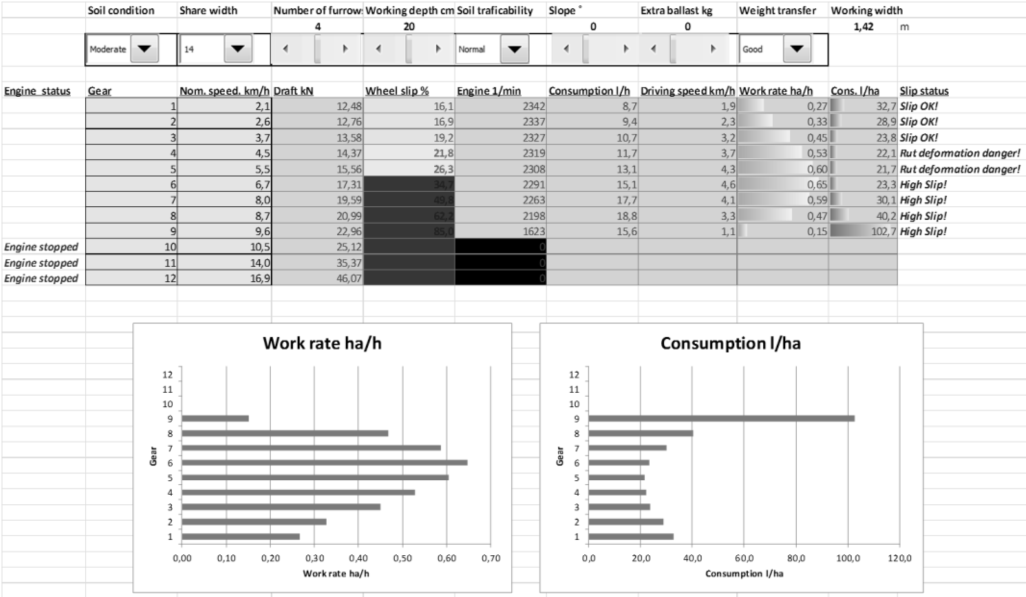

	Soil condition	Share width	Number of furrow:	Working depth cm	Soil traficability	Slope °	Extra ballast kg	Weight transfer	Working width	
			4	20		0	0		1,42	m
	Moderate	14			Normal			Good		

Engine status	Gear	Nom. speed. km/h	Draft kN	Wheel slip %	Engine 1/min	Consumption l/h	Driving speed km/h	Work rate ha/h	Cons. l/ha	Slip status
	1	2,1	12,48	16,1	2342	8,7	1,9	0,27	32,7	*Slip OK!*
	2	2,6	12,76	16,9	2337	9,4	2,3	0,33	28,9	*Slip OK!*
	3	3,7	13,58	19,2	2327	10,7	3,2	0,45	23,8	*Slip OK!*
	4	4,5	14,37	21,8	2319	11,7	3,7	0,53	22,1	*Rut deformation danger!*
	5	5,5	15,56	26,3	2308	13,1	4,3	0,60	21,7	*Rut deformation danger!*
	6	6,7	17,31	34,7	2291	15,1	4,6	0,65	23,3	*High Slip!*
	7	8,0	19,59	49,8	2263	17,7	4,1	0,59	30,1	*High Slip!*
	8	8,7	20,99	62,2	2198	18,8	3,3	0,47	40,2	*High Slip!*
	9	9,6	22,96	85,0	1623	15,6	1,1	0,15	102,7	*High Slip!*
Engine stopped	10	10,5	25,12		0					
Engine stopped	11	14,0	35,37		0					
Engine stopped	12	16,9	46,07		0					

Figure 4. Simulation of ploughing.

Fig. 5 shows an example of ploughing result. The minimum fuel consumption is gained with gears M3L and M2H while the maximum work rate is gained with gears M4L, M3H or H1L. Wheel slip is however high with these gears, which means that the tractor needs more ballast. It is also common that the minimum fuel consumption and maximum work rate do not occur with the same gear.

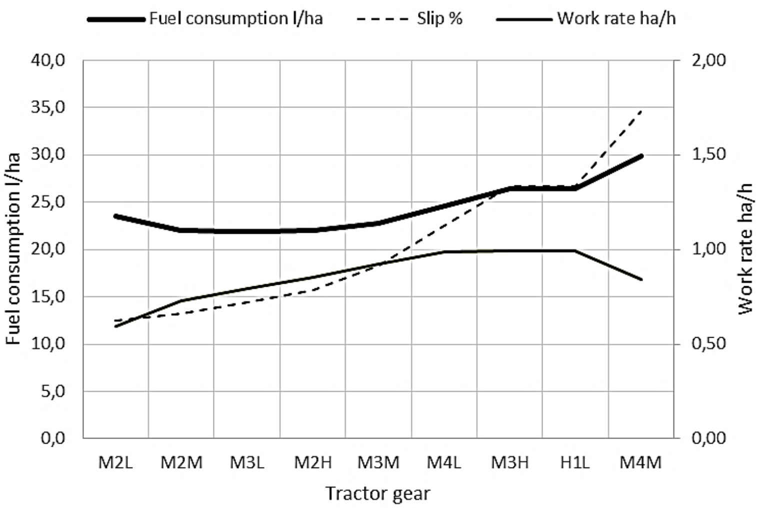

Figure 5. Result from ploughing simulation.

CONCLUSIONS

Tractor simulator was programmed in Excel spreadsheet. Users can experiment with their own tractor and implement and see how different adjustments and conditions affect on the operation parameters in hard tillage work.

The spreadsheet program was chosen because it is commonly used and it is easy to make calculations in it. However, simulation in this environment has some restrictions and it would be easier to make it in normal programming language. The restrictions in the spreadsheet programming occur especially when there are several choices to make or the results should be chosen depending on different conditions.

There can be lot of variation in the soil conditions as well as in implement type and function. This means that the assumptions and simplifications made in the simulator calculations do not have much influence on the results because more variation is caused by the soil, implement and tractor parameters.

REFERENCES

Abdulrahman, A. Al-Janobi & Saad, A. Al-Hamed. 2002. An Object-Oriented Program to Predict Tractor and Machine System Performance. In F.S. Zazueta and J. Xin (eds.): *Proceedings of the World Congress of Computers in Agriculture and Natural Resources. ASAE Publication Number 701P0301*. Iguacu Falls, Brazil, pp. 477–483.

Al-Hamed, S.A., Grisso, R.D., Zoz, F.M. & Von Bargen, K. 1994. Tractor performance spreadsheet for radial tires. *Computers and Electronics in Agriculture* **10**, 45–62.

ASAE D497. 2003. Agricultural machinery Management Data. American Society of Agricultural and Biological Engineers.

Evans, M.D., Clark, R.L., & Manor, G. 1989. A traction prediction and ballast selection model. ASAE Paper 89-1054. St. Joseph, Mich., 14 pp.

Buckmaster, D.R. & Beheshti Tabar, I. Integrated Model for Teaching Tractor-Implement Performance. 2013 ASABE Annual International Meeting, Kansas City, Missouri July 21– 24, 2013. Paper No 131620219, 12 p.

Grisso, R.D., Perumpral, J.V. & Zoz, F.M. 2007 Spreadsheet for Matching Tractors and Drawn Implements. *Applied Engineering in Agriculture*, American Society of Agricultural and Biological Engineers. **23**(3), 259–265.

Renius, K.T. 1999. Tractors: Two Axle Tractors. In B.A. Stout and B.Cheze, eds. CIGR Handbook of Agricultural Engineering, **3**, Plant Production Engineering. Copyright ASAE. St. Joseph, Michigan, USA: American Society of Agricultural Engineers, pp. 115–184.

Valtra T140. DLG-Data Sheet Tractors 2003. DLG–Top Agrar–Test Issue No. 12/2002.

Agronomy Research **12**(1), 25–32, 2014

Constructive and kinematics parameters of the picking device of blueberry harvester

M. Arak* and J. Olt

Institute of Technology, Estonian University of Life Sciences, Kreutzwaldi 56, EE51014 Tartu, Estonia; *Correspondence: margus.arak@emu.ee

Abstract. The article focuses on the selection of constructive and kinematics parameters of the picking device intended for picking lowbush blueberry, cultivated on milled peat fields. The constructive parameters of the picking device are reel radius, the height of the picking device's axis of rotation from the ground, the number of picking rakes (or the displacement angle of neighbouring rakes) and the angle of inclination of rake teeth in relation to the upward direction. The kinematics parameters include the angular speed of the picking reel, the machine velocity and the kinematics number.

Key words: agricultural engineering, blueberry harvester, picking reel, constructive and kinematics parameters.

INTRODUCTION

Lowbush blueberries, the height of which is between 10…60 cm depending on the variety and the berries of which ripen more or less at the same time (Starast et. al, 2005; Strik, 2009), could be harvested most reasonably with a machine, where the functional working unit is a drum or a picking reel (Olt & Käis, 2006). Picking rake contains teeth attached to the axis of rotation (Olt & Arak, 2012). Blueberries do not ripen after harvesting and therefore the berries have to be picked at their full maturity (Albert et al., 2009). Ripened blueberries do not defoliate easily and could thus stay on the bush ca 10 days when ripened (Starast et. al, 2009).

The principle layout of the blueberry harvester has been presented in Fig. 1. It is the so-called rough harvester, i.e. the additives of the blueberry harvester (leaves, pieces of stems and peat, etc) and bruised berries are not separated from the berry mixture. Thus, the technological operations of the blueberry harvester comprise removing the berries harmlessly from the stems and collecting the berries into berry boxes or containers, meant for handling.

Picking reel 3 contains picking rakes 12 that have been attached to the axes between side discs; rake teeth 13 have been rigidly attached to the picking rakes. Berries are separated from the stems with the help of rake teeth 13 that are put into motion through the blueberry stems. The diameter of the rake teeth 13 is 5 mm and their interval from each other on the picking rake 6 is 8 mm.

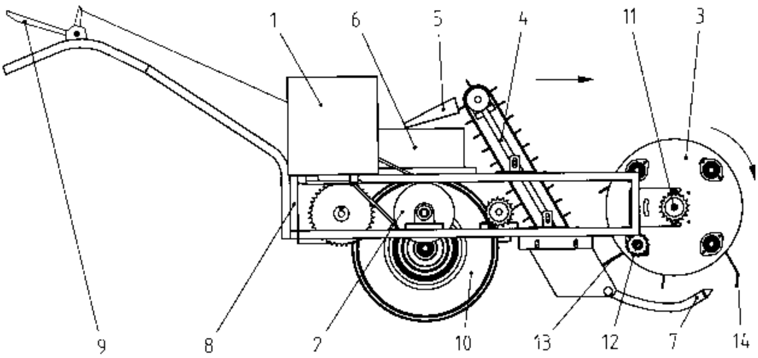

Figure 1. Main assemblies and parts of a motoblock-type harvester (Patent EE05488 B1): 1 – engine, 2 – power transmission elements, 3 – picking reel, 4 – conveyor, 5 – chute, 6 – berry box, 7 – copying unit, 8 – frame, 9 – steering levers, 10 – wheels, 11 – reel shaft, 12 – picking rake, 13 – rake tooth, 14 – hook spring-tine.

MATERIALS AND METHODS

The article studies the constructive parameters of the picking reel of the blueberry harvester: radius r_A, the height of the picking reel shaft from the ground H, (Fig. 2) the number of picking rakes z (or the angle of displacement of neighbouring rakes) and the angle of inclination of the rake teeth of the picking rake γ in relation to the vertical direction, as well as the angular speed of the kinematic parameters' picking reel ω_r, velocity of the machine v_m, and the selection principles of the kinematic indication number λ.

The picking reel 3 is a parallelogram reel, which is characterised by the fact that the rake tooth 13 of the picking rake 12 is located with a permanent (constant) rake angle toward the ground, and, thus, the following condition has to be followed

$$|\omega_r| = |\omega_p|, \quad (1)$$

where: ω_r – the angular speed of the picking reel 3; ω_p – the angular speed of the picking rake 12.

The rake angle γ of the rake teeth 13 of the picking rake 12 can be changed according to need.

The picking rake 12 participates in unitary movement: linear moving with the machine and rotary relative movement around the horizontal axis. According to the scheme presented in Fig. 2, the coordinates of point B, the free tip of the rake teeth of the picking reel are expressed as follows:

$$x(t) = v_m \cdot t + r_A \cdot \cos\varphi - l_p \sin\gamma; \quad (2)$$

$$y(t) = 0; \quad (3)$$

$$z(t) = -r_A \cdot \sin\varphi - l_p \cos\gamma; \qquad (4)$$

where: v_m – speed of the blueberry harvester; r_A – radius of the picking reel 3 (the distance of the centre-axle A of the picking rake from the axis of rotation O of the picking reel); $\varphi = \omega_r t$ – angle of rotation of the picking reel; ω_r – angular speed of the picking reel; γ – rake angle of the picking rake teeth; γ = const; β – the angle characterising the position of the picking rake; $\beta \neq$ const; l_p – length of the picking rake teeth; t – time.

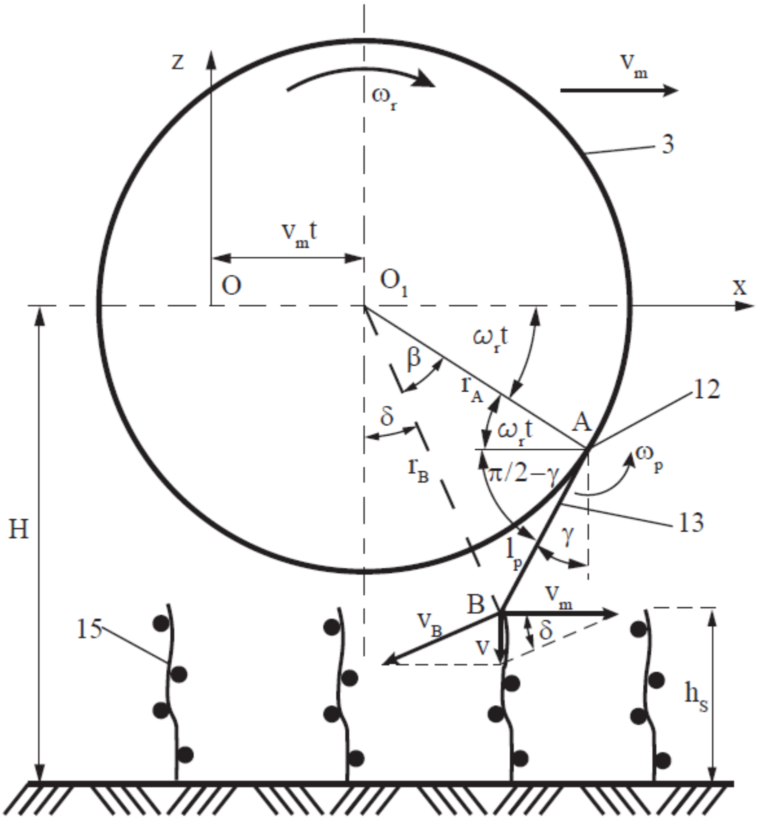

Figure 2. Calculation scheme for compiling equations of the trajectory of picking reel's rakes and for determining the height of the picking reel shaft from the ground: 3 – picking reel, 12 – picking rake, 13 – rake teeth, 15 – blueberry plant.

The trajectory of the picking reel has been studied by Heinloo (2007), but in this case we are not interested in the trajectory of the picking reel and the picking rake. Nevertheless, some important analytical relations for the technological calculation of the picking reel can be indicated with the trajectory equations (2, 3, 4). Firstly, this includes a relation for the selection of the rotational speed of the picking reel. So that the picking of berries could at all occur, the following condition has to be met:

$$v_x = \frac{dx}{dt} < 0,$$

Thus, after differentiation of the first equation (2) according to time t, the result is

$$v_m - \omega_r r_A \sin \omega_r t < 0. \tag{5}$$

Dividing the inequality (5) with the machine velocity v_m and marking $\lambda = \omega_r r_A / v_m$, which indicates the kinematic indication number of the picking reel, the result is

$$\lambda > \frac{1}{\sin \omega_r t}.$$

That is, calculating that the maximum value of sine is 1, then $\lambda > 1$, whereas the value of λ changes practically in the limit of $\lambda \approx 2 \ldots 2.5$, and the absolute velocity of the picking reel is expressed as follows:

$$v = v_m \sqrt{1 + \lambda^2 - 2\lambda \sin \omega_r t}, \tag{6}$$

and the angular velocity of the picking reel ω_r is expressed thus:

$$\omega_r = \frac{\lambda \cdot v_m}{r_A}. \tag{7}$$

As this is a motoblock-type machine, the machine velocity v_m is limited with the operator's velocity, that is, $v_m < 1$ m s^{-1}. The velocity of the machine prototype is changeable in the interval of $v_m = 0.30 \ldots 0.78$ m s^{-1}. During tests, most suitable working velocity is $v_{m,opt} = 0.55$ m s^{-1}.

The task of the picking reel 3 is to remove blueberries from the stems without any damage. In real working conditions, during the rotation of the picking reel 3, the movement direction of the rake teeth tips has to be vertical, directed top-down, when the rake teeth 13 tips of the picking reel (point B) reach the top of the blueberry plant; in this way the picking rake teeth can penetrate between the blueberry plants 15, that is, at the moment of penetrating between the stems carrying berries the absolute speed vector of the rake teeth tips (Fig. 2) has to be directed vertically top-down. In this case, the height H of the picking reel 3 shaft from the ground is expressed as follows:

$$H = h_s + l_p \cdot \cos\gamma + r_A \cdot \sin\omega_r t \tag{8}$$

where: h_s – the average height of the blueberry plant from the ground to the top, as $\lambda = 2.5$, then it is reasonable to implement the condition $l_p \geq 0.5 h_s$.

RESULTS AND DISCUSSION

Analysing equation (8), it is evident that except for the angle $\omega_r t$ all other parameters can be determined. Thus, for the purpose of being able to use the equation (8), an unknown angle has to be expressed $\omega_r t$. This is possible if we express the fictive radius r_B from the triangle O_1AB (Fig. 2), using a cosine sentence as follows:

$$r_B^2 = r_A^2 + l_p^2 - 2r_A l_p \cos\left[\frac{\pi}{2} + (\omega_r t - \gamma)\right]. \tag{9}$$

Considering that

$$\cos\left[\frac{\pi}{2} + (\omega_r t - \gamma)\right] = -\sin(\omega_r t - \gamma) = -\sin\omega_r t \cdot \cos\gamma + \cos\omega_r t \cdot \sin\gamma,$$

the relation (9) can be expressed as follows

$$r_B^2 = r_A^2 + l_p^2 + 2r_A l_p[\sin\omega_r t \cdot \cos\gamma - \cos\omega_r t \cdot \sin\gamma]. \tag{10}$$

Also, the following relation can be drawn from the Fig. 2

$$r_B \cdot \cos\delta = r_A \cdot \sin\omega_r t + l_p \cdot \cos\gamma. \tag{11}$$

by squaring both sides of the relation (11) and formulating from this fictive radius r_B

$$r_B^2 = \frac{r_A^2 \cdot \sin^2\omega_r t + 2r_A l_p \sin\omega_r t \cdot \cos\gamma + l_p^2\cos^2\gamma}{\cos^2\delta}, \tag{12}$$

where δ – positional angle of the rake tooth tip B.

If we apply a sine low for the triangle formed from velocity vectors (Fig. 2):

$$\frac{\sin\delta}{v} = \frac{\sin\left(\frac{\pi}{2} - \delta\right)}{v_m} \tag{13}$$

and considering relation (6) as well as the fact that $\sin\left(\frac{\pi}{2} - \delta\right) = \cos(\delta)$, then we can express it after the conversions as this

$$\frac{1}{\cos^2\delta} = \lambda^2 - 2\lambda\sin\omega_r t + 2. \tag{14}$$

When solving together relations (10), (12) and (14), grouping the units and after squaring and converting of both sides, we can formulate the following equation for the angle $\omega_r t$:

$$\begin{aligned} 4\lambda^2 r_A^4 \sin^6\omega_r t + r_A^2\left(\lambda^2 r_A - 4\lambda l_p + 2r_A\right)^2 \sin^4\omega_r t + \\ + 4l_p^2[\cos^2\gamma(r_A - \lambda^2 r_A + \lambda - 2r_A)^2 + \\ + r_A\sin^2\gamma]\sin^2\omega_r t - l_p^4[(\lambda^2+2)^2\cos^2\gamma - 1] + r_A^4 = 0. \end{aligned} \tag{15}$$

If we mark

$\sin^6\omega_r t = z^3$

$\sin^4 \omega_r t = z^2$
$\sin^2 \omega_r t = z$
and $4\lambda^2 r_A^4 = a$
$r_A^2\left(\lambda^2 r_A - 4\lambda l_p + 2r_A\right)^2 = b$
$4l_p^2[\cos^2 \gamma (r_A - \lambda^2 r_A + \lambda - 2r_A)^2 + r_A \sin^2 \gamma] = c$
$l_p^4[(\lambda^2 + 2)^2 \cos^2 \gamma - 1] + r_A^4 = d,$

We can write the relation (15) in this form

$$az^3 + bz^2 + cz - d = 0$$

that is,

$$z^3 + \frac{b}{a}z^2 + \frac{c}{a}z - \frac{d}{a} = 0. \tag{16}$$

If we mark $A = b/a$; $B = c/a$ and $C = -d/a$, then the satisfactory result of the equation (16) is expressed in the following form:

$$\sin \omega_r t_1 = \sqrt{z} = \sqrt{K_1 - \frac{K_2}{K_1} - K_3}, \tag{17}$$

where

$$K_1 = \left(\sqrt{\frac{B^3}{27} - \frac{C^2}{4} + \frac{A^3 C}{27} - \frac{A^2 B^2}{108} - \frac{ABC}{6}} - \frac{A^3}{27} + \frac{AB}{6} - \frac{C}{2}\right)^{\frac{1}{3}},$$

$$K_2 = \frac{1}{3}\left(B - \frac{A^2}{3}\right),$$

$$K_3 = \frac{A}{3}.$$

Because in different plantations the height of the blueberry plant h_s (the length of the stems) (Starast et. al, 2005) can differ, then the position of the axis of rotation of the picking device shall be changeable, so as to ensure harvesting without any loss.

Considering the fact that the average height of the blueberry plant from ground to top is $h_s = 0.2$ m and the technical parameters of the picking reel correspond to the ones indicated in Table 1, then the angle of rotation of the picking rake is $\omega_r t = 8°$, and we get the minimum height of the picking reel shaft according to relation (8) as $H_{\min} = 330$ mm.

Table 1. Technical characterisation of the picking reel

Parameter	Symbol	Unit	Value
Radius of the picking reel	r_A	mm	165
Length of the picking rake teeth	l_p	mm	135
Rake angle of the picking rake teeth	γ	degree	30

If we consider that the working speed of the machine is $v_{m,opt} = 0.55\ \mathrm{m\ s^{-1}}$, then according to the relation (7),the angular speed of the picking reel is $\omega_r = 8.33\ \mathrm{rad\ s^{-1}}$.

Rake teeth tips B of the picking rake have to reach the ground in their lower position. Deducing from this, we can check the distance of the picking rake axis from the shaft centre r_A with the following relation:

$$r_A \leq \frac{H - l_p \cdot \cos\gamma - d_c}{\cos\beta}, \tag{18}$$

where: d_c is the thickness of the copying unit runner, β – the angle characterising the position of the picking rake; $\beta \neq$ const; $\beta = 0\ldots360°$.

Thus, if $H = 330$ mm, the rake angle of the picking rake teeth is $\gamma = 30°$, the thickness of the runner $d_c = 30$ mm of the copying unit 7 (Fig. 1), the angle characterising the position of the picking rake $\beta = 20°$ if $\omega_r t = \pi/2$ and considering also the fact that the berries may be located close to the ground, then the maximum radius of the picking unit according to relation (19) has to be $r_A \leq 173$ mm. The radius of the picking reel of the blueberry harvester prototype (Fig. 3) is 165 mm, which prevents clutching peat pieces and other litter from the ground during the harvesting process.

Figure 3. Prototype of the blueberry harvester.

The number of rakes depends both on the kinematics of the picking reel as well as the positioning of its shaft. During design, it would be most reasonable to choose the number of the reel rakes in the limit of $z = 4\ldots6$ (Landtechnik, 1999). Following from these recommendations, the number of rakes has been chosen $z = 4$ when designing the prototype of this machine.

CONCLUSIONS

The article has pointed out methodology and explanation for the selection of the most important part of the motoblock-type blueberry harvester - the constructive and kinematics parameters of the picking reel. The constructive parameters of the prototype of the blueberry harvester (Fig. 3) are the following:

1) the diameter of the picking reel $2r_A = 330$ mm,
2) the height of the axis of rotation of the picking reel from the ground $H = 330$ mm,
3) the number of picking rakes $z = 4$.

Kinematics parameters are the following:

1) angular speed of the picking reel $\omega_r = 8.33$ rad s^{-1},
2) machine movement speed $v_m = 0.55$ m s^{-1},
3) kinematic indication number $\lambda = 2.5$.

REFERENCES

Albert, T., Starast, M., Karp, K., Kaldmäe, H., Vool, E. & Paal, T. 2009. The influence of propagation method on growth of the half-highbush blueberry 'Northblue'. *Acta Horticulturae*, vol. 812, pp.141–146.

Heinloo, M. 2007. A virtual reality technology-based method for the study of the working process of blueberry harvester´s picking reel. *Agricultural Engineering International: the CIGR Ejournal*, 12 pp.

Landtechnik / Herausgegeben von H. Eichhorn. 7. Aufgabe.– Hohenheim, Verlag Eugen Ulmer GmbH & Co, 1999, 688 S.

Olt, J. & Arak. M. 2012. Moto block-type structure and development of the blueberry harvester reel. *Journal of Agricultural Science* **XXIII** (2), 21–26.

Olt, J. & Käis, L. 2006. Kinematics of the working unit of the blueberry harvester. *Journal of Agricultural Science* **XVII**(2), 101–105.

Starast, M., Karp, K., Paal, T. & Värnik, R. 2005. Kultuurmustikas ja selle kasvatamine Eestis. Eesti Põllumajandusülikool, 65 pp. (in Estonian).

Starast, M., Paal, T., Vool, E., Karp, K., Albert, T. & Moor, U. 2009. The Productivity of Some Blueberry Cultivars under Estonian Conditions. *Acta Horticulturae*, 810, p. 103–108.

Strik, B. 2005. Blueberry: An Expanding World Berry Crop. *Chronica Horticulturae* **45**(1), 7–12.

Agronomy Research **12**(1), 33–40, 2014

Technical and economical analysis of harvesting and ensilaging of corn grain

J. Barwicki[1], S. Gach[2], K. Koprysz[2], S. Ivanovs[3,*], A. Adamovics[3] and O. Valainis[3]

[1]Institute of Technology and Life Sciences in Falenty, Warsaw Branch, Warsaw, Poland
[2]Department of Production Engineering, Warsaw Agricultural University – SGGW, Warsaw, Poland
[3]Latvia University of Agriculture, Research Institute of Agricultural Machinery, Ulbroka, Latvia; [*]Correspondence: semjons@apollo.lv

Abstract. Elaborated test results concerning two technologies of corn grain harvesting using grain harvesters. One technology called ZKP was using a mill crusher unit with direct filling system of a plastic bag and the other one was using a mill crusher connected to a silo press and was called ZKG. Provided research and calculations enabled evaluation of the values of critical coefficients, which were the following: unitary fuel consumption and unitary labour cost requirement. Because of different corn grain yields, these values referred to a unitary area of crop and also unitary mass of corn grain. It has been proved that the total costs of harvesting and conservation of corn grain with the technology ZKP equalled 321.83 € ha^{-1}, but the same costs with the technology ZKG equalled 245.69 € ha^{-1}. However, when taking into consideration the unitary mass of harvested grain, lower costs appeared with the technology ZKP at the value 21.89 € t^{-1} compared to the 31.02 € t^{-1} for the technology ZKG.

Key words: maize, harvesting technology, grain ensilaging, plastic bag, costs, labor, harvesting, transportation, fuel consumption.

INTRODUCTION

Increasing demand for maize, but especially for corn grain, designated for feed as well as for other goals, such as the needs of distillery industry and energy production, leads to dynamic growth of the cultivated area of this grain (Sokhansanij et al., 2002; Kowalczyk & Rzepiński, 2003). However, usage of corn as high energetic feed for all animal groups is of the highest importance (Gach & Kowalski, 2010; Gach et al., 2011).

Maize can be grown for silage as whole plants, for silage using corn cobs only (LKS – corn cobs with leafs or CCM) as well as for grain itself only (Niedziółka, 1999; Podkówka & Michalski, 2003; Bulghakov et al., 2006).

Making silage using chaff from whole maize plants is quite rational, because it utilizes all food components and can be used as a fundamental base for feeding of ruminant animals. (Podkówka & Michalski, 2003; Ustinovs & Ivanovs, 2003; Weinberg & Ashbell, 2003; Gach & Kowalski, 2010; Kowalski, 2010).

Growing maize for corn grain also holds an important position, but requires quite a high energy input for the drying process. The moisture content of the corn grain for storage must be lower (Eckl, 2003). Because of the high energy prices, the costly drying is replaced by grain ensiling using special conservation additives (Płonka, 2002; Chlebowski et al., 2008).

Ensiling of maize for feeding purposes is effective from the perspective of small losses of food components and silage can be stored for several month, so it can solve the problems of feeding animals. Grain silage contains less non-nitrogen extraction compounds, but it contains more protein and is characterized by higher digestibility of food compounds by animals compared to dried grain (Podkówka & Michalski, 2003). Total utilization of the components contained in feed is possible by using proper methods of harvesting and ensiling (Niedemaier, 1998; Gach et al., 2011).

Harvesting is usually done by using properly adapted grain harvesters (Szymanek et al., 2008), however, before storage, grain is crushed by using special mill crushers, the operation of which is known as the so-called Mursk method (Plonka, 2002). It is possible to use different variations of the technology, such as utilization of mill crushers in a separate operation and then filling the crushed grain into a plastic bag using a silo press or utilization of an aggregate performing both of these operations together (Gach et al., 2011). There are not many research results published in literature concerning harvesting and ensiling of corn grain in a plastic bag (Csermley et al., 2000).

It shows that evaluation of the exploitation parameters concerning preparation of crushed corn grain silage is very important as a research task. Fuel consumption, labor input, the costs involved according to the elementary area of maize designated to ensiling, or taking into account the dry matter involved can be good parameters to compare when evaluating different technologies. It can also be utilized for verification of elaborated models of similar processes, during simulation for better knowledge and for development and modelling the technology for ensiling of whole maze plants (Zaliwski & Hołaj, 2006; Kowalski & Gach, 2009).

The goal of this elaboration was evaluation of exploitation parameters, as well as to discover the material and cost inputs during harvesting and ensiling of corn grain using field test results taken directly from the production activity in a farm.

MATERIAL AND METHODS

The research work and evaluation of the whole process were provided for two technologies of maize harvesting for corn grain named ZKP and ZKG. A scheme of these technologies is presented on Fig. 1.

The tests for the technology ZKP were performed during 2009 in the Agricultural Experiment Research Station of the Warsaw Agricultural University (SGGW) in Obory near Warsaw. Corn grain harvesting was carried out using an adapted grain harvester Claas MEGA 360. The harvesting assembly was replaced by a six row adapter Conspeed 6-75FC for corn cobs separation from maize plants. After separation of corn cobs, maize stalks were shredded and left on the field, where the process of decomposition of the green mass could begin easily. This situation helped to prepare the field for after-harvest growing of other cultures.

During corn grain harvesting using high capacity harvesters, it is essential to prepare a proper amount of means of transport for delivering the corn grain. In the case of the present technology, the corn grain from the harvester was transported to the reloading area using a trailer PP14 Metaltech Mirosławiec Co. with the capacity of

14 tons, which transported the corn grain to the main truck SCANIA 114L with the capacity of 29 m^3. Reloading of the trailer was provided by using a screw conveyor located on the trailer. Then, the corn grain was transported to the place of storage and ensiling located 16 km from the field. Unloading of the corn grain from the truck was performed by tripping of the carrying body.

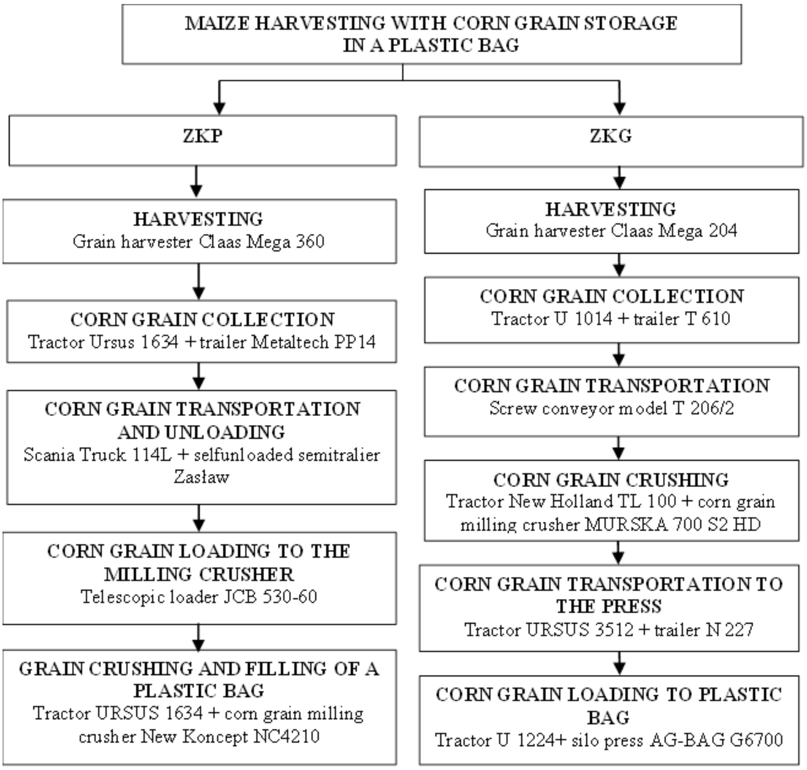

Figure 1. Scheme of the technology for corn grain ensilaging in a plastic bag.

Transportation and loading of corn grain to the mill crusher were performed by using a telescope loader JCB 530-60 equipped with a bucket for loose materials. For corn grain crushing, a roller mill crusher NC4210 New Concept Co. driven from a tractor Ursus 1634 using the PTO system were utilized. Crushed corn grain was compressed into a plastic bag. The size of the plastic bag was: 60 m long and 2.4 m in diameter.

The technology ZGK was presented as follows:

Corn grain harvesting and corn cubs separation were performed directly on the field using an adapted grain harvester CLAAS Dominator 204 Mega. The grain harvester was adapted by replacing the header unit with a 5-row adapter, which separates corn cobs from plants. Further, some changes were made to the harvester shredding and cleaning units.

Utilization of stalk rotation shredders working in vertical position and placing them under corn cobs separation unit. All chaff left after separation and shredding were spread on the ground behind the harvester and made good material for developing organic fertilizer.

The obtained corn grain was loaded on type T 610 trailers and transported with U 902 tractors to the shredding and ensilaging area, where it was filled into a plastic bag.

Unloading of the corn grain was performed directly on the entry table of the milling crusher MURSKA, equipped with a magnetic and rock separator. The mill crusher had two rollers 70 cm long each. The distance between the rollers was set on 0.3 mm. The mill crusher was powered by the PTO unit of a New Holland tractor. The crushed grain was charged through an unloaded pipe on the transporter, which directed it into a press. The transportation process was performed by using two sets of tractors C-360 and trailers type N227. Unloading of the trailer was performed using a flour conveyor powered by the PTO system of a tractor.

The corn grain from the charging hopper was fed into a plastic bag type B 820 by a silo press type AG-BAG, which was powered by a tractor Zetor 1211. The size of the plastic bag equalled 2.4 m width and 60 m length and had the capacity from 180 to 220 ton depending on the grain moisture content.

The exploitation tests of the machinery utilized in this technology were performed according to the requirements of the relevant standards and methodology developed at the Warsaw Institute of Technology and Life Sciences (ITP) (Barwicki et al., 2011).

On the basis of tests results described above, the yield per ton of corn grain was calculated. Moreover, the cost structures of the presented technologies were calculated taking into account: fuel costs, material costs, labor input and machinery costs.

RESULTS AND DISCUSSION

The main parameters of the provided experiments are presented in Table 1. As we can see, plants were harvested at a proper moisture content and the corn grain yield was quite high compared to the average yields on a country scale.

The values of exploitation and economical parameters were evaluated on the basis of typical standards and methodology, taking into account the actual prices of farm machinery (Barwicki et al., 2011).

Table 1. Characteristics of test conditions

Description of parameters	Units	Value	
Tested material	-	Corn grain	
Technology	-	ZKP	ZKG
Variety	-	PIONEER – PR39D23	PIONEER – PR39D81
Yield	t ha^{-1}	14.70	7.92
Moisture content	%	36	31.4
Row spacing	m	0.75	0.75
Number of plants on m^2	Piece m^{-2}	8.2	6.02
Average height of plants	m	2.91	2.43
Average height of corn cobs location	m	1.23	1.08

The yield of different technologies of the utilized machinery and aggregates were different, and are presented in table 2.

Table 2. Values of performance indicators

Description of parameters	Technology	
	ZKP	ZKG
	Yield [t h^{-1}]	Yield [t h^{-1}]
Harvester Claas Mega 360	13.50	7.56
Tractor U1634 + trailer Metaltech PP14	13.5	-
Truck Scania 114L + selfunloaded semitrailer Zasław	10.9	-
Telescopic loader JCB 530-60	8.9	-
Trailer U1634 + milling crusher NC4210	8.9	-
Tractor New Holland TL 100 + milling crusher MURSKA 700 S2 HD	-	8.0
Tractor U 1224+ silo press AG-BAG -G 6700	-	8.39

The calculated values refer to a specific area and also to a specific mass, because the yields for both technologies were considerably different. Fuel consumption is characterized in connection with a specific area or a specific yield and is presented in table 3. Taking into account the higher yield for the first technology when looking for a mass of the harvested corn grain, lower fuel consumption was present in the case of the technology ZKP – 3.42 dm^3 t^{-1} – compared to the technology ZKG – 4.10 dm^3 t^{-1}.

Table 3. Fuel consumption during harvesting and ensilaging of corn grain using different technologies

Description of parameters	Technology	
	ZKP	ZKG
	dm^3 t^{-1}	dm^3 t^{-1}
Harvesting	1.55	2.24
Loading and transportation	0.78	0.38
Loading of corn grain to milling crusher	0.35	-
Grain crushing and filling of plastic bag	0.74	-
Grain crushing	-	0.36
Transportation and loading to silo press	-	0.18
Plastic bag filling using silo press	-	0.94
Total	3.42	4.10

In the case of both technologies, fuel consumption was highest during harvesting with the following results: technology ZKP – 1.55 dm^3 t^{-1}, technology ZKG 2.24 dm^3 t^{-1}.

In the case of the technology ZKP, the lowest fuel consumption was related to loading of the corn grain to the milling crusher – 0.35 dm^3 t^{-1} –, but in the case of the technology ZKG, transportation and loading of the corn grain to the silo press – 0.18 dm^3 t^{-1}.

The total labour input values concerning specific areas in both technologies were quite close and were as follows: ZKP – 6.66 rbh t^{-1}, ZKG – 6.89 rbh t^{-1}. However, concerning the specific mass of corn grain, for the technology ZKP, it equalled 0.45 rbh t^{-1} and 0.87 rbh t^{-1}, which is almost twice higher because of different yields as shown Table 4. The highest labour consumptions during operations were those related to loading-unloading and transportation, the lowest one, however, was related to harvesting as a very efficient operation.

Table 4. Labour input for harvesting and ensilaging using different technologies

Description of parameters	Technology	
	ZKP	ZKG
	rbh t^{-1}	rbh t^{-1}
Harvesting	0.07	0.13
Loading and transportation	0.16	0.26
Loading of corn grain to milling crusher	0.11	-
Grain crushing and filling of plastic bag	0.11	-
Grain crushing	-	0.12
Transportation and loading to silo press	-	0.12
Plastic bag filling using silo press	-	0.24
Total	0.45	0.87

When taking into account the specific mass of collected grain, lower costs were obtained with the technology ZKP at the value of 21.89 € t^{-1} compared to the technology ZKG with the value of 31.02 € t^{-1}, as presented in Table 5.

In the cost structures of the tested technologies, in the case of the technology ZKP, corn grain harvesting had the highest impact on final expenditure– 7.50 € t^{-1} – but for the technology ZKG, the result equals 15.18 € t^{-1}.

Besides that, a considerable share of the costs is related to grain crushing and filling of the plastic bag: ZKP – 7.36 € t^{-1}; there is a similar situation in the case of the technology ZKG, where filling of the plastic bag using a silo press consumes 9.37 € t^{-1}. The costs related to transportation and loading-unloading operations are considerably lower.

Table 5. Specific costs of harvesting and ensilaging of corn grain in different technologies

Description of parameters	Technology	
	ZKP	ZKG
	€ t^{-1}	€ t^{-1}
Harvesting	7.50	15.18
Loading and transportation	5.08	2.07
Loading of corn grain to milling crusher	1.95	-
Grain crushing and filling of plastic bag	7.36	-
Grain crushing	-	3.30
Transportation and loading to silo press	-	1.10
Plastic bag filling using silo press	-	9.37
Total	21.89	31.02

In addition to the above, the costs of some other analysis were provided, taking into account the following costs: machinery, fuel consumption, labour consumption, additional materials. All this is presented in Table 6.

In the second place was fuel consumption with the following values for each technology: ZKP – 3.30 € t^{-1} – and the technology ZKG – 4.0 € t^{-1}. The costs of additional materials such as the plastic foil used for the plastic bag and the conservation agent supporting better development of the ensilaging process were equal: ZKP – 3.15 € t^{-1} – and for the technology ZKG – 2.17 € t^{-1}. The lowest values were the costs of labour input, which equalled: ZKP – 1.23 € t^{-1} – and the technology ZKG – 1.81 € t^{-1}.

Table 6. Comparison of specific costs involved in harvesting and ensilaging of corn grain in a plastic bag

Description of parameters	Technology	
	ZKP	ZKG
	€ t^{-1}	€ t^{-1}
Machinery	14.21	23.04
Fuel	3.30	4.0
Labour	1.23	1.81
Other materials – plastic foil	3.15	2.17
Total	21.89	31.02

The described experiment can be very helpful in determining values and structural inputs of harvesting and ensiling of corn grain. This area of research is very important and should be continued in the future, because we should consider the improvement of efficiency of each step of harvesting and ensilaging process described in this research work. The knowledge presented in this paper can be utilized for developing new technologies, but also for verifying elaborated models of old technologies for harvesting and ensiling of corn grain (Zaliwski & Hołaj, 2006, Kowalski & Gach, 2009).

CONCLUSIONS

On the basis of the provided research and analysis, the following conclusions can be made:

1. When taking into account the specific mass of the collected corn grain, lower fuel consumption took place in the technology ZKP – 3.42 dm^3 t^{-1} – than in the technology ZKG – 4.10 dm^3 t^{-1} –, because of the higher yield in the first technology compared to the second one. The highest fuel consumption was present during harvesting, but the lowest occurred during loading of the corn grain to the milling crusher in the case of the technology ZKP and during transportation and loading of the corn grain to the silo press in the case of the technology ZKG.

2. However, when taking into account the mass of corn grain in the technology ZKP, the labor input was twice lower than in the technology ZKG, because of the considerably higher yield of the first technology. The highest labor input occurred during grain loading, unloading and transportation.

3. When taking into account the specific mass of the collected corn grain, lower costs were achieved with the technology ZKP – 21.89 € t^{-1} – compared to the technology ZKG – 31.02 € t^{-1}.

4. In the structure of all costs for both technologies, the costs were highest for harvesting and the results were as follows: for the technology ZKP – 7.50 € t^{-1} – and for the technology ZKG – 15.18 € t^{-1}. Further, the costs related to corn grain crushing and filling of the plastic bag had a considerable influence: ZKG – 7.36 € t^{-1} – and also for the technology ZKG using silo press – 9.37 € t^{-1}.

5. In the cost structure related to the machinery, fuel consumption, labour requirement and additional materials, machinery costs had the highest share with the

following values: for the technology ZKP – 14.21 € t^{-1} – and for the technology ZKG – 23.04 € t^{-1}. Fuel consumption costs had the following values: for the technology ZKP – 3.30 € t^{-1} – and for the technology ZKG – 4.0 € t^{-1}.

REFERENCES

Barwicki, J., Gach, S. & Ivanovs, S. 2011. Inputs analyses of maize harvesting and ensilaging technologies. *Agronomy Research* **9**, 31–36.

Bulgakov, V., Shpokas, L. & Petkavicius, S. 2006. Issledowanije uborki kukuruzy na zerno. Motorization and powerindustry in agriculture. ISSN 1730 – 8568. Lublin, Vol. 8, 58–68. (in Russian).

Chlebowski, J., Gach, S., Gozdalik, I. & Kowalski, P. 2008: Analiza nakładów ponoszonych na zbiór i zakiszanie ziarna kukurydzy. *Inżynieria Rolnicza* 1, 71–76 (in Polish).

Csermely, J., Bellus, Z., Herdovics, M., Komka, Gy., Schmidt, J. & Sipöcz, J. 2000. Fodder preservation by fermentation in plastic bags. Hung. *Agricult. Eng.* **13**, 32–35.

Eckl, J. 2003. Wenn trocken zu teuer ist. *DLZ-Agrarmagazin*. Jg 54 nr 9, 80–82 (in German).

Gach, S. & Kowalski, P. 2010. Technologiczne i techniczne aspekty zbioru kukurydzy na kiszonkę. *Postępy Nauk Rolniczych* **1**, 91–99 (in Polish).

Gach, S., Korpysz, K. & Polańczyk, M. 2011. Nakłady ponoszone na zbiór i zakiszanie ziarna kukurydzy w worku foliowym. *Journal of research and applications in agricultural engineering*, **56**(2), 44–48 (in Polish).

Kowalczyk E. & Rzepiński, W. 2003: Kiszenie ziarna kukurydzy jako metoda poprawy efektywności ekonomicznej produkcji pasz lub etanolu. [w:] Kierunki wykorzystania wysokoenergetycznych odmian kukurydzy do produkcji biopaliw. Instytut Biotechnologii Przemysłu Rolno-Spożywczego. Monografie. Warszawa: 20–31. (In Polish)

Kowalski, P. & Gach, S. 2009. Model matematyczny zbioru i zakiszania kukurydzy. Zeszyty Probl. Post. Nauk Roln., 543, 167–180 (in Polish).

Niedemaier, H. 1998. Mais- Gaskorn silage – eine alternative zu CCM? *Top Agrar* **6**, 12–16 (in German).

Niedziółka, I. 1999. Analiza energetyczno-ekonomiczna technologii produkcji ziarna kukurydzy. *Inżynieria Rolnicza*, R. 3, **4**(10), 89–95 (in Polish).

Niedziółka, I. & Szymanek M. 2003. Przemysłowe i energetyczne wykorzystanie ziarna kukurydzy. *Motoryzacja i Energetyka Rolnictwa* **5** (in Polish).

Płonka, S. 2002. Zabezpieczenie bazy paszowej w gospodarstwie. Kiszenie ziarna o wysokiej zawartości wilgoci. [w:] Wdrażanie nowych proekologicznych technologii w zakresie roślin uprawnych. Puławy, pp. 441–448 (in Polish).

Podkówka, W. & Michalski, T. 2003. Technologie zbioru i użytkowania kukurydzy ziarnowej. Kukurydza rośliną przyszłości. Agro Serwis, pp. 41–45 (in Polish).

Sokhansanj, S., Turhollow, A., Cushman, J. & Cundif, J. 2002. Engineering aspects of collecting corn stover for bioenergy. *Biomass Bioenergy* **23**(5), 347–355.

Szymanek, M., Tanaś, W., Zagajski, P. & Dreszer, K.A. 2008. Możliwości wykorzystania kombajnów zbożowych do zbioru kukurydzy. *Technika Rolnicza Ogrodnicza Leśna* **3**, 21–24 (in Polish).

Zaliwski, A. & Hołaj, J. 2006. Modelowanie technologii produkcji kukurydzy na ziarno w aspekcie efektywności ekonomicznej. *Inżynieria Rolnicza*r **6**, 407–413 (in Polish).

Ustinovs, V., Ivanovs, S., 2003. Improvements in the technologies and technical means of growing maize for silage. Engineering. Lithuanian University of Agriculture. Research papers 6(1). Akademija, pp. 97–101.

Weinberg, Z.G & Ashbell, G. 2003. Engineering aspects of ensiling. *Biochemical Engineering Journal*, **13**, 181–188.

Agronomy Research **12**(1), 41–58, 2014

Mathematical model of vibration digging up of root crops from soil

V. Bulgakov[1,*], V. Adamchuk[2], G. Kaletnik[3], M. Arak[4] and J. Olt[4]

[1]National University of Bioresources and Nature Management of Ukraine, 15 Heroiv Oborony St., 03041 Kyiv, Ukraine; *Correspondence: vbulgakov@meta.ua
[2]National Scientific Centre 'Institute for Agricultural Engineering and Electrification' National Academy of Agrarian Sciences of Ukraine (NAASU), 11 Vokzalna St., Glevakha-1, Vasylkiv District, Kyiv Region, 08630, Ukraine
[3]Vinnitsa National Agrarian University, 3 Soniachna Str., 21008 Vinnytsia, Ukraine
[4]Institute of Technology, Estonian University of Life Sciences, Kreutzwaldi 56, EE51014 Tartu, Estonia

Abstract. A new theory of vibrational digging up of root crops from the soil has been developed. The Hamilton-Ostrogradski variational principle is used, on the basis of which we have received the differential equation of longitudinal oscillations of the root in the soil with an infinite number of degrees of freedom. Solution of the given equation provided the possibility to determine the main parameters of the tools that are used in modern beet harvesters.

Key words: root crop, digging tool, vibrational digging up, variational principle, differential equation, constructive parameters.

INTRODUCTION

The reason for large-scale use of vibrational digging tools in root harvesters of the modern technical level is their significantly lower draught level, actual ability to dig up beetroots from the soil without damage and losses. Oscillations of the digging tool create conditions, under which the soil that adheres to roots is intensely beaten down when they are dug up, which facilitates high level of qualitative indicators. That's why development of new constructions of vibrational digging tools, as well as research of their operation for the purpose of determination of the optimal constructive and kinematic parameters is a current task of the branch of mechanisation of sugar beet growing (Sarec et al., 2009; Lammers, 2011).

Statement of the problem. Analytical research of the process of interaction between working elements of the vibration digging tool with the root, that allows to obtain kinematic, constructive and technological parameters, and gives the opportunity to determine their optimal value.

MATERIAL AND METHODS

Fundamental theoretical and experimental research of the vibrational digging up of the root crops of sugar beet was published in the paper (Babakov, 1968), in which the root is modelled as a body having elastic properties, and it is presented as a rod with variable cross section with one attached end. Transverse oscillations of the root analysed in the given paper are described using the differential equation, in particular derivatives of fourth order. The technological process of digging up of the root from the soil with vibrational application of forces is not actually analysed here; instead it is stated that using the additionally prepared equations of kinetostatics the conditions are found for its digging up from the soil under the action of the disturbing force applied in the cross vertical plane. It is stated in the given paper that this particular direction of oscillations will be the best way to foster high quality digging up of the root crops from the soil.

Paper (Vasilenko et al., 1970) presents the theory of the digging tool of a regular digging share type, and states the conditions for digging up of the root from the soil with translational motion of the digger, taking the condition of avoiding damage to the root into account. The given paper demonstrates how the expression is obtained for determination of the allowed velocity of translational motion of the digging tool with its pre-set constructive parameters. In the given case the process of digging up of the root from the soil is performed under the action of forces that emerge on the working surfaces of the digging shares as a result of the transitional motion of the digging tool along the rows of the roots.

The developed theory of own and forced oscillations of the body of the root (Pogorely et al., 1983) is necessary for assessment of the action of the given oscillations on the process of destruction of connections of the root with the soil.

However, the given methods are not sufficient for performance of full analysis of the actual process of digging-up of the root from the soil.

Goal of the research. To develop a calculation and mathematical model and to analytically analyse the root – tool system in order to study the process of oscillations of the root during its vibrational digging-up from the soil.

RESULTS OF THE RESEARCH

The case where oscillatory motions of the vibration digging-up tool are applied to the beetroot in longitudinal vertical area will now be analytically analysed. It will be assumed that the root that is located in the soil is a complex solid elastic system with an infinite number of degrees of freedom, also modelled as the rod with variable cross section with the attached low end.

At the same time, since the Lagrange equation of the second kind in generalised coordinates serves as theoretical basis for most research of oscillations of holonomic systems with a finite number of degrees of freedom, for the purpose of performance of oscillations of holonomic systems with an infinite number of degrees of freedom the so called Hamilton-Ostrogradski principle of stationary action is used (Babakov, 1968).

In the theory of longitudinal, torsional and transverse oscillations of straight rods the Hamilton-Ostrogradski functionals are applied, which in the most generalised form look as follows:

$$S = \int_{t_1}^{t_2}\int_0^h L\left(t, x, y, \frac{\partial y}{\partial t}, \frac{\partial y}{\partial x}, \frac{\partial^2 y}{\partial t^2}, \frac{\partial^2 y}{\partial t\,\partial x}, \frac{\partial^2 y}{\partial x^2}\right) dx\,dt \tag{1}$$

where: $L = T - \Pi$ is the Lagrange function; T is kinetic energy of the system; Π is the potential energy of the system.

It will be assumed that the root that is located in the soil to be the rod with variable cross section along its length with one end attached (Fig. 1). The Hamilton-Ostrogradski principle will now be applied for research of longitudinal oscillations of the root that occur under the action of the vertical disturbing force that changes according to the harmonic law of the following type (Bulgakov et al., 2005):

$$Q_{зб.} = H \sin \omega t \,, \tag{2}$$

where: H is the amplitude of forced oscillations; ω is the frequency of forced oscillations.

As we can see from the scheme (Fig. 1), the root having a cone-like body (the top angle of which equals 2γ, and the top part of which is located above the level of the surface of the soil), is modelled as the rod with variable cross section with the attached low end (point O). In the centre of gravity, designated as point C, the force $\overline{G}$ is applied – the weight force of the root. h is its total length. Through the axis of symmetry of the root the vertical axis x is drawn, the beginning of which matches the point O. Connection of the root with the soil is determined by the general reaction of the soil $\overline{R}_x$, which is located along the axis x.

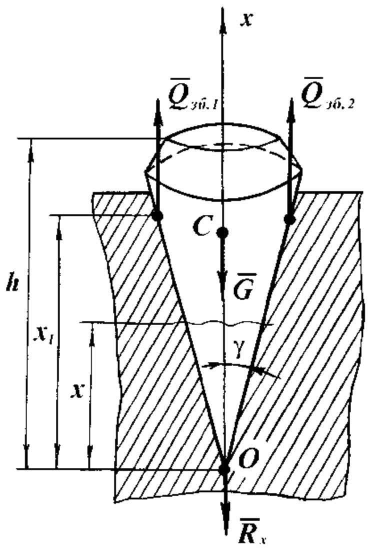

Figure 1. Scheme of the forces having an action on the root at the time of gripping by the vibration digging tool.

The disturbing force $\overline{Q}_{зб.}$ stated above is simultaneously applied to the root from two digging-up plough shares from its two sides, and that's why it is presented in the scheme by two components $\overline{Q}_{зб.1}$ and $\overline{Q}_{зб.2}$. The given forces are applied on the distance x_1 from the origin of coordinates (point O), and they are the source of oscillations of the root in longitudinal vertical area, that destroy connection of the root with the soil and form conditions for digging up of the latter from the soil. The functional S of Hamilton-Ostrogradski for the analysed vibrational process will now be made. For this purpose the necessary symbols will be applied:

$F(x)$ is the area of cross section of the root at some point located at the distance x from the low end m^2; E is the Young's modulus for material of the root N m^{-2}; $y(x,t)$ is the longitudinal dislocation of some cross section of the root at the time point t, m; $Q(x,t)$ is the intensity of longitudinal external load directed along the axis of the root N m^{-1}; $\mu(x)$ is the mass per length of the root kg m^{-1}.

Then kinetic energy of the oscillatory motion of the root will be:

$$T=\frac{1}{2}\int_o^h \mu(x)\left(\frac{\partial y}{\partial t}\right)^2 d\,x \tag{3}$$

Potential energy of the elastic deformation is designated as follows:

$$\Pi_1=\frac{1}{2}\int_o^h E\cdot F(x)\left(\frac{\partial y}{\partial x}\right)^2 d\,x \tag{4}$$

Potential stretching energy of the longitudinal load $Q(x,t)$ will look as follows:

$$\Pi_2=\frac{1}{2}\int_o^h Q(x,t)y\,d\,x \tag{5}$$

The Lagrange function L will be made.
Since

$$L=T-\Pi_1+\Pi_2, \tag{6}$$

then, taking the expressions (3), (4) and (5) into consideration, we get:

$$L=\frac{1}{2}\int_o^h\left[\mu(x)\left(\frac{\partial y}{\partial t}\right)^2-E\cdot F(x)\left(\frac{\partial y}{\partial x}\right)^2+Q(x,t)y\right]d\,x. \tag{7}$$

By inserting the expression (7) into the expression (1), we will have:

$$S=\frac{1}{2}\int_{t_1}^{t_2}\int_{o}^{h}\left[\mu(x)\left(\frac{\partial y}{\partial t}\right)^2-E\cdot F(x)\left(\frac{\partial y}{\partial x}\right)^2+Q(x,t)y\right]dx\,dt. \tag{8}$$

Further, expressions of all values that are included in the functional (8) will be found. Since the root has the shape of a cone, we find that its area of cross section $F(x)$ at the point that is located at an arbitrary distance x from the point O, will be:

$$F(x)=\pi x^2\tan^2\gamma. \tag{9}$$

It is obvious that the mass per length of the root can be determined using the following expression:

$$\mu(x)=\rho\cdot F(x),$$

or, given the (9),

$$\mu(x)=\rho\cdot\pi x^2\tan^2\gamma, \tag{10}$$

where ρ is the density of the root in kg m^{-3}.

Since the value $Q(x,t)$, included in the functional (8), is the intensity of distributed load, that is measured in N m^{-1}, then in each specific case the disturbing force must correspond to dimension of the intensity of the load. By using the so called impulse function of the first order $\sigma_1(x)$ (Babakov, 1968) it is possible to determine the intensity of the distributed load, and to include into the composition of the load divided along the length the concentrated forces and moments of forces.

Respectively, if $Q_{зб.}(t)$ is the concentrated disturbing force applied to point x_1 and measured in Newtons, then the function:

$$Q_{зб.}(x,t)=Q_{зб.}(t)\cdot\sigma_1(x-x_1) \tag{11}$$

has the dimension in N m^{-1} and expresses intensity of the concentrated load in the point x_1.

The function $\sigma_1(x-x_1)$ equals zero for all x, except for $x=x_1$, where it is transformed into infinity.

Let the disturbing force acting according to the law

$$Q_{зб.}(t)=H\sin\omega t, \tag{12}$$

be applied to the root at the distance x_1 from the starting point (point O in Fig. 1). Then, according to (11) we can write:

$$Q_{зб.}(x,t)=H\sin\omega t\cdot\sigma_1(x-x_1). \tag{13}$$

Since the root is connected with the soil, which is an elastic environment, application of the disturbing force of type (12) to the root leads to emergence of the force of resistance of the soil to movement of the root due to its oscillations. This force also has an action on the process of own oscillations of the root in the soil, especially at the beginning of the oscillations process, until connections of the root with the soil are destroyed.

It is obvious that the force of resistance of the soil (for the entire body of the root) is the distributed load along the area of contact of the root with the soil, and that's why we must determine its intensity as the force of resistance of the soil to movement of a length unit of the root.

Let c be the coefficient of the elastic deformation of the soil applied to the area of the contact measured in N m^{-2}. It will now be assumed that the soil surrounding the root, under the action of the disturbing force $H\sin\omega t$, performs forced oscillations according to the same harmonic law with the amplitude that is determined by elastic properties of the soil. Then the intensity $P(x, t)$ in N m^{-1} of resistance of the soil to movement of the root in point x will be:

$$P(x,t) = 2\pi c x \cdot \tan\gamma \cdot \sin\omega t, \tag{14}$$

Respectively, we will have the following relation for longitudinal external load:

$$Q(x,t) = Q_{зб.}(x,t) - P(x,t).$$

Given the expressions (9), (10), (13) and (14), the Hamilton-Ostrogradski functional (8) will look as follows:

$$\begin{aligned} S = \frac{1}{2}\int_{t_1}^{t_2}\int_{0}^{h} \Bigg\{ & \rho \cdot \pi x^2 \tan^2\gamma \left(\frac{\partial y}{\partial t}\right)^2 - E\pi x^2 \cdot \tan^2\gamma \left(\frac{\partial y}{\partial x}\right)^2 + \\ & + \left[H\sin\omega t \cdot \sigma_1(x - x_1) - 2\pi c x \cdot \tan\gamma \cdot \sin\omega t\right] y(x,t) \Bigg\}\, dx\, dt. \end{aligned} \tag{15}$$

In order to find natural forms and frequencies of longitudinal oscillations of the root in the soil, the Ritz method can be applied (Babakov, 1968). According to the given method we will need to find harmonic longitudinal oscillations of the root as follows:

$$y(x,t) = \varphi(x)\sin(pt + \alpha), \tag{16}$$

where $\varphi(x)$ is the natural form of primary oscillations, i.e. the function that determines continuous population of amplitude longitudinal deviations of cross section of the root from their equilibrium positions, and p is the natural frequency of primary oscillations.

Since natural forms and natural frequencies are related to free oscillations of the system, in the functional (15) we must highlight the part that specifically describes free oscillations of the system. Obviously the functional will look as follows:

$$S_1 = \frac{1}{2}\int_{t_1}^{t_2}\int_{o}^{h}\left[\rho\pi x^2 \tan^2\gamma\left(\frac{\partial y}{\partial t}\right)^2 - E\pi x^2 \tan^2\gamma\left(\frac{\partial y}{\partial x}\right)^2\right]dx\,dt \tag{17}$$

The expression (16) will now be inserted into the functional (17), and we will get:

$$\begin{aligned} S_1 = \frac{1}{2}\int_{t_1}^{t_2}\int_{0}^{h}\Big\{ & \rho\cdot\pi x^2\cdot\tan^2\gamma\cdot\varphi^2(x)\cdot p^2\cdot\cos^2(p\,t+\alpha) - \\ & - E\pi x^2\cdot\tan^2\gamma\,[\varphi'(x)]^2\sin^2\Big(p\,t+\alpha\Big)\Big\}\,d\,x\,d\,t. \end{aligned} \tag{18}$$

The expression (18) will be integrated over t within the limits of one period $T = \dfrac{2\pi}{p}$, and we will have:

$$S_2 = \frac{\pi}{2p}\int_0^h\left\{\rho\cdot\pi x^2\cdot\tan^2\gamma\cdot\varphi^2(x)\,p^2 - E\,\pi x^2\cdot\tan^2\gamma\,[\varphi'(x)]^2\right\}dx. \tag{19}$$

The basis of the Ritz method is reduction of the variational problem to the problem of search of extremum of function of any independent variables.

According to the Ritz method the value of the functional (19) is analysed on population of linear combinations of functions, i.e. expressions looking as follows:

$$\psi(x) = \sum_{i=1}^{n}\alpha_i\cdot\psi_i(x), \tag{20}$$

where: α_i are the parameters, variations of which enable us to obtain the required class of allowed functions; $\psi_i(x)$ are the basis functions that are specifically chosen and are known functions, that correspond to geometrical boundary conditions of the problem.

Respectively, we insert the expression (20) into the expression (19), and get:

$$\begin{aligned} S_2 = \frac{\pi}{2p}\int_0^h\Bigg\{ & \rho\cdot\pi x^2\tan^2\gamma\left[\sum_{i=1}^{n}\alpha_i\psi_i(x)\right]^2 p^2 - \\ & - E\pi x^2\tan^2\gamma\left[\left(\sum_{i=1}^{n}\alpha_i\cdot\psi_i(x)\right)'\right]^2\Bigg\}d\,x. \end{aligned} \tag{21}$$

After respective transformations the functional (21) will look as follows:

$$S_2 = \frac{\pi}{2p}\int_0^h \left[\rho\pi x^2 \tan^2\gamma\, p^2 \sum_{i,k=1}^{n}\psi_i(x)\psi_k(x)\,\alpha_i\alpha_k - \right.$$

$$\left. - E\pi x^2 \tan^2\gamma \sum_{i,k=1}^{n}\psi_i'(x)\psi_k'(x)\,\alpha_i\,\alpha_k\right]dx. \tag{22}$$

The following symbols will now be entered:

$$\begin{gathered}
\int_0^h \rho\cdot\pi x^2\cdot\tan^2\gamma\cdot\psi_i(x)\cdot\psi_k(x)\,dx = T_{ik},\\
\int_0^h E\pi x^2\cdot\tan^2\gamma\cdot\psi_i'(x)\cdot\psi_k'(x)\,dx = U_{ik},\\
(i,k = 1,2,...,n).
\end{gathered} \tag{23}$$

By inserting (23) into (22), we will get a functional as a function from parameters $a_1, a_2, \ldots, a_n$:

$$S_2(\alpha_1, \alpha_2, ..., \alpha_n) = \frac{\pi}{2p}p^2\sum_{i,k=1}^{n}T_{ik}\alpha_i\alpha_k - \frac{\pi}{2p}\sum_{i,k=1}^{n}U_{ik}\alpha_i\alpha_k. \tag{24}$$

The extremum analysis of the functional (24) will now performed. For this purpose we will differentiate the expression (24) with respect to parameters α_i, $(i = 1,\ 2,\ldots,n)$ and equate the obtained particular derivatives to zero. As a result of that we will get a set of linear homogeneous equations with respect to the unknowns $a_1, a_2, \ldots, a_n$, from which, in turn, we can find the Ritz frequencies equation for longitudinal oscillations of the root attached in the soil:

$$\begin{vmatrix}
U_{11} - p^2T_{11} & U_{12} - p^2T_{12} & \ldots & U_{1n} - p^2T_{1n}\\
U_{21} - p^2T_{21} & U_{22} - p^2T_{22} & \ldots & U_{2n} - p^2T_{2n}\\
\cdots & \cdots & \cdots & \cdots\\
U_{n1} - p^2T_{n1} & U_{n2} - p^2T_{n2} & \ldots & U_{nn} - p^2T_{nn}
\end{vmatrix} = 0 \tag{25}$$

It is known, that with $n > 4$ the given equation cannot be solved in radicals, that's why it is necessary to apply numerical methods using a PC.

However, in reality, as a rule, only the lower frequencies are determined, most often the first and the second ones, which have the most significant action on the technological process that is being analysed.

Therefore, the first and the second frequencies of natural oscillations of the root will now be determined.

For the purpose of determination of the first and the second frequencies the equation (25) will look as follows:

$$\begin{vmatrix} U_{11}-p^2T_{11} & U_{12}-p^2T_{12} \\ U_{21}-p^2T_{21} & U_{22}-p^2T_{22} \end{vmatrix} = 0 \tag{26}$$

As a result of the solution of the given equation we will obtain expressions for finding the value of the first (primary) frequency:

$$p_1 = \frac{0.662422}{h}\sqrt{\frac{E}{\rho}}, \tag{27}$$

and the second frequency:

$$p_2 = \frac{27.931592}{h}\sqrt{\frac{E}{\rho}}. \tag{28}$$

Now the calculation will be performed of the values of the first and the second frequencies for the beetroot having the following parameters (Pogorely et al., 1983) $h = 250$ mm; $E = 18.4 \cdot 10^6$ N m^{-2}; $\rho = 1{,}300$ kg m^{-3}. As a result of the calculations we get:

$$p_1 = \frac{0.662422}{250 \cdot 10^{-3}}\sqrt{\frac{18.4 \cdot 10^6}{1{,}300}} = 315 \text{ s}^{-1},$$

$$p_2 = \frac{27.931592}{250 \cdot 10^{-3}}\sqrt{\frac{18.4 \cdot 10^6}{130}} = 13{,}292 \text{ s}^{-1}.$$

Next, the analysis of the forced oscillations of the root will be discussed. The exclusively forced oscillations will happen according to the following law:

$$y(x,t) = \varphi(x)\sin\omega t, \tag{29}$$

where φ(x) is the form of the forced oscillations.

In order to determine the form of the forced oscillations of the root the expression (29) will now be entered into the functional (15), and we will get the following functional:

$$\begin{gathered} S_3 = \frac{1}{2}\int_{t_1}^{t_2}\int_0^h \Big\{\rho\pi x^2 \tan^2\gamma\omega^2\varphi^2(x)\cos^2\omega t - E\pi x^2\tan^2\gamma\left[\varphi'(x)\right]^2\sin^2\omega t + \\ + \left[H\sigma(x-x_1) - 2\pi cx\tan\gamma\right]\ \varphi(x)\sin^2\omega t\Big\}\,dx\,dt. \end{gathered} \tag{30}$$

By integrating the expression (30) over t within the limits of one period $T = \dfrac{2\pi}{\omega}$, we will get:

$$S_4 = \frac{\pi}{2\omega}\int_0^h \Big\{ \rho\pi x^2 \tan^2\gamma \varphi^2(x)\omega^2 - E\pi x^2 \tan^2\gamma\,[\varphi'(x)]^2 + \qquad (31)$$
$$+ H\sigma_1(x - x_1)\varphi(x) - 2\pi c x \tan\gamma\varphi(x)\Big\} d\,x.$$

According to the Ritz method let's analysis will now performed of the value of the functional (31) with respect to population of linear combinations of the following type:

$$\varphi(x) = \alpha\psi(x) \qquad (32)$$

where: α is the parameter, variations of which let us obtain the class of the allowed functions; $\psi(x)$ is the basis function.

The expression (32) will now be inserted into the functional (31), and we will obtain:

$$S_4 = \frac{\pi}{2\omega}\int_0^h \Big\{ \rho\pi x^2 \tan^2\gamma\alpha^2\psi^2(x)\omega^2 - E\pi x^2 \tan^2\gamma\alpha^2\,[\varphi'(x)]^2 + \qquad (33)$$
$$+ H\sigma_1(x - x_1)\alpha\psi(x) - 2\pi c\, x \tan\gamma\alpha\psi(x)\Big\} d\,x.$$

The following symbols will now be inserted:

$$\int_0^h \rho\,\pi\, x^2 \cdot \tan^2\gamma \cdot \psi^2(x)\, d\,x = T\,, \qquad (34)$$

$$\int_0^h E\,\pi\, x^2 \cdot \tan^2\gamma \cdot [\psi'(x)]^2 d\,x = U\,, \qquad (35)$$

$$\int_0^h [H\sigma_1(x - x_1)\cdot\psi(x) - 2\pi\, c\, x \tan\gamma\psi(x)] d\,x = L. \qquad (36)$$

The expressions (34), (35), (36) will now be inserted into (33), and we will have:

$$S_4(\alpha) = \frac{\pi}{2\,\omega}\left(\omega^2 T\alpha^2 - U\alpha^2 + L\,\alpha\right) \qquad (37)$$

So, in the population of functions, (32) the functional (33) is transformed into the function of the independent variable α, looking as (37).

The necessary condition of the stationary functional (37) (i.e. existence of the extremum) is that its first variation equals zero:

$$\frac{\partial S_4}{\partial\alpha}\cdot\delta\alpha = 0 \qquad (38)$$

from which we receive the following equation:

$$2\omega^2 T\alpha - 2U\alpha + L = 0 \tag{39}$$

from which we find the required value of the parameter α . It will be:

$$\alpha = \frac{L}{2\left(U - \omega^2 T\right)} \tag{40}$$

The form of the forced longitudinal oscillations of the rod with the constant cross section with one end firmly attached, emerging under the action of the longitudinal harmonic force of frequency ω, applied at the point $x = x_1$ will now be assumed as the basis function $\psi(t)$.

According to Babakov (1968) the form of the forced oscillations of the given rod looks as follows:

$$\psi\left(x\right) = D_1 \sin a x \qquad \text{with} \quad x \le x_1 \tag{41}$$

$$\psi\left(x\right) = D_2 \cos\, a\, \left(h - x\right) \qquad \text{with} \quad x > x_1, \tag{42}$$

where,

$$D_1 = -\frac{1}{a\,EF} \cdot \frac{\cos a\left(h - x_1\right)}{\cos a h} \tag{43}$$

$$D_2 = -\frac{1}{a E F} \cdot \frac{\sin a x_1}{\cos\, a h} \tag{44}$$

$$a = \omega \sqrt{\frac{\mu}{EF}} \tag{45}$$

μ is the mass per length of the rod; F is the area of the longitudinal section of the rod; E is the Young’s module for material of the rod; h is the length of the rod; ω is the frequency of the forced oscillations of the rod.

Having calculated the parameters of T, U and L according to the expressions (34), (35) and (36), we obtain the required value of the parameter α according to the expression (40), in case of which the functional (33) will have a stationary value.

Taking into consideration the expressions (32), (41) and (42), we get expression for the form of the forced oscillations of the root attached in the soil. They look as follows:

$$\begin{aligned} &\varphi\left(x\right) = \alpha \cdot D_1 \sin a\, x, \quad \text{with} \\ &x \le x_1,\ \varphi\left(x\right) = \alpha \cdot D_2 \cos a\left(h - x\right), \quad \text{with } x > x_1 . \end{aligned} \tag{46}$$

Having inserted the expressions (46) into (29), we get the final law of the forced oscillations of the root attached in the soil. If we take into consideration the action of the disturbing force $H\sin\omega t$, the given law will look as follows:

$$y(x,t)=D_1\alpha\sin ax\cdot\sin\omega t\,,\quad \text{with } x\le x_1\,,$$
$$y(x,t)=D_2\,\alpha\,\cos a\,(h-x)\cdot\sin\omega t\,,\quad \text{with } x>x_1\,. \tag{47}$$

Based on the results of the theoretical research of the forced oscillations of the beetroot attached in the soil we will perform specific calculations of the amplitude of the given oscillations.

The length of the root h, its cone angle γ, Young's module E for the body of the root, density ρ of the root, coefficient of elastic deformation of the soil c will be assumed to be equal, according to Pogorely et al. (1983): $h = 250\cdot10^{-3}$ m; $\gamma = 14°$; $E = 18.4\cdot106$ N m^{-2}; $\rho = 1{,}300$ kg m^{-3}; $c = 1\cdot10^{-5}$ N m^{-2}.

The amplitude H of the disturbing force will be chosen within the limits 100...600 N. We will assume the frequency ω of the disturbing force, according to (Vasilenko et al., 1970), to equal ω = 20 Hz.

The calculation is performed using the Mathcad program in order to determine the relations between the amplitude of the forced longitudinal oscillations of the body of the root and changes of the disturbing force within the range 100...600 N for different cross sections of the root.

The result of the given calculation is the graph shown in Fig. 2.

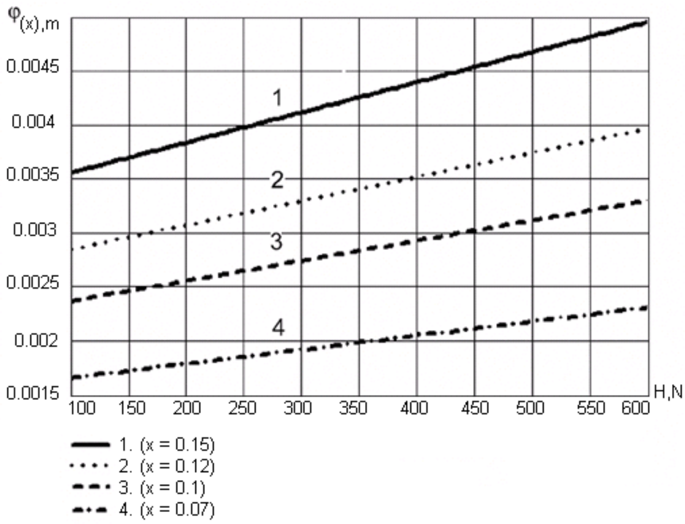

Figure 2. Relation between the amplitude of forced longitudinal oscillations of the body of the root and the value of the disturbing force.

As it is seen from the given graph, increase of the value of the disturbing force leads to the increase of the amplitude of the longitudinal forced oscillations of the body of the root according to the linear law.

It should also be noted, that with increase of the distance of the area of cross section of the root from the origin of coordinates O the amplitude is also increased. For example, with x = 0.07 m the amplitude is within the limits of 1.7…2.3 mm with x = 0.1 m – within the limits of 2.3…3.5 mm, with x = 0.12 m – within the limits of 2.8…3.9 mm, with x = 0.15 m (the point of gripping) – within the limits 3.2…4.8 mm.

Further, analysis will be presented of the calculation performed on a PC of the amplitude of longitudinal oscillations of the body of the root attached in the soil from the coefficient c of the elastic deformation of the soil surrounding the root, and the distance of the cross section of the root from the conditional point of its attachment for the frequency of the disturbing force $\nu = 10\,\text{Hz}$ and $\nu = 20\,\text{Hz}$.

On the basis of the calculations we get the following graphs (Fig 3).

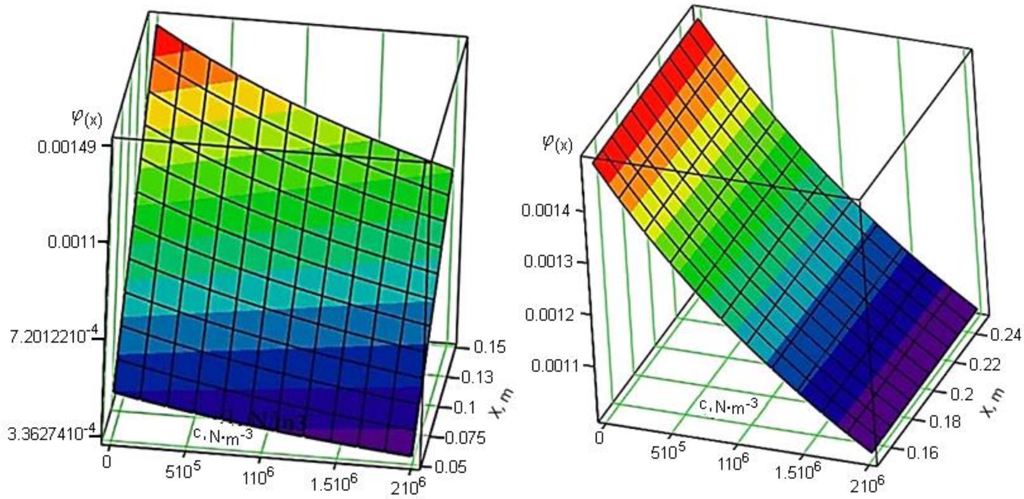

a) b)

Figure 3. Relation between the amplitude of the forced longitudinal oscillations of the root as an elastic body attached in the soil, and the coefficient c of the elastic deformation of the surrounding soil, and between the distance x of the cross section of the root and the conditional point of attachment: a) $x \le x_1$,) b) $x \ge x_1$), (x_1 – point of gripping, $\nu = 20$ Hz).

As it is seen from the graphs stated above, in case of increase of the coefficient c of the elastic deformation of the surrounding soil, the amplitude of the forced oscillations of the root is reduced, and in case of increase of the distance x of the cross section of the root from the point of conditional attachment with $x \le x_1$ it is increased, and with $x \ge x_1$ it almost doesn't change.

Fig. 4 shows the given relation for a number of specific cross sections of the root, in particular: for *x* = 0.07 m; 0.1 m; 0.12 m; 0.15 m (point of gripping).

On the given graph we can quite clearly see the tendency of increase of the amplitude of the forced longitudinal oscillations in case of increase of the distance of the cross section from the conditional point of attachment and the tendency of its reduction due to increase of the coefficient c of the elastic deformation of the surrounding soil.

For example, with x = 0.07 m and change of the coefficient c within the limits c = 0…20·105 N m-3, the amplitude is changed within the limits of 0.7…0.47 mm; with x = 0.1 m – within the limits of 0.99…0.67 mm; with x = 0.12 m – within the limits of 1.19…0.81 mm; with x = 0.15 m (point of gripping) – within the limits of 1.49…1.01 mm.

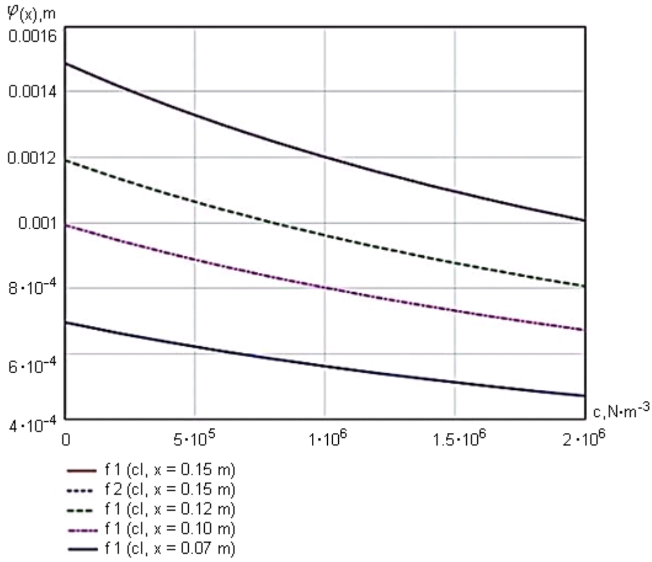

Figure 4. Relation between the amplitude of the forced longitudinal oscillations of the root as an elastic body and the distance x of the cross section of the conditional point of attachment $x \le x_1$, $\nu = 20$ Hz.

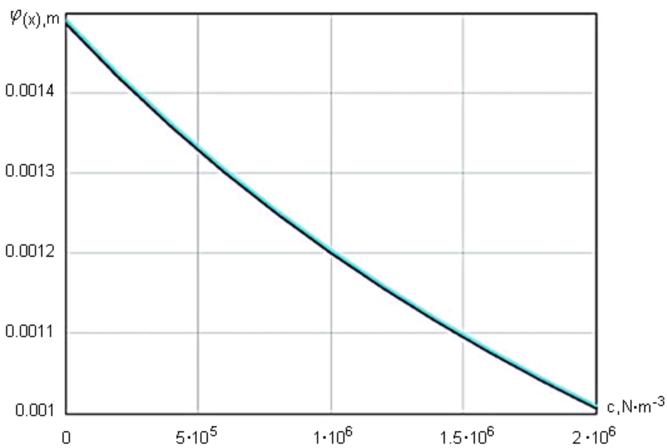

Figure 5. Relation between the amplitude of the forced longitudinal oscillations of the root as an elastic body and the distance x of the cross section from the conditional point of attachment $(x \ge x_1)$, $\nu = 20$ Hz.

However, as the graph in Fig. 5 shows, for cross section of the root above the point of gripping ($x \geq 0.15$ m) the amplitude of forced oscillations of the body of the root with increasing distance of the cross section from the conditional point of attachment almost doesn't change and remains the same as in case of x = 0.15 m. However, the tendency of decrease of the amplitude from increase of the coefficient c is the same as for the sections below the point of gripping (x ≤ 0.15).

In case of the frequency of the disturbing force $\nu = 10$ Hz values of the amplitude are slightly lower. For example, with x = 0.07 m the value of the amplitude remains within the limits of 0.66…0.45 mm; with x = 0.1 – within the limits of 0.94…0.65 mm; with x = 0.12 m – within the limits of 1.13…0.78 mm; with x = 0.15 m (point of gripping) – within the limits of 1.41…0.97 mm.

Also, we have obtained the estimated relation between the amplitude of the forced longitudinal oscillations of the body of the root and the amplitude of the disturbing force for the frequency of the disturbing force $\nu = 20$ Hz (Figs 6 and 7).

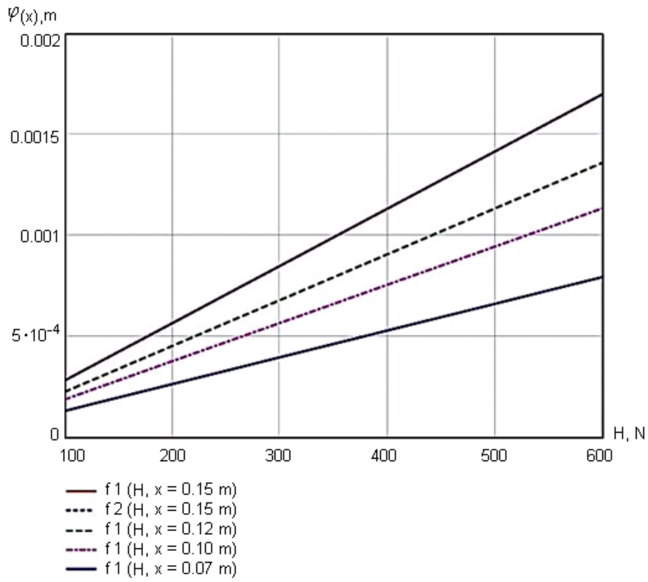

Figure 6. Relation between the amplitude of the forced longitudinal oscillations of the body of the root and the amplitude of the disturbing force ($x \leq x_1$, $\nu = 20$ Hz).

As it is seen from the presented graphs, increase of the amplitude of the disturbing force leads to increase of the amplitude of longitudinal forced oscillations of the body of the root according to the linear law.

It should also be noted, that below the point of gripping ($x \leq 0.15$ m), with increase of the distance of the cross section of the root from the conditional point of attachment O the amplitude also increases (Fig. 6). For example, with *x* = 0.07 m the amplitude remains within the limits of 0.13...0.8 mm; with *x* = 0.1 m – within the limits of 0.19...1.14 mm; with *x* = 1.12 m – within the limits of 0.23...1.36 mm; with *x* = 0.15 m (point of gripping) – within the limits of 0.28...1.7 mm. However, above the point of gripping ($x \geq 0.15$ m), in case of increase of distance of the cross section from the conditional point of attachment O the amplitude almost doesn't change, as it is shown on the graph in Fig. 7.

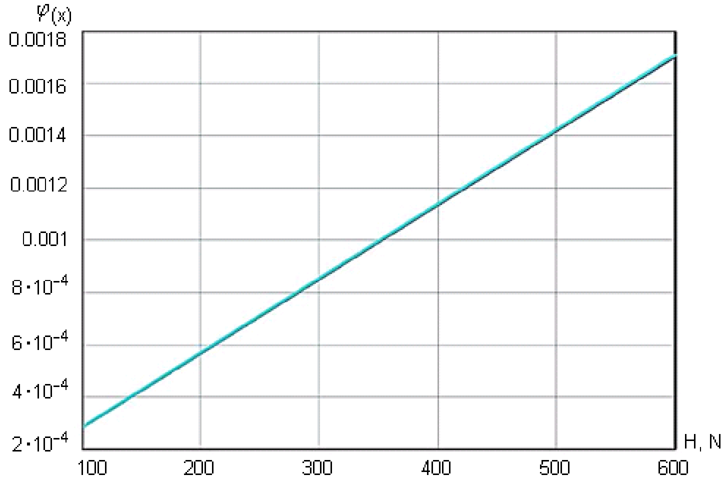

Figure 7. Relation between the amplitude of the forced longitudinal oscillations of the body of the root and the amplitude of the disturbing force ($x \geq x_1$, $\nu = 20$ Hz).

In case of the frequency of the disturbing force $\nu = 10$ Hz the obtained values of amplitudes were a little bit lower, however for $\nu = 10$ Hz they were the same. For example, with $x = 0.07$ m the amplitude remains within the limits of 0.12...0.76 mm; with $x = 0.1$ m – within the limits of 0.18...1.08 mm; with $x = 0.12$ m – within the limits of 0.21...1.3 mm; with $x = 0.15$ m (point of gripping) – within the limits of 0.27...1.62 mm.

Respectively, the obtained values of the frequencies of natural longitudinal oscillations and amplitudes of the forced longitudinal oscillations of the body of the root foster the process of intense knocking of the soil that adhered to the roots off their surface, and in case of such values of the amplitudes tearing of the bodies of the roots is unlikely.

CONCLUSIONS

1. The new theory has been developed with regard to longitudinal oscillations of the root of sugar beet as a body attached in the soil, as an elastic body in an elastic environment, that emerges under the action of the vertical disturbing force that changes according to the harmonic law. The Hamilton-Ostrogradski variational principle of stationary action is used for longitudinal oscillations of the root taking into account the physical and mechanical properties of the root of sugar beet as an elastic body and the surrounding soil.

Using the Ritz direct variational method the Ritz frequencies equation has been obtained, from which different frequencies of free longitudinal oscillations of the root as an elastic body are determined. This, for example, allowed to obtain the analytical expression for calculation of the first natural frequency depending on the physical and mechanical properties of the root and elasticity of the soil surrounding it, which plays the main role in destruction of the tights of the root with the soil. According to the calculations performed, when the coefficient c of the elastic deformation of the soil is changed, the first frequency of natural oscillations of the body of the root is monotonously increased within the limits of 76.4…93.4 Hz, which sufficiently precisely corresponds to the experimental data stated in (Pogorely et al., 1983; Pogorely & Tatyanko, 2004). At the same time the second frequency is changed within the limits of 528…532 Hz, i.e. it has little dependency on the coefficient c of the elastic deformation of the soil.

2. The Hamilton-Ostrogradski functional for forced longitudinal oscillations of the root as an elastic body was constructed, on the basis of which the theory of forced oscillations of the beetroot in the soil was created. The results of theoretical research of the forced oscillations of beetroot attached in the soil were the basis for finding of the algorithm for calculation on a PC of the specified oscillations, in particular, finding of the law of the forced longitudinal oscillations and amplitude under the condition of prevention of damage (tearing) of the beetroot depending on the coefficient c of the elastic deformation of the soil and the amplitude of the disturbing force.

3. It was analytically established that the amplitude of the forced oscillations of the body of the root decreases in case of increase of the coefficient c of elastic deformation of the soil, and increases in case of increase of distance of the cross section of the beetroot from the conditional point of its attachment in the soil. For example, with $x = 0.07$ m and the change of the coefficient c within the limits of $c = 0 \ldots 20 \cdot 10^5$ N m^{-3}, the amplitude is measured within the limits of 0.7…0.47 mm; with $x = 0.1$ m – within the limits of 0.99…0.67 mm; with $x = 0.12$ m – within the limits of 1.19…0.81 mm; with $x = 0.15$ m (point of gripping) – within the limits of 1.49…1.01 mm.

However, for the cross sections of the root above the point of gripping ($x \geq 0.15$ m) the amplitude of the forced oscillations of the body of the root almost doesn't change in case of increase of the distance of the cross section from the conditional point of attachment and remains the same as in case of $x = 0.15$ m. However, the tendency of decrease of the amplitude from increase of the coefficient c is the same as for sections below the point of gripping ($x \leq 0.15$ m).

4. The paper also presents the calculations performed of the amplitude of forced longitudinal oscillations in case of change of the amplitude of the disturbing force within the limits of 100…600 N. As the calculations demonstrated, the increase of the amplitude of the disturbing force leads to the increase of the longitudinal forced oscillations of the body of the beetroot according to the linear law, and increase of the distance of the area of cross section of the root from the conditional point of its attachment in the soil also leads to increase of the amplitude.

For example, with $x = 0.07$ m, the amplitude remains within the limits of 0.13…0.8 mm, with $x = 0.1$ m – within the limits of 0.19…1.14 mm, with $x = 0.12$ m – within the limits of 0.23…1.36 mm, with $x = 0.15$ m (point of gripping) – within the limits of 0.28…1.7 mm. However, above the point of gripping in case of increase of the distance of the cross section from the conditional point of attachment the amplitude almost does not change.

REFERENCES

Babakov, I.M. 1968. *Theory of Oscillations*. Nauka, Moscow, 560 pp. (in Russian).

Bulgakov, V., Golovats, I., Špokas, L. & Voitjuk, D. 2005. Theoretical investigation of a root crop cross oscillations at vibratinal digging up. *Research papers of IAg Eng LUA & LU of Ag.* **37**(1), 19–35. (in Russian).

Lammers, P.S. 2011. Harvest and loading machines for sugar beet – new trends. *International Sugar Journal* **113(**1348), 253–256.

Pogorely, L.V., Tatyanko, N.V., & Bray, V.V. 1983. *Beet-harvesting machines (designing and calculation)*. Under general editorship of Pogorely, L. V. Tehnika, Kyiv, 232 pp.

Pogorely, L.V., & Tatyanko, N.V. 2004. *Beet-harvesting machines: History, Construction, Theory, Prognosis*, Feniks, Kyiv, 232 pp. (in Ukrainian).

Sarec, P., Sarec, O., Przybyl, J., & Srb, K. 2009. Comparison of sugar beet harvesters. *Listy cukrovarnicke a reparske* **125**(7-8), 212–216. (in Czech).

Vasilenko, P.M., Pogorely, L.V., & Brey, V.V. 1970. Vibrational Method of Harvesting Root Plants. *Mechanisation and Electrification of the Socialist Agriculture* **2**, 9–13 (in Russian).

Agronomy Research **12**(1), 59–64, 2014

Influence of soil compaction by farm machinery and livestock on water infiltration rate on grassland

J. Chyba[1,]*, M. Kroulík[1], K. Krištof[2], P.A. Misiewicz[3] and K. Chaney[3]

[1]Czech University of Life Sciences Prague, Kamýcká 129, Prague 6 – Suchdol, 16521, Czech Republic; *Correspondence: chyba@tf.czu.cz
[2]Slovak University of Agriculture in Nitra, Tr. A. Hlinku 2, 94976 Nitra, Slovak Republic
[3]Harper Adams University, Newport, Shropshire, TF10 8NB, United Kingdom

Abstract. The objective of this study was to investigate the rate of water infiltration into the soil under different soil compaction levels caused by livestock and farm machinery. Measurements were performed on grassland which is situated at Harper Adams University, UK. The soil type is classified as a sandy loam – *Eutric Cambisols*. The following treatments were evaluated: non-compacted soil, compaction by cattle hooves and compaction by tractor with trailer. Infiltration rate was measured by simplified falling-head and cone index to a depth of 0.3 m using a cone penetrometer.
Results of the simplified falling-head infiltration method showed a significantly higher water infiltration rate in the non-compacted soil than the compacted soil. There was no statistical difference in the infiltration rate following compaction by cattle hooves and compaction by tractor. The mean values of water infiltration rate measured on compacted soil by cattle hooves and tractor with trailer showed 2.6% difference. The measurements of cone index showed a significant difference only in the case of compaction by cattle hooves, where a decrease of cone index values by approximately 20% in the depth from 0.15 to 0.25 m occurred. Overall it was found that the ground pressure of 200–250 kPa reduces water infiltration properties of the soil more than 80% in comparison to the non-compacted soil.

Key words: cone index, saturated hydraulic conductivity, soil compaction, water infiltration rate.

INTRODUCTION

Soil compaction is an important factor that influences the water infiltration rate and is one of the factors responsible for the degradation of the physical quality of soils. Soil compaction is mainly caused by agricultural machinery, which reduces porosity and increases the density of soils, thus reducing water infiltration rate in comparison with non-compacted soil (Liebig et al., 1993; Yuxia et al., 2001; Hamza & Anderson, 2005; Raper & Kirby, 2006). A non-compacted soil has 4–5 times higher water infiltration rate than the soil compacted by agricultural machines. Yuxia et al. (2001) showed that the effect of agricultural machinery on soil has a greater influence on water infiltration rate than soil tillage.

Soil compaction is not only caused by farm machinery, but also by livestock trampling. Preliminary results on the impact of livestock on bulk density and soil infiltration were obtained by Castellano & Valone (2007) on gravelly sandy loam soils. In this experiment it was found that free-moving livestock increases soil infiltration in comparison with non-compacted soil and thus also increase the abundance of grass on the land. It was also found that the cone index values of soil compacted by cattle hooves and tractor with trailer had lower values than non-compacted soil in the upper layer of soil (0–0.1 m). Da Silva et al. (2003) conducted an experiment evaluating the influence of the animal unit per hectare on soil cone index. The results showed that there was no difference between 3.5 and 4.42 of livestock unit per hectare, however, the load of 5.68 of animal unit per hectare showed significant increase cone index by 88%. Another experiment showed that a grazed site has a 16% higher value of cone index and about 60% lower water infiltration rate than the non-grazed sites (Moret-Fernández et al., 2011). A cone index increase on grazed sites was also observed by Evans et al. (2012) and Schmalz et al. (2013).

MATERIALS AND METHODS

Bird´s Nest field is situated at Harper Adams University farm, Shropshire, UK (latitude 52.776; longitude -2.430). The grassland test areas were prepared by a grassland subsoiler (OPICO sward lifter) to the depth 0.12–0.15 m. The soil water infiltration rate and cone index measurements were performed on sandy loam soil (Beard, 1988) – *Eutric Cambisols* (World Reference Base for Soil Resources – WRB). The average annual rainfall of 653.2 mm and mean annual temperature of 10.1°C. Further soil characteristic is given in Table 1. The measurements were performed on non-compacted soil, soil compacted by cattle hooves with the target ground pressure of 200–250 kPa and compaction by loaded tractor and trailer with the target ground pressure of 200–250 kPa. Both types of soil compaction were conducted three times with a ten day interval in February 2012 and the measurements were taken in June 2012.

Table 1. The soil of Bird´s Nest (Beard, 1988)

Topsoil characteristics	Subsoil characteristics	Soil water regime
Very slightly stony sandy loam	Deep permeable very slightly stony sandy loam often becoming loamy sand below 0.6 m depth.	Well drained. Subsoil is rarely wet.

The simplified falling-head method (SFH) was used for assessment of water infiltration rate into the soil. The SFH method measures saturated hydraulic conductivity (K_{fs}). K_{fs} was measured using a ring of known diameter A [mm] (for this measurement the ring diameter was 0.152 m). The ring was inserted into the soil down to 0.05 m (encloses an area for application of water on the soil surface). SFH uses a small water volume V [l] which is applied to the soil surface. The time t_a [s] was measured from pouring water onto the soil surface until complete water absorption by soil. The soil moisture content was measured before and after water application by Theta Probe (type HH2 Moisture meter, Delta T Devices). The saturated hydraulic conductivity was calculated based on the equation of Bagarello et al. (2004):

$$K_{fs} = \frac{\Delta\theta}{(1-\Delta\theta)t_a}\left[\frac{D}{\Delta\theta} - \frac{\left(D+\frac{1}{\alpha^*}\right)}{1-\Delta\theta}\ln\left(1+\frac{(1-\Delta\theta)D}{\Delta\theta\left(D+\frac{1}{\alpha^*}\right)}\right)\right] \tag{1}$$

where $\Delta\theta$ [$m^3 \cdot m^{-3}$] is the difference between the saturated water content (inside the cylinder θfs) and initial water content (outside the cylinder θi), $D = V / A$ [$l\ mm^{-1}$] is the depth of water in the cylinder at the beginning of measurement and α^* [m^{-1}] is saturation potential coefficient for K_{fs} (Elrick et al., 1989). All measurements used the same volume of water of 0.3 litres and five replications were conducted for each measurement. Saturation potential coefficient of $\alpha^* = 12\ m^{-1}$ was selected (structured sandy loam soils).

An Eijkelkamp penetrologger (ART.NR. 06.15.01) with a 30° cone with an area of 100 mm^2 was used for the cone index determination. The measurements were conducted based on the ASABE standard S313.3 (ASAE Standards, 2004).

STATISTICA 12 software with ANOVA and graph tools was used to analyse the data statistically.

RESULT AND DISCUSSION

The values of saturated hydraulic conductivity measured by the SFH method are shown in Fig. 1. The results show that the non-compacted soil has higher values of saturated hydraulic conductivity (5.62 mm h^{-1}) than the soil compacted with cattle hooves (1.09 mm h^{-1}) and tractor with trailer (1.12 mm h^{-1}), which equates for an 80% decrease in soil infiltration rate. There is no significant difference between the levels of soil compaction caused by cattle hooves and compaction caused by the tractor with trailer.

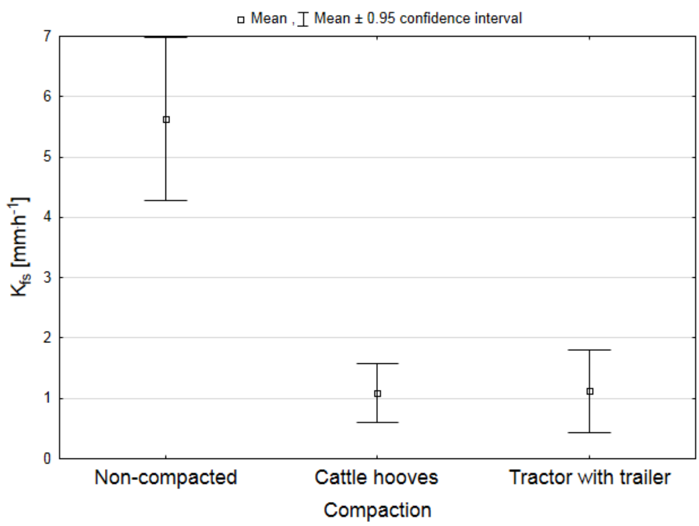

Figure 1. Relationship between different compaction levels and saturated hydraulic conductivity.

Tukey´s HSD test of homogenous groups (Table 2) confirmed that there is no significant statistical difference between compaction types levels (compaction by cattle hooves and compaction by tractor with trailer) and non-compacted soil is in its own homogenous group.

Table 2. *Tukey´s* HSD test of homogenous groups for saturated hydraulic conductivity

Homogeneous groups, α = 0.05			
Compaction type	Mean of K_{fs} [mm h^{-1}]	1	2
Non-compacted	5.626206	****	
Cattle hooves	1.088804		****
Tractor with trailer	1.121352		****

The penetrometer results showed that there was no significant statistical difference between compaction type levels at depths from 0 to 0.10 m, where the upper layer of the soil (from 0 to 0.05) was less compacted for all treatments due to the presence of root concentration and activity of micro-organisms. The results also showed that there were no statistically significant differences between the non–compacted soil and compaction by tractor with trailer in the entire observed depth of the soil profile. The only exception was compaction by cattle hooves, where there was a reduction in cone index values at the depth of 0.10–0.25 m. This is confirmed by *Tukey´s HSD* test of homogenous groups which is shown along with the average values of cone indexes in Table 3.

Similar reduction in cone index values at the depths from 0.10 to 0.35 m, under the soils compacted by cattle hooves, were observed by Martínez & Zinck (2002) on fine- and coarse-textured soils (Acrisols).

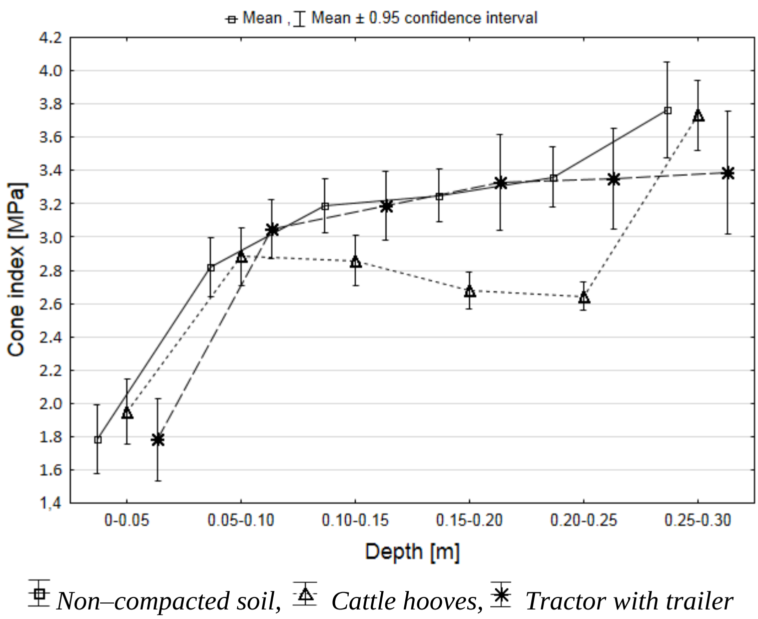

Figure 2. Values of cone indexes for different compaction levels.

Table 3. *Tukey´s HSD* test of homogenous groups for cone indexes
a, b – *homogenous groups in rows;* 1, 2, 3, 4 – *homogenous groups in columns;* α = 0.05

	Cone indexes for different types of soil compaction [MPa]					
Depth	Non-compacted		Cattle hooves		Tractor with trailer	
0–0.05	1.78	a 1	1.95	a 1	1.78	a 1
0.05–0.10	2.82	a 2	2.88	a 2	3.04	a 2
0.10–0.15	3.19	b 2, 3	2.86	a 2	3.19	b 2
0.15–0.20	3.25	b 3	2.68	a 2	3.33	b 2
0.20–0.25	3.36	b 3	2.64	a 2	3.35	b 2
0.25–0.30	3.77	a 4	3.73	a 3	3.39	a 2

CONCLUSIONS

The results showed that the water infiltration rate was influenced by soil compaction. Compaction by cattle hooves and tractor with trailer caused a decrease in saturated hydraulic conductivity values by 80%. However, there were no statistically significant differences between the compaction by cattle hooves and tractor with trailer at the same ground pressure. Further research of the differences between these types of soil compaction and its influence on saturated hydraulic conductivity is recommended.

The cone index values revealed only one case of a statistical difference between the types of soil compaction, as observed with compaction by cattle hooves at a depth of 0.10 to 0.25 m. All variants were influenced by root system in topsoil to a depth of 0.05 m.

Based on these results it can be concluded that there was no statistical difference in penetrometer resistance between the non-compacted soil and compaction by tractor with trailer. However, the saturated hydraulic conductivity measurements confirmed the negative effect of soil compaction on soil water infiltration.

ACKNOWLEDGMENTS: The project was conducted on an experiment investigating the effect of soil compaction on nitrous oxide emissions founded by DiaryCo.

REFERENCES

ASAE Standards, 49th Ed. 2004. S313.3. Soil cone penetrometer. St. Joseph, Mich.: ASAE.

Bagarello, V., Iovino, M. & Elrick, D.A. 2004. Simplified Falling-Head Technique for Rapid Determination of Field-Saturated Hydraulic Conductivity. *Soil Science Society of America Journal* **68**, 66–73.

Beard, G.R. 1988. The soils of Harper Adams Agricultural College, Newport, Shropshire. Published by *Soil Survey and Land Research Centre*, Silsoe.

Castellano, M.J. & Valone, T.J. 2007. Livestock, soil compaction and water infiltration rate: Evaluating a potential desertification recovery mechanism. *Journal of Arid Environments* **71**(1), 97–108.

Da Silva, A.P., Imhoff, S. & Corsi, M. 2003. Evaluation of soil compaction in an irrigated short-duration grazing system. *Soil & Tillage Research* **70**(1), 83–90.

Elrick, D.E., Reynolds, W.D. & Tan, K.A. 1989. Hydraulic conductivity measurement in the unsaturated zone using improved well analyses. *Ground Water Monitoring & Remedition* **9**(3), 184–193.

Evans, C.R.W., Krzic, M., Broersma, K. & Thompson, D.J. 2012. Long-term grazing effects on grassland soil properties in southern British Columbia. *Canadian Journal of Soil Science* **92**(4), 685–693.

Hamza, M.A. & Anderson, W.K. 2005, Soil compaction in cropping systems: A review of the nature, causes and possible solutions. *Soil & Tillage Research* **82**(2), 121–145.

Liebig, M.A., Jones, A.J., Mielke, L.N. & Doran, J.W. 1993. Controlled Wheel Traffic Effects on Soil Properties in Ridge Tillage. *Soil Science Society of America Journal* **57** 1061–1066.

Martínez, L.J. & Zinck, J.A. 2002. Temporal variation of soil compaction and deterioration of soil quality in pasture areas of Colombian Amazonia. *Soil & Tillage Research* **75**(1), 3–18.

Moret-Fernandéz, D., Pueyo, Y., Bueno, C.G. & Alados, C.L. 2011. Hydro-physical responses of gypseous and non-gypseous soils to livestock grazing in a semi-arid region of NE Spain. *Agricultural Water Management* **98**(12), 1822–1827.

Raper, R.L. & Kirby, J.M. 2006. Soil compaction: How to do it, undo it, or avoid it. In: *Agricultural Equipment Techonology Conference*. Louisville, Kentucky, USA, pp. 1–14.

Schmalz, H.J., Taylor, R.V., Johnson, T.N., Kennedy, P.L., DeBano, S.J., Newingham, B.A. & McDaniel, P.A. 2013. Soil Morphologic Properties and Cattle Stocking Rate Affect Dynamic Soil Properties. *Rangeland Ecology & Management* **66**(4), 445–453.

Yuxia, L., Tullberg, J.N. & Freebairn, D.M. 2001. Traffic and residue cover effects on infiltration. *Australian Journal of Soil Research* **39**, 239–247.

Agronomy Research **12**(1), 65–72, 2014

Determination of silage density in bunker silos using a radiometric method

T. Hoffmann* and S. Geyer

Leibniz-Institute for Agricultural Engineering Potsdam Bornim, Max-Eyth Allee 100, 14469 Potsdam, Germany, *Correspondence: thoffmann@atb-potsdam.de

Abstract. Wilted grass and chopped maize have to be compressed in bunker silos in order to achieve storability for high quality silage. High losses can occur if the compaction is too low. The aim of the project was to develop a measuring device to determine the density of the ensiled material during the compaction drives. The measuring method is based on the radiometric density determination by backscattered gamma-photons. Cesium Cs-137 is used as photon source. The cesium source and the detector were located in a measuring wheel, which is trailed by the compaction vehicle over the silo. In conjunction with data from a Differential Global Positioning System (DGPS), the density values can be related to certain positions in the silo. An assessment of the costs and benefits showed that the radiometric measurement method is cost-effective if the number of dairy cows exceeds 135 cows.

Key word: Silage, compression, radiometry, bunker silo, costs, benefits.

INTRODUCTION

When storing wilted grass or chopped maize in bunker silos, the ensiled material has to be compacted in order to avoid losses. At present, in order to measure the density of silage, samples are taken out of the silo using special drills or silage blocks are cut out with a silo block cutter. The density is calculated from the volume withdrawn and the associated mass. However, both these methods can only be applied after the storage period when the silage is removed.

For a relatively long time radiometric methods have been used for measuring densities of natural materials such as wood (Malan & Marais, 1992; Macedo et al., 2002); tobacco (Okumoto, 1987), ice cream (Badr, 2012), starch suspensions (Kempf et al., 1976), grain (DLG, 2001), straw and silage bales (Mumme & Katzameyer, 2007; Gläser et al., 2007; Sun et al., 2012) and silages (Kuhn, 1976; Gläser & Kuhn, 1997).

On the bases of the experiences of Gläser & Kuhn (1997) and Fürll (2008), the radiometric measuring method was chosen as the most promising measuring principle to determine the density of the ensiled material during the compaction drives.

MATERIAL AND METHODS

The measuring principle is based on the interaction of gamma photons with the electrons of the scattering material.

The used measuring unit consists of a cesium radiator with an activity of 37 MBq and a sodium iodide scintillation detector. The measuring system detects the gamma photons radiated back from the material. That means the higher the density of electrons, the higher is the material density.

First of all preliminary experiments were done to find out the optimal geometric arrangement of source and detector. Afterwards the radiometric measuring device was calibrated. For this, natural raw materials of known density were placed beneath the measuring wheel and the impulses of the radiation backscattering were measured. This method is based on the principle that organic materials are similar in their stochiometric composition and thus also display similar mass absorption coefficients (Gläser, 1992; Macedo et al., 2002). The materials used were hemp shives (woody fragments of the hemp stem), balsa, spruce and oak, as well as oats and rye grains. In addition, the impulse rates for air and water were measured. One spruce sample was measured in the natural density state with 430 kg m^{-3}, the other after a mechanical compression with 880 kg m^{-3}.

For each sample the backscattered photons were counted for 1 second with 100 repetitions. This means every measurement series consists of 100 values. A quadratic regression was done with all values of all series by using the statistical software SAS 9.3.

Based on these examinations, a wheel-like measuring device with optimized arrangement of source and detector was developed (Fig. 1) and tested while driving over the silo (Fig. 2). The measuring wheel is connected with the tractor by the three point linkage at the rear. The design is suitable for road transportation as well. The measuring wheel has a diameter of 1 m and a design width of 0.4 m.

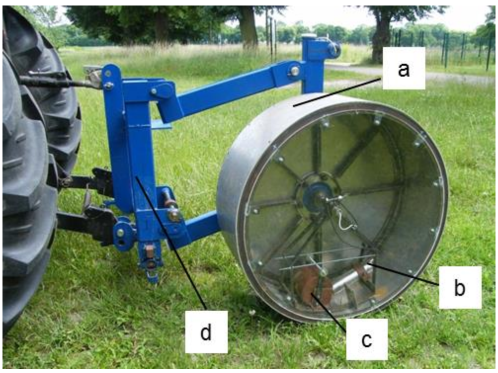

Figure 1. Measuring wheel with cesium source and detector (a – measuring wheel, b – detector, c – cesium source with lead casing, d – frame for three-point linkage).

Figure 2. Measuring pass on a bunker silo with chopped maize.

The necessary number of dairy cattle for a profitable application of a radiometric measuring device was calculated based on a cost-benefit calculation. Cost criteria were silage losses, compaction work, employment of veterinarian, and costs for insemination. Revenues are gained from milk and calves sale. No coherent information were available in literature for every stage from the storage of the ensiled material to the milk sale or cow health. Data for assessing the measurement system were therefore collected from different publications with differing backgrounds. For each criterion a standard value and, in addition, a value with an assumed improved level was determined. Often an improvement of 5% was assumed.

RESULTS

The calibration by various organic materials and water shows a quadratic connection between the given material density and the impulse rate (Eq. 1, Fig. 3). After transformation of Eq. 1, the density can be calculated by using the minus sign in front of the root (Eq. 2).

$$I = -0.222268 \cdot \rho^2 + 6.87148 \cdot \rho + 6517.57751 \tag{1}$$

$$r^2 = 0.99$$

$$\rho_{1,2} = 15.87654 \pm \sqrt{1514.87654^2 - \frac{I - 6517.57751}{0.002268}} \tag{2}$$

with: I – impulse rate, (s^{-1}); ρ – density, (kg m^{-3}); r^2 – coefficient of determination, (-). As expected, the calibration curve (Fig. 3) shows a higher impulse rate with increased density.

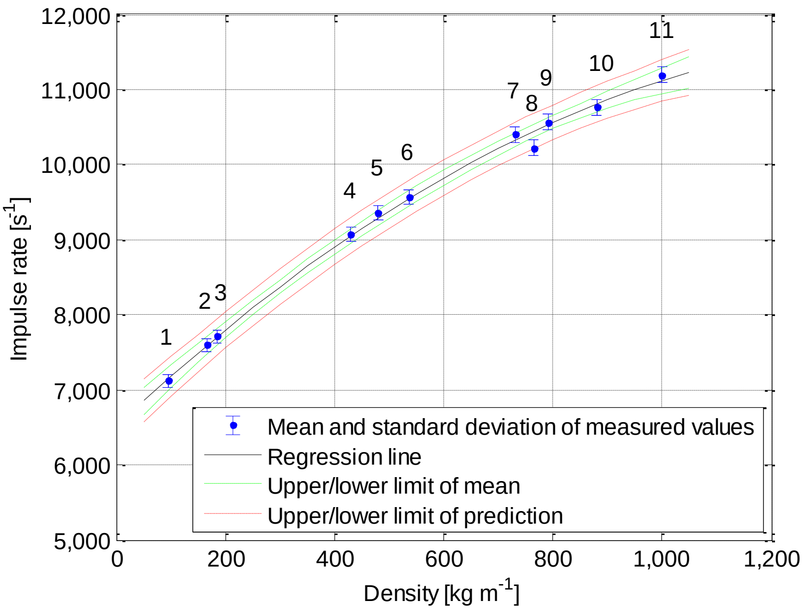

Figure 3. Calibration curve with confidence areas for the radiometric measuring device: 1 balsa, low density; 2 hemp shives; 3 balsa, high density; 4 spruce, natural; 5 oats, loosely poured; 6 oats, firmly tapped; 7 rye, loosely poured; 8 oak; 9 rye, firmly tapped; 10 spruce, compressed; 11 water.

The measuring wheel was tested eight times on bunker silos with maize and wilted grass (Fig. 2). In conjunction with data from a Differential Global Positioning System (GPS), the density values can be related to certain positions in the silo (Fig. 4).

For displaying to the driver of the compaction vehicle the current density on a monitor inside of the cabin of the compaction vehicle a software program was developed. The current density is graduated using a color scale. The colour 'red' represents low densities and 'green' indicates high densities.

The measuring wheel gives the density for one site of the compaction vehicle. No values are available for the second site and for the area between the wheels. The software menu option 'Associated width of a measured value' allows the selection of whether the displayed line represents only the site of the vehicle measured or it is extrapolated on the entire vehicle width (Fig. 4).

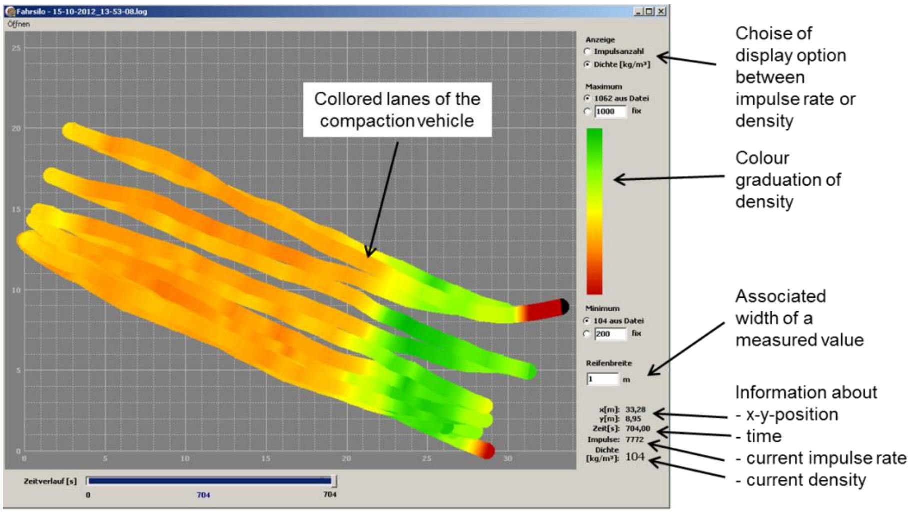

Figure 4. Measured silage density as a function of the position inside a bunker silo with wilted grass (green colour indicates high density, red colour indicates low density).

The acquisition of the measuring system leads to cost. However, financial incentives are to be expected if the ensiled material is compacted properly. The values for the dry matter mass losses given in literature are 7.95% (Ruppel at al., 1995), 9.0% (Köhler et al., 2012), 11.0% (Thaysen, 1993), 11.7% (Böttcher, 1957), 12.0% (Köhler et al., 2012), 13.5% (Hell, 1966), 15.0% (LFL, 2006), 18.0% (DOW, 2012) up to 43.0% (Ruppel et al., 1995).

It is assumed that the losses can be reduced from 13% to 10% (Table 1, row 2) if the ensiled material is compacted as required. For further calculations, a reduction of losses of 3 percentage points is assumed independent of the total level of losses. The calculation results in a cost benefit of 18.05 EUR cow^{-1} a^{-1} (row 6).

The driver of the compaction vehicle controls the next drives based on the current density value. However, because it is not known whether and to what extend compaction time can be saved, no effects due to time losses or savings were applied (row 15).

Table 1. Comparison of the standard cost to the improved costs by using the radiometric density measurement system

Row	Position	Unit	Standard variant	Improved variant
Costs of losses				
1	Need for silage	$m^3\ cow^{-1}\ a^{-1}$	26.72	
2	Losses, relative	%	13.00	10.00
3	Losses, absolute, (OS)	$m^3\ cow^{-1}\ a^{-1}$	3.47	2.67
4	Costs of silage (OS)	$EUR\ m^{-3}$	22.52	22.52
5	Costs of losses	$m^3\ cow^{-1}\ a^{-1}$	78.21	60.16
6	Cost advantage	$EUR\ cow^{-1}\ a^{-1}$		18.05
Costs of compaction work				
7	Standard value for maize (OS)	$min\ t^{-1}$	1	1
8	Standard value for wilted grass (OS)	$min\ t^{-1}$	3	3
9	Relation 1/3 maize, 2/3 grass	$min\ t^{-1}$	2.33	2.33
10	Mass of silage (0.65 t/m³)	$t\ cow^{-1}\ a^{-1}$	2.56	2.56
11	Time for compaction	$min\ cow^{-1}\ a^{-1}$	2.48	2.48
12	Time for compaction	$h\ cow^{-1}\ a^{-1}$	2.51	2.51
13	Costs for driver and tractor	$EUR\ h^{-1}$	2.50	2.50
14	Costs for compaction	$EUR\ cow^{-1}\ a^{-1}$	6.26	6.26
15	Cost advantage	$EUR\ cow^{-1}\ a^{-1}$		0.00
Costs of veterinarien				
16	Data from literature	$m^3\ cow^{-1}\ a^{-1}$	89.00–02.75	
18	Assumed reduction	%		5
17	Standard value	$m^3\ cow^{-1}\ a^{-1}$	95.88	91.09
18	Cost advantage	$EUR\ cow^{-1}\ a^{-1}$		4.79
Costs of insemination				
19	Data from literature	$m^3\ cow^{-1}\ a^{-1}$	25.00–45.00	
20	Assumend reduction	%		5
21	Standard/reduced value	$m^3\ cow^{-1}\ a^{-1}$	30.00	28.50
22	Cost advantage	$EUR\ cow^{-1}\ a^{-1}$		1.50
Proceeds of milk sale				
23	Number of milk cows in Germany	cows	4,164,789	
24	Amount of milk in Germany	$t\ a^{-1}$	29,198,675	
25	Encreased quantity of milk	%		10
26	Quantity of milk	$l\ cow^{-1}\ a^{-1}$	7,010.84	7,711.93
27	Profit	$EUR\ l^{-1}$	0.02	
28	Proceeds of milk sale	$EUR\ cow^{-1}\ a^{-1}$	140.22	154.24
29	Cost advantage	$EUR\ cow^{-1}\ a^{-1}$		14.02
Proceeds of calves sale				
30	Improvement	%		5
31	Number of lactations	cow^{-1}	2.50	2.63
32	Average proceeds of calf	$EUR\ a^{-1}$	174.00	174.00
33	Proceeds	$EUR\ cow^{-1}$	435.00	456.75
34	Age of milk cow	a	5	5
35	Proceeds	$EUR\ cow^{-1}\ a^{-1}$	87.00	91.35
36	Cost advantage	$EUR\ cow^{-1}\ a^{-1}$		4.35

It is assumed that high quality fodder stimulates the health of cows and therefore leads to reduced costs for veterinarian. Averages of costs for animal care are between

89.00 EUR cow^{-1} a^{-1} (Wattendorf-Moser, 2001) and 102.75 EUR cow^{-1} a^{-1} (Dummer, 2010). As standard variant in the calculation 95.88 EUR cow^{-1} a^{-1} (row 18) is used and 91.09 EUR cow^{-1} a^{-1} as improved variant, that is 5% cost reduction. The financial benefit amounts to 4.79 EUR cow^{-1} a^{-1} (row 18).

A good cow health is also reflected in lower insemination costs. The insemination costs are estimated at 25.00 – 45.00 EUR cow^{-1} a^{-1} (LFL, 2006). The evaluation calculates with 30.00 EUR cow^{-1} a^{-1} as standard value (row 21). The assumed benefit amounts to 1.50 EUR cow^{-1} a^{-1} (row 22).

Kressel (2008) reported, that cows give 38.33 kg milk day^{-1} if they were fed with good maize silage and only 33.83 kg day^{-1} if they were fed with molded silage. This means a reduction of approx. 10%. From the point of view of a quality improvement due to the density measurement, an increased milk amount of 10% (row 26) was used in the calculation. The benefit amounts to 14.02 EUR cow^{-1} a^{-1} (row 29).

It can be expected that a healthy cow is more efficient and gets more calves. In average a cow gets 2.5 calves (row 31) (LKV, 2012). If the number of lactations increases to 2.63 calves (plus 5%), a financial benefit of 4.35 EUR cow^{-1} a^{-1} be the result (row 36). The total lifetime of cows is set to 5 years in the calculation.

The compilation of cost advantages shows that the reduction of losses and the increase of milk production deliver the greatest cost benefits (Table 2, rows 37 and 41).

Table 2. Compilation of cost adavantages

Row	Position	Unit	Improved variant
37	Costs of losses	EUR cow^{-1} a^{-1}	18.05
38	Costs of compaction work	EUR cow^{-1} a^{-1}	0.00
39	Costs of veterinarien	EUR cow^{-1} a^{-1}	4.79
40	Costs of insemination	EUR cow^{-1} a^{-1}	1.50
41	Proceeds of milk sale	EUR cow^{-1} a^{-1}	14.02
42	Proceeds of calves sale	EUR cow^{-1} a^{-1}	4.35
43	SUM	EUR cow^{-1} a^{-1}	42.71

A financial benefit of 42.71 EUR is the result underlying these conservative assumptions.

The purchase price of the measuring device is not fixed yet. Presumably, the invest will be between 10,000 EUR and 13,000 EUR (Tab. 3, row 44). Assuming an eight-year-lifetime, the fixed costs will be between 2,997.50 EUR a^{-1} and 3,746.75 EUR a^{-1} (row 54). These costs include training courses regarding the radiological protection of the labour of 500 EUR a^{-1} (row 52). There are also variable costs of 42.72 EUR a^{-1} (row 58). The sum of cost ranges between 3,040.22 EUR a^{-1} and 3,789.47 EUR a^{-1}.

With a financial benefit of 42.71 EUR/cow/a between 71.2 and 88.7 milk cows are necessary for a profitable employment of the radiometric measuring device (Table 3, row 60), considering positive effects only. Due to uncertainties in calculation, an excess charge of 50% on highest value is recommended. Economic viability is given if the stock of dairy cattle is 135 or more.

In Germany, about 3,600 farms have a stock of between 100 and 200 dairy cows (Destatis, 2012). Approximately 1,530 farms keep more than 200 dairy cows. Thus, there are a sufficient number of potential users.

CONCLUSIONS

The radiometric measuring principle by using a cesium radiator is well suited to determine the density of ensiled material. By arranging source and detector in a trailed measuring wheel, the silage density can be measured online during movement. In conjunction with data from a Differential Global Positioning System (DGPS), the density values can be allocated to certain positions in the silo. By that, the driver is enabled to plan the next passes.

A conservative assumption of the costs of the measuring device and the benefit shows that approximately 135 milk cows are necessary to guarantee an economic employment of the measuring system presented here.

Table 3. Calculation of the costs and minimum number of cows

Row	Position	Unit	Variant 1	Variant 2	Variant 3
44	Purchase price	EUR	10,000.00	11,500.00	13,000.00
45	Residual value	EUR	500.00	575.00	650.00
46	Lifetime of device	a	8.00	8.00	8.00
47	Depreciation	EUR a^{-1}	1,187.50	1,365.63	1,543.75
48	Interest rate	%	4.00	4.00	4.00
49	Interest	EUR a^{-1}	210.00	241.50	273.00
50	Assurance	EUR a^{-1}	500.00	575.00	650.00
51	Housing	EUR a^{-1}	100.00	115.50	130.00
52	Education	EUR a^{-1}	500.00	500.00	500.00
53	Maintenance cost	EUR a^{-1}	500.00	575.00	650.00
54	**Sum of fixed costs**	**EUR a^{-1}**	2,997.50	3,372.63	3,746.75
55	Service	h	2.67	2.67	2.67
56	Cost of labor	EUR h^{-1}	15.00	15.00	15.00
57	Allocable labor costs	EUR a^{-1}	40.05	40.05	40.05
58	**Sum of variable costs**	**EUR a^{-1}**	42.72	42.72	42.72
59	**Sum of costs**	**EUR a^{-1}**	3,040.22	3,415.35	3,789.47
60	Minimum number of milk cows		71.2	80.0	88.7

REFERENCES

Badr, H.M. 2012. Improving the microbial safety of ice cream by gamma irradiation. *Food and Public Health* **2**(2), 40–49.

Böttcher, H. 1957. Futterkonservierung durch Silage. Deutscher Bauernverband, Berlin, 132 p.

Destatis. 2012. Land- und Forstwirtschaft, Fischerei. Statistisches Bundesamt, https://www.destatis.de/DE/Publikationen/Thematisch/LandForstwirtschaft/ViehbestandTierischeErzeugung/Viehhaltung2030213109004.pdf?__blob=publicationFile, access: 25.02.2014.

DLG. 2001. Ertragsermittlung im Mähdrescher – Ertragsmessgeräte für die lokale Ertragsermittlung. Ergänzte und überarbeitete Neuauflage. Ed.: Deutsche Landwirtschafts-Gesellschaft (DLG), DLG-Merkblatt 303. 19 p.

DOW. 2012. Bewertung der Trockenmasseverluste bei der Silageherstellung. Information material of Dow Chemical Company, http://www.dow.com/silage/, acsess 31.07.2012.

Dummer, C. 2010. Auswertung der Tierarztrechnungen. http://www.aelf-co.bayern.de/tierhaltung/29344/auswertung_mlp_11_11.pdf, access 18.02.2014.

Fürll, C., Schemel, H. & Köppen, D. 2008. Prinziplösungen für die Dichtemessung in Siliergütern. *Landtechnik* **63**(2), S. 94–95.

Gläser, M. & Kuhn, E. 1997. Forschungssonde für die Dichtemessung an landwirtschaftlichen Gütern. *Agrartechnische Forschung* **3**(1), 44–51.

Gläser, M. 1992. Grundlagenuntersuchungen zur radiometrischen Bestimmung der Masse geförderter Güter, insbesondere in der landwirtschaftlichen Forschung und Praxis. Forschungsberichte VDI Reihe 14, Düsseldorf, Germany, VDI-Verlag GmbH.

Gläser, M., Jahnke, W. Pütz, M & Mumme, M. 2007. Zerstörungsfreie radiometrische Bestimmung des Dichteverlaufs an Rund- und Quaderballen. *Landtechnik* **62**(3), 146–147.

Hell, K.W. 1966. Optimale Investitionen in der Silowirtschaft bei Grassilagen als Futtergrundlage in der Rinderhaltung. Arbeitsgemeinschaft landwirtschaftliches Bauen, ALB-Heft-Schriftenreihe 28, Frankfurt am Main.

Kempf, W., Friedrich, I., Hoepke, C.-H., Veldenkamp, J., Vierhuf, J. & Brandtmöller, W. 1976. Kontinuierliche Mengen- und Dichtemessung von Stärkesuspensionen. Die Stärke 28(2), 54–68.

Kressel, U. 2008. Erstellung eines Konzeptes für ein dynamisches Qualitätssicherungssystem für Milcherzeugerbetriebe im Kontrollbereich Stoffwechselgesundheit. Ph.D. thesis, Technical University München, München, 338 p.

Kuhn, E. 1976. Die Aussagefähigkeit radiometrischer Messungen zur Bestimmung der mittleren Gärfutterdichte in Horizontalsilos. *Agrartechnik* **26**(11), 532–533.

Köhler, B., Diepolder, M., Ostertag, J., Thurner, S. & Spiekers, H. 2012, Dry matter losses of grass and maize silages in bunker silos. In: Proceedings of the XVI International Silage Conference, 2-4 July 2012, Hämeenlinna, Finnland, Hrsg.: MTT Agrifood Research Finland und University of Helsinki 2012, 318–319.

LFL. 2006. Materialsammlung Futterwirtschaft. Bayerische Landesanstalt für Landwirtschaft (Ed.), Freising-Weihenstephan, 143 p. www.lfl.bayern.de/mam/cms07/publikationen/daten/informationen/p_22478.pdf, access 20.02.2014.

LKV. 2012. Jahresbericht 2012. Landeskontrollverband Brandenburg e.V., Waldsieversdorf, 76 p.

Macedo, A., Vaz, C. M. P., Pereira, J. C. D., Naime, J.M., Cruvinel, P.E. & Crestna, S. 2002. Wood density determination by X- and Gamma-ray Tomography. *Holzforschung* **56**(5), 535–540.

Malan, F.S. & Marais, P.G. 1992. Some Notes on the direct gamma ray densitometry of wood. *Holzforschung* **46**(2), 91–97.

Mumme, M. & Katzameyer, J. 2008. Mobiler Prüfstand zur radiometrischen Messung der Dichteverteilung in Ballen. *Landtechnik* **63**(6), 341–343.

Okumoto, Y. 1987. Device for controlling contents of tobacco on cigarette manufacturing machine. European Patent EP 0268124 A1.

Ruppel, K.A., Pitt, R.E., Chase, L.E. & Galton, D.M. 1995. Bunker silo management and its relationship to forage preservation on dairy farms. J. Dairy Sci. **78**, 141–153.

Sun, Y., Cheng, Q., Meng, F., Buescher, W., Maack, C. & Lin, J. 2012. Image-based comparison between a γ-ray scanner and a dual-sensor technique for visual assessment of bale density distribution. *Computer and Electronics in Agriculture* **82**, 1–7.

Taysen, J. 1993. Silagebereitung II. Sonderdruck aus der Kartei für Rationalisierung. Rationalisierungs-Kuratorium für Landwirtschaft (RKL), Rendsburg-Osterronfeld, 678–792.

Wattendorf-Moser, F. 2001: Betriebszweigauswertung. http://milchgeld.de/, access 20.02.2014.

Agronomy Research **12**(1), 73–80, 2014

Detection of anchoring columns in low trellis

D. Hoffmann*, A. Rybka, M. Linda and M. Kříž

Czech University of Life Sciences Prague, Faculty of Engineering, Kamýcká 129, 16521 Prague 6 – Suchdol, Czech Republic; *Correspondence: dhoffmann@tf.czu.cz

Abstract. Low trellis of hop field was emerged in the Czech Republic in the mid-nineties of the 20th century. Growing hops in a low trellis has already been tested in 1991 by Hop Research Institute Ltd. in Žatec. However, at that time, the lack of adequate (the dwarf) varieties and special techniques prevent to their expansion. For full use low trellis is necessary mechanization, that is already currently being developed.

The main advantage of growing hops at low trellis is costs reduce. Some experts say cost reduction to 50%. Cost reduction is the result of simplifying the spring and harvest work (using a mobile harvester).

Currently, a prototype of a mechanical cutter is tested in field conditions. Activity of mechanical cutter is now controlled directly by the tractor driver. This control of mechanical cutter (or rather inter-axle carrier on which it is cutter mounted) puts on the tractor driver too high demands on precision. Failure to comply with the conditions set comes in contact the trimming disc with anchor pillar and the mutual damage.

The movement of inter-axle carrier would therefore be appropriate automatically. But at first, it is necessary to solve recognition (detection) anchoring columns of the low trellis.

During the cutting of hops needed to ensure the most accurate copy of the columns by the trimming disc, to be trimmed hop vines and hops growing in close proximity (distance hops from the anchoring column is about 150 mm).

The paper presents several types of sensors and describes their advantages and disadvantages. For laboratory test was developed model low trellis comprising also hop vine, at which were referred sensors tested. This article analyzes the measured results of individual sensors and it is shown, that not all sensors are suitable for this field application. In conclusion are recommendations for follow-up research.

Key words: hops, sensor, low trellis.

INTRODUCTION

A highly important aspect in the technology of hop growing on low trellis is the spring mechanical pruning, on the quality of which depends later yield (Ebersold, 2004; Srečes et al., 2013). An experimental model of mechanical pruner (Fig. 1) is being developed in the Department of Agricultural Machines, Faculty of Engineering CULS in Prague. This mechanical pruner is placed on the inter-axle carrier of tractor which owing to its rectilinear hydromotors secures the necessary motion for the carried mechanical pruner. The mechanical pruner's cutting disc moves directly in the axis of hop rows (under the supporting net) of low trellis. In the same axis, however, there are also placed supporting wooden poles which need to be avoided as closely as possible during the agrotechnical operation.

Despite all the advantages mechanical pruning may bring, currently mechanical pruners are not produced in series (Křivánek et al., 2008; Křivánek & Ježek, 2010; Krofta & Ježek, 2010; McAdam et al., 2013).

Figure 1. Experimental model of mechanical pruner placed on tractor.

MATERIALS AND METHODS

Detection of the right position for supporting poles of low trellis is the key step for automation of the whole operation of mechanical hop pruning. Tractor's operator pays full attention to driving through hop inter-rows. Manual control of the motion of inter-axle carrier with mechanical pruner would be too dangerous. At imprecision (delay) of supporting arm deflection, the cutting disc would come into contact with low trellis supporting pole, which would cause a damage to the machine or hop-field equipment. At the same time, there is an attempt to copy a supporting pole as precisely as possible with the cutting disc in a way so that even hop rootstocks growing in its immediate proximity were cut (distance of a rootstock from a supporting pole is app. 150 mm, though the recommended distance is 500 mm), (Štranc et al., 2007).

At imprecise driving in the hop inter-rows a tractor can damage the supporting net or uproot (eventually break) the supporting poles of the low trellis.

Steps in copying are depicted in Fig. 2. To achieve the right copying effect it is necessary to detect a precise position of supporting poles.

Direction of the mechanical pruner motion

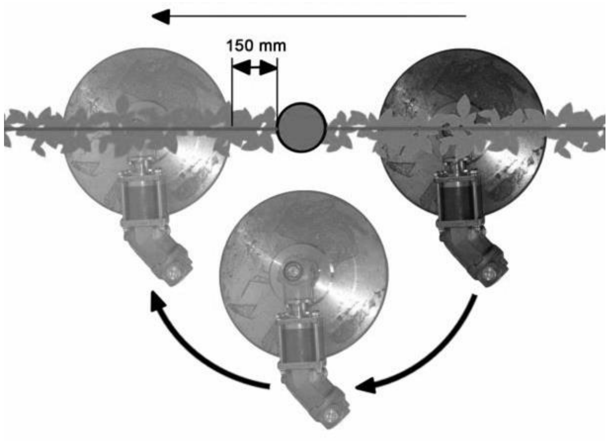

Figure 2. Copying of a supporting pole by a cutting disc.

Laboratory model of low trellis

For the purposes of sensors measurement a model of low trellis was created in the laboratory of the Department of Agricultural Machines.

The model is a faithful copy of a common low trellis construction for hop growing with one difference in the height which is only 1,300 mm. The model is formed of two supporting poles of 80 mm in diameter (Fig. 3 – left pole) and 100 mm in diameter (Fig. 3 – right pole), and of a white plastic supporting net covered with dry hop bines (amount of plant residues is the same as in field conditions). Between the supporting poles there are stretched two steel wire ropes of 6 mm in diameter which increase the firmness of the supporting plastic net. The lower stretching rope is situated 250 mm above the ground and the other is 1,200 mm above the ground. The axial distance of the supporting poles is 1,200 mm and are fixed to the floor by L-shaped anchors. The laboratory model and its placement in the laboratory is to be seen in Fig. 3.

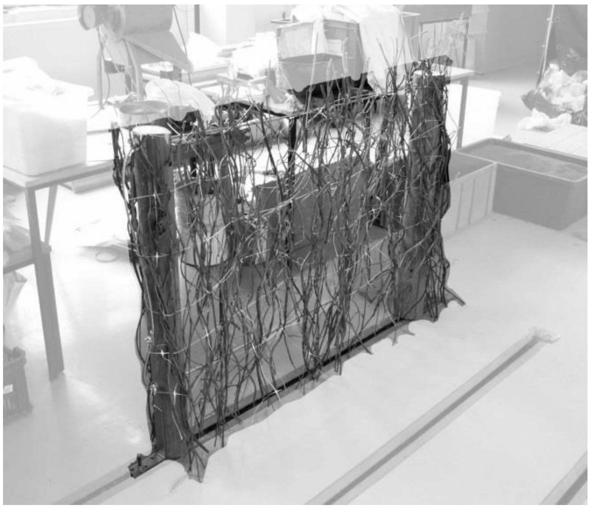

Figure 3. Laboratory model of low trellis.

The laboratory measurement was supposed to verify the suitability of using different sensor types. Our object was to find out whether a measured sensor is able to distinguish repeatedly a wooden supporting pole from the supporting plastic net with plant residues.

Measuring by means of Efector pmd 3d sensor

For the purpose of our measurement with the laboratory model we used Efector pmd 3d camera 03D201 infrared sensor (IR), which was during the whole measurement placed on its own photo tripod fitted with a special handle.

Efector pmd 3d (Fig. 4) is an IR sensor by Ifm Electronic intended to measure distance. It operates using the time-of-flight method: light passing through needs certain amount of time to get to the object (where it reflects) and comes back to the sensor. This stretch of time is directly proportional to its trajectory (PMD technology, 2013).

PMD is an abbreviation for Photo Mixer Device: both sensor and evaluation electronics are integrated into one silicon chip.

The resolution of this device is 64 x 50 pixels (px), which means the amount of image dots of the sensor. (According to the producer, the minimal resolution is 13 mm for a distance of 500 mm.)

Big advantage is innovative design with maximum performance in a compact, industrially compatible housing. Waterproof and dustproof is a very important property suitable into field conditions.

Figure 4. Efector pmd 3d camera 03D201 IR sensor.

RESULTS AND DISCUSSION

Survey image

First of all we measured so called survey images at a distance of 2,000 mm from the edge of the hop-field model, illustrating both supporting poles and the supporting net.

During the measurement we measured the distance of all the dots within a segment of the sensor's lens and according to RV we assigned them a shade of grey colour. RV mean relative value of the intensity and distance. Red colour in the figure (Fig. 5) marks the places which, due to their distance, were outside the measuring range of the sensor.

The lighter the colour gets, the closer to the sensor the measured object is. The supporting pole is well noticeable, despite the fact that some of the dry hop bines were up to 70 mm closer to the sensor.

After the data had been recorded, we carried out a visualization of the image, particularly of the 32nd line of image dots – counted from the top edge of the image (Fig. 5 – the horizontal line). When conducting the visualization, each RV is matched with a colour shade. Therefore the output voltage of a given line is able to be chosen and depicted independently in a graph. The visualized measured data of the 32nd line are to be found in Fig. 6.

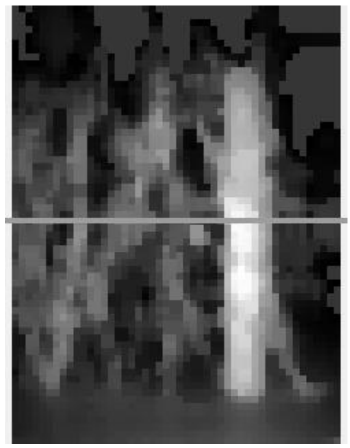

Figure 5. Survey image with marked position of visualized image data (intensity mode).

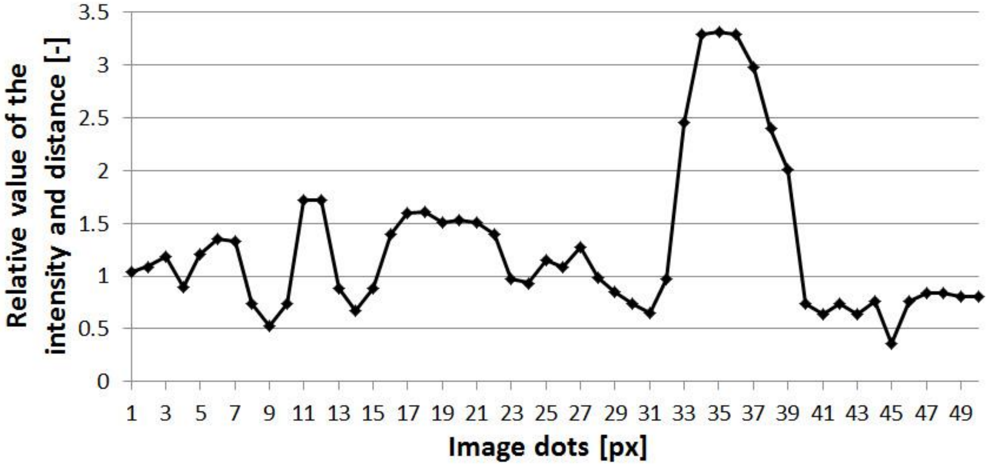

Figure 6. Measured RV of the right survey image.

In the graph there is a well visible deflection which almost reaches the value of 3.5. In exactly this place a pole is detected – in Fig. 5 it is marked with the lightest colour. To get a clearer idea it is possible to place the graph of the measured RV onto the survey image. The result of the overlap is depicted in Fig. 7. In it we may notice a clear dependency of the measured RV (yellow curve) on the colour shade. Analysed data are displayed in Table 1.

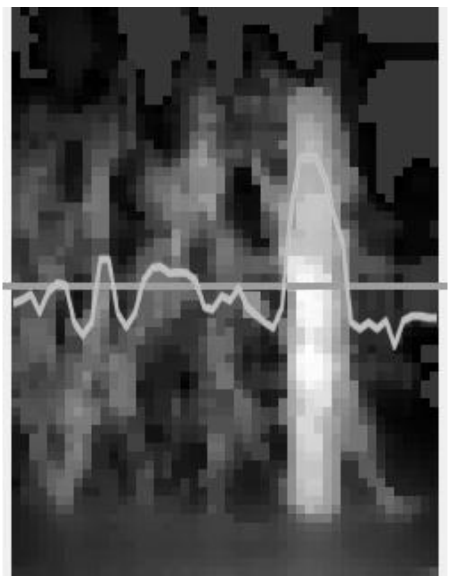

Figure 7. Graph of the measured RV overlapping the survey image.

Table 1. Analysis of measured data

Relative value of the intensity and distance	
Mean value	1.274705
Error of the mean value	0.10337
Median	1.009531
Modus	0.735344
Standard deviation	0.730938
Sampling variance	0.534271
Spikiness	2.092599

Measuring at a distance of 900 mm

Another image was taken at a distance of 900 mm from the edge of the low trellis model. The sensor was placed on a photo tripod, just as it was with the survey image.

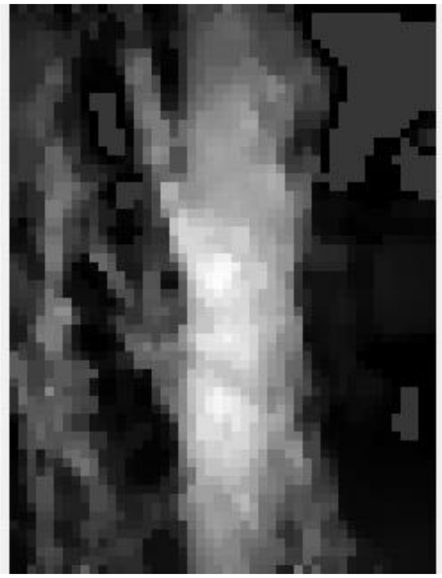

Table 2. Analysis of measured data

Relative value of the intensity and distance	
Mean value	3.874797
Error of the mean value	0.548159
Median	2.220263
Modus	2.961701
Standard deviation	3.876071
Sampling variance	15.02393
Spikiness	-0.18257
Skewness	1.12963
Minimum	0.276654
Maximum	12.60698
Sum	193.7399
Number	50
Confidence level	1.101567

Figure 8. Supporting pole, distance of 900 mm.

A graphic analysis of a supporting pole of 100 mm in diameter (Fig. 8) is depicted in the graph of Fig. 9. The course of graphic dependency makes noticeable the position of the supporting pole, which ranges between 20–35 px. The supporting plastic net with hop bines ranged about the RV of 4, namely between 1 and 20 image dots. Analysed data are displayed in Table 2.

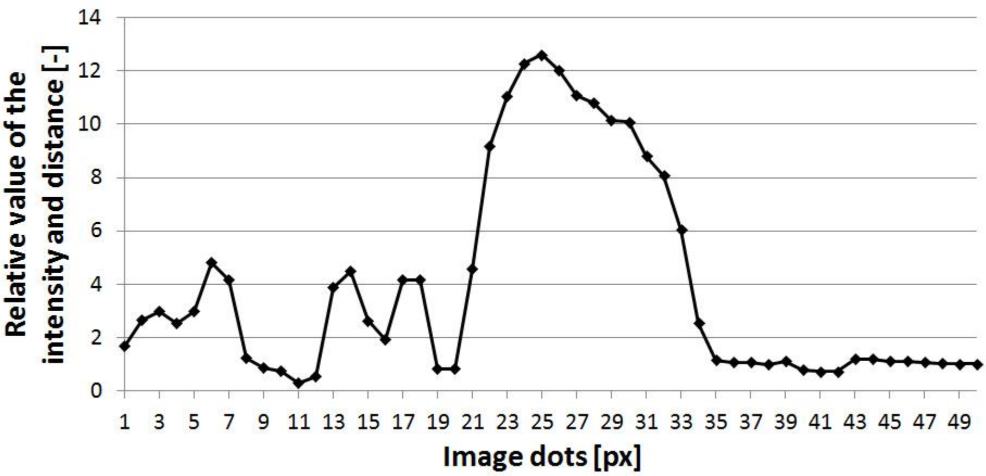

Figure 9. Graphic dependency of RV on image dots.

Measuring at a distance of 200 mm

Figure 10. Right supporting pole of 100 mm in diameter, with dry bines.

Table 3. Analysis of measured data

Relative value of the intensity and distance	
Mean value	45.32024
Error of the mean value	3.906432
Median	52.66297
Modus	4.420968
Standard deviation	27.62264
Sampling variance	763.0104
Spikiness	-1.16161
Skewness	-0.05245
Minimum	3.998318
Maximum	94.14951
Sum	2266.012
Number	50
Confidence level	7.850268

The graph in Fig. 11 illustrates the graphic dependency of the RV on image dots of a supporting pole of 100 mm in diameter with dry bines (Fig. 10). This image contains two parts which are vertically divided: in the left part there is the supporting net with hop bines, and in the right part there is the supporting pole of 100 mm in diameter. In the graph the pole is visible from 23rd to 50th line of image dots. Analysed data are displayed in Table 3.

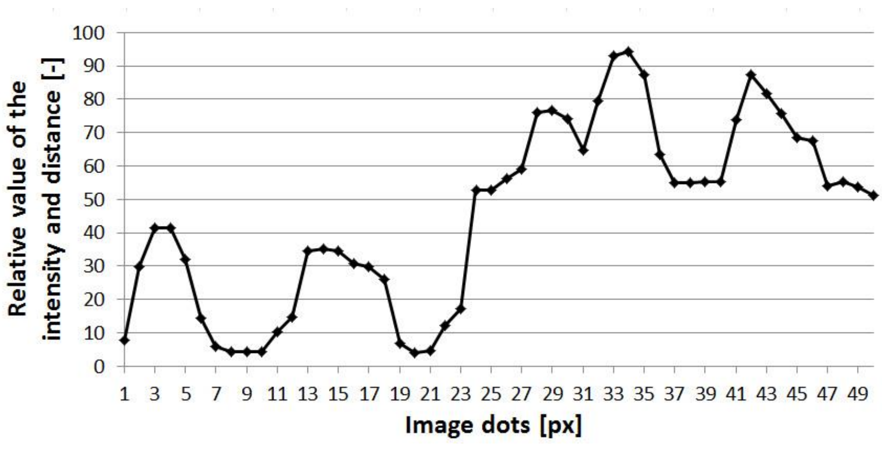

Figure 11. Dependency of RV on image dots.

CONCLUSION

The graphic analysis makes evident that to detect the position of supporting poles as more convenient proves to be the sensor distance of 900 mm from measured hop row. At such a distance the sensor detects old bines with the supporting plastic net as being one unit, therefore no IR beam passes through the measured object. Also the supporting poles, measured at this distance, are much better recognizable from the rest of the low trellis equipment. The position of poles at a measured distance of 900 mm is well visible as it is shown in Fig. 8 and its graphic illustration (Fig. 9).

Measuring at a distance of 2,000 mm is inconvenient, as the sensor would have to be placed on the other side of the tractor to the one where the cut is executed.

A measuring distance of 200 mm is inconvenient as well, because then the supporting poles in the image are distinguishable from the supporting net with hop bines only with difficulties.

Currently we have been carrying out a measurement using the laboratory model with another sensors, such as e.g. the infrared IR SHARP sensor (GP2Y0A21YK0F) or an ultrasonic sensor (UK1C-E1-0E). The last step will be to create an application which based on a detection of a supporting pole would produce a controlling impulse to deflect the inter-axle carrier.

Other measurements show that as the best distance measuring for technology growing hops at a low trellis is IR sensor SHARP GP2Y0A21YK0F.

ACKNOWLEDGEMENTS. This article was written as an output of MZe NAZV No. QI101B071 and IGA 2013:31160/1312/3112 research projects.

REFERENCES

Ebersold, R. 2004. Feasiblity study on low-trellis hop production. Chambre d´Agriculture du Bas-Rhin (CABR), Rome, Italy, pp. 3. Available at: <http://adha.us/sites/default/files/downloads/French%20Low%20Trellis%20Feasability.pdf>

Krofta, K. & Ježek, J. 2010. *The effect of time of cutting on yield and the quality of the hop hybrid varieties* Harmonie, Rubín and Agnus. Plant, Soil and Environment. Volume **56**, Issue 12, pp. 564-569. ISSN: 1214117

Křivánek, J. & Ježek, J. 2010. The importance of cut and verification German prototype machines for hop cutting designed for a low trellis system in ÚH Stekník. *Chmelařství* **83**(4), 45–48. (in Czech).

Křivánek, J., Pulkrábek, J., Chaloupský, R., Kudrna, T. & Pokorný, J. 2008. Response of the Czech hybrid hop cultivar Agnus to the term of pruning, depth of pruning and number of trained bines. Plant, Soil and Environment, Volume 54, Issue 11, pp. 471-478. ISSN: 12141178

McAdam, E.L., Freeman, J.S., Whittock, S.P., Buck, E.J., Jakse, J., Cerenak A., Javornik, B., Kilian, A., Wang, C.H., Andersen, D., Vaillancourt, R.E., Carling, J., Beatson R., Graham, L., Graham D., Darba P. & Koutoulis, A. 2013. Quantitative trait loci in hop (Humulus lupulus L.) reveal complex genetic architecture underlying variation in sex, yield and cone chemistry. BMC Genomics, Volume 14, Issue 1, 30, Article number 360. ISSN: 14712164

PMD technology, 2013. PMD technology. Available at: <http://www.ifm.com/ifmuk/web/pmd.htm>

Štranc, P., Štranc, J., Jurčák, J., Štranc, D. & Pázler, B. 2007. Řez chmele (Hop cuting). ČZU in Prague, pp. 42-43. ISBN 978-80-87111-03-1. (in Czech).

Agronomy Research **12**(1), 81–94, 2014

Energy consumption in different grain preservation methods

T. Jokiniemi*, S. Jaakkola, M. Turunen and J. Ahokas

University of Helsinki, Department of Agricultural Sciences, P.O. Box 28, 00014, University of Helsinki, Finland; *Correspondence: tapani.jokiniemi@helsinki.fi

Abstract. The energy consumption of hot air drying and alternative feed grain preservation methods was examined. Alternative methods were airtight preservation, acid preservation and grain crimping. The results indicate that significant energy savings can be achieved by using any of these methods instead of hot air dying for preservation of home-grown grain used for animal feeding. Remarkable differences in the energy consumption between the alternative methods were also found. Grain crimping showed the lowest energy consumption, but the effect of the used additive and especially the storage system was large. A suitable option for different farm animal species can be found among these methods, and the limitations, when they exist, are set rather by the feeding technology than the nutritive value of the preserved grain.

Key words: Agriculture, grain preservation, energy consumption, hot air grain drying, airtight preservation, acid preservation, grain crimping.

INTRODUCTION

Energy use and energy efficiency have become notable issues in all sectors of life. This trend is driven by the climate change scenarios and declining fossil energy resources. European Union has obligated the member states to achieve 20% savings in primary energy consumption by the year 2020, compared to the projections made in 2007 (European Union 2012).

One of the most energy intensive processes in agriculture cereal production in boreal- and northern temperate climate zone countries is grain preservation. Due to the short growing season the harvest moisture of grain is usually high, and degradation of the yield has to be prevented by some kind of preservation. Current common practice for grain preservation is hot air drying. In Finland it is applied to ca. 85–90% of the grain yield (Palva et al., 2005). Grain drying is one of the biggest direct energy inputs in cereal production in Finland. For example in barley production it represents ca. 30% of all direct energy inputs (Mikkola & Ahokas, 2009). In unfavourable harvest conditions the energy consumption of grain drying may be as large as in all the field operations added together.

However, almost 70% of the domestic grain consumption is used as animal feed, either directly at the farm or through a feed factory (Tike 2013a). In animal nutrition maintaining the grain viability is not necessary and the grain could be preserved also by some other methods than drying. Advantages of drying are well-established technology, reliability and the flexibility of the method; it does not limit the end-use possibilities of the yield and the dried grain is easy to store, handle and transport.

Therefore one rational approach would be to apply drying when the grain is to be transported for longer distances, and some alternative preservation method when the grain is to be used on site or in its vicinity. Finnish farms used their own grain for feed ca. 1.3 billion kg during the season 2012–2013, which represented ca. 35% of the total grain yield of 3.7 billion kg (Tike 2013b). According to the approach presented above, this is hence the approximate maximum amount of grain that could be realistically preserved by alternative grain preservation methods.

The aim of this paper was to evaluate the energy efficiency and achieved energy savings of several alternative feed grain preservation methods compared to the hot air drying. In addition to the energy efficiency, also the nutritive value of the grain preserved by different methods was taken into consideration. Also some economical assessments were made on the basis of previous studies. The examined methods were:

- Hot air drying.
- Airtight preservation.
- Acid preservation of whole grains.
- Grain crimping.

All of the examined methods have been known for a long time but they are still relatively seldom used. They are technologically mature and could thus be implemented directly into current farming practices. Also some other grain preservation methods exist, for example grain cooling, but they are not discussed in this paper. The analyses made in this paper ended when the grain was in the storage. The energy consumption of unloading the storage and the feeding system were not included in the calculations. However, these systems may still be discussed when evaluating the overall functionality of the examined grain preservation methods.

,

MATERIALS AND METHODS

Surfaces of grains are always infected by some yeast, fungi and bacteria, which will contaminate the grain if they are allowed to reproduce. For this they need moisture, oxygen and suitable environmental conditions, such as temperature and pH-level (Loewer et al., 1994). All the grain preservation methods aim to alter at least one of these factors to create circumstances where the micro-organisms cannot grow and reproduce. The examined grain preservation methods are introduced briefly in the following chapters. This concerns the technical solutions as well as animal nutritional perspective with different farm animal species. It must be noted that some other techniques may also exist. Also the initial data for calculating the energy inputs for each method is presented.

The energy consumption of all preservation methods was calculated per one kilogram of grain dry matter (grain DM) to ease the comparison between different methods. The size of the farm operation has little effect on the specific direct energy consumption (J kg^{-1}) of grain preservation. However, it has notable influence on the indirect energy consumption. To enable the comparison of the preservation methods, the analysis were based on barley production on a field area of 40 ha, which is quite typical farm size in Finland. The yield level was assumed to be 3,500 kg ha^{-1} at storage moisture content of 14% in wet basis (w.b.). Some storage losses occur in preservation due to decomposition of grain protein and carbohydrates (Palva et al., 2005). Storage dry matter losses used in the analysis were: drying and airtight storage 1%, acid preservation 0.5% and grain crimping 4% (Palva & Siljander-Rasi, 2003). These were taken into account in all calculations.

One remarkable difference in the alternative grain preservation methods compared to drying is the low content of vitamin E. Moisture and acidity during the storage increase the oxidation of vitamin E. While dried barley has E-vitamin content of 34 mg kg^{-1} (in dry matter), the high-moisture grains have only few milligrams (Palva & Siljander-Rasi, 2003; MTT 2013). This applies to all the examined methods. Although it does not have any influence on the energy consumption of preservation, it has to be noted and taken into account in the feeding.

Hot air drying

Moisture is the most important factor for the reproduction of microbes. The growth of fungi is possible when the air relative humidity (RH) is higher than 62%. When the RH exceeds 90%, also the growth of bacteria begins. (Ross et al., 1973, ref. Loewer et al., 1994) When the grain is stored, the humidity of air between the grain particles settles to equilibrium with the grain. The equilibrium moisture of grain can be calculated by Eq. (1) (Pfost 1976, ref. Pabis et al., 1998):

$$M_{eq} = E - Fln[-(T + C)lnRH] \tag{1}$$

where: M_{eq} is grain equilibrium moisture, decimal (dry basis, d.b.); E, F, C are grain dependent coefficients; T is temperature, *°C* and *RH* is relative humidity, decimal.

For example for barley, the air relative humidity of 62% equals to equilibrium moisture of about 12% (w.b.) in temperature of 20°C. In Finnish climate conditions the grain moisture of 14% has been considered to be sufficiently low for long term storage (Lötjönen & Pentti, 2005). This does not mean that the microbial activity in the grain would have stopped completely, but it has become slow enough to avoid the spoilage of the grain.

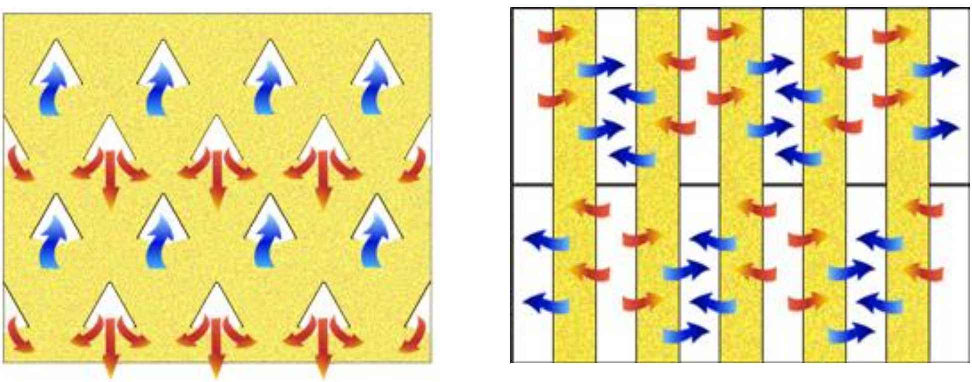

Figure 1. Cross-section of one possible duct configuration for mixed flow drying cell (on the left) and cross flow drying cell (on the right).

Hot air drying can be conducted by very many different techniques. In Finland the dominant dryer type is recirculating batch dryer, where the grain batch is circulated in the drying silo until it is dry. The advantages of this dryer type, compared to the continuous flow dryers, are the ability to dry also very moist grain, as well as even drying due to mixing of the grain and tempering that occurs in the storage space above the drying section. The drying section of the dryer usually consists of several drying cells, which use cross-flow or mixed flow design (Fig. 1).

Energy needed for drying is usually obtained from light fuel oil and carried into the grain by air. Water enthalpy of vaporization is ca. 2.3 MJ kg^{-1}, and this is thus the minimum amount of energy needed to evaporate 1 kg of water. In practice there are always some heat losses caused by unsaturated dryer exhaust air and heat convection and radiation through the dryer structures. Therefore the energy consumption measured from practical grain dryers varies between 4 to 8 MJ kg^{-1} [water], depending on dryer type and design (Peltola, 1985; Nellist, 1987; Suomi et al., 2003). In this paper an average value of 6 MJ kg^{-1} was used as base for calculations.

The amount of evaporated water can be calculated from the average harvest moisture and the storage moisture. The average harvest moisture of all grains in Finland between years 1999–2007 was 20.5% (w.b.) (Sieviläinen, 2008). The storage moisture content of 14% (w.b.) was used in calculations. These figures correspond to 25.8% and 16.3% in dry basis, respectively. The amount of evaporated water can thus be calculated by Eq. (2):

$$m_w = m_d(w_w - w_d) \tag{2}$$

where: m_w is the mass of evaporated water, kg; m_d is the mass of grain dry matter, kg; w_w is the harvest moisture (d.b.) decimal; and w_d is the storage moisture (d.b.), decimal.

When specific energy consumption and the mass of evaporated water are known, the heat energy consumption of drying can be calculated. With the figures given above, this equals to 576 kJ per one kg of grain dry matter. In addition to heat energy, dryer consumes also electricity and indirect energy via building and manufacturing the structures and the dryer machinery. The amount of electric energy is relatively small, ca. 5–8% of total direct energy consumption (Peltola, 1992). The figure used in calculations was 7%., which equals to 43.4 kJ kg^{-1} [grain DM]. The indirect energy is much more complex to calculate, as there is lack of information about the energy inputs, and the size, utilization rate and lifetime of facilities have a strong influence on the results. Mikkola et al. (2010) suggested energy consumption of 18.8 GJ per year for constructing, repair and maintenance of grain dryer building and machinery for 45 ha farm. The assumed lifetime of the dryer was 25 years. With the average yield level of 3,500 kg ha^{-1} (at storage moisture), this equals to 158 kJ kg^{-1} [grain DM].

Airtight storage

Airtight grain preservation is based on gas proof storage conditions. When the gas exchange between the grain and the environment is prevented, the respiration of the grain and the microbial activity consume the existing oxygen quickly (Loewer et al., 1994). When all of the oxygen has been drained, the growth of fungi and aerobic bacteria is suppressed. The microbiological activity does not stop completely, as for example yeasts grow in anaerobic conditions, but they are not harmful in feeding. (Klemola et al., 1994) Some lactic acid fermentation may also occur if the grain moisture is relatively high. This lowers the pH of the grain mass and thus suppresses the microbe activity. The effect of the fermentation is not, however, significant until the grain moisture content is ~35% or more (Loewer et al., 1994, Palva et al., 2005).

Airtight preservation does not have any significant influence on the chemical composition of the grain, and it is hence a suitable feed option for all essential production animals. After the grain is unloaded from the storage, the conventional feeding systems, designed for dried grain, can be used. The quality of the grain will also remain good until the next harvest season if the preservation system is managed properly (Siljander-Rasi et al., 2000; Perttilä et al., 2001).

The most widely used technical solution for airtight grain preservation is airtight steel silo, which can be galvanized, stainless or glass-lined steel. Apart from very small farms, the steel silo is the only realistic option for this preservation method. (Palva & Siljander-Rasi, 2003) The grain silo is usually filled by a pneumatic conveyor (Klemola et al., 1994). This is virtually the only direct energy input in this preservation method. Also a bucket elevator can be used. It has lower energy requirement, but it is more expensive. Additionally, the pneumatic conveyor is more flexible as it can serve several silos on the farm.

The information about grain moisture is needed to calculate the energy consumption of filling the silo, as it affects the mass that has to be moved, as well as the indirect energy input according to silo capacity. In Finnish conditions the upper limit to the grain moisture is probably set by the unloading technology, since high moisture may cause the grain to freeze in the silo in wintertime. In Swedish studies, the maximum grain moisture of 28–30% (w.b.) has been suggested for airtight storage (Granö, 1990). According to Siljander-Rasi et al., (2000), the optimal grain moisture for airtight preservation is 20–25% (w.b.). In the analysis of the present paper an average value of 22.5% was used. The mass of the 3,500 kg ha^{-1} grain yield is hence, converted to correspond this moisture, 3,884 kg ha^{-1}. According to Pokki (1982), the power demand of pneumatic conveyor was in average 5.5 kW with the lifting height of 10 m and capacity of 2.5 t h^{-1}. Conveyors used nowadays have higher capacities, but the efficiency, however, has assumingly remained at the same level. The energy requirement to fill the silo can thus be calculated from the values presented above, and it results as 10.3 kJ kg^{-1} [grain DM].

Mikkola et al. (2010) suggested indirect energy consumption of 18.5 GJ per year for constructing and maintenance of an airtight silo with capacity of 194 m^3 and lifetime of 25 years. The silo needed in this analysis for the given field area and yield was 259 m^3, with the barley bulk density of 600 kg m^{-3}. The figure from Mikkola et al. (2010) can thus be scaled to this size, with the result of an annual indirect energy consumption of 24.7 GJ. This equals to 207 kJ kg^{-1} [grain DM].

Acid preservation

In acid preservation method the whole grains are treated with organic acid based additive. The aim of the treatment is to terminate all the vital functions of the grain, as well as the microbiological activity. The acid preservative absorbs quickly to the grain and suppresses the microbiological activity within one day. Treatment lowers the pH of the grain, but the preservation effect is actually based on the amount of undissociated acid. The most suitable acid for whole grain preservation is propionic acid. Also acetic acid and formic acid have been used in the past, but due to mycotoxin findings in the preserved grain, they have since been abandoned for this purpose. (Palva & Siljander-Rasi, 2003) As the airtight preservation, the acid preservation does not alter the chemical composition of the grain significantly, and it can therefore be used as feed for all essential production animals. Limitations are rather set by the feeding systems, which are usually designed for dried grain (Palva et al., 2005).

Acid preservation is a very simple and straightforward method: the grain is dumped from tractor trailer into a screw conveyor, where the acid is dosed into the grain. The conveyor mixes the acid to the grain effectively. To achieve adequately even mixing, it is recommended that the conveyor is at least three meters long. Wide variety of storage systems can be used for acid-preserved grain, since no coverage or compressing is necessary. However, the surfaces of the storage facilities must be able to tolerate the corrosiveness of the acid. Furthermore, the dosage of the acid is crucial for the successful preservation, and it is strongly influenced by the moisture of the grain. Therefore a great care must be taken in the dosage and the dosage instructions of the additive must me followed. If the preservation is managed correctly, the grain will keep well until the next harvest (Palva et al., 2005).

The largest energy input in acid preservation is the indirect energy of the additive. The screw conveyor consumes also electric energy, but the energy requirement is assumingly so small that it may be disregarded. According to Ekman & Börjesson, (2011), the energy input in manufacturing propionic acid is ca. 19 MJ kg^{-1}. The propionic acid concentration in the additives is high, for example one commercial product contains 99.5% of propionic acid (Agrimarket 2013). As the dosage depends on the grain moisture, the moisture level must be determined for the calculations. Basically the grain should be harvested as dry as possible to reduce the amount of required additive. However, one of the benefits of alternative preservation systems is the possibility to earlier harvest or cultivation of later varieties. Therefore the same moisture content as with the airtight storage (22.5% w.b.) was used. The dosage of the acid for grain in this moisture is 8.5 l t^{-1}, and the indirect energy input of the acid equals to 206 kJ kg^{-1} [grain DM].

The indirect energy input of the storage facilities is, again, more complicated to calculate, as the acid preservation enables several storage possibilities. One approach is to use old, existing storage facilities. In this case no indirect energy of storage is allocated to the preservation. Other option is to use new silage bunker. Both of these options were analyzed. For the bunker, only the energy input for manufacturing the concrete was taken into account. With the volume of 259 m^3, element thickness of 15 cm, lifetime of 25 years and concrete manufacturing energy of 2.88 GJ m^{-3} (Hammond & Jones, 2011), the indirect energy input of the bunker was 25.3 kJ kg^{-1} [grain DM] for the given field area and yield level.

Very similar method to acid preservation is urea preservation. Urea is applied to the grain as water solution similarly to acid preservation. Microbial enzymes in the grain decompose the urea into carbon dioxide and ammonia, which creates the preservation effect. Urea-preserved grain is suitable feed for ruminants (Klemola et al., 1994). Urea preservation is not further discussed in this paper.

Grain crimping

Principle of grain crimping is similar to silage preservation. It is based on the lactic acid fermentation in anaerobic conditions. When the grain is compressed to high density and covered by plastic or some other air tight material, the grain respiration and microbial activity deplete the existing oxygen rapidly. In anaerobic conditions lactic acid bacteria becomes active, producing fermentation acids (mainly lactic acid) that lower the pH of the grain mass. When the pH has decreased to about 4, the microbiological activity virtually stops. The process is further contributed by adding acid to grain to initially lower the pH, or sugars to enhance the lactic acid bacteria activity. Crimping of the grain contributes the compaction and increases the surface area on which the bacteria can survive and function.

In addition to absence of oxygen, sufficient moisture is required for the lactic acid bacteria to function effectively. Optimal grain moisture for grain crimping preservation is hence 35–45% (w.b.), which means that the grain is harvested when it has started ripening (Bern, 1998, Klemola et al., 1994, Palva et al., 2005). Successful trials have also been conducted with considerably dryer grain, with moisture content of 16–25% (w.b.). In this case the preservation effect is based mainly on absence of oxygen rather than lactic acid fermentation. Additionally, different kinds of preservatives are required with dryer grain to avoid the growth of moulds. This method is not further discussed in this paper.

Crimped grain is basically suitable feed for all farm animal species. Equal or even better nutritional value of crimped grain has been observed in feeding trials compared to the dried grain (Siljander-Rasi et al., 2000, Perttilä et al., 2001, Jaakkola et al., 2004). Limitations are set, again, rather by the feeding technology than the nutritive value. Problems occur especially in automated feeding system in poultry and pork production (Siljander-Rasi et al., 2000). On the other hand, crimped grain is technically very well suited for the increasingly popular total mixed ration (TMR) method in cattle feeding (Jaakkola et al., 2004).

The additives on crimped grain are the same as used in silage preservation, for example commonly used formic acid based products. Recommended dosage is 3 l per ton of moist grain, when the grain moisture is 35–45% (w.b.) and the concentration of formic acid in additive is ca. 80% in mass basis. If the grain is dryer than this, the dosage must be increased. However, it is advisable to preserve the grain at around 40% moisture to ensure proper compaction and fermentation. If the grain is too dry, some water can also be added during the crimping. (Klemola et al., 1994, Palva et al., 2005) Grain moisture of 40% was used in the present analyses. The yield of 3,500 kg at 14% moisture equals then 5,017 kg at 40% (w.b.). According Grönroos & Voutilainen, (2001), the energy input to produce one liter of AIV 2+ -additive is 3.68 MJ, which corresponds to 19.1 kJ kg^{-1} [grain DM]. When molasses is used as preservative, the needed amount is 10 kg sugar per ton of moist grain (Klemola et al., 1994, Palva et al., 2005). The energy input of molasses was calculated by the energy consumption in sugar beet production and processing, and the shares and energy contents of the process products (Mikkola & Ahokas, 2009, Nurmi, 2014). The received figures were 2.84 MJ kg^{-1} [molasses] and 69 kJ kg^{-1} [grain DM]. The actual energy content of molasses is useful energy for animals, and it was therefore ignored in the analysis.

Crimping is conducted by a crimper machine (or mill), which breaks and flattens the whole grains. Energy consumption can be estimated by the power requirement and throughput of the crimper machine. According to Aimo Kortteen konepaja Oy, (2014), the power requirement is at minimum ca. 2 kW per t h^{-1} of throughput. The crimper machines are usually powered by a tractor. If the tractor runs at efficiency of 30%, the fuel power requirement is hence 6.67 kW. This equals to 41.6 kJ kg^{-1} [grain DM].

Crimped grain can be stored in a clamp, silage bunker, plastic tube or airtight silo. If an airtight silo is used, it must be glass-lined to withstand the low pH of the grain. Storage method has a strong influence on the indirect energy inputs. The lowest energy consumption can be achieved with a simple clamp, but this was not examined here due to the higher risk of storage losses. The indirect energy inputs for silage bunker and airtight silo were already presented in previous chapters, and the same principles were used with crimped grain. The storage space requirement was updated to correspond the larger grain mass caused by the higher moisture. The received figures were 49 kJ kg^{-1} [grain DM] for the silage bunker and 265 kJ kg^{-1} [grain DM] for the airtight silo.

When the crimped grain is stored in a plastic tube, the indirect energy input is caused by the plastic material. According to Granvik (2014), the energy consumption in manufacturing the plastic film for the tube is 5.4 MJ kg^{-1}. The diameter of the tube is 1.52 m, weight of one m^2 of the film is 0.2 kg and the volume of grain mass at 40% moisture (w.b.) is 334 m^3, which equal to plastic energy input of 2.73 kJ kg^{-1} [grain DM] with the given yield and field area. This does not include the energy content of plastic. If the used plastic will be utilized as energy by combustion, the energy content will be recovered and there is no need to allocate it to grain preservation. If the plastic is disposed as landfill waste, the energy content will be lost, and it should be allocated to grain preservation. The lower heating value (LHV) of plastic is similar to that of oil, ca. 43 MJ kg^{-1}, and together with the energy for manufacturing the plastic, this equals to 63.4 kJ kg^{-1} [grain DM].

Potential energy savings in Finnish agriculture

As stated in the introduction chapter, the amount of the grain used directly at farms was ca. 1.3 billion kg in Finland during the season 2012–2013. While the share of drying as preservation method was 85–90%, the amount of grain preserved by other methods is in maximum 15% of the total yield of 3.7 billion kg, which equals to 0.56 billion kg. It is most likely that the alternative preservation methods, which are already in use, are applied on livestock farms. Therefore it can be assumed that the amount of grain that is preserved by drying, but still used as feed directly at farm is 1.3 - 0.56 = 0.74 billion kg. The amount of the achievable energy savings can thus be estimated by the difference in the energy consumption, when preservation of this 0.74 billion kg is done by the alternative methods, instead of drying. The estimation was done by assuming that equal shares of airtight preservation, acid preservation and grain crimping were used to preserve this grain mass.

RESULTS AND DISCUSSION

Energy consumption of the examined grain preservation methods is presented in Table 1 and Fig. 2. Hot air drying has overwhelmingly high energy consumption compared to most of the other methods, which is obvious as large amount of oil is used as heat energy source. Also the indirect energy embodied in structures is high in drying as well as in airtight preservation, since manufacturing of large metal structures consumes lot of energy. In practice the dryers are often bigger than the one used in the analysis, which further increases the indirect energy consumption. Airtight preservation has comparable indirect energy consumption with drying, but with the minor direct energy consumption, the total energy consumption remains considerably lower.

Table 1. Total energy consumptions in kJ per 1 kg of grain dry matter

Preservation method	E, kJ kg^{-1} [grain DM]
Hot air drying	777
Airtight preservation	217
Acid preservation, existing storage	206
Acid preservation, new silage bunker	232
Crimped grain, acid additive, silage bunker	95
Crimped grain, acid additive, airtight silo	350
Crimped grain, acid additive, tube, used plastic for energy	63
Crimped grain, acid additive, tube, used plastic for landfill waste	124
Crimped grain, molasses additive, silage bunker	147
Crimped grain, molasses additive, airtight silo	402
Crimped grain, molasses additive, tube, used plastic for energy	116
Crimped grain, molasses additive, tube, used plastic for landfill waste	176

In acid preservation method the high embodied energy in the acid together with relatively high dosage cause a high indirect energy input. The examined storage systems with acid preservation were old, existing building, when no indirect energy was allocated to the preservation, and a new silage bunker. The storage method does not have a significant effect on the energy consumption, as the lifetime of the silage bunker is relatively long, 25 years. Only the energy embodied to the concrete was examined here, so the total energy input for building the silo would be somewhat larger, but it would not have any crucial effect on the results.

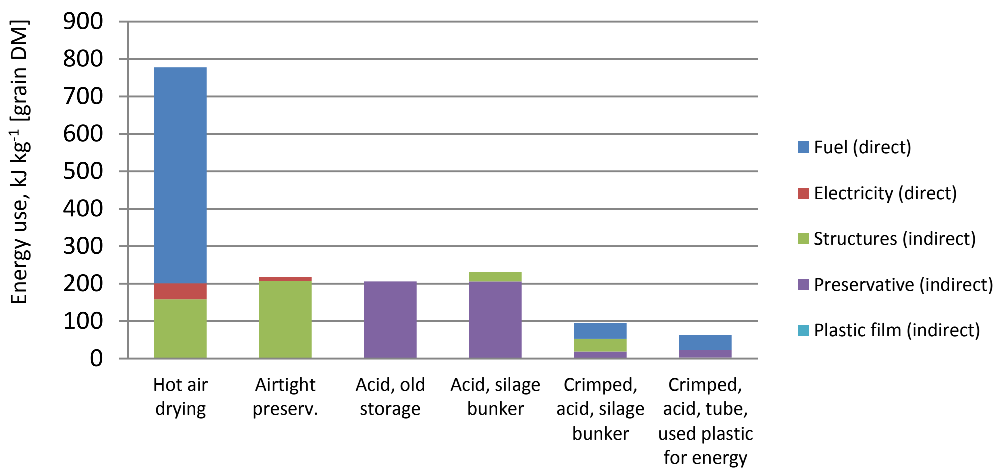

Figure 2. Energy consumption of the examined grain preservation methods.

Clearly the lowest energy consumption was achieved by grain crimping. In the best case, the energy use was only 63 kJ per 1 kg of grain dry matter, and the largest energy input was the tractor fuel for crimping. However, it was also strongly influenced by the storage method, the used additive, and in case of tube storage, the disposal of the used plastic (Fig. 3). When the crimped grain was stored in an airtight silo, the large indirect energy inputs caused high energy consumption. It was in fact higher than in airtight preservation because of the bigger storage space requirement due to considerably higher grain moisture. When molasses was used as preservative, the energy use was larger than with acid due to the higher application rate. The energy consumption of crimping was highest when molasses additive and airtight silo were used, but even then it was about half compared to that of drying.

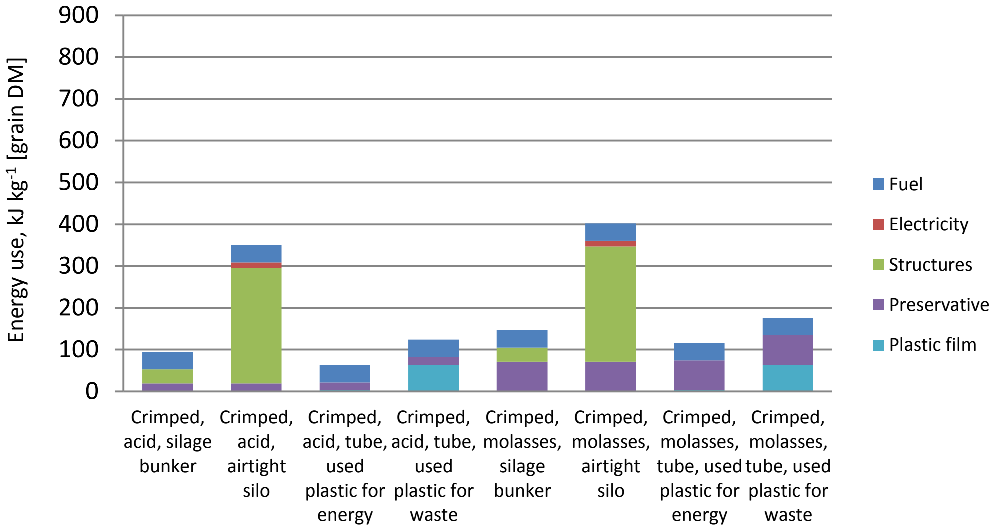

Figure 3. Energy consumption of different storage systems and additives in grain crimping preservation.

In tube storage the crucial factor is the disposal of the used plastic. If the waste plastic is used as energy, either on farm or in a power plant, only the plastic production energy is allocated to grain preservation. In this case the energy input is small, and it is not even visible in Figs 2 and 3. If the plastic is disposed as landfill waste, the energy content will be lost, and it must be thereby allocated to grain preservation. In this case, the energy input from the plastic is of the same magnitude with the crimper machine fuel consumption.

The potential energy savings of by the alternative grain preservation methods in Finnish agriculture were estimated by the received results. Equal shares of alternative preservation methods were used to preserve the 0.74 billion kg of feed grain. Storage method for acid preservation and crimped grain was silage bunker and acid was used as preservative in grain crimping. The potential energy saving with these figures was 106 GWh, which equals ca. 15% of all grain preservation current energy inputs. In comparison, this corresponds ca. 1% of the total direct energy use in agriculture (10 TWh) and ca. 3% of the fuel oil use (3.5 TWh) (Tike 2012).

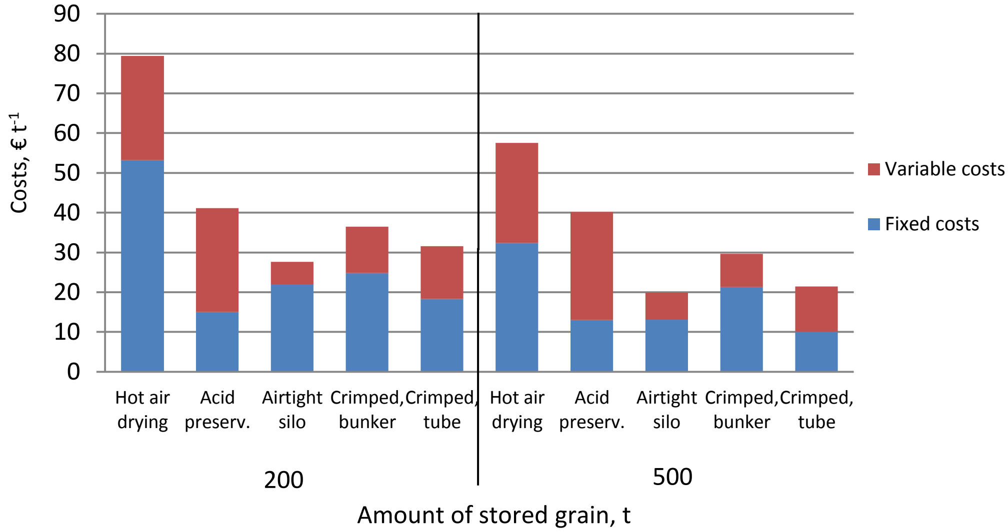

Figure 4. Costs of different preservation methods without storage losses (Palva, 2008).

For a farmer, the energy consumption is rather irrelevant compared to costs of the preservation system. Result of one model cost calculation is presented in Fig. 4. The costs were calculated for storage capacities of 200 and 500 tons. When the amount of preserved grain increased, the fixed costs decreased, while variable costs remained at the same level. It must be noted that similar behaviour occurs in energy inputs; an increase in size results a decrease in indirect energy consumption, while direct energy inputs remain constant.

CONCLUSIONS

The present study indicates that significant energy savings can be achieved by using alternative methods for feed grain preservation. When a combination of airtight preservation, acid preservation and grain crimping is used with equal shares for preserving the grain that is used directly on farms, a total energy saving of ca. 15% can be achieved compared to the current situation. The most beneficial method considering energy consumption is grain crimping with formic acid as additive and silage bunker or plastic tube as storage. However, the storage system and used preservative have a high impact on the energy consumption of the method. The lowest production costs altogether were achieved by airtight preservation.

High moisture grain preservation methods demand management with certain degree of caution to avoid the storage failures. This may be one reason limiting the popularity of these methods. As the specialization and expertise in farming increase due to the ongoing structural change in agriculture, and energy prices rise at the same time, the interest towards the high moisture grain preservation is likely to increase.

In addition to energy savings, alternative systems posses several other advantages, such as lower costs and enhanced harvest season, which reduces workload peaks. They also enable earlier harvesting, which reduces the risk of yield losses, and cultivation of late varieties with higher yields.

Grain moisture concentration has a strong influence on energy consumption especially in drying and acid preservation. However, the storage systems are big investments and the farmer cannot change the selected system from year to year. Therefore the decisions must be based on the most probable situation. Since the grain moisture variation due to the weather conditions is most likely random, the historical average, which was also used in this analysis, can be used as basis for decision making. Airtight preservation is likely to be the most sensitive to the grain moisture variation of the examined methods, since there are few possibilities to adjust the preservation according to grain moisture.

All of the examined alternative grain preservation methods can be used for all farm animal species. The limitations are mainly set by the operation of the automated feeding systems. In addition, it should be noticed that airtight-preserved and crimped grain will be spoiled in few days after unloading from the storage, and especially poultry animals are sensitive to poor quality grain. However, among the studied alternatives a suitable option for different farm animal species can be found. There are no principal barriers for preserving all of the feed grain stored and used directly at the farm by some of these methods. As the problems, when they exist, are found mainly in the feeding technology, there is no doubt that they could and will be solved if the economical gap between drying and other options grows large enough.

ACKNOWLEDGEMENTS. This study was funded by the foundation of Marjatta and Eino Kolli.

REFERENCES

Agrimarket 2013. Propion, kostean rehuviljan jyväsäilöntäaine. Package label. *http://www.agrimarket.fi/Maatalous_ja_Elaimet/Maatalouskemikaalit/Sailontaaineet/propion-30-kg/*. Accessed 29.1.2014.

Bern, C.J. 1998. Preserving the Iowa corn crop: energy use and CO_2 release. *Applied engineering in agriculture* **14**(3), 293–299.

Ekman, A. & Börjesson, P. 2011. Environmental assessment of propionic acid produced in an agricultural biomass-based biorefinery system. *Journal of Cleaner Production* **19**, 1257–1265.

European Union 2012. Directive 2012/27/EU. *Official journal of the European Union. http://eur-lex.europa.eu/LexUriServ/LexUriServ.do?uri=OJ:L:2012:315:0001:0056:EN:PDF*. Accessed 21.5.2013.

Granvik, T. 2014. Energy consumption in plastic film production. Raniplast Oy. Personal communication, 1.2.2014.

Granö, U-P. 1990. Våtlagring och hantering av fuktig spannmål. *Röbäcksdalen meddelar* **1990:7**. 49 p.

Grönroos, J. & Voutilainen, P. 2001. *Maatalouden tuotantotavat ja ympäristö*. Helsinki: Suomen ympäristökeskus. 62 p.

Hammond, G. & Jones, G. 2011. Inventory of carbon & energy (ICE). University of Bath, UK. *http://www.circularecology.com/ice-database.html#.UvCLyfvcArA*. Accessed 30.1.2014.

Jaakkola, S., Saarisalo, E., Kangasniemi, R., Sariola, J. & Khalili, H. 2004. Murskeviljan käyttö lypsylehmien ruokinnassa. Conference paper, Maataloustieteen päivät 2004. *http://www.smts.fi/MTP%20julkaisu%202004/esi04/ti52.pdf*. Accessed 30.1.2014.

Klemola, E., Järvenpää, M. & Peltola, A. 1994. Viljansäilöntäopas. *Työtehoseuran maataloustiedote* **441**. 15 p.

Loewer, O.J., Bridges, T.C. & Bucklin, R.A. 1994. *On-farm drying and storage systems*. ASAE publication 9. 560 p.

Lötjönen, T. & Pentti, S. 2005. Kuivausteknologia. In: Palva, R., Kirkkari, A.-M. & Teräväinen, H. (ed.). Viljasadon käsittely ja käyttö. *ProAgria Maaseutukeskusten Liitto, Tieto tuottamaan* **108**, 34–51.

Mikkola, H. & Ahokas, J. 2009. Energy ratios in Finnish agricultural production. *Agricultural and food science* **18**, 332–346.

Mikkola, H., Pahkala, K. & Ahokas, J. 2010. Energy consumption in barley and turnip rape cultivation for bioethanol and biodiesel production. *Biomass and bioenergy* **35**, 505–515.

MTT 2013. Vitamin concentration of feeds. MTT Agrifood research Finland. https://portal.mtt.fi/portal/pls/portal/rehu_mtt.REHU_MTT_VITAMIINI_PACK.report?p_kieli=1. Accessed 28.1.2014.

Aimo Kortteen konepaja Oy 2014. Murska crimper machines, product information. *http://www.murskabiopacker.fi/fin/1000-valssimylly*. Accessed 30.1.2014.

Nellist, M.E. 1987. Modelling the performance of a cross-flow grain drier. *Journal of Agricultural Engineering Research* 37, 43–57

Nurmi, H. 2014. Energy use in molasses production. Sucros Oy. Personal communication, 6.2.2014.

Pabis, S., Jayas, D.S. & Cenkowski, S. 1998. *Grain drying. Theory and practice*. New York: John Wiley & Sons, Inc. 303 p.

Palva, R. 2008. Costs of different grain preservation methods. TTS research. Personal communication, 3.2.2014.

Palva, R. & Siljander-Rasi, H. 2003. Kuivaamattoman viljan käyttö lihasikoja kasvattavalla tilalla. *Työtehoseuran julkaisuja* **388**. 51 p.

Palva, R., Jaakkola, S., Siljander-Rasi, H., Valaja, J., Root, T. & Peltonen, S. 2005. Viljan tuoresäilöntä. In: Palva, R., Kirkkari, A.-M. & Teräväinen, H. (ed.). Viljasadon käsittely ja käyttö. *ProAgria Maaseutukeskusten Liitto, Tieto tuottamaan* **108**, 55–66.

Peltola, A. 1985. Energiansäästö viljan lämminilmakuivauksessa. In Laitinen, A., Orava, R., Peltola, A., Salasmaa, O. & Ylönen, A-L (Eds.), Energiansäästö viljankorjuussa. *Työtehoseuran julkaisuja* **272**, 121 p.

Peltola, A. 1992. Viljan lämminilmakuivauksen mallintaminen energiankulutuksen perusteella taulukkolaskimella. *Työtehoseuran maataloustiedote* **412**. 7 p.

Perttilä, S., Valaja, J., Partanen, K., Jalava, T., Kiiskinen, T. & Palander, S. 2001. Effects of preservation method and β-glucanase supplementation on ileal amino acid digestibility and feeding value of barley on poultry. *British poultry science* **42**, 218–229.

Pokki, J. 1982. Rehuviljan ilmatiivis varastointi. *Työtehoseuran julkaisuja* **240**. 75 p.

Sieviläinen, E. 2008. Viljan laatuseuranta. [Available at The Finnish Food Safety Authority – EVIRA]. (In Finnish).

Siljander-Rasi, H., Valaja, J., Jaakkola, S. & Perttilä, S. 2000. Tuoresäilötty ohra sikojen ja siipikarjan rehuna. *Työtehoseuran maataloustiedote* **518**. 6 p.

Suomi, P., Lötjonen, T., Mikkola, H., Kirkkari, A.-M. & Palva, R. 2003. Viljan korjuu ja varastointi laajenevalla viljatilalla. *Maa- ja elintarviketalous*, **31**, 100 p.

Tike 2012. Irrigation and energy (Kastelu avomaalla ja energia). Information Centre of the Ministry of Agriculture and Forestry, official statistics of Finland. 17 pp. *http://www.maataloustilastot.fi/e-lehti-kastelu-energia/*. Accessed 30.1.2014.

Tike 2013a. Viljavuosi 2012–2013. Information Centre of the Ministry of Agriculture and Forestry, official statistics of Finland. *http://www.maataloustilastot.fi/e-lehti-viljavuosi-2012-2013/index.html*. Accessed 10.12.2013. 14 p.

Tike 2013b. Maatilojen sadonkäyttö 2012–2013. Information Centre of the Ministry of Agriculture and Forestry, official statistics of Finland. *http://www.maataloustilastot.fi/maatilojen-sadonkaytto*. Accessed 16.1.2014. 14 p.

Agronomy Research **12**(1), 95–100, 2014

Adaptive tillage systems

M.H. Jørgensen

Department of Mechanical and Manufacturing Engineering, Aalborg University, 16 Fibigerstraede, DK-9220 Aalborg, Denmark; e-mail: MHJ@m-tech.aau.dk

Acstract. This paper addresses the perspective of developing autonomous tillage robots. The aim is to analyze the possible perspectives in site specific tillage performed by autonomous units, including the additional effects that can be achieved by self-propelled systems in contrast to the classic tractor-tool units.

In general, soil tillage can be defined with two different main purposes. One is the close-to-surface seed bed preparation for optimal conditions regarding seed germination. The deeper soil tillage normally involves other types of implements such as the chisel cultivator or the plough. For this operation, the aim is more complex, including mixing soil and organic residues, weed control and losing the soil structure.

Site specific tillage has great potential. The result of the tillage operation can be improved dramatically when the intensity of the operation is adapted to the local needs. The autonomic unit will by nature be a light weight and less intensitive design compared to the traditional tractor-tool unit. This means that soil tillage by autonomic implements is also the solution for reducing soil compaction. In fact, site specific tillage has great potential gains in addition to the optimized quality of the operation; substantial energy savings can be achieved, negative soil compaction and erosion risks can be reduced, and in general, the reduced and the less intensive soil tillage will support a naturally rich micro biology life, characterized by the occurrence of worms etc.

Key words: Adaptive soil tillage, agricultural engineering, implements, autonomous systems, adaptive systems, sensors.

INTRODUCTION

Overall, the purpose of the different tillage operations is to obtain the best possible conditions for seed germination, root development and crop growth. An important element in this is the weed control that which is closely linked to the tillage system; this also applies to biological life and soil structure. In the ideal situation, the tillage system helps to maintain good soil fertility. From a fundamental perspective, the aim is to ensure sufficient supply of oxygen to the roots and to the microbial life. In the ideal situation the tillage also contributes to stabilize a fertile soil structure including a pore structure that ensures the availability of water around plant roots, and allows the drainage of excess water (Andersen et al., 2013). In the process of optimizing the tillage tool system it is very important to keep in mind these side effects, which influence soil fertility. Good soil fertility leads to improved absorption of nutrients, better root development, and a faster and better turnover of biological residues. This again helps to maintain a good soil structure and fertility (Carter, 1992). For a given soil texture, the healthy fertility itself enables easier tillage operation to obtain the right conditions.

In an overall description, the porosity must be composed of small pores that, by capillary effect, can raise the water level to an area in which the plant roots can absorb this. Medium pores that enable the water drainage, and macro pores enable the oxygen availability in the soil (Andersen et al., 2013). Tillage operations disturb this structure, which must then regenerate after the operation. Due to this, light treatments are preferred. High compressive loads, primarily from wheels in the actual operation or other operations in the field, can cause the capillary pores to collapse (Alakukku, 1999) and to become so small in diameter that the roots cannot absorb the water, which will then be fixed in the soil (Glab, 2007). Furthermore, the access of the oxygen to the roots and the microbiological organisms is reduced by the collapse of the bigger pores. The top soil layer is also sensitive to tillage intensity. Too high intensity or a non-matching method causes soil aggregates in the soil layer to be broken into small particles (Atkinson, 2009). The effect is that soil particles become closely compressed, resulting in a dense surface with limited passage of oxygen and water sensitive to erosion caused by wind or water.

Different implement types each have their own positive or negative effect on soil tillage. Classic spring tines used for top soil tilling loosen and separate the aggregates by tension forces, adding a minimal glazing and crushing effect to the soil aggregates. Stiff tines or tines on rotor/ pendulum harrows have a more precise working depth, and their intensity can be controlled by the angle of operation in relation to the horizontal surface. However, the operation of these tines is more sensitive to the performance of negative effects such as the kneading and crushing of soil aggregates in the zones around the working implement in which compaction occurs. The sensitivity to these negative effects is highly controlled by the moisture content and the texture of the soil. The deeper tillage operations are traditionally performed by chisel plowing or mouldboard ploughing. These deeper operations are always effective in loosening the soil and mixing surface matters and organic residues into the soil. These operations always result in both positive and negative effects for the soil. However, a soil characterized by healthy fertility regenerates faster from these negative effects than a soil which is less healthy.

Today’s traditional tillage tools and systems are designed to perform an acceptable result over the entire area of a field. At a closer look, the soil conditions vary substantially across the field. Due to this, the intensity of the operation is designed to handle the most challenging parts of the field, which means that large areas are overworked. Consequently, much of the area is also overexposed to the negative effects of the tillage operation.

It seems that the potential for obtaining a better result is quite large, and much energy may be saved if the tillage intensity is locally adapted to the actual soil conditions. The concept of and potential for site specific farming has now been analyzed and developed over more than two decades. One might wonder why so little focus has been directed towards soil tillage operations.

Over the past decades, technical research in agricultural engineering has been focused on finding systems that could provide better results through considering synergies between the effect of tooling and natural biological effects. The major systems analyzed were ‘moldboard ploughing/ chisel ploughing’; ‘reduced tillage/

mulch tillage' and 'no tillage'. In the no-tillage system, the only operation in the soil is sowing. Moldboard ploughing is known as the classic way of operating the soil. Reduced tillage covers a wide range of technical systems in between these two extremes. Results generally show that there are big potential gains in reducing tillage intensity, such as energy savings, improvements in microbiological life, stabilization of soil aggregates and pore structure (Tebrugge & During, 1999). The main problem for the systems tested so far is the emergence of a compact zone of the soil under the depth of tillage. Reduced no turning tillage also causes another challenge in controlling weeds, as this is one of the main tasks of traditional tillage operations.

As evidenced in the above, a very complex relationship exists between tillage systems, soil microbial activity and soil structure. Introducing non-tractor-powered implements expands this complexity by a new dimension of possibilities. The following analysis is based on a design in which the primary tillage operations which are deeper than seeding depth are carried out with a tractor-powered system based on the use of a moldboard plow, and the seed bed preparation and seeding is performed by an integrated autonomous implement. This is to maintain an overview, and to analyze opportunities in both tractor-powered systems and new integrated autonomous systems. The hypothesis is that substantial potential exists in both types of systems, and that the development will gradually show the change from the classic systems as they appear today to the fully integrated autonomous systems (Atkinson, 2007; Jørgensen, 2012).

Potentials and results of locally adapted soil tillage

The idea and potentials of reduced tillage operations have been investigated by research. Results show big potentials for the saving of energy. One aspect of this is ensuring that the operation is adapted to local condition. The moldboard plough constitutes one example; results show that focus on the correct adjustment of the implement to local conditions implies assumed energy savings of app. 20% in compared to average consumption (Guul-Simonsen et al., 2002). Investigations on reduced tillage systems and no tillage systems show potentials energy savings of up to 50% measured by fuel consumption. In the systems tested a big variation in yield was observed, showing an average net effect close to zero. The main problems for these systems are soil compaction due to traffic, and weed problems. Challenging these related problems in the design of the new technical systems there might result in a realistic savings potential in the range of 30 to 40%. It is well documented that reduced tillage and no tillage systems adapted to the soil and field conditions caused by biological residues and weed pressure can cause improvements in soil structure and porosity, soil aggregates and stability and microbiological activity in the soil. However, it has been difficult to set up general systems or descriptions generating yield increases of more than 5–10%. The expectation is that systems adapting to the local soil tillage will lead to a net reduction in fuel consumption of 30 to 40%, and that the yield will increase by 10% or more; more importantly, this increase will be stable, due to existing systems without big Fluctuation

Design of the autonomous robotic implement

Modern tractors support systems of integrated implement control. The commercial systems are described as Tractor-Implement-Automation (TIA/TA), Tractor Implement Management (TIM) etc. Literature shows operative examples of controlling a wagon, a baler and a fertilizer machine. This demonstrates that the system is ready and could be developed to control a moldboard plough, for instance. A simple way of defining optimal adjustment could be to define a small load on the lifting arms and on the rear land wheel. If the bearing load on these components is becoming too heavy, a substantial amount of energy will be spent on rolling resistance. The correct adjustment can be implemented by using the existing adjustment options. The angle of the chisel (foreshare) may enhance efficiency so that the force to keep the plow into the ground is adjusted to perform a stable operation. To ensure a good quality when using this system, it is still important that the overall orientation of the plow is correct. A measure to be used could be the side oriented force measured on the landside in the furrow. The actuator could be the top link arm. In addition to this process control, the plowing depth could be controlled according to the local need. A possibility here could be to set the max depth at 20 cm and the minimum at 10 to12 cm. The restriction on the minimum depth of ploughing is defined to ensure that the ground strips worked by the individual plough shares are effectively reversed, so that crop and plant residuals are effectively mixed into the soil and covered by a top layer of soil. The need for a larger ploughing depth could be determined by the tracking resistance of the plough as an indicator of the need for loosening the soil. For this to take place, the operator must define some reference numbers, as the correlation between these data relies on soil moisture, soil texture and other elements. To make it even more effective, an adjustable soil loosening tine could be mounted immediately behind the main share, so that the soil-loosening below ploughing depth can take place without lifting the soil in the ploughing zone. The assumption is that the fuel consumption for ploughing can be reduced substantially by introducing this type of adaptive plow design. Also, the effect of the plowing operation will be optimized so as to ensure the best conditions for the subsequent seed bed preparation. If the goal is to investigate the possibilities and perspectives for smaller autonomic tooling units, it is important to also analyze the possibility for optimizing the comparable tractor powered operation.

The process of seed bed preparation and seeding seems to fit quite well into the development of a fully autonomous integrated system. One immediate benefit from such a system is to get rid of the tractor driving in front of the implement, making compacted tracks in the wheel track that have to be treated separately afterwards. In the integrated implement, the bearing and traction systems must be designed to work over the full working with to distribute the load and designed such that it if possible contributes to the tillage process. After a slight positive compaction of the loose top layer, the seed bed has to be prepared so as to obtain the best possible aggregate structure possible on the basis of the soil texture and the actual local conditions. The properties of the seed bed have been analyzed by more research studies, among these (Atkinson, 2007), who analyze the possibility of predicting the properties of the seedbed for the purpose of predicting crop establishment. Input to the model are selected physical soil properties, and the intensity of the prior preparing tillage operation. It is a hard challenge to find or develop sensors that are able to collect the data needed for an online setup. A first approach here could be to use image analysis to analyze the micro-scale roughness of the soil surface as a measure of the size and distribution of aggregates before and after the tillage operation. The driver must also supply some reference data to make the system operate. The final seeding operation can be designed by the use of classic components. The assumption is that such an implement for integrated seed bed preparation and seeding is an example of a new implement that performs better than the comparable tractor-powered unit. This is due to more reasons: reduced energy consumption, quality improvements due to seed germination and crop growth, and also to the environmental impact of erosion and the need for subsequent pesticides, mostly herbicides.

RESULTS AND DISCUSSION

It is believed that the systems described for plowing and sowing are realistic, both from a technological and an economic perspective. The TIM/TIA systems have been commercially available for the past five years. As the manufactures of the implements takes the opportunity to benefit from these new solutions and designs, many different implements will be introduced to the market. Among these, new tooling systems for tillage operations will also emerge. It is realistic to assume that the autonomic unit be developed due to navigation, tracking and sensor/tooling systems. Here the obstruction is the safety aspect. One might wonder why free moving autonomic robots are allowed in industrial surroundings, but not in outdoor solutions. The safety aspect has not been a part of this paper. Also on this topic much research is being carried out. State of the art in this is that sensors and control systems are available, so that the challenge is to design the standards for such systems to obtain acceptance from the authorities.

CONCLUSION

The systems described are intended as examples of a possible next generation of agricultural tools. However, it seems very likely that these types of sensor controlled systems will enter the market. As the technology for the tractor-based systems are already commercially available in the market, it seems obvious that these systems will be the first to be introduced.

In the same way as self-propelled sprayers and other similar types of implements are taking over in the market, it is believed that the autonomous systems will also enter the market in the next few years.

REFERENCES

Alakukku, L. 1999. Subsoil compaction due to wheel traffic. *AGRICULTURAL AND FOOD SCIENCE IN FINLAND* **8** (4–5) SI 333–351.

Andersen, Mathias N., Munkholm, Lars J. & Nielsen, A. Lisbeth. 2013. 'Soil compaction limits root development, radiation-use efficiency and yield of three winter wheat (Triticum aestivum L.) cultivars' *ACTA AGRICULTURAE SCANDINAVICA SECTION B-SOIL AND PLANT SCIENCE* **63**(5), 409–419.

Atkinson, B.S. 2009. Effect of seedbed cultivation and soil macrostructure on the establishment of winter wheat. *Soil & Tillage research* **103**, 291–301

Atkinson, B.S. 2007. Using selected soil physical properties of seedbeds to predict crop establishment. *Soil & Tillage Research* **07**, 218–228.

Carter, M.R. 1992. Influence of reduced tillage systems on organic matter, microbial biomass, macro-aggregate distribution and structural stability of the surface soil in a humid climate. *Soil & Tillage Research* **23**, 361–372.

Glab, T. 2007. Effect of soil compaction on root system development and yields of tall fescue, Int. *Agrophysics* **21**, 233–239.
Guul-Simonsen, F., Jørgensen, Martin Heide, Have, H. & Håkansson, I. 2002. Studies on Plough Design and Ploughing Relevant to Conditions in Northern Europe. *Acta Agriculturae Scandinavica* **52**(2), 57–77.
Jørgensen, M.H. 2012 Agricultural Field Machinery for the future – from an engineering perspective. *Agronomic Research* **10**, 109–113.
Tebrugge, F. & During, R.A. 1999. Reducing tillage intensity – a review of results from a long-term study in Germany. *SOIL & TILLAGE RESEARCH* Volume: **53**(1), 15–28.

Agronomy Research **12**(1), 101–114, 2014

Development of an active boom controller for field sprayers

H. Karadöl[1] and S. Arslan[2]

[1]Kahramanmaraş Sütçü İmam University, Graduate School of Natural and Applied Sciences, 46100, Kahramanmaraş, Turkey
[2]Kahramanmaraş Sütçü İmam University, Biosystems Engineering Department, 46100 Kahramanmaraş, Turkey; Correspondence: sarslan@ksu.edu.tr

Abstract. The objective of this study was to develop an electronic control system to automatically control the boom of an agricultural sprayer. This paper addresses the electronic circuits and programmes used to accomplish active boom control under laboratory conditions. The boom sections were mounted on two sides of the frame in the laboratory and ultrasonic sensors were placed at the tips of boom sections. The sensors were tested at varying heights from 50 cm to 150 cm to obtain a calibration equation correlating voltage output of the sensors to the boom height. In the lab experiments, the calibration of the ultrasonic distance sensors could be done with a high coefficient of determination ($R^2 = 0.999$). Both PLC and PIC programming were used to develop the control programmes. The simulations of control programs were written in PIC C and Ladder programming languages and were executed on a computer. The sensor data were interpreted with the control programme loaded on the control device and automatically controlled the hydraulic valves and cylinders. The control program was programmed to neglect vertical oscillations with magnitudes less than 3.5 cm under laboratory conditions, which can be varied for field conditions. It was concluded that PLC and PIC circuits could work fast enough to sample analogue signals generated by the sensors at a forward speed of 6–8 km h^{-1} when used in real field conditions. Further research is ongoing to adapt the system to a field sprayer for field experiments.

Key words: Sensors, electro-hydraulic control, field sprayer, active boom control.

INTRODUCTION

One of the most important characteristics of agricultural field sprayers is the wide working width of these machines in field operations. Boom width may vary from 6 m to 48 m, even wider in some self-propelled sprayers. Big spray width increases field capacity however increased working width also causes more vibration on the boom sections, resulting in ossilation problems in longitudinal and vertical directions. The outcome of this is poorer chemical spray distribution on the target. To prevent from undesired ossilations of the boom sections, boom control systems are used. Such control systems are used to level the boom sections when vibration occurs due to uneven terrain conditions (Sartori et al., 2002; Güler et al., 2010; Okada & Mucheroni, 2012).

The mechanisms that control the boom height may be passive or actice type boom control systems. Passive systems try to overcome ossilations by using the dead weight of the boom using different types of parallelograms while active boom control systems utilize sensors to measure and control the height of boom sections (Deprez et al., 2003; Çilingir & Dursun, 2009).

Although there are many domestic sprayer manufacturers, field sprayers lack boom control systems in Turkey. The general purpose of this study was to develop a controller system that can be adapted to a field sprayer. The specific objectives of the study were to build a simple frame in a laboratory to simulate boom sections of a sprayer, which can be moved in vertical directions using hydraulic cylinders, to develop and simulate a PIC and a PLC program, and then control the boom sections of the laboratory frame.

MATERIALS AND METHODS

Laboratory test set up consists of three sections: a simple frame with so-called boom sections, hydraulic system and control system with a computer code. In the laboratory, two lightweight wooden bars were mounted on a simple frame in such a way that each bar could move up and down vertically (Fig. 1). Each bar representing a boom section was 1.2 m in length. An ultrasonic sensor was mounted at the tip of the each section. The bars were moved using two hydraulic cylinders that were controlled by electro hydraulic directional control valves (DCVs). Solenoids of the DCVs were connected to the PLC or PIC controller. A DC voltage source was used to supply power to the sensors and a hydraulic power pack was used to supply hydraulic power to the cylinders. The solenoids were powered with 24 V DC using the power suppy.

To develop a PIC controller, a microcontroller with 10 bit A/D converter (model 16f877) was used in the study. An ultrasonic distance sensor (LV Maxsonar EZ1) was used to measure and control the boom section heights. The sensors work with 5 V at 42 kHz, can detect distances within the range of 15–645 cm, and generate an output signal of 9.766 mV per 2.54 cm.

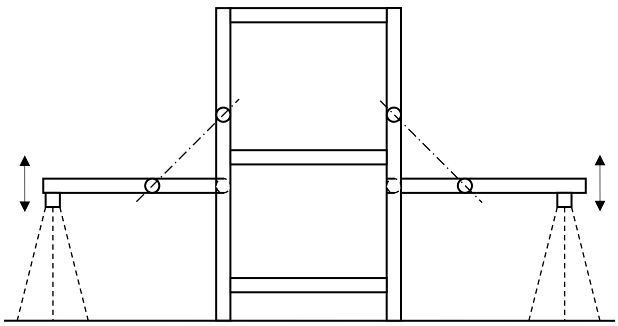

Figure 1. Schematic of the frame used in the laboratory experiments.

The instantaneous output signals of the ultrasonic sensors were measured using a digital multimeter that was connected to a laptop using the USB port. The multimeter was also used to plot the system response while the controllers were adjusting boom height after different disturbances were introduced between the sensors and the ground.

After the laboratory tests were completed to develop the controllers, some initial testing was done on a real field sprayer. A 600 L field sprayer with 10 m working width was used adapting the controllers to a real field sprayer. The tractor had a hdyraulic power suppy with a flow rate of 35 L min^{-1} and a pressure of 175 bars. The boom of the commercial sprayer was modified so that boom sections could be moved vertically with two hdyraulic cylinders at each side. The hydraulic system consisted of a pressure control valve, solenoid controlled directional control valves, hydraulic cylinders and flow control valves. The hydraulic system components used on the sprayer are the second set of system elements and are different from the ones in the laboratory. The flowrate and pressure of the hydraulic power pack were different from the tractor's specifications as well as the physical dimentions of the laboratory test set up and the actual sprayer. Therefore, the software programmes developed in the laboratory were changed accordingly before the programmes could be used on the tractor.

Both PLC and PIC control programs were developed for active boom control in the laboratory. First, a PLC program was written in Siemens S7-1200 Totally Integrated Automation Portal V10 Editor and was loaded on to the computer. Additionally, software was also developed in PIC C language. Simulations were done for both software programs before the programs were used on the test set up.

Sensor power was supplied by a regulator with 12 V DC and was reduced to 5 V DC by using a power regulator. Analog output of the sensor depends on the distance between the sensor and the target. The following equation was used to calculate the distance measured by the sensor:

$[(V_{cc}/512) = V_i]$

V_{cc} = Voltage

V_i = Voltage generated per 1 inch (2.54 cm)

V_{cc} = Generated voltage for a height of 80 cm

$[(5.0 \text{ V}/512) = 0.009766 \text{ V} = 9.766 \text{ mV}]$

$[(9.766 * 80) / 2.54] = 307.6 \text{ mV}]$

Control program should determine the height of each boom section and automatically adjust the height to the set value for each section independently. The system in the laboratory measures the distances and automatically intends to adjust the height of the boom to the set value by measuring the error, which was set to 3.5 cm. Therefore, the controllers were expected to detect any disturbances between the sensor and the ground and readjust the boom height so that the distance between the object and the sensor is at the set value within ±3.5 cm. The reference (set) height for the boom sections were 45 cm in the laboratory.

Closed loop control block diagram for this system is given in Fig. 2. Due to the disturbances, the boom height may be higher or lower than the desired set value. The ultrasonic sensors detect these disturbances, the controller calculates the error using the feedback signal, and activates the solenoid valves to maintain the preset height value when necessary.

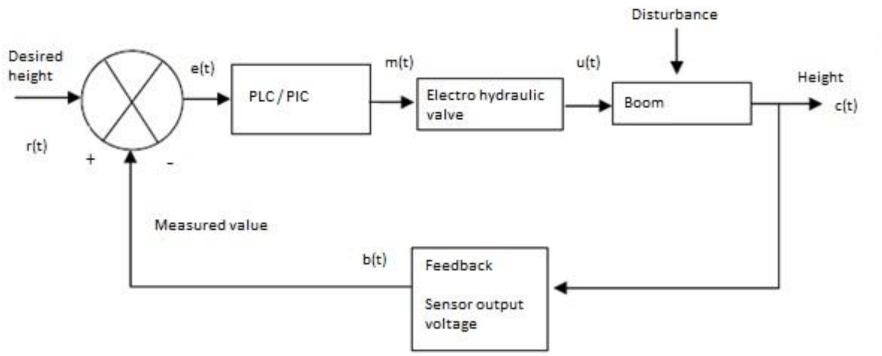

Figure 2. Closed loop control block diagram of the boom control system.

First program was written in PIC C programlamming language (Fig. 3). Analog output value of the sensors (0–5 V) was used as reference for A/D conversion. As a result, analog signals could be sampled with a resolution of 4.88 mV ($5V/2^{10}$). The sensors used in this study generates analog signal of 9.766 mV for 2.54 cm and hence each boom section could be theoretically controlled within 1.27 cm for a set value of 4.88 mV.

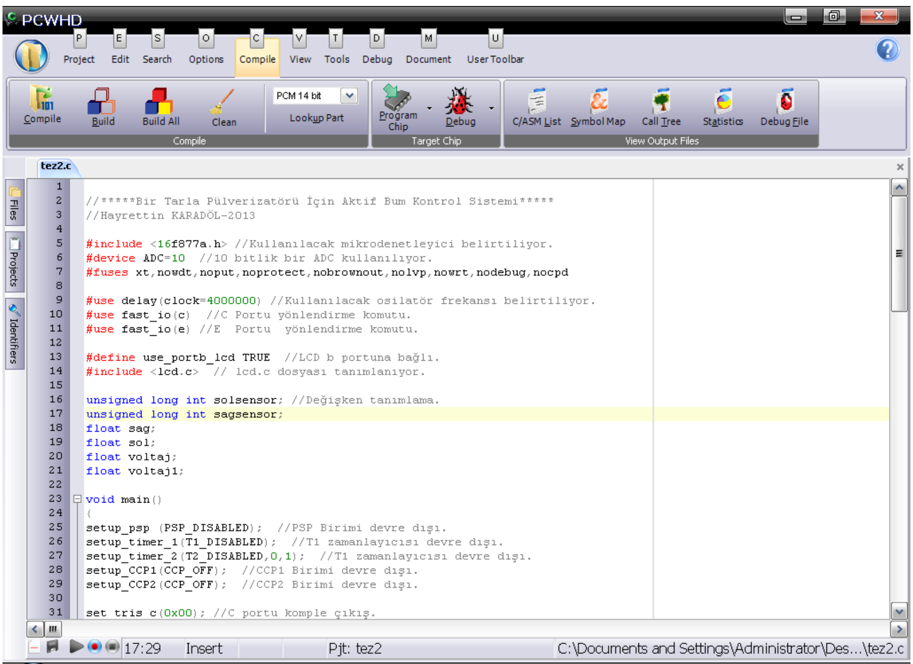

Figure 3. Picture of editor for PIC C programming.

Second control program was written using PLC. However, analog signals cannot be measured using PLC. Therefore, an analog input-output module was used to read analog signals using the PLC (S7 1200 Siemens). Analog inputs of 0–10 V were used and the data were converted to digital values. The analog signals from the sensors were compared to the values between 0 and 27,648 by the analog module of PLC and if the error was greater than 3.5 cm the solenoids of the directional control valves were activated to operate the hydraulic cylinders (Fig. 4). PLC editor and a part of the program is given in Fig. 5.

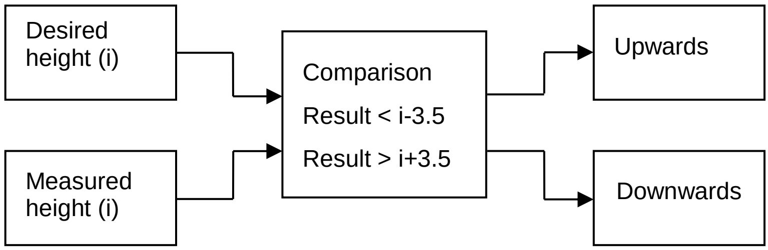

Figure 4. Output control based on error signal.

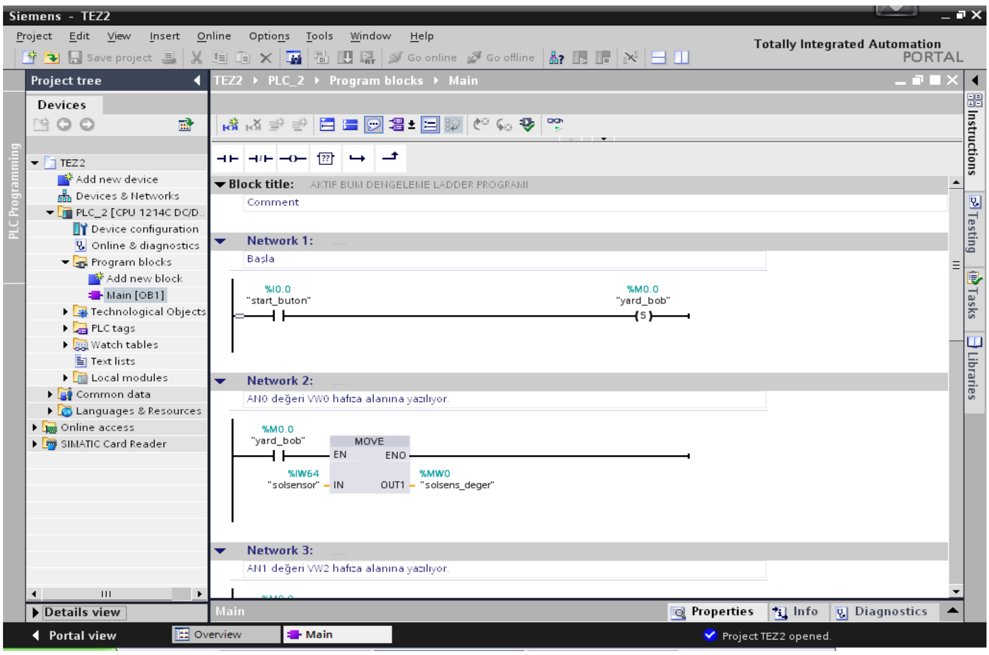

Figure 5. Picture of editor for PLC 1200 Simatic program.

Simulation of PIC C Program

Fig. 6 shows the circuit drawn in proteus program. Control software developed in PIC C editor was loaded on to the microcontroller. The program was tested by applying DC voltage to the corresponding pins using potentiometers. The LCD in Fig. 6 shows the distance value generated as a result of voltage applied to the microcontroller. The potantiometer represents the sensor on the right boom section and the potentiometer voltage values were greater than the control set value, resulting in activation in the outuput. As a result, the simulated program seems to work properly based on set values and artificial disturbances.

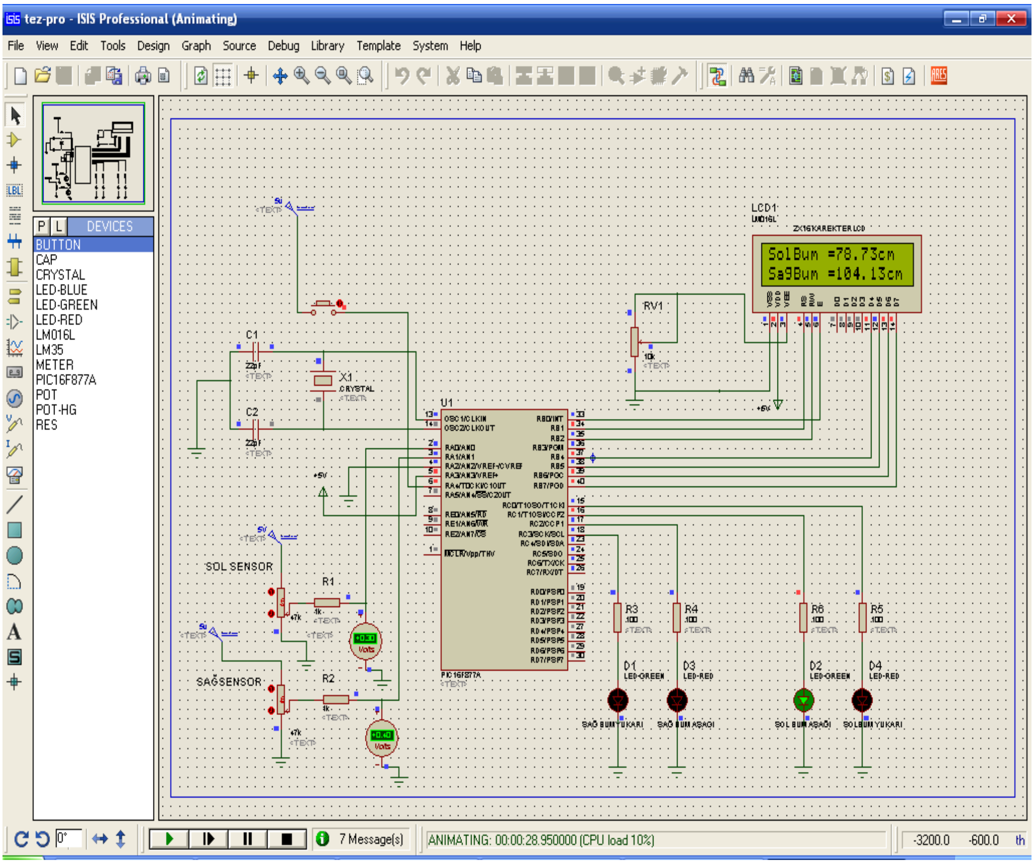

Figure 6. Simulation of the control program in PIC C programming language.

Simulation of PLC Program

PLC S7 200 PLC Simulator was used to observe how the program would work on the computer. Appropriate CPU type was chosen to read analog data and output was observed based on applied voltages. Fig. 7 shows that output (Q0.0) generates a signal to increase the height of left boom section whereas output (Q0.3) produces a signal to reduce the height of right boom section based on the inputs. Hence the program seems to work properly based on set values using the PLC.

Electro hydraulic control circuit

Electro hydraulic circuit designed for boom control is given in Fig. 8. Hydraulic power pack provides the power to two hydraulic cylinders that are controlled by electro hydraulic solenoid controlled valves. The solenoid valves are activated based on PLC outputs determined by output voltage values from ultrasonic distance sensors. Solenoids 1 and 2 activate left boom cylinder and 3 and 4 activate the right boom cylinder in Fig. 8. The cylinders could be operated independently.

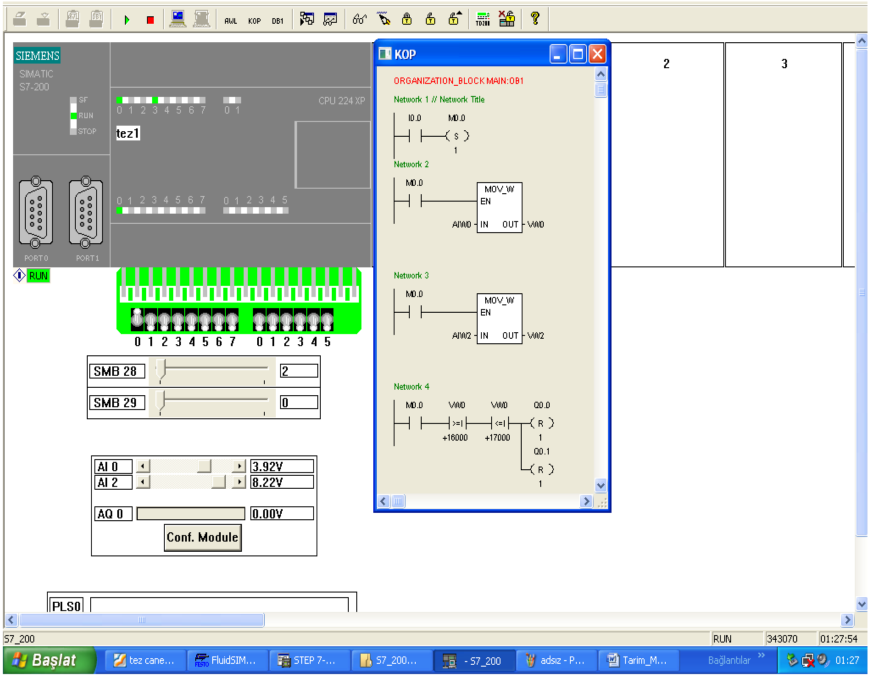

Figure 7. Simulation of control program for the PLC.

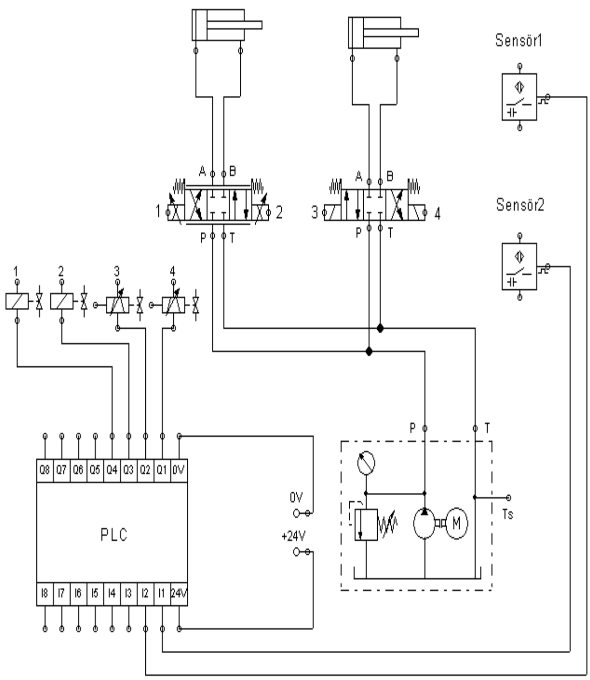

Figure 8. Circuit of the electro hydraulic system designed for active boom section control.

RESULTS AND DISCUSSION

Experimental results of laboratory tests

It was estimated that the boom height could be maintained within 1.27 cm error, corresponding to about 2% of a set value of 80 cm for boom height. However, the software was designed to ignore oscillation amplitudes less than 3.5 cm due to difficulties in stabilizing the boom sections. This was due to the fact that conventional solenoids were used with on-off control in the closed loop control system. Proportional directional valves are costly compared to common solenoid valves and one of the purposes of this study was to be able to do the boom levelling automatically in a cost effective way as much as possible. Thus, on-off control was used to adjust the distance between the sensor and the target. Analog outputs at the milivolt levels caused large oscillations even in the laboratory tests. As a result, the controller attempted to activate the solenoids frequently, resulting in unstable system response. An op amp circuit was integrated to the control system to amplify the output signals with a gain factor of ten to reduce some of the vibrations observed in the preliminary tests (Fig. 9).

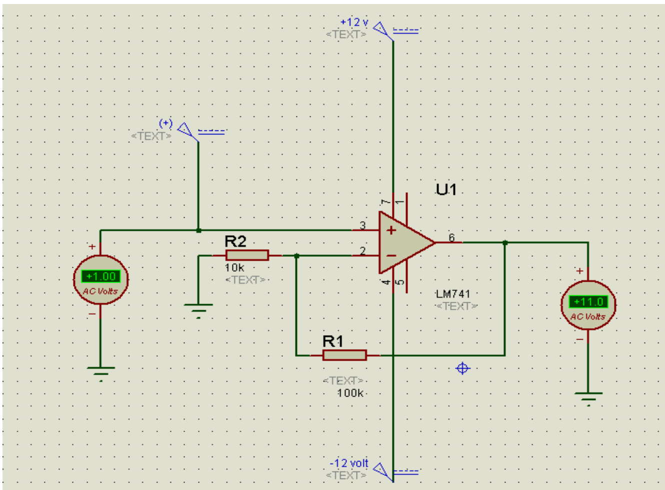

Figure 9. Op-amp circuit desinged to eliminate unstable system response due to frequent oscillations.

Output of the ultrasonic distance sensors was measured at different heights from 0 cm to 150 cm to obtain the calibration equation of the sensors. Fig. 10 shows the measured data, linear regression line and the regression equation with coefficient of determination ($R^2 = 0.999$). The calibration equation was derived from the regression equation as follows with height y in cm and measured voltage output V in mV: $y = 0.260654V–0.303115$ (cm).

In laboratory tests, a reference height of 45 cm was set for boom sections. Then different objects were placed between the sensor and the ground. It was observed that the change in height between the object and the sensor was detected immediately and the hydraulic valves were activated accordingly to actuate the hydraulic cylinders. The distance between the sensor and the object was automatically readjusted to the set value in two or three attempts with on-off control of the solenoids. The dynamic response of the system in the laboratory was good with smooth movements of the boom section. It should be noted that the pressure and the flow rate of the hydraulic power unit were much smaller compared to a tractor's hydraulic output characteristics. Therefore, the electro hydraulic system circuit shown in Fig. 8 was sufficient without speed control of the cylinders since the cylinders moved smoothly without additional flow control in the system.

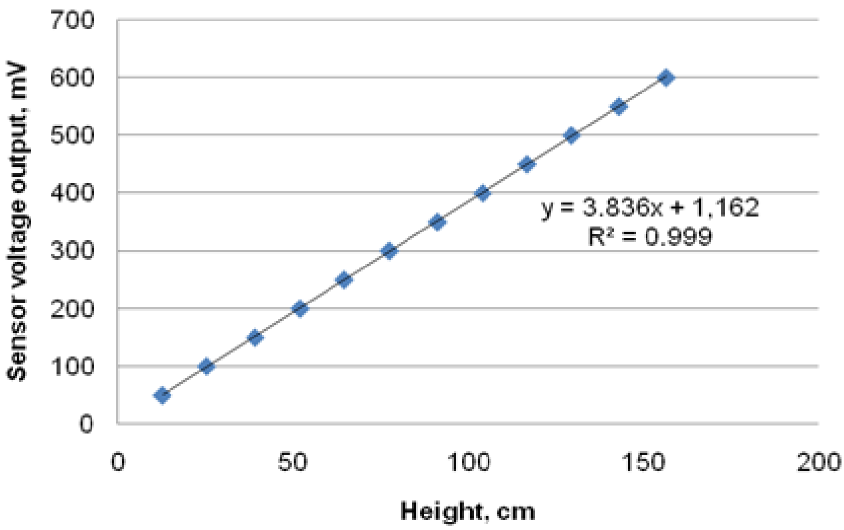

Figure 10. Relationship between boom section height and output of the sensor.

Soil was placed in a small container and the container was passed under the sensor to roughly simulate height variations that can be seen in field conditions. The soil bin was moved slowly forward and backward in a random manner in these tests for about 90 seconds. The resulting height changes of the sensor were recorded using the digjital multimeter (Fig. 11). The test results showed that the amplitude of the signal could be kept within 1.5 and 2.15 Volts, corresponding to 3.5 cm deviatiatins from the set value.

A data acquisition system was not used in this study to record the output voltage or height data. Instead a digital multi meter with USB port was used to read the processed output voltages of the sensors. The sensor produces output signals at 42 kHz that is much faster than the sampling frequency of the measuring device (3 Hz). It should be noted that the dynamic system response using the controller may be sufficient but the measurement system response was slow. This can be observed in rise up durations in the graphs shown in this subsection. Another reason for slow response may be the low flowrate in the hydraulic system resulting in a controlled and smooth movement of the boom sections.

Figs 12–13 shows the responses of the system to soils moved under the sensors at two different speeds. The soil was moved in forward and backward directions and the system responded to the height variations by comparing the output singal values to the acceptable output voltage range of 1.65–2.00 V. As observed, the height of the boom was not allowed to deviate more than 3.5 cm compared to the set height value of 45 cm.

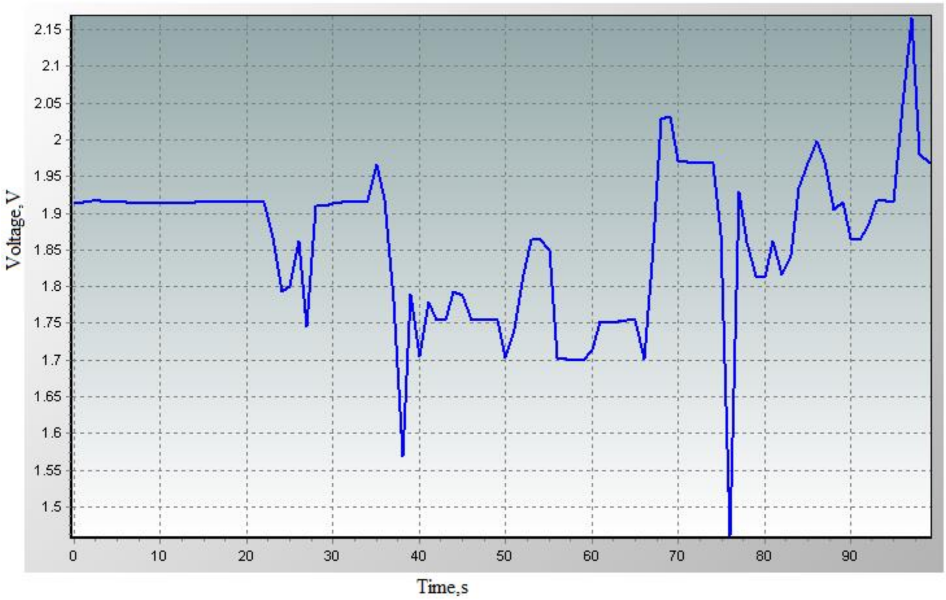

Figure 11. Changes in measured voltage output based on artificial height disturbances in the laboratory.

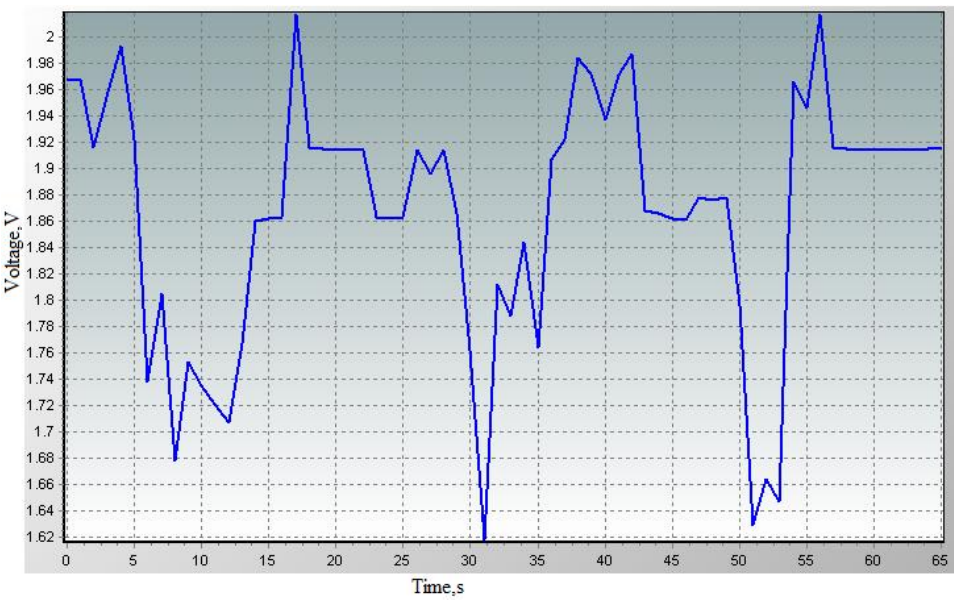

Figure 12. Measured output voltage from the sensor when soil is moved at 4 m min^{-1}.

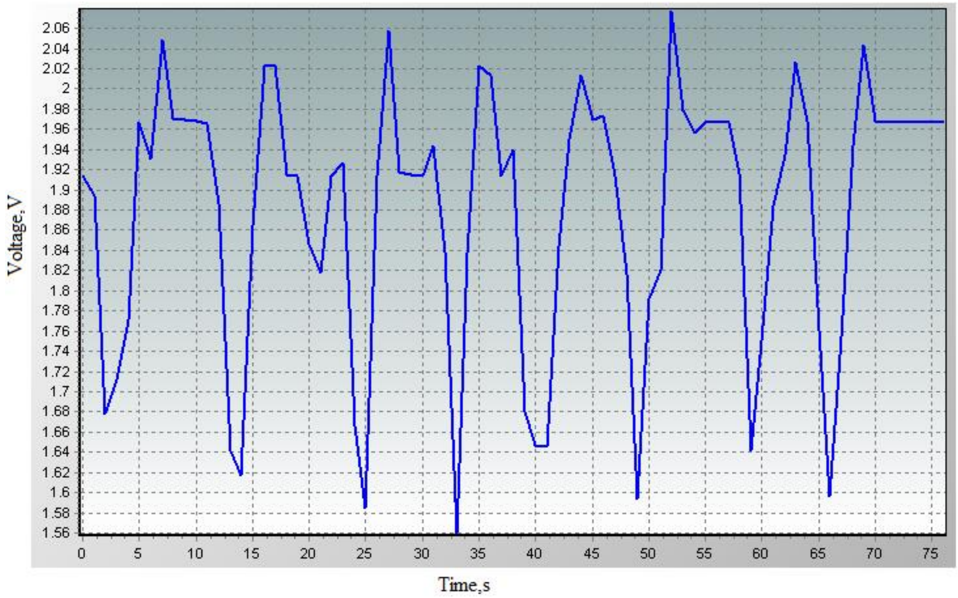

Figure 13. Measured output voltage from the sensor when soil is moved at 10 m min^{-1}.

Experiments under the laboratory conditions showed that the height change under the sensors mounted at the tip of the boom sections could be measured accurately. Boom sections could be moved up and down depending on the disturbance between the sensor and the target. The dynamic response of the sensors and the controller was considered fast and satisfactory. The hydraulic cylinders worked smoothly to control the boom height. The drawback of the system seemed to be the measurement device that had a much lower sampling frequency compared to the output frequency of the sensor. It should also be recalled that the test frame was stationary and the disturbances could not be moved fast enough under the boom sections. Additionally, the metal bars representing the boom sections were short (1.2 m) and there were no forced vibrations on the boom sections. Finally, the oil flowrate was low in the laboratory hydraulic power pack and did not require speed regulation of the cylinders. All these factors might have made it easier to measure, compare, and automatically control the boom height using on-off control method. The controller that was developed in this study is flexible and can be modified or further developed to compansate for changes in operating conditions. Nevertheless, the capabilities of the system will be somewhat limited due to on-off control used in the closed loop control system.

The sensor was able to detect the distance variations between the sensor and the ground. However, it was not likely to activate and deactivate the hydraulic cylinders as fast as sensor outputs. The solenoids need some time to open and close the circuit to drive the DCVs. By reasoning, it was estimated that signals may be sampled for every 100 ms so that the system can respond to variations in the field for ground speeds of 6–8 km h^{-1}. This corresponds to about 20–25 cm distance in the forward direction once a disturbance is detected by the sensor. Thus, the system will attempt to respond to the variations in less than half a meter with an output sampling frequency of 100 ms.

It was concluded that main objective of the study was accomplished by developing functional controllers under laboratory conditions. At the second stage of the study, the controllers and the hydraulic system was mounted on a field sprayer. First, the boom sections were modified so that each boom section can be folded up and down. The cylinders were mounted on the frame of the sprayer and piston rods were mounted on the foldable boom sections. Electro hydraulic valves, pressure control valve and relevant components were also mounted. The middle boom section is 2 m wide, and right and left boom sections are of 4 m on the field sprayer. The same hydraulic circuit was used as the laboratory tests but the components used on the tractor-sprayer combination were different due to diffferences in physical dimensions and hydraulic requirements.

The pressure was set to 100 bars on the tractor hydraulic system. According to FAO (2001), the allowable oscillation at the boom sections could be 2% of the boom length. Therefore, for a 4 m boom section on each side, the ampitude of the natural oscillation may be up to 8 cm. This is why the controller should ignore the height variations at the tip of boom sections as long as vibrations are not greater than this value. Due to the high flowrate of the tractor’s hydraulic system, the pistons tended to move too fast, resulting in very fast boom folding action. The response of the controller to this fast hidromechanical behaviour was unstable oscillation. The system was not able to provide damping, rather a response with no damping was observed for a couple of seconds. The conclusion from the initial testing on the field sprayer was that the speed of the hydralic cylinders and hence the boom sections was too fast to control with on-off control of the electro hydraulic valves. Next, the deviations from the set value were allowed to be 30 cm to observe the dynamic response of the system. The controller had enough time to recalculate the sensor output and compare it with the reference value and was able to control the boom height withing 30 cm from the reference height. Obviously 30 cm oscillation is higher than allowable amplitude of 8 cm for the sprayer under consideration.

Therefore, in the next stage, four flow regulating valves were integrated into the hydraulic system to control the speed of each cylinder both during extraction and retraction. Although testing has not been done after the flow regulating valves were mounted on the inlet and outlet ports of the cylinder yet, two conclusions were drawn based on initial trials on the field sprayer. First, due to natural vibrations of the boom sections, it is not likely to prevent boom sections to oscillate within about 10 cm from the reference height settting. Therefore the controller should not take such oscillations into account. Second, high speed at the hydraulic cylinders result in even much higher speed at the point the sensors are mounted. The controller should have enough time to detect, compare and send necessary signal to the solenoids and the hydraulic system should have acceptable speed for closed loop control of the system with on-off control of the hydraulic valves.

Caner et al. (2012) observed significant natural oscillations in field conditions in Turkey using 12, 15 ve 18 m field sprayers. Wider sprayers will experience more vibrations with larger amplitudes compared to the 10 m sprayer that will be used for further tests. Therefore the control system developed in this study needs to be developed further.

In order to improve the system dynamics that was tested in this study, precise speed and pressure control can be done using proportional valves or servo valves

(Anthonis et al., 2000; Kartal, 2007). Proportional valves are cost-effective compared to servo valves but more expensive compared to solenoid valves used in this study. The materials used in this study were sufficient to activate the hydraulic cylinders using on-off control. The system used in the laboratory was smooth and stable, mainly due to low flowrate of the supply and short bom sections with no natural or forced oscillations. That is why the height of boom tips could be automatically adjusted within 3.5 cm of the reference height value. The system in the laboratory did not require speed control of the hydraulic cylinders wheareas the hydraulic system on the actual sprayer needed flow control valves in addition to the pressure control valve to be able to stabilize the boom leveling system.

The main objective of the study was to focus on developing controllers that could be eighter directly used or modified to be adapted to a field sprayer for boom height levelling. The experimental system had only one sensor on each side of the boom, and hence the capability to detect soil or plant height variations would be limited in real conditions due to the fact that sensor could only determine height variations over a limited area under the tip the boom sections. Therefore, monitoring the leveling problems along the boom would require more than one sensor on each side. A single sensor at the tip of the boom would help leveling the boom to some extent and also protect the boom from ossilating and hitting the ground. Despite the drawback regarding number of sensors used, both PIC and PLC sytems were sufficient to level the booms using the feedback information provided by ultasonic sensors.

CONCLUSIONS

The followings could be summarized and concluded as a result of this study:

- Two types of controllers were designed and implemented for active boom section control using PIC and PLCs. Both systems were tested in the laboratory and only PIC contoller was mounted on the field sprayer for initial testing. Both systems had fast responses to the disturbances under laboratory conditions.
- Calibration equation for the ultrasonic distance sensor had a very high determination coefficient in the laboratory ($R^2 = 0.999$).
- Analog output signals were at the mV levels, causing oscillations. An op-amp was integraged to improve the stability of the system. The laboratory test system could be automatically leveled within 3.5 cm of the set value.
- The hydraulic system on the field sprayer required flow regulation valves to control the speeds of folding at boom sections. The boom tips could be kept within 30 cm compared to reference height and therefore the system needs to be improved by appropriate flow control in the tests to be done next in field conditions.

ACKNOWLEDGEMENTS. This study (Project No: 2013/3-23) was supported by the Coordination Unit of Scientific Research Projects, Kahramanmaraş Sütçü İmam University.

REFERENCES

Anthonis, J., Ramon, H. & De Baerdemaeker, J. 2005. Implementation of an active horizontal suspension on spray boom. *Transactions of the ASAE* **43**(2), 213–220.

Caner, Ö., Kaya, E. & Yılmaz, E. 2012. Ege Bölgesi'nde süne (eurygasterspp., hemiptera: scutelleridae) mücadelesinde farkli rampa uzunluklarinin kaplama oranina ve ilaçlama başarisina etkileri. Ege Üniv. Ziraat Fak. Derg. **49**(3), 213–221 ISSN 1018–8851 (in Turkish).

Çilingir, İ. & Dursun, E. 2009. *Plant Protection Machinery (Bitki Koruma Makinaları)*. AÜZF Yayın No: 1531 (in Turkish).

Deprez, K., Anthonis, J., Ramon, H. 2003. System for vertical boom corrections on hilly fields. *Journal of Sound and Vibration* **266,** 613–624.

FAO. 2001. *Guidelines on Minimum Requirements for Agricultural Pesticide Application Equipment*, International Code of Conduct on the Distribution and Use of Pesticides, Volume Two: Vehicle Mounted and Trailed Sprayers. Rome.

Güler, H., Urkan, E., Tozan, M., Tekin, A.B. & Caner, Ö. 2010. Technical developments in plant protection mechanization (Tarımsal Savaşım Mekanizasyonunda Teknolojik Gelişmeler). *Ziraat Mühendisliği VII. Teknik Kongresi Bildiriler Kitabı* 1–2.Ankara.

Kartal, F. 2007. *Industrial Hydraulic (Endüstriyel Hidrolik).* ISBN: 978–975–00336–1-2. Modül Ders Araçları ve Özel Eğitim Hizmetleri Ltd. Şti. İzmir (in Turkish).

Okada., C.F. & Mucheroni, M.F. 2012. Co-Simulation procedure for PID and fuzzy logic active controls strategies applied to a sprayers boom suspension. *Technology and Engineering Applications of Simulink*, Prof. Subhas Chakravarty (Ed.). 78–953-51-0635-7. InTech, Available from http://www.intechopen.com/book/technology-and-engineering-applications-of-simulink

Sartori, S., Domingues, E.L., Kimura, J.B. & Garrito, S.A. 2002. Automatic control of boom height and positioning on a self propelled sprayer. In *Proceedings of the World Congress of Computers in Agriculture and Natural Resources*, Iguacu Falls, Brazil, pp. 421–431. ASAE Publication Number 701P0301.

Agronomy Research **12**(1), 115–120, 2014

The effect of soil tillage intensity on carbon dioxide emissions released from soil into the atmosphere

K. Krištof, T. Šima*, L. Nozdrovický and P. Findura

Slovak University of Agriculture in Nitra, Faculty of Engineering, Department of Machines and Production Systems, Tr. A. Hlinku 2, 94976 Nitra, Slovak Republic; *Correspondence: tomasko.sima@gmail.com

Abstract. Soil tillage is among the factors which affect the amount of carbon dioxide (CO_2) emissions released from soil into the atmosphere. The objective of the study was to compare three tillage systems which overall represents the most commonly used systems. No-tillage, reduced tillage (shallow disc cultivation) performed by LEMKEN Rubin 9/600 KU disc cultivator and ploughing performed by LEMKEN EuroDiamant 8 mouldboard plough. Experimental area was divided into three replications of each tillage treatment as a randomized block design and the effect of soil tillage intensity on CO_2 emissions were observed in field conditions by using ACE device (Automated Soil CO_2 Exchange Station, ADC Bio-Scientific Ltd., UK). There were found an effect of soil tillage intensity on CO_2 emissions released from soil into the atmosphere. Increasing tillage intensity resulted in increasing rate of CO_2 emissions released from soil into the atmosphere where reduced tillage was reflected as 43% and ploughing as114% of this escalation. The results of our study supporting the more ecological effects of reduced tillage and no-tillage systems in comparison with widespread conventional systems by using mouldboard ploughs.

Key words: carbon dioxide, soil emissions, soil tillage.

INTRODUCTION

Chirinda et al. (2011) concluded that gas exchange between soil and atmosphere is an important factor which affects release of greenhouse gases into the atmosphere. There are three most important gases: carbon dioxide (CO_2), nitrous oxide (N_2O) and methane (CH_4). Global climate change is a phenomenon which negatively affects the entire mankind. In this regard, among the most mentioned gases overall is a carbon dioxide (Goh, 2004). Agriculture is considered as one of the significant producer of carbon dioxide (IPCC 2007). The amount of emissions released from soil into the atmosphere is relatively low though in regards on total area of cultivated soils it represents a huge amount of carbon dioxide emissions (Krištof et al., 2011).

The research on CO_2 emissions released from soil into the atmosphere is realised by many, mostly terrain, methods: absorbing, gasometrical, gradient and micrometeorological (Pumpanen et al., 2006; Šima et al., 2012). The extensive research on global climatic change leads to an extensive discussion about releasing of CO_2 emissions from soil into the atmosphere inducted by soil tillage. As Reicosky a Saxton (2007) indicated, conventional soil tillage based on using plough contributes on higher soil carbon losses through CO_2 emissions. But they also point, soil conservation tillage has a great potential to reduce the release of greenhouse gases from soil into the atmosphere. This phenomenon can be explained by the way how each tillage technology affects the soil environment (Carter et al., 2003a and 2003b). Since soil conservation tillage technologies are characterised by lowered tillage intensity and soil surface which reduce the extent of soil organic matter by oxidation processes (Batey, 2009) and therefore the release of CO_2 emissions from soil into the atmosphere. However, as Robertson et al. (2000) had stated, issue of the soil tillage technologies effect is only one of the whole complex system how agriculture affect the environment through production of greenhouse gases such as CO_2.

The primary process which is responsible for CO_2 emissions releasing from soil into the atmosphere is diffusion (Buchmann, 2000). It is affected by roots of plants and organisms of soil respiration, and soil organic matter decomposition (Normanet al., 1992). Future more, among other factors which directly affect the amount of produced emissions are counted: temperature, atmospheric pressure (Garcia et al., 2004), soil type (Welles et al., 2001), organic matter (Reicosky & Saxton, 2007), fertilisers (Li et al., 2004; Chirinda et al., 2011; Ludwig et al., 2011), soil compaction (Buc et al., 2011; Šima & Dubeňová, 2013; Šima et al., 2013a), soil tillage (Krištof et al., 2011; Šima et al., 2013b) and moisture (Norman, et al., 1992).

The objective of the study was to compare three tillage systems which overall represents the most commonly used systems (no-tillage, reduced tillage and ploughing) and its effect on carbon dioxide emission released from soil into the atmosphere.

MATERIALS AND METHODS

The experiment was placed in lands of AGRO Divízia ltd. Selice, cca 40 km from Nitra city during spring 2012 (Temperature range: 2–15°C; Average temperature: 7.9°C; Air humidity range: 31–81%; Air pressure range: 980–1,010 hPa; Rainfall: 0.6 mm). As a study area was selected flat land with balanced microrelief, high uniformity of soil conditions after year of dormancy. After soil sampling and following analysis where soil identified as a sandy loam (particles < 0.01 mm below 20–30%) with high soil organic matter and humus (3.00–4.99%) and neutral soil reaction (pH in H_2O: 6.9–7.3; pH in KCl: 6.5–7.2)

The area were divided and marked by wooden stakes in three replication of each tillage treatment as a randomized block experiment. Reduced tillage (shallow disccultivation) was performed by LEMKEN Rubin 9/600 KU disc cultivator, ploughing was performed by LEMKEN EuroDiamant 8 mouldboard plough and no-tillage areas with no cultivation.

For measurement of CO_2 emissions released from soil into the atmosphere were used ACE device (Automated soil CO_2 Exchange station produced by ADC Bio-Scientific Ltd., UK). The device is designed for automatic long term terrain measurement of soil respiration. The basis of device is infrared gas analyser which is placed directly inside of the gas chamber supplement. It allows tubeless and shortened transfer of gases between the chamber and analyser and prevents any leakage from the system. In addition, short distance between soil chamber and analyser provides immediate responsiveness on change of CO_2 exchange between soil and the air.

The data of CO_2 exchange between soil and air was observed for 30 days until seeding was conducted.

Obtained data where analysed by ANOVA analysis, LSD test after normality test by Kolmogorov-Smirnov procedure and homogeneity of variance by using Levene's test ($P < 0.05$ at 95% confidence level).

RESULTS AND DISCUSSION

Table 1 shows the effect of soil tillage intensity on carbon dioxide emissions released from soil into the atmosphere. While mean value measured on non-tilled areas was 2.014 $\mu mol\ m^{-2}\ s^{-1}$ it is in contrast with obtained value at areas which was cultivated by LEMKEN Rubin 9/600 KU and even greater difference was observed in contrast with areas cultivated by LEMKEN EuroDiamant 8 mouldboard plough, 2.889 and 4.318 $\mu mol\ m^{-2}\ s^{-1}$, respectively.

Table 1. The effect of soil tillage intensity on carbon dioxide emissions released from soil into the atmosphere, $\mu mol\ m^{-2}\ s^{-1}$ (n = 60)

Parameter	CO_2 emissions, $\mu mol\ m^{-2}\ s^{-1}$		
	No-tillage	Reduced tillage	Ploughing
Mean	2.014^{a}	2.889^{b}	4.318^{c}
Standard deviation	0.444	0.346	0.421
Min.	1.150	2.310	3.180
Max	2.960	3.380	4.990
Range	1.810	1.070	1.810
Coefficient of variation, %	22.064	11.993	9.750

Different letters in superscript (^{a,b,c}) mean the effect of the soil tillage intensity on carbon dioxide emissions released from soil into the atmosphere. It indicates that means are significantly different at $P < 0.05$ according to the LSD multiple-range test at the 95.0% confidence level.

While selected variants used in our study also represents a different systems of soil tillage it is possible to conclude that direct drilling (no-tillage) system is characterised by lowest influence on soil and therefore causes lowest CO_2 emissions released from soil into the atmosphere. If direct drilling will be taken as a basis for comparison then using reduced tillage system will be reflected as escalation by 43.44% in regards to CO_2 emissions released from soil. In comparison with systems using conventional ploughs it was increase by 114.39% which is more than double amount of CO_2 emissions and carbon loss from the soil. While in case of difference between reduced tillage and conventional tillage by using mouldboard plough it was only 49.46% increase it still means almost a half more CO_2 emissions released from soil.

As it was stated (Goh, 2004; Reicosky, 2007), the agriculture can change its role from CO_2 producer into CO_2 absorber. There are still many problems in terms of establishment and development of some crops in reduced tillage and no-tillage systems (Jones et al., 2006); however the global pressure to reduce air pollution should be taken into account even more. The measurement methods may be divided into many incomparable methods (Pumpanen et al., 2004), but all of them are trying to send out the same message. Greater intensity of soil tillage have an effect on CO_2 emissions released from soil into the atmosphere and lower intensity can reduce greatly the way how agriculture pollute the environment, moreover how agriculture can contribute in reduction of air pollution by greenhouse gases widely supported by many researchers (Reicosky, 2001; Lloyd % Taylor, 2004; Reicosky et al., 2005; Lal et al., 2007; Reicosky and Saxton, 2007, Khaledian et al., 2012).

CONCLUSION

From the analysis of measured data it is possible to conclude that no-tillage, direct drilling technology caused the lowest carbon dioxide emissions released from soil into the atmosphere in comparison with other tested technologies. Reduced tillage technology caused higher amount of CO_2 emissions then no-tillage but lesser then it was observed in case of use of conventional technology with using mouldboard plough. There is a great effect of soil tillage intensity on CO_2 emissions released from soil into the atmosphere and therefore a great effect from environmental perspective.

ACKNOWLEDGEMENTS. The paper reflects the results obtained within the research project NFP No. 26220220014 'Application of information technologies to increase the environmental and economic sustainability of the production agrosystem' (Activity 3.1 Creation of the department of transfer of technology to practice) (OPVaV– 2008/2.2/01-SORO).

REFERENCES

Batey, T. 2009. Soil compaction and soil management, a review. *SoilUse and Management* **25**, 335–345.

Buc, M., Krištof, K., Nozdrovický, L. & Šima, T. 2011. Skúmanie vplyvu riadeného pohybu strojov na množstvo uvoľňovaných emisií CO_2 z pôdy do atmosféry. In: *XIII. International conference of young scientists 2011*, Prague: CULS in Prague, 2011. pp 16–21. (in Slovak, English abstract).

Buchmann, N. 2000. Biotic and abiotic factors controlling soil respiration rates in PiceaAbiesstands. In: *SoilBiology and Biochemistry* **32**, 1625–1635.

Carter, A., Jordan, V. & Stride, C. 2003a. A Guide to Managing Crop Establishment. *Soil Management Initiative,* Chester 2003.

Carter, A., Stride, C. & Jordan, V. 2003b. Improved Soil Management for Agronomic and Environmental Gain. *Soil Management Initiative,* Chester 2003.

Chridina, N., Kracher, D., Laegdsmand, M., Porter, J.R., Olesen, J.E., Petersen, B.M., Doltra, J., Kiese, R. & Butterbach-Bahl, K., 2011. Simulating soil N_2O emissions and heterotrophic CO_2 respiration in arable systems using FASSET and MoBiLE-DNDC. In: *Plant Soil* **343**. 139–160.

Ellert, B.H. & Janzen, H.H. 1999. Short-terminfluence of tillage on CO_2 fluxes from semi-arid soil on the Canadian praires. *Soil and Tillage Research* **50**, 21–32.

Garcia, R.L., Demetriades-Shah, T.H., Welles, J.M., McDermitt, D.K. & Norman, J.M. 2004. Measurements of Soil CO_2 Flux. LI-COR, inc., Environmental Division, 4421 Superior Street, Lincoln, NE 68504, and [1]Dept. of Soil Science, University of Wisconsin, Madison, WI 53706 USA.

Goh, K.M. 2004. Carbon sequestration and stabilization in soils: Implications for soil, productivity and climate change. In. *Soil Science and Plant Nutrition* **50**, 467–476.

Guzman, J.G., Godsey, CH.B., Pierzynski, G.M., Whitney, D.A. & Lamond, R.E. 2006. Effects of tillage and nitrogen management on soil chemical and physical properties after 23 years of continuous sorghum. *SoilTill. Res*. **91**, 199–206.

Houghton, R.A., Hackler, J.L. & Lawrence, K.T. 1999. The U.S. carbonbudget: contributionsfromland-usechange. *Science* **285**, 574–578.

IPCC 2007. *Intergovernmental panel on climatechange 2007*. Synthesis report. IPCC, Geneva

Jones, C.A., Basch, G., Baylis, A.D., Bazzoni, D., Bigs, J., Bradbury, R.B., Chaney, K., Deeks, L.K., Field, R., Gomez, J.A., Jones, R.J.A., Jordan, V., Lane, M.C.G., Leake, A., Livermore, M., Owens, P.N., Ritz, K., Sturny, W.G. & Thomas, F. 2006. Conservation Agriculture in Europe: An Approach to Sustainable Crop Production by Protecting Soil and Water? SOWAP, Jealott'sHill, Bracknell, UK.

Khaledian, M.R., Mailhol, J.C. & Ruelle, P., 2012. Impacts of direct seeding into mulch on the CO_2 mitigation. *Agronomy research* **10**, 303–310.

Krištof, K., Buc, M., Nozdrovický, L. & Šima, T. 2011. Vplyv technológie spracovania pôdy na množstvo uvoľňovaných emisií CO_2 z pôdy do atmosféry. In: *XIII. International conference of youngs cientists 2011*, Praha, 19.-20. září 2011. Praha: ČZU Praha, 2011. pp 111-115. ISBN 978-80-213-2194-6 (in Slovak, Englishabstract).

Lal, R., Reicosky, D.C. & Hanson, J.D., 2007. Evolution of the plough over 10,000 years and the rationale forno-till farming. *Soil&Tillage Research* **93**, 1–12.

Li, C., Mosier, A., Wassmann, R., Cai, Z, Zheng, X., Huang, Y., Tsuruta, H., Boonjawat, J. & Lantin, R. 2004. Modeling greenhouse gas emissions from rice-based production systems: Sensitivitiy and upscaling. *Global Biogeochemical cycles***18**.

LI-COR Biosciences. 1998. Application Note 124 (1998). Considerationformeasuringground CO2 fluxeswithchambers. LI-COR Biosciences, Lincoln, NE, USA 68504.

Lloyd, J. & Taylor, J.A. 1994. On the temperature dependence of soil respiration. *Functional Ecology* **8**, 315–323.

Ludwig, B., Jäger, N., Priesack, E. & Flessa, H., 2011. Application of the DNDC model to predict N_2O emissions from sandy arable soils with differing fertilization in a long-term experiment. In: *Journal of Plant Nutrition and Soil Science* **174**, 350–358.

Norman, J.M., Garcia, R. & Verma, S.B. 1992. Soil surface CO_2 fluxes and the carbon budget of a grassland. In: *Journal of Geophysical Research,* **97** 18,845–18,853.

Pumpanen, J., Kolari, P., Ilvesnieni, H., Minkkinen, K., Vesala, T., Niinistö, S., Loliha, A., Larmola, T., Morero, M., Pihlatie, M., Janssens, I., Yuste, J.C., Grünzweig, J.M., Reth, S., Subke, J.A., Savage, K., Kutsch, W., Østreng, G., Ziegler, W., Antoni, P., Lindroth, A. & Hari, P. 2004. Comparison of different chamber technique for measuring soil CO_2 flux. *Agric. and . For. Meteorol.* **123**, 159–176.

Rajaniemi, M., Mikkola, H. & Ahokas, J., 2011. Greenhouse gas emissions from oats, barley, wheat and rye production. *Agronomy research* **9**, 189–195.

Reicosky, D.C. 2007. Carbon is the ‚C' that starts ‚C'onservation. *Proceedings of the South Dakota No-Till Association*, 17–23.

Reicosky, D.C. 2001. Tillage-inducted CO_2 emissions and carbon sequestration: effect of secondary tillage and compaction. In: *GARCIA, R., TORRES, L. et al. (eds.). Conservation Agriculture: A World wide Chalenge XUL*, Cordoba, Spain, p. 265–274.

Reicosky, D.C., Lindstrom, M.J., Schumacher, T.E., Lobb, D.E., Malo, D.D. 2005. Tillage-inducted CO_2 loss across aneroded landscape. *Soil and Tillage Research*.***81***, 183–194.

Reicosky, D.C. & Saxton, K.E. 2007. Reduced Environmental Emissions and Carbon Sequestration. In: *BAKER, C.J. et al. 2007. No-Tillage Seeding in Conservation Agriculture. 2nd Edition*. FAO, 2007. 257–267.

Robertson, G.P., Klingensmith, K.M., Klug, M.J., Paul, E.A., Crum, J.R. & Ellis, B.G. 1997. Soil resources, microbial activity, and primary production across an agricultural ecosystem, *Ecological Applications* **7**, 158–170.

Šima, T., Nozdrovický, L., Krištof, K., Dubeňová, M. & Macák, M. 2012. A comparison of the field and laboratory methods of measuring CO_2 emissions released from soil to the atmosphere. *Poljoprivredna tehnika* **37**, 63–72.
Šima, T., Nozdrovický, L., Dubeňová, M., Krištof, K. & Krupička, J., 2013a. Effect of crop residues on nitrous oxide flux in the controlled traffic farming system during the soil tillage by LEMKEN Rubin 9 disc harrow. *Agronomy research* **11**(1), 103–110.
Šima, T., Nozdrovický, L., Krištof, K., Dubeňová, M. & Krupička, J. 2013b. Effect of the vertical and horizontal soil tillage technology to nitrous oxide flux from soil. *Trends in agricultural engineering 2013*, proceeding of CULS in Prague, 586–589.
Šima, T. & Dubeňová, M. 2013. Effect of crop residues on CO_2 flux in the CTF system during soil tillage by a disc harrow Lemken Rubin 9. *Res. Agr. Eng.* **59**, Special Issue, S15–S21.
Welles, J.M., Demetriades-Shah, T.H. & Mcdermitt, D.K. 2001. Considerations for measuring ground CO_2 fluxes with chambers. Chemical Geology **177**, 3–13.

Agronomy Research **12**(1), 121–128, 2014

Soil damage reduction and more environmental friendly agriculture by using advanced machinery traffic

Z. Kviz, M. Kroulik and J. Chyba

Department of Agricultural Machines, Technical Faculty, Czech University of Agriculture in Prague, Kamycka 129, 16521 Prague, Czech Republic; *Correspondence: kviz@tf.czu.cz

Abstract. Nowadays, the agriculture technologies using guidance systems during field operations are more and more common all around the world. Machines without satellite navigation in fields have a tendency to pass-to-pass errors, especially unwanted overlaps, resulting in waste of fuel and pesticides, longer working times and also environmental damage. Finally, such errors can be taken as useless additional costs of farming. When utilising satellite guidance for field operations, the pass-to-pass accuracy can be significantly improved and thus it is possible to make the agriculture production more efficient.

The purpose of this paper was to evaluate advantages and real possibilities of using advanced machinery guidance systems with regard to energy consumption and efficiency and also more environmental friendly agricultural operations. Real pass-to-pass errors (omissions and overlaps) in a field were measured on different tractor-implement units with and without guidance system utilization.

The outcomes from our measurements revealed that there is a statistically significant difference between the total area treated by machinery without any guidance system and machinery using precise guidance systems. It means, better accuracy of machinery passes in fields with guidance systems could help with energy and material savings. Namely the fuel, seeding material or chemicals can be saved up to 6% from a single field operation.

Key words: soil compaction, reduction, energy and material efficiency, machinery passes, satellite navigation, traffic intensity.

INTRODUCTION

The GPS (global positioning system) based means can be used with a great advantage for important data gathering during field operations when talking about soil protection farming systems. Nowadays, using of satellite guidance systems is more and more common in agriculture practice and have become a synonym for precision farming and modern farming systems. Utilization of such equipment can be remarkably beneficial concerning minimizing of machine errors in fields, setting precise production inputs, and therefore lower costs for agriculture production. Machinery traffic monitoring and detailed analysis of machines passes across a field can be a tool for the field area determination which is heavily loaded with tyre contacts. Right the field traffic is connected with soil compaction phenomena and its unfavourable effects. Also passes arrangement in fields is usually without any system and therefore random and therefore GPS with a precise traffic system can help soil protection.

During the last two decades much research has been carried out within developing and analyzing GPS based guidance systems. Now, these systems are commercially available from leading tractor brands. In normal operations, the driver operates the vehicle manually during the turning operation in the headland, but in the field the auto guidance takes over. At present, the technology is available to take over the full guidance of the vehicle. This implies not only a release of the drivers work. It also opens a big potential for redesigning the tractor. Due to this, the task for the driver now changes from controlling the driving to taking care of the overall operation performance (Jorgensen 2012).

Several authors such as Dunn et al. (2006), Han et al. (2004), Stoll and Kutzbach (2000), Debain et al. (2000), Cordesses et al. (2000) summarize the following general benefits from the use of guidance systems:

– reduction in driver fatigue: guidance systems reduce the effort associated with maintaining accurate vehicle paths;

– reduction in costs: accuracy is increased by reducing ‘skip’ (omissions) and ‘double-up’ (repeated application-overlaps) between neighbouring passes in the field;

– increase in productivity: higher operating speeds are possible;

– improved quality: the driver can focus attention elsewhere to ensure better quality;

– improved safety of work in fields;

– less impact on the environment (reduction of machinery pass frequency, reduction of soil compaction…);

– possibility for work at night and when visibility is poor.

It is possible to use many different types of guidance systems such as ground based sensing systems (Hague et al., 2000), laser systems (Chateau et al., 2000), vision-based machine guidance systems (Debain et al., 2000; Han et al., 2004) and satellite navigation systems (Ehsani et al., 2002; Karimi et al., 2006) in almost all machines used in agriculture. Finally, satellite navigation appears to be the most promising and useful way for agricultural machinery guidance in general. GPS-based navigation systems are the only navigation technologies that have become commercially available for navigation of farm vehicles (Batte and Ehsani 2006). Differential Global Positioning System (DGPS) technology has introduced many possibilities for better input management by enabling growers and farmers to apply the right amount of inputs at the right location with acceptable accuracy. As a result, DGPS technology has made the precision agriculture concept more appealing to the agricultural community (Ehsani et al., 2002).

The accuracy of these systems varies from meters down to even millimeters. This range of accuracy is influenced by two factors. First factor are different means of receiving GPS signal corrections and the second is a degree of steering system automation.

Working accuracy for agriculture should be quite high in the range of centimetres and therefore it is necessary to receive coordinates corrections – necessity for differential signals reception. Concerning guidance systems, there are GPS guidance-aided systems and fully automated or ‘hands-free’ GPS guidance systems.

Berglund and Buick (2005) also point out that it is necessary to distinguish between two different levels of accuracy called *´Year-to-Year´* and *´Pass-to-Pass´*.

Pass-to-pass accuracy when using satellite navigation depends on many factors. There is a difference between a vehicle with an assisted guidance and fully automated steering. The assisted guidance involves human factor errors because the operator still has to turn the steering wheel according to light-bar indication. When using fully automated steering systems, the human factor is excluded and the driver has only to concentrate on the first run and turns on headlands. Implement response to tractor steering, its direction control, is usually delayed which could be a source of errors. A specific problem case is where the tractor-implement unit is moving on a slope in a field in the direction of the contour lines. The implement behind the tractor does not run in line with the tractor direction. Despite the fact that the tractor can be equipped with a slope compensation system, the implement has always a tendency for turning aside.

Further problem connected with agricultural machinery and its passes across fields is soil compaction. Trafficking by wheeled heavy farm machines is common in most agricultural operations even in zero tillage systems (Tullberg, 1990) therefore the vast majority of arable land is endangered by soil compaction. Intensity of trafficking (number of passes) plays an important role in soil compaction as well, because deformations can increase with the number of passes (Bakker and Davis, 1995). Also another fact has to be stated, soil compacted by machinery tyres is not only a problem for one year or even one season. Undesirable compaction and changed soil structure may be found even after several years. Compaction of soil by traffic reduces soil infiltration, hydraulic conductivity, porosity and aeration and increases bulk density and impedance for root exploration (Gan-Mor & Clark 2001; Radford et al. 2007). McPhee at al. (1995) stated that up to 30% of tractor engine power can be wasted due to soil compaction which increases pulling force demand by 25%.

Soil compaction can be reduced by a certain passes arrangement system which needs GPS guidance system utilization. One possible tool for soil compaction reduction could be Controlled traffic farming (CTF). The use of the technology named controlled traffic farming (CTF) may minimize or eliminate the need for deep tillage or subsoiling, since CTF is based on maintaining the same wheel lanes for several years (Hadas et al. 1990). Control traffic farming with precisely set tyre tracks could be a tool for minimising of soil compaction risk. Together it means, that GPS utilized in precise traffic arrangement, like for example CTF, is again very important electronic means for better environmental friendly agricultural production and for significant savings for a farmer.

The aim of this paper was to summarize and evaluate advantages and real possibilities of using advanced machinery guidance systems with regard to energy consumption and efficiency and also more environmental friendly agricultural operations. This work evaluates the working accuracy of agriculture machines during different field operations. Real pass-to-pass errors during field jobs were monitored. Differences between pass-to-pass errors during manual machinery steering without any automated guidance and with using GPS – RTK based machinery navigation were analysed.

MATERIAL AND METHODS

Analysis of field operations working accuracy – pass-to-pass errors

Firstly, the most commonly used agricultural machinery units in the Czech Republic with different working widths with different drivers were evaluated during field operations without using any GPS guidance system. The experimental arrangements measured and all the details and experiment conditions are in Table 1.

Table 1. Field operations for pass-to-pass errors analysis (manual steering) – season 2012

Driver	Machinery operation	Operating width	Driver experience	Orientation in a filed
1	soil tillage	6 m	8 years	by estimation of driver
2	soil tillage	6 m	5 years	by estimation of driver
3	plant protection – spraying	18 m	6 years	by estimation of driver
4	plant protection – spraying	18 m	13 years	foam marker
5	seeding	6 m	5 years	disc marker
6	plant protection – spraying	18 m	6 years	tramlines
7	plant protection – spraying	18 m	6 years	by estimation of driver

The measurements were carried out under normal field conditions in a even field without any obstacles in the line of vision. Measured values of pass-to-pass errors were obtained with the help of a laser rangefinder by means of the so-called matrix method. The method principle is the measurement of the distance between axes or tyre tracks of two neighbouring passes (Beel, 2000). For each experimental run and further statistical evaluation of the pass-to-pass accuracy, 36 values were obtained in the following way. Firstly, 7 adjacent passes with the tractor-implement unit were carried out continuously. These passes were consequently evaluated with regard to their true widths (overlaps or missing areas taken into account and actual operation performed by one single pass was calculated). Distances between tyre tracks of neighbouring passes were measured, with the accuracy of 10 mm, and thus 6 values of actual widths were obtained. Further, another 6 measurements of tyre track distances were carried out farther along the passes (the distance between points of measurement along the pass should be equal to the designed working width of the implement). This procedure was repeated completely six times. It resulted in a square sampling grid with one six-unit (6x working width) long side and it provided 36 measured values.

The deviations between the actual working width in the field and the implement design width were calculated. The method and distance measurement described above must be used directly after the unit's pass when the tyre tracks or other identification marks (for instance tramline marks) are clearly visible.

Secondly, the field operation working accuracy was monitored on three machinery units (Table 2) alternately with the navigation using RTK signal and without navigation use. The experiment was carried out on larger fields (acreage more than 35 ha) in order to ensure longer undisturbed passes. Each machinery unit has its driver who was used to operate the machine and utilize RTK navigation during field operations. A very simple equipment to monitor vehicle trajectory was placed into every machine – DGPS receivers and data loggers. The task for the driver was to run approximately 10 passes or to do at least 45 minute his field job with and further without navigation use. These two variants were repeated at least 3 times for each machine.

Table 2. Field operation for pass-to-pass errors analysis (RTK guidance) – season 2012

Driver	Machinery unit	Operating width	Driver experience	Differential signal type
1	seed bed preparation	8 m	4 years	RTK
2	tillage – shallow loosening	15 m	6 years	RTK
3	row seeding	6 m	8 years	RTK

Statistical processing of logged data and graphical visualisation of machinery trajectories was done by means of STATISTICA Cz 8.0 (Statsoft, Tulsa, USA) and ArcGIS 9.2 (Esri, Redlands, CA) software. The deviations between the actual working width in the field and the implement design width were calculated (overlaps or omissions).

RESULTS AND DISCUSSION

Analysis of field operation working accuracy – pass-to-pass errors – manual steering

Table 3 shows a basic statistical overview on deviations for the pass-to-pass error measurements when no guidance system was used during field job. The statistics illustrates the variability of measured values together with maximum and minimum values measured.

Table 3. Statistical analysis of pass-to-pass errors for machines without using any guidance system (values in meters)

(m)	Driver						
	1	2	3	4	5	6	7
Mean	0.17	0.20	0.43	0.09	0.17	0.48	0.02
Median	0.15	0.18	0.79	0.18	0.16	0.50	0.13
Standard Deviation	0.08	0.11	0.94	0.61	0.04	0.22	1.01
Skew	-0.72	0.83	-0.10	-0.87	0.59	-0.70	0.02
Difference min-max	0.44	0.48	3.10	2.29	0.19	1.11	4.13
Minimum	-0.10	-0.02	-1.10	-1.27	0.09	-0.2	-1.8
Maximum	0.34	0.46	2.00	1.02	0.28	0.91	2.33

The best results with the lowest errors (standard deviation) performed drivers 1, 2 and 5 probably because of smaller working width (6 m) as opposed to the arrangements with sprayer (18 m). It is evident from the results that working width has a significant influence on the accuracy of field operation. The driver with the tiller was able to continue the next pass more precisely than the one with the sprayer. The sprayer performed with better accuracy when using foam markers. The best result had the driver 5 during seeding when disc marker use is necessary form the precision of seeding point of view.

Positive mean values of errors indicate that the implement mainly overlapped the preceding pass during the field operation.

Analysis of field operation working accuracy – pass-to-pass errors – RTK navigation versus manual steering

The outcomes from our measurements revealed that there is a statistically significant difference between the total area treated by machinery without any guidance system and machinery using precise guidance systems.

The results from the analysis of the same machine unit with the same driver alternately with the navigation using RTK signal and without navigation use showed that the utilization of guidance system gives significant benefits. Manual operation of the machine and its pass-to-pass errors were obviously bigger than with autonomous (fully automated) steering systems with RTK navigation. The outcome values show prevailing overlaps of passes in the range between 1 and 6% of machine's working width. This value can be significantly minimized by utilization of precise guidance systems, based on RTK signal. Therefore these systems can be a possible way for fuel, chemicals, changeable tool parts and other additional material savings.

The statistical analysis and graphical visualisation of the results is in Table 4.

Table 4. Statistical analysis of pass-to-pass errors – RTK navigation versus manual steering (values in %)

(%)	Driver 1					
	omission		overlap		total error	
Guidance	with	without	with	without	with	without
Mean	0.20	1.22	0.25	1.93	0.46	3.15
Median	0.20	1.14	0.23	2.04	0.42	3.08
Standard Deviation	0.05	0.63	0.07	0.79	0.10	0.79
Skew	0.84	0.96	0.81	0.16	0.94	0.85
Difference min-max	0.20	2.62	0.24	3.16	0.35	3.71
Minimum	0.12	0.36	0.18	0.51	0.34	1.75
Maximum	0.32	2.98	0.41	3.67	0.69	5.45
(%)	Driver 2					
	omission		overlap		total error	
Guidance	with	without	with	without	with	without
Mean	0.00	0.51	1.04	2.20	1.04	2.71
Median	0.00	0.27	1.13	1.87	1.14	2.49
Standard Deviation	0.01	0.64	0.20	1.55	0.20	1.43
Skew	3.49	2.10	-0.63	0.65	-0.63	0.62
Difference min-max	0.05	2.72	0.66	5.71	0.66	4.97
Minimum	0.00	0.00	0.64	0.09	0.64	0.84
Maximum	0.05	2.72	1.30	5.81	1.30	5.81
(%)	Driver 3					
	omission		overlap		total error	
Guidance	with	without	with	without	with	without
Mean	1.11	0.37	1.39	2.09	2.50	2.47
Median	1.07	0.31	1.39	2.17	2.41	2.46
Standard Deviation	0.21	0.28	0.41	0.56	0.56	0.60
Skew	-0.29	1.10	0.17	-0.66	0.12	-1.20
Difference min-max	0.84	0.95	1.65	2.47	2.02	2.42
Minimum	0.61	0.08	0.54	0.67	1.50	0.82
Maximum	1.45	1.03	2.20	3.14	3.53	3.24

The measurements and further analysis of the driver steering without any guidance means show mainly overlaps of passes. Similar outcomes discussed Han et al. (2004) and Dunn et al. (2006) in their papers. The range between 1 and 6% of machine's working width is in accordance with published papers as well. This fact is most important concerning costs and generally inputs for agricultural plant production (savings of fuel, chemicals, changeable tool parts, etc.) and GPS guidance system has a great potential for more environmental friendly and cost-effective agriculture.

CONCLUSIONS

General benefits following from the utilization of guidance systems based on RTK GPS signal such as reduction in costs by reducing repeated applications –overlaps within neighbouring machinery passes in the field were proved.

To summarize the results from the machinery pass-to-pass errors analysis, it is possible to give the following statements. It is evident that the utilization of guidance systems on agricultural machines gives the chance to perform a particular field operation in a more precise way with saving of time and fuel.

When machine steering was dependent on the driver's action (manual steering), the pass-to-pass errors were bigger than with autonomous (fully automated) steering systems with RTK navigation. The errors were mainly overlaps of passes in the range between 1–6% of machine's working width. It means that the field is at the area of overlaps treated uselessly twice which results in additional costs for agriculture production.

The worst results were recorded when the machine was without any guidance and any additional aids (disc markers, foam markers…) and the steering was completely dependent on driver estimation.

Also another outcome can be stated – wider the working width, the worse was the working accuracy. Utilization of precise guidance systems based on RTK signal can be a remarkable source for savings in farming when considering number of field operations during one season.

Taking into account number of field operations per one season – in average 6 entries are necessary for each field on a common farm during one year. According to the results, it means up to 6% of overlaps when evaluating connecting the adjacent passes of agriculture machinery. Therefore it can be stated in a simplified way that up to 36% of total farm acreage is uselessly treated each year as additional costs to one year farm production.

REFERENCES

Bakker, D.M. & Davis, R.J. 1995. Soil deformation observations in a vertisol under field traffic. *Australian Journal of Soil Research* **33**, 817–832.

Batte, M.T., Ehsani, M.R. 2006. The economics of precision guidance with auto-boom control for farmer-owned agricultural sprayers. *Computers and Electronics in Agriculture* **53**, 28–44.

Beel, T. 2000. Automatic tractor guidance using carrier-phase differential GPS. *Computers and electronics in agriculture* **25**(1–2), 53–66.

Berglund, S. & Buick, R. 2005. Guidance and automated steering drive resurgence in precision farming. In: Stafford, J.V. (ed.) *Proceedings of the 5th European Conference on Precision Agriculture, Precision Agriculture '05.* Wageningen Academic Publishers, Wageningen, The Netherlands, pp. 39–45.

Chateau, T., Debain, C., Collange, F., Trassoudaine, L. & Alizon, J. 2000. Automatic guidance of agricultural vehicles using a laser sensor. *Computers and Electronics in Agriculture* **28**, 243–257.

Cordesses, L., Cariou, C., Berducat, M. 2000. Combine harvester control using Real Time Kinematic GPS. *Precision Agriculture* **2**, 147–161.

Debain, C., Chateau, T., Berducat, M., Martinet, P. & Bonton, P. (2000). A guidance-assistance system for agricultural vehicles. *Computers and Electronics in Agriculture* **25**, 29–51.

Dunn, P.K., Powierski, A.P. & Hill, R. 2006. Statistical evaluation of data from tractor guidance systems. *Precision Agriculture* **7**, 179–192.

Ehsani, M.R., Sullivan, M., Walker, J.T. & Zimmerman, T.L. (2002). A Method of Evaluating Different Guidance Systems. Paper number 021155, ASAE, St Joseph, MI, USA.

Gan-Mor, S. & Clark, R.L. 2001. DGPS-Based Automatic Guidance – Implementation and Economical Analysis. Paper No. 011192, ASAE, St Joseph, MI, USA.

Hadas, A., Shmulevich, I., Hadas, O. & Wolf, D. 1990. Forage wheat yield as affected by compaction and conventional vs. wide frame tractor traffic patterns. Transactions of ASAE 33(1): 79–85.

Hague, T., Marchant, J.A. & Tillett, N.D. 2000. Ground based sensing systems for autonomous agricultural vehicles. *Computers and Electronics in Agriculture* **2**5, 11–28.

Han, S., Zhang, Q., Ni, B. & Reid, J.F. 2004. A guidance directrix approach to vision-based vehicle guidance systems. *Computers and Electronics in Agriculture* **43**, 179–195.

Jorgensen, M.H. (2012). Agricultural Field Machinery for the future – from an Engineering Perspective. *Agronomy Research* **10**(1), Special Issue, 109–113.

Karimi, D., Mann, D.D. & Ehsani, R. 2006. A New Methodology for Evaluating Guidance Systems for Agricultural Vehicles. Paper No. 06148, ASABE, St Joseph, MI, USA.

McPhee, J.E., Braunack, M.V., Garside, A.L., Reid, D.J. & Hilton, D.J. 1995. Controlled traffic for irrigated double cropping in a semi-arid tropical environment: part 2, Tillage operations and energy use. *Journal of Agricultural Engineering Research* **60**, 183–189.

Radford, B.J., Yule, D.F., McGarry, D. & Playford, C. 2007. Amelioration of soil compaction can take 5 years on a Vertisol under no till in the semi-arid subtropics. *Soil & Tillage Research* **97**, 249–255.

Stoll, A. & Kutzbach, H.D. 2000. Guidance of a forage harvester with GPS. *Precision Agriculture* **2**, 281–291.

Tullberg, J.N.(2001. *Controlled traffic for sustainable cropping. In: Proceedings of the 10th Australian agronomy conference*. Australian Society of Agronomy, Hobart, Australia, pp. 217–224.

Agronomy Research **12**(1), 129–134, 2014

The quality evaluation of different soil tillage technologies

J. Mašek*, P. Novák, M. Kroulík and J. Chyba

Faculty of Engineering, Czech University of Life Sciences Prague, Kamycka 129, 16521 Prague, Czech Republic; *Correspondence: masekj@tf.czu.cz

Abstract: Soil tillage technologies are one of the most important processes having huge influence on sowing, germination, growing and yield of cultivated crops. At the same time soil tillage is one of the most consuming processes of crop production. There are lots of differences in conventional and other soil tillage technologies. Substitution of the deep cultivation based on ploughing with the technologies of shallow tillage or no tillage allows the reduction of the negative impact on the environment and decreasing of labour and energy cost for soil tillage. Described below is a field experiment based on different soil tillage technologies and its influence on soil condition. Among main research objectives are impact of different intensity soil tillage on the main physic-mechanical properties of soil and overall assessment of the technologies in terms of environmental protection. To evaluate the reliability of the achieved results the data was assessed by statistical analysis methods, using 'Statistica' software. In a field experiment there were evaluated two kinds of tillers typically used in conservation soil tillage technologies. Experiment was focused on working quality and influence of working tolls on soil properties.

Key words: soil tillage, conservation tillage, crop residue, erosion.

INTRODUCTION

Ways of farming change notably the structure of soils and conditions for crops growing. Structure is changed by all external pressure mechanization agents, the way of fertilization, weather conditions and last but not least a very significant influence also have different way soil tillage systems, which was confirmed in study of Powers & Skidmore (1984) and Lhotsky (2000). The main goal of conservation soil tillage systems is restriction of the soil textures destruction, elimination of soil compaction and protection the soil against erosion. Minimum soil tillage includes above all summary proceedings progress cultivation (Hůla et al., 2002), that is based on jointing or reduction of the number of single operations, reduction of depth or intensity of tillage processes and soil could be tilled only in zone treatment or only in a certain soil profile layer.

The constant addition of crop residues leads to an increase in the organic matter content of the soil. In the beginning this is limited to the top layer of the soil, but with time this will extend to deeper soil layers. Organic matter plays an important role in the soil: fertilizer use efficiency, water holding capacity, soil aggregation, rooting environment and nutrient retention, which all depend on organic matter (Johnson, 1988). Residues on the soil surface reduce the splash-effect of the raindrops, and once the energy of the raindrops has dissipated the drops proceed to the soil without any harmful effect. This results in higher infiltration and reduced runoff, leading to less erosion. The residues also form a physical barrier that reduces the speed of water and wind over the surface. Reduction of wind speed reduces evaporation of soil moisture.

Keeping the soil covered is a fundamental principle of conservation agriculture. Crop residues are left on the soil surface, but cover crops may be needed if the gap is too long between harvesting one crop and establishing the next. Cover crops improve the stability of the conservation agriculture system, not only on the improvement of soil properties but also for their capacity to promote an increased biodiversity in the agro-ecosystem. Conservation agriculture systems utilize soils for the production of crops with the aim of reducing excessive mixing of the soil and maintaining crop residues on the soil surface in order to minimize damage to the environment (Andrews et al., 2013). Leaving the plant residues on the top or in the upper layer of soil could lead to the problem with creation deposits of harmful organisms. The problem is to find the ratio of plant residues mixed in upper and top layer of the soil – to have enough soil protection and good soil structure with minimalizing pests' risk. Second problem of the research is quality of work which could be represented by size of clods after tillage. Size of clods plays very important role in soil tillage quality chain because clods with average bigger than 50 mm create problems in following working operations (seed bed preparation and seeding) (Anken et al., 1997). The soil tillage working mechanism plays a crucial role in soil protection system. Different working tools take different quantity of plant residues on the soil surface. The main aim of our observation is working quality evaluation by different soil tillage.

MATERIAL AND METHODS

Observation took place in field conditions for different soil tillage technologies provided by different working tools. On first experimental field evaluated difference between sweep and disc tillers work quality was evaluated with accent on plant residues distribution and size of clods after shallow ploughing. On the second experimental field were marked divers' variants according to different working speed and different working depth. Very important for observation is distribution of plant residues after stubble ploughing in work-in-process level and rate of plant residues on the top of soil. For evaluation of surface covering by crop residues we used image analysis with help of software Photoshop 7 (Fig. 1). For taking pictures of the surface of the soil we used digital camera Olympus C-70. Distance between camera and soil surface was 1.5 m. There is very easy way to recognize grade of covering according to count white and black pixels in the picture of surface. Every variant of tillage (different work speed and depth) has five repetitions. For image analysis 30 pictures per variant was taken. Places for taking pictures were randomized.

For influence of speed and working depth evaluation on a working quality, especially on a crop residue distribution in a working profile and surface we used sweep tiller Horsch Tiger (Fig. 2) in typical setting with original thin chisel working tools. There were evaluated four working depth and four working speeds in a cross combination. It means 16 variants of soil tillage. The disc tiller was Disc Cover Corp DBx made by SMS Rokycany (Czech Republic), it has double working sections in an 'x' arrangement and working angle of section was 18 degrees. On the both experimental fields is there light sandy loam soil. Experimental tillage was made one week after harvest. Previous crop was winter wheat with average yield 7.1 $t \cdot ha^{-1}$.

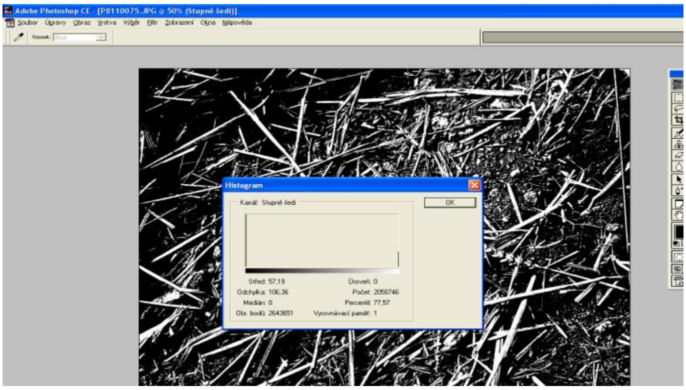

Figure 1. Photoshop tools for picture analysis.

Figure 2. Sweep tiller Horsch Tiger.

RESULTS AND DISCUSSION

In the field experiment we prepared 6 variants of tillage. I – 1x sweep tiller, II – 2x sweep tiller, III – 1x sweep tiller and 1x discs tiller, IV – 1x discs tiller, V – 2x discs tiller and VI 1x discs and 1x sweep tiller. Option 0 is without tillage. Average amount of plant residues on the surface of the soil before tillage was 680 $g \cdot m^{-2}$ (range 390–780 $g \cdot m^{-2}$).

The sweep tiller left more plant residues on the soil surface than disc tiller (Fig. 3). By using disc tiller two times it was observed that crop residues are going up back on surface. Size of clods is smaller by sweep tiller cultivation (Fig. 4). There was recognized significant statistical difference of plant residues distribution in different working depth. The statistical significant differences are between depth 180 mm versus 240 mm and 210 mm; 150 mm versus 240 and 210 mm. There is no significant difference between 150 mm and 180 mm working depth.

For determination of clods‘ fraction we used sieve analyses with 4 sieves followed by weighing the fraction of clods. There is minimum clods fraction with size more than 50 mm. This value is very important because size of clods greater than 50 mm can create problems for secondary tillage and for seeding also.

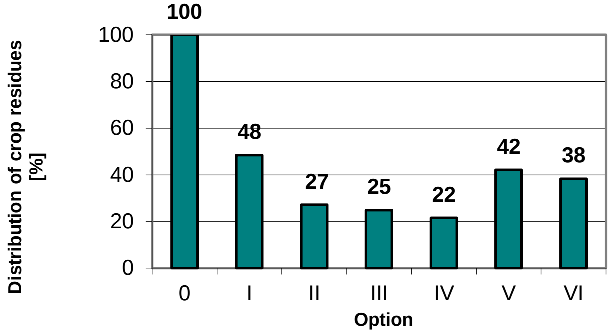

Figure 3. Distribution of crop residues by different variant of tillage.

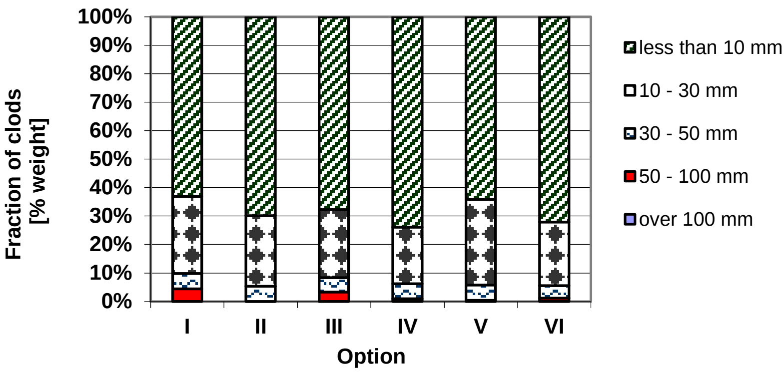

Figure 4. Clods fraction by different soil tillage.

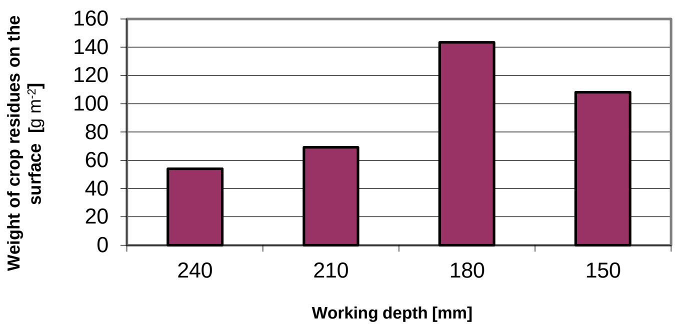

Figure 5. Weight of crop residues according to working depth.

In the measurements on the second field sweep tiller work quality was evaluated according to work speed and work depth (evaluation of sweep tiller by stubble ploughing after winter wheat harvest without straw collection). On the experiment field divers' variants were marked according to different working speed and different working depth. Very important for observation is distribution plant residues after stubble ploughing in work-in-process level and rate of plant residues on the top of soil. There was recognized significant important difference of plant residues distribution in different work depth (Fig. 5). The working speed (Fig. 6) did not have statistically significant difference in the variants with different working speed by the same depth level.

Plant residues distributions in soil level were evaluated according to working speed, for 4 different speeds in 4 depth levels. Working speeds didn´t have significant influence on crop residues distribution in different depth levels. Experiment had 5 repetitions for each working speed with the same results.

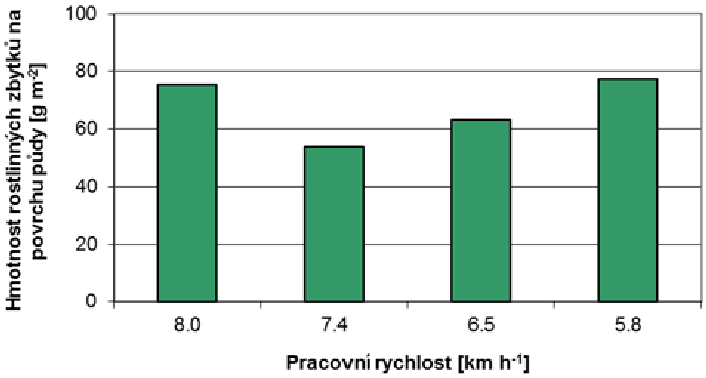

Figure 6. Weight of crop residues according to working speed.

Evaluations of crop residue distribution in a tilled soil profile give these results. The most of residues is covered by soil in depth from 0 to 60 mm and on the soil surface (Table 1). Evaluation was made for 4 different working speed (5.8; 6.5; 7.4 and 8.00 km h^{-1}) and every measurement was five time repeated (numbers 1–5 in Table 1). In depth 60 to 120 mm is it smaller part of total quantum crop residues and in a lower layer there aren´t any crop residues. By tillage by this kind of tiller by different working speed and different working depth the plant rests are covering up to maximum 120 mm depth. Between variants there isn't significant statistical difference.

Table 1. Weight of crop residues in different working layers

Working layer	Weight of crop residues, g m^{-2}				
	1	2	3	4	5
Surface	94	156	104	241	122
Depth 0–60 mm	514	403	320	520	213
Depth 60–120 mm	59	62	62	32	160
Depth 120–180 mm	0	0	0	0	0

In the Fig. 7 is described different ratio of covering the soil surface. According to Johnson (1988) surface must be covered more than 30%. This is the main signature of conservation soil tillage technologies. By measurement on experimental field was soil surface covered from 28 to 42%. So this tiller is suitable for conservation soil tillage technologies.

CONCLUSIONS

Results of this work are important because conservation (minimal) soil tillage technologies play an important role in plant production. Especially conservation tillage systems with their modification are increasingly being introduced under an economic pressure on the fields around the world. By evaluation working quality of sweep tiller and discs tiller we can say that sweep tiller puts more residues on the surface than disc tiller. But by second tillage by discs tiller covered plant residues are coming up on the surface and the number of plant rests is similar to tillage by sweep tiller.

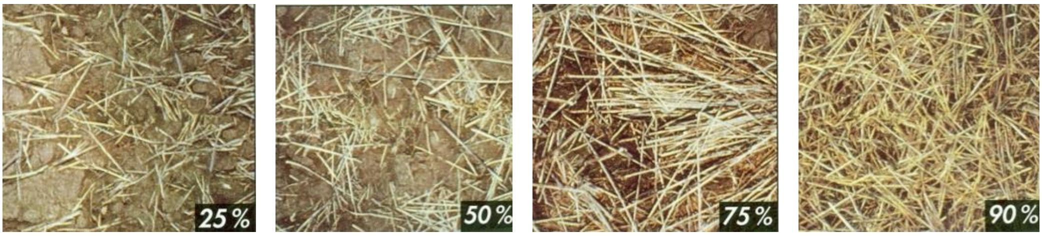

Figure 7. Soil surface covered by plant residues.

It is interesting that by shallow tillage by sweep tiller the crop residues are put in to upper layer and soil surface as well. In all scale of working depth the soil contains crop residues to the depth of 120 mm. Lower layers are only tilled but without crop residues which are normally found in deep layer by classical ploughing. It means that soil tillage based on shallow tillage have a very good influence on a soil protection against water and wind erosion.

ACKNOWLEDGEMENT. This paper has been supported by the Ministry of Agriculture of Czech Republic as part of research project QH82191.

REFERENCES

Anken, T., Hilfiker, T., Sandri, R. & Sartori, L., 1997. *Bodenbearbeitungssysteme*. FAT Bericht Nr. 484, FAT, Taenikon, 14 p. (in German).

Andrews, A.C., Clawson, R.A., Gramig, B.M. & Raymond, L. 2013. Why do farmers adopt conservation tillage? An experimental investigation of framing effects. *Journal of soil and water conservation* **68**(6), 501–511.

Hůla, J., Procházková, B., Badalíková, B., Kovaříček, P., Kumhála, F., Dryšlová, T., Kroulík, M., Neudert, L., Křen, J. & Mayer, V. 2002. *Vliv minimalizačních a půdoochranných technologií na plodiny, půdní prostředí a ekonomiku*. ÚZPI, Praha, 104 pp. (in Czech).

Johnson, R.R., 1988. Soil engaging effects on surface residue and roughness with chisel-type implements. *Soil Science Society of America Journal* **52**, 237–243.

Lhotský, J. 2000. *Zhutňování půd a opatření proti němu*. ÚZPI, Praha, 63 p. (in Czech).

Powers, D.H. & Skidmore, E.L. 1984. Soil structure as influenced by simulated tillage. *Soil Science Society of America Journal* **48**(4), 879–884.

Agronomy Research **12**(1), 135–142, 2014

Measurement of stubble cultivator draught force under different soil conditions

P. Novák[1], J. Chyba[1], F. Kumhála[1,*] and P. Procházka[2]

[1]Czech University of Life Sciences in Prague, Faculty of Engineering, Department of Agricultural Machines, Kamýcká 129, CZ; *Correspondence: kumhala@tf.czu.cz
[2]BEDNAR FMT s.r.o., Lohenická 607, Prague-9 Vinoř, 19017 Prague, Czech Republic

Abstract. Knowledge of the energy demands of the machines for soil tillage is a useful factor for machinery design as well as farm management. It was decided to measure the draught force necessary for the operation of the stubble cultivator Ecoland 4000 from BEDNAR FMT Co.
The measuring set was composed as follows: pull tractor John Deere 8220 pulled by a rod in which the load cell was placed, another tractor John Deere 8345R. A cultivator type Ecoland 4000 (4 m working width) was mounted on the second pulled tractor. Measurements were carried out on two different soil types (light sandy and loamy) at operational speeds 6, 8 and 10 km h^{-1} and at two different adjusted depths of loosening.
The soil physical properties were characterized by cone index measurements which were measured with a penetrometer PN-10 with cone angle 30° and area 100 mm^2.
The results showed an about 30% increase in the draught force at work in clayey soil in comparison to sandy soil. Different quality of tillage was also observed on different soil types.

Key words: soil tillage, draught forces, soil properties.

INTRODUCTION

Soil mechanical resistance is an indicator of the mechanical properties of the soil. Soil mechanical resistance may be influenced by many factors such as: soil compaction, soil texture, water content, and other parameters (Adamchuk & Christenson, 2005). In trailed machines for soil tillage, the volume of draught force is critical with respect to the field operation energy demands. The draught force of soil tillage machines is affected by conditional parameters such as: tool type, working width, working depth, and working speed. The second area of factors influencing draught force are the factors dependent on the site, such as soil type, soil bulk density, soil moisture (Arvidsson et al., 2004), and relief (Schutte & Kutzbach, 2003). Other factors affecting the final value of draught force are tool condition and tool adjustment.

Paul (1992) performed mapping of draught force on the experimental plot of the Federal Agricultural Research Centre Institute in Braunschweig. A data logger recorded the signal from the strain gauge pins of the tractor and the speed measured by a radar. Besides the abovementioned, the author also recorded the overall slippage. The result of the measured values was in compliance with the dependence of draught force on various soil types within the experimental plot. Based on the results, Paul (1992) concluded that soil moisture significantly influenced the overall slippage of the tractor.

Van Bergeijk & Goense (1996) attached sensors on a modified mouldboard plough which sensed the working width and depth. Draught force was measured by strain gauge pins attached on the lower links of a three-pint hitch and by an additional measuring frame between the tractor and the mouldboard plough. The immediate position was recorded by a GPS receiver. The draught force when ploughing ranged between 30–50 kN m^2. Van Bergeijk & Goense (2001) repeated the measurement on the same field to determine the effect of the clay content in the soil on the draught force. After two years of experiments, the draught force values and maps prepared by the Kriging method showed high dependence of draught force on clay content.

Droll (1999) estimated the main sources of errors during measuring, such as: soil roughness, tractor and tool oscillations, speed differences, soil moisture content differences, variability of plot, etc. McLaughin et al. (2000) reached similar conclusions.

Kheiralla et al. (2004) used three steel octagonal ring transducers to measure draught on a three-point hitch. During the experiment on sandy clay loam soil, the following equipment was compared: mouldboard plough, disk plough, disk harrow, and rotary tiller. A similar experiment was performed by Chen et al. (2013). Chen performed an experiment with 180 mm wide sweep and with the angle of 80°. The experiments were performed at working speed 3.19 km·h^{-1} on three different soil types: coarse sand, loamy sand, and sandy loam. The results showed that the lowest values of draught force were observed with coarse sand soil (0.292 kN) compared to loamy sand soil (0.430 kN) and the highest values were observed with sandy loam soil (0.585 kN). These results were used for a discrete element model for soil-sweep interaction. Similar measurements were performed even before 1996 by Glancey et al. (1996).

Current knowledge of draught force could be a useful tool in many ways. The results can be used in routine practice to compare the energy performances of tillage technologies, for verification of technical changes to working tools, working tool optimization, and verification of agronomical measures (Kroulík, 2013).

MATERIALS AND METHODS

Field measurements took place in Písková Lhota in Central Bohemia. The measurements were taken on the 10^{th} of October, 2013.The soil type was classified as mostly sandy and loam. Spring barley was grown on the field before the measurements with an average yield of 5.2 t ha^{-1}. Straw was crushed and dispersed on the land during harvest. After the harvest, the stubble was loosened by a mounted disk cultivator of Stromexport (BEDNAR FMT) ltd. to the depth of 0.1 m in August 2013. The fields were sprayed three weeks before measurement (liquidation of second growth) with a non-selective herbicide (glyphosfate).

The tractor John Deere 8220 and cultivator Stromexport (BEDNAR FMT) ltd. Ecoland EO 4000were used to measure the tensile draught force. The working width of the machine was 4 m. For actual measurement, an instrument for measuring draught force developed in collaboration of the Czech University of Life Sciences and BEDNAR FMT ltd. (formerly Stromexport) was used. John Deere 8345R (Fig. 1) served as the pulling tractor. The tractor John Deere 8220 had an engaged gear and was released during measurements and served only for lifting and lowering of the cultivator. The draught force was provided only by the tractor John Deere 8345R.

Figure 1. Measuring set. From right: pulling tractor John Deere 8345R, measuring instrument, pulled tractor John Deere 8220 for lifting and lowering of the cultivator, cultivator Ecoland EO 4000.

A basic part of the measurement apparatus was a strain gauge load cell S-38 with the measuring range of up to 200 kN. The load cell had to be placed into a steel cage so that forces were applied only in tension or compression. Bending of the load cell may cause its destruction. The load cell was calibrated on a stationary workplace. Callibration was carried out on a tensile testing machine ZDM 50t. The data from the load cell were sensed every 2s into a laptop which was situated in the cabin of the tractor. The measuring equipment was complemented by hinges for mounting between the pair of tractors (Fig. 2).

Figure 2. Measuring equipment between the pair of tractors.

Firstly, series of measurements were performed without recess of the cultivator. This measurement was used to determine the rolling resistance of the tractor with a tiller. Then the cultivator was set at processing depth 0.1 m. The measurements were performed with the tiller lowered at speeds of 6, 8 and 10 km h^{-1}. The measurements were performed on light sandy soil and consequently on loamy soil in the second part of the plot. Then, the working depth was set to the depth of 0.15 m. Again, the measurements were made for alternative speeds 6, 8 and 10 km·h^{-1}. The measurements were also performed for both types of soil.

Additional measurements of the physical properties of the soil were carried out by a penetrometer PN-10 which was developed at CULS Prague. It uses a probe with a cone angle of 30° and area of 100 mm^2. Furthermore, the transverse profile of the soil was uncovered for determination of the quality parameters of the tillage.

RESULTS AND DISCUSSION

The calibration results and calibration curve can be seen in Fig. 3. The linear dependence of the measuring apparatus output frequency on tensile force was proved. The resulting linear dependence was used as a calibration equation for draught force calculation.

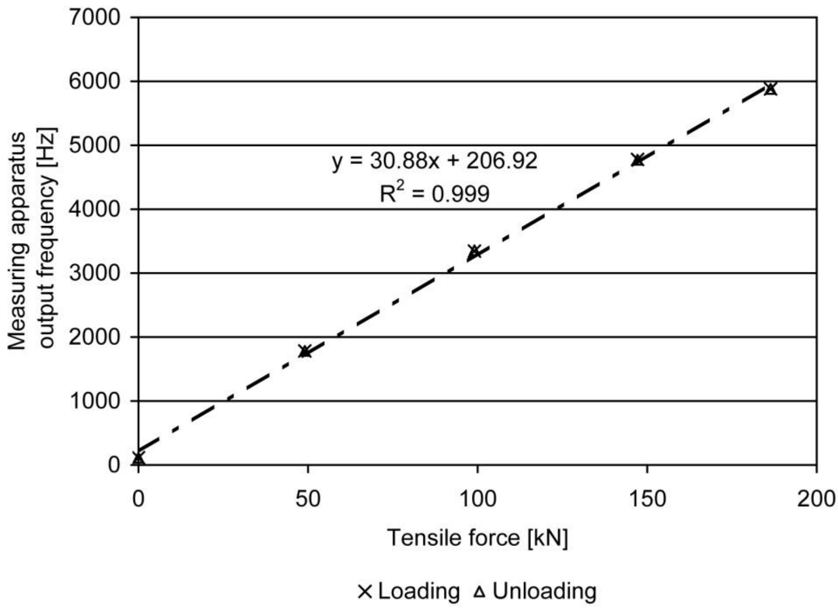

Figure 3. Dependence of the measuring apparatus output frequency on tensile force. Load cell calibration curve.

The graph in Fig. 4 shows the measured results of the loosened soil to the depth of 0.1 m, the measured values are relative to 1 m of width. The cultivator worked at the upper limit of its working range. The soil was intensively lifted and blended by the tines. Only the upper part of the soil profile and the crushing effect caused by the tines were cut off. These facts also correspond to the process of measuring. The results showed a linear increase in draught force along with the working speed. This applied for sandy soil and loamy soil. Furthermore, the results demonstrated the influence of soil type on draught force. Increased traction in soils with a high content of clay particles was observed at all operating speeds.

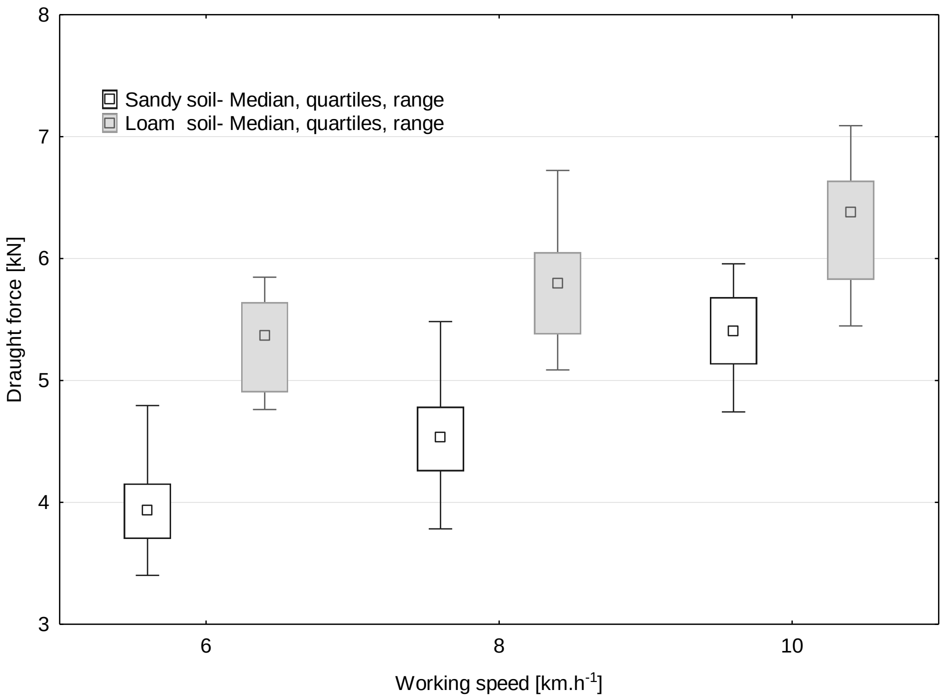

Figure 4. Dependence of draught force on working speed for sandy and loamy soil – working depth 0.1 m.

Fig. 5 shows the results of the measurement of tensile force at the depth of 0.15 m. The cultivator worked very intensively with the change of the working depth. The soil was picked up and intensively mixed with crop residues by the tines. The work of the cultivator showed improvement of qualitative parameters (soil mixing, breast size, cross profile of bottom). The course of tensile draught force was quite different from the measurements at the depth of 0.1 m. No correlation between the increased tensile force and working speed was found. Conversely, a greater dependency on the soil type can be observed. This is probably caused by movement of the soil over coulter and its surrounding areas. A soil layer was created in the course of work that was moved with the tines during the movement forward. The weight of this material probably increased draught force. At the same time, it may not decrease with decreasing working speed.

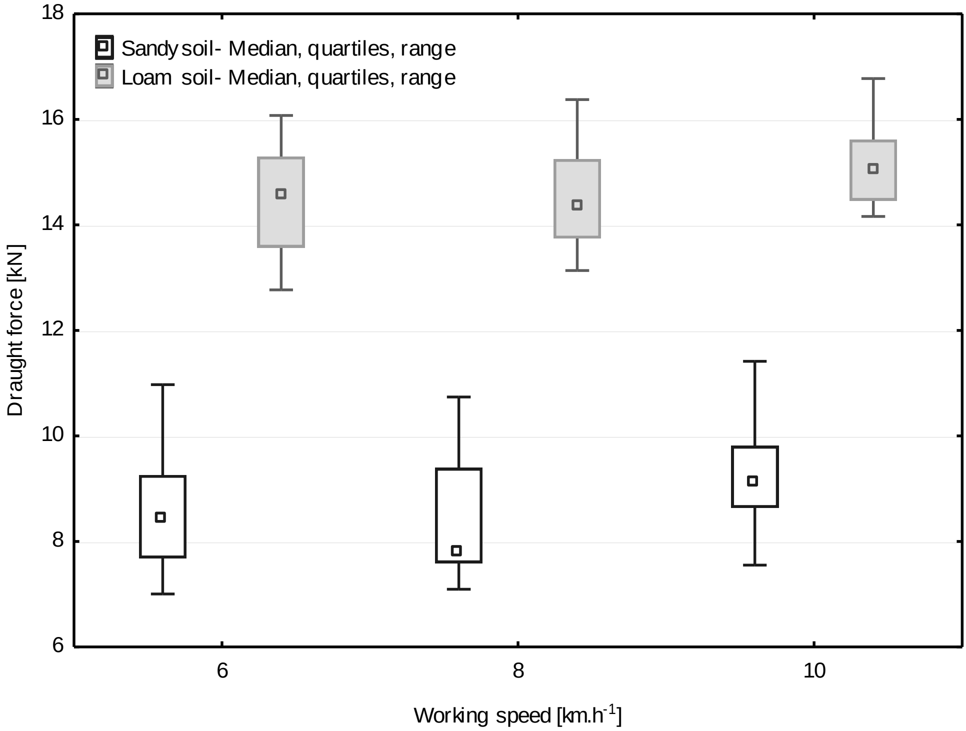

Figure 5. Dependence of draught force on working speed for sandy and loamy soil – working depth 0.15 m.

Measurement of the cone index is shown in Fig. 6. The cone index is graphically expressed for 4 depths. The figure shows that a higher content of clay particles in the soil influenced the cone index values. This is likely due to the different soil moisture content. For example, in the surface layer, the average moisture content of sandy soil is below 8.7%. The cone index value increased significantly with measured depth, which can be expected in these types of soils. The impact of soil tillage technology was also evident. In this case, reduced soil tillage had been conducted for several years. There was no obvious layer of soil, which would be significantly compacted (e.g. technogenic compaction). In contrast, relative to the absolute values of the cone index of soil, the soil was in good condition in terms of physical properties.

The research results confirmed the conclusions about draught force research in the area of soil tillage (Chen, 2013; Glancey, 1996; Paul, 1992; Arvidsson et al., 2004; Schutte & Kutzbach, 2003).

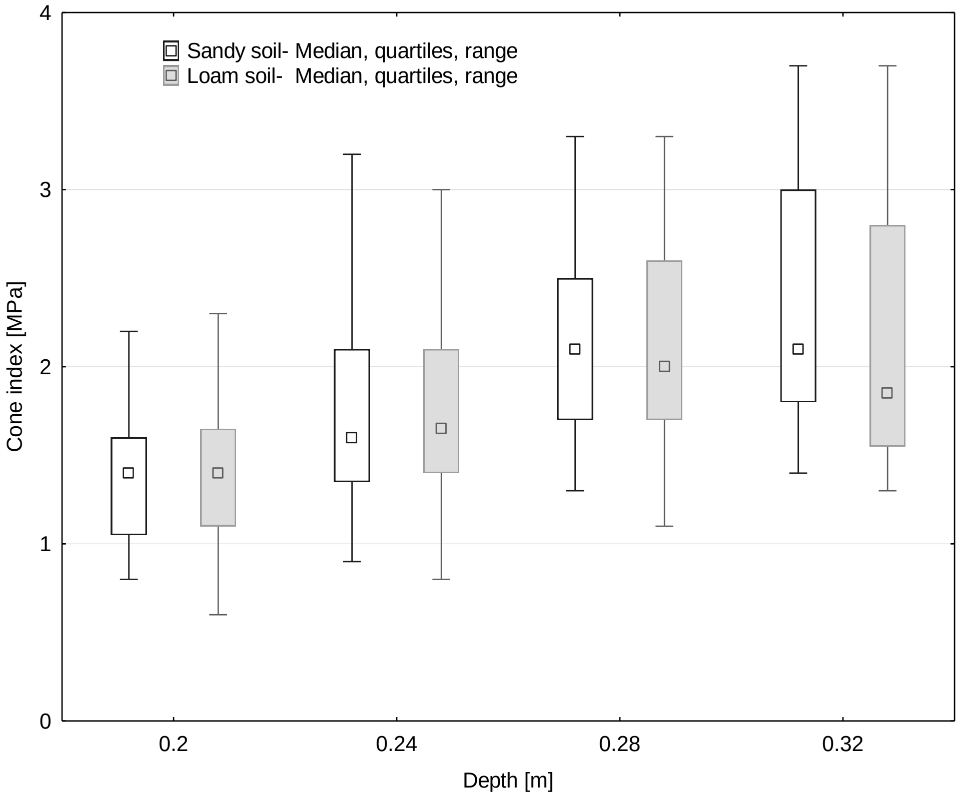

Figure 6. Results of the cone index measured by a penetrometer PN-10 on sandy and loam soil.

CONCLUSIONS

The measurements showed the influence of soil type on draught force during the measurement of ploughshare plow. Conversely, the influence of working speed on draught force has not been proven when using this cultivator. However, it can be assumed that a different type of cultivator tines with different geometries would behave in a different way in terms of tensile strength under these soil conditions, depending on the depth and forward speed. When selecting the cultivator, it is always advisable to perform a test operation in the conditions where the cultivator will be used. It is used to optimize the costs in terms of fuel consumption, wear of the tines, and time management in compliance with agro-technical terms.

ACKNOWLEDGEMENT. This work was supported by BEDNAR FMT Co. by kindly lending a cultivator and by measuring device design and manufacturing, and by Agriculture Cooperative Písková Lhota by kindly lending tractors and agricultural land.

REFERENCES

Adamchuk, V.I. & Christenson, P.T. 2005. An integrated system for mapping soil physical properties on the- go: the mechanical sensing component. preceded **In**, *Precision Agriculture ’05*, Wageningen Academic Publishers, pp. 449–455.

Schutte, B. & Kutzbach, H.D. 2003. Evaluierung von ortsspezifischen Zugkraftmessungen bei der Bodenbearbeitung. Preceded **In**, *Agricultural Engineering 2003*, Tagng Landtechnik, Hannover, pp. 299–304.

Paul, W. 1992. Zugkraftmessungen zur Teilschlagkartierung. *Landtechnik*, **47**, 490–491.

Van Bergeijk, J. & Goense, D. 1996. Soil Tillage Resistance as a Tool to Map Soil Type Differences. Preceded **In**, *the 3rd Int. Conf. On Prec. Ag. (1996)*, Minneapolis, Minnesota/USA.

Van Bergeijk, J. & Goense, D. 2001. Soil Tillage Restiance as a Tool to Map Soil Type Differences. *Journal of Agricultural Engineering Research* **79(**4), 371–387.

Droll, P. 1999. Erstellung von geokodierten Karten mit Bodenkennwerten. Msc, thesis (Diplomarbeit Hohenheim), unpublished (unveröffentlicht), (in German).

Mclaughin, N.B. & Burtt, S.D. 2000. Spatial Mapping of Tillage Energy. Preceded **In**, *the 5th Int. Conf. On Prec. Ag. (2000)*, Bloomington, Minnesota/USA.

Chen, Y., Munkholm, L.J. & Nyord, T. 2013. A discrete element model for soil–sweep interaction in three different soils. *Soil & Tillage Research* **126**, 34–41.

Kheiralla, A.F., Yahya, A., Zohadie, M. & Ishak, W. 2004. Modelling of power and energy requirements for tillage implements operating in Serdang sandy clay loam, Malaysia. *Soil & Tillage Research* **78**(1), 21–34.

Glancey, J.L., Upadhyaya, S.K., Chancellor, W.J. & Rumsey, J.W. 1996. Prediction of agricultural implement draft using an instrumented analog tillage tool. *Soil & Tillage Research* **37**(1), 47–65.

Kroulík, M. 2013. Technique in precision agriculture technology. Thesis submitted in fulfilment of the requirements for the associate professor. Czech University of Life Sciences Prague. (in Czech).

Agronomy Research **12**(1), 143–150, 2014

Research of a material and structural solution in the area of conventional soil processing

P. Novák[1,*], M. Müller[2] and P. Hrabě[2]

[1]Czech University of Life Sciences in Prague, Faculty of Engineering, Department of Agricultural Machines, Kamýcká 129, CZ; *Correspondence: novakpetr@tf.czu.cz
[2]Department of Material Science and Manufacturing Technology, Faculty of Engineering, Czech University of Life Science

Abstract. Sustainability in the area of agricultural commodities production depends on soil processing. Ploughshare is one of the most strained parts of a ploughing body and huge requirements are put on it. It has to meet relatively high strength requirements on one hand and high wear resistance on the other hand.
The aim of the research is to increase the service life of the ploughing body by means a structural and material solution. Increasing the service life of a ploughshare by means of overlaying is a much discussed topic. The types of overlay materials of carbides (Soudokay A43-0, OK Tubrodur 14.70, OK Tubrodur 15.82) and martensitic (Filarc PZ 6159) were used. Further, new a functional surface was distinguished for reinforcement of the ploughshare cutting edge. A method of size and mass analysis in field tests was chosen for measurements of the ploughshares service life.

Key words: functional surface, overlays, ploughshare, service life, wear.

INTRODUCTION

The main problem connected with using soil processing machines is their wear owing to the particles embedded in the soil (Chotěborský et al., 2008; Doubek & Filípek, 2011; Hrabě & Müller, 2013; Kejval & Müller, 2013; Müller et al., 2013).

The abrasive wear can be decreased to an acceptable level by means of suitable technologies and choice of material for the production of the whole tool or its part in the area of the highest wear (Horvát et al., 2008; Hrabě & Müller, 2013; Valášek & Müller, 2013). The newest researches try to find and use such procedures in ploughshare production which would ensure decreasing of the friction between the working tool and the soil (Votava et al., 2007; Horvát et al., 2008; Chotěborský et al., 2008; Doubek & Filípek, 2011; Hrabě & Müller, 2013; Kejval & Müller, 2013). This would lead partly to increasing the service lives of the parts under the heaviest load and partly to decreasing soil resistance which would save fuel (Müller & Valášek, 2012).

There are a lot of approaches to increasing the ploughshare service life (Müller & Hrabě, 2013). A significant problem is changing the ploughshare geometry when the reaction of the vertical force is also changed which affects the depth of the plough in the furrow (Hrabě & Müller, 2013).

The properties of the functional surface of the tools and parts are can be usefully changed at keeping original properties below the surface. One of the effective solutions is increasing the wear resistances of the tools processing the soil by means of overlays while creating a new functional surface with an aim to improve the current properties (Chotěborský et al., 2009).

It is possible not only to create a wear resistant surface, but also to use various geometric settings of the overlaying layer (that means the bead) at the same time with the aim to copy the course of draining off of processed soil and to create a serrated cutting edge. An example of a serrated cutting edge is combined shares of tactical knives. A significant benefit of this solution is a possibility to divide the material in an effective way and to sink. These elements taken over from observing the nature enable to process the soil in an effective way and simultaneously decrease the tool wear at the application on the ploughshares.

Recently, creation of a new functional surface or renovation of a relatively large area have been preferred (Natis et al., 2008). A negative of this solution is the change of the geometry, increasing of the cross-section and the related energetic demands and significantly increasing the price of the tool (Natis et al., 1999).

Soil is a considerably abrasive medium which affects the tools processing the soil in a negative way. The aim of the research is to increase the service life of the ploughing body by means of a structural and material solution.

MATERIALS AND METHODS

The solution is based on creation of a new functional surface. The research was focused on increasing the service life of ploughshares by overlaying oblique deposited overlay material which is abrasive wear resistant. Increasing the ploughshare service life by means of overlaying is a much discussed topic. Further, a new functional surface was distinguished for reinforcement of the ploughshare cutting edge. A method of size and mass analysis in field tests was chosen for measurements of the service life of ploughshares.

A change to the tool's shape, a mass loss and changes to the cutting edge shape were observed within testing the tool's service life under field conditions. A five-share plough was used for the field tests. The experiments took place on a piece of land in the settlement Neperská Lhota near Benešov and mainly gravelly soil was found on this piece of land. The ploughing resistance was very high and the abrasive wear was above the average. This soil was chosen on purpose owing to the extreme wear at ploughing under these conditions. Changes to the sizes, the mass and the geometry were observed after each 2 ha of ploughing. The entire ploughed area within the experiment was 18 ha. The reason for that was keeping approximately the same soil conditions within the chosen piece of the land. Measurements were performed at all five ploughshares, of which four were overlaid and one had not been treated (a comparing etalon). The comparing etalon was a standardized share from the final manufacturing.

Overlay materials of types carbides (Soudokay A43-0 (described as M4), OK Tubrodur 14.70 (described as M1), OK Tubrodur 15.82 (described as M2)) and a martensitic one (Filarc PZ 6159 (described as M3)) were used.

A new functional profile was created by means of overlaying electrodes on a conventional tool in such a way that the draining off of the processed soil was respected (that means oblique overlays). The oblique depositing of the overlaying bead, i.e. locating of the overlays was chosen with respect to the direction of the action of abrasive particles on the share at its relative motion through the soil. An angle cca 45° to the share cutting edge was set according to the wear of the used share. The necessity to reinforce the peak and the end of the cutting edge was obvious from previous experiments. In addition to increasing the service life, a serrated self-sharpening effect was also expected with this solution. Fig. 1 shows a schematic presentation of the geometrical solution.

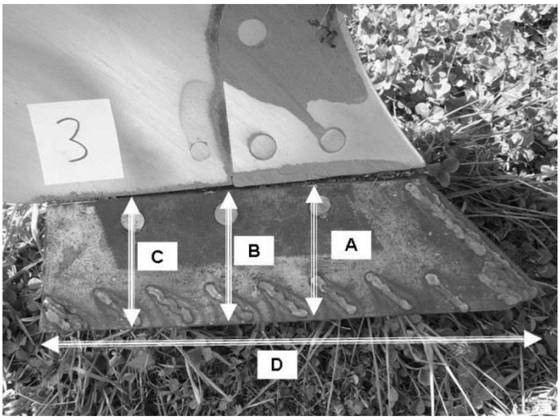

Figure 1. Ploughshare with oblique overlay and positions of the measurement points.

A method of a dimension and mass analysis was chosen for measuring the ploughshare service life. During the field test, single dimensions (marked A to C) of adjusted and standard ploughshares were measured after approximately each 2 ha of ploughing. The places for measuring the dimensions passed through the axis of the holes for fitting to the frog.

Further, the bottom edge of the ploughshare cutting edge (marked D) and the length of the share face (marked F) were measured.

At first, the layer of the finishing coat was removed manually from the shares. The shares were overlaid with hard faced metal in the form of tube wires of a mean 1.6 mm by means of an automatic welding machine. It was a technique of overlaying by an electric arc flashing by a continually passed electrode. Because of the semi-automatic way of the overlaying, it can be stated that all overlays reached the same quality.

After each bead overlaying, the share was cooled to the temperature of approximately 60°C so that the basic material was not considerably heat influenced.

RESULTS AND DISCUSSION

The amount of deposited overlaid material with the oblique overlaying technique was 0.1 kg (share mass increased of 2%) for OK TUBRODUR 14.70 (M1), 0.05 kg (share mass increased of 1.02%) for OK TUBRODUR 15.82 (M2), 0.15 kg (share mass increase of 2.86%) for Filarc PZ 6159 (M3), and 0.1 kg (share mass increase of 1.90%) for Soudokay A43-0 (M4).

The results of single measurements are visible in Figs. 2 to 6. For correct evaluation, it is also important to determine the determination index R^2. It is the problem of the correlation analysis. The values of the determination index can range from 0 to 1.

The functions presented in Figs. 2 to 6 are determined by the equations in Table 1.

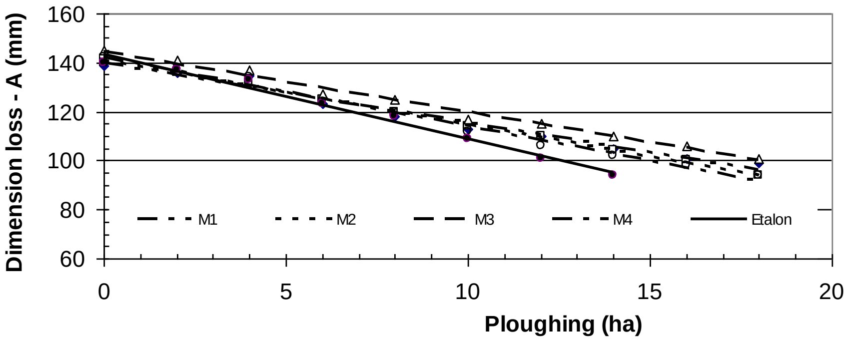

Figure 2. Course of share wear – dimension parameter A.

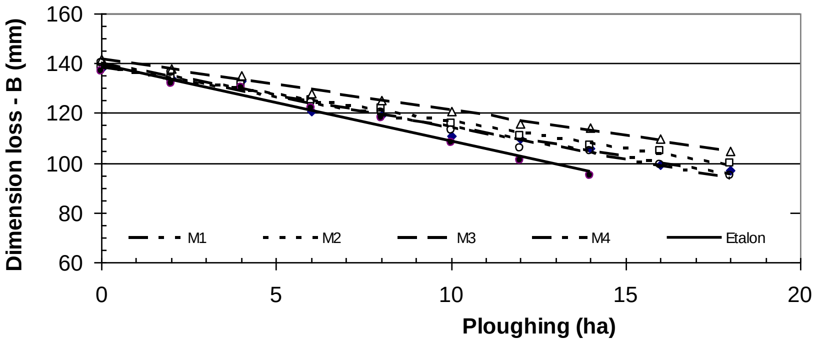

Figure 3. Course of share wear – dimension parameter B.

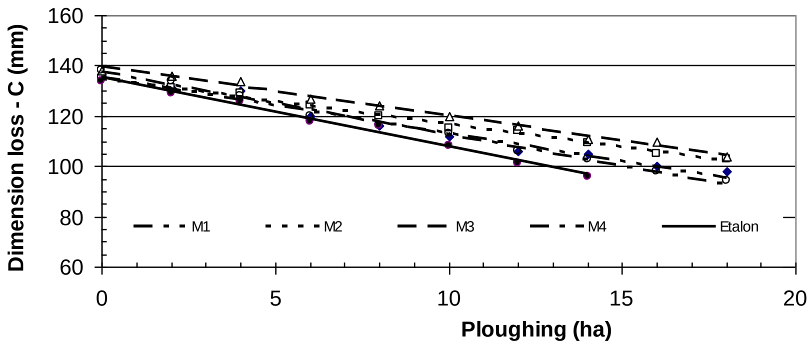

Figure 4. Course of share wear – dimension parameter C.

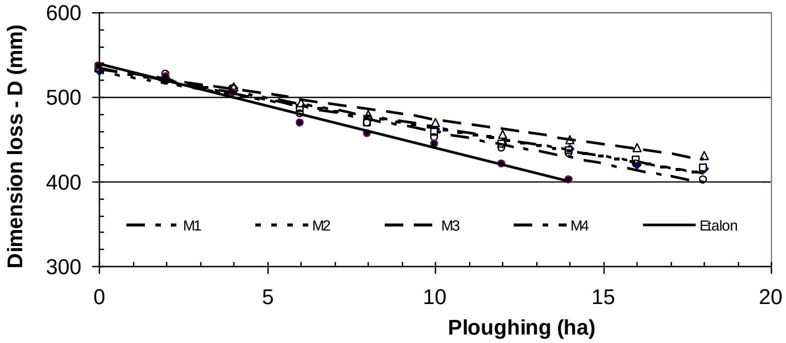

Figure 5. Course of share wear – dimension parameter D.

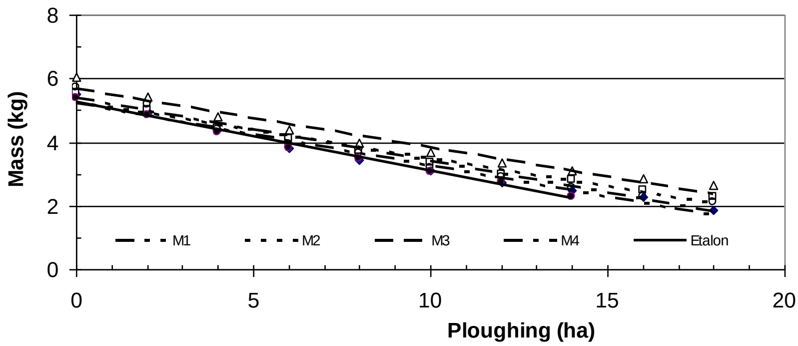

Figure 6. Course of share wear – mass.

Table 1. Equations of linear functions

Description	Functional equations	R^2	Description	Functional equations	R^2
M1 / A	y = -2.4212x + 139.69	0.97	M1 / C	y = -2.2121x + 135.31	0.98
M2 / A	y = -2.597x + 140.87	0.99	M2 / C	y = -1.8333x + 135	0.99
M3 / A	y = -2.4848x + 144.76	0.99	M3 / C	y = -1.9394x + 139.45	0.99
M4 / A	y = -2.8091x + 142.18	0.99	M4 / C	y = -2.4788x + 137.31	0.99
Etalon / A	y = -3.4464x + 143.5	0.99	Etalon / C	y = -2.75x + 135.25	0.99
M1 / B	y = -2.3939x + 138.35	0.98	M1 / D	y = -6.8242x + 532.22	0.99
M2 / B	y = -2.1606x + 138.35	0.99	M2 / D	y = -6.7121x + 529.91	0.99
M3 / B	y = -2.0424x + 141.78	0.99	M3 / D	y = -5.9212x + 532.89	0.99
M4 / B	y = -2.5758x + 139.98	0.99	M4 / D	y = -7.503x + 533.93	0.98
Etalon / B	y = -3.0893x + 139.5	0.98	Etalon /D	y = -9.8333x + 538.33	0.99
M1 / mass	y = -0.1952x + 5.22	0.98	M4 / mass	y = -0.1986x + 5.3827	0.97
M2 / mass	y = -0.1779x + 5.28	0.98	Etalon / mass	y = -0.2158x + 5.2542	0.99
M3 / mass	y = -0.1841x + 5,69	0.98	ploughshare type / place of measuring		

The graphical presentation of the results was performed by means of ANOVA by the least square method (Fig. 7). Tukey's HSD test was used for statistical comparison of the mean values. From the results of Tukey's HSD test, it was obvious that there were not statistically significant differences between the data sets at the significance level $\alpha = 0.95$. From the wear point of view, the comparing etalon already stopped being functional after 14 ha. This conclusion is essential from the perspective of keeping even shape of the share.

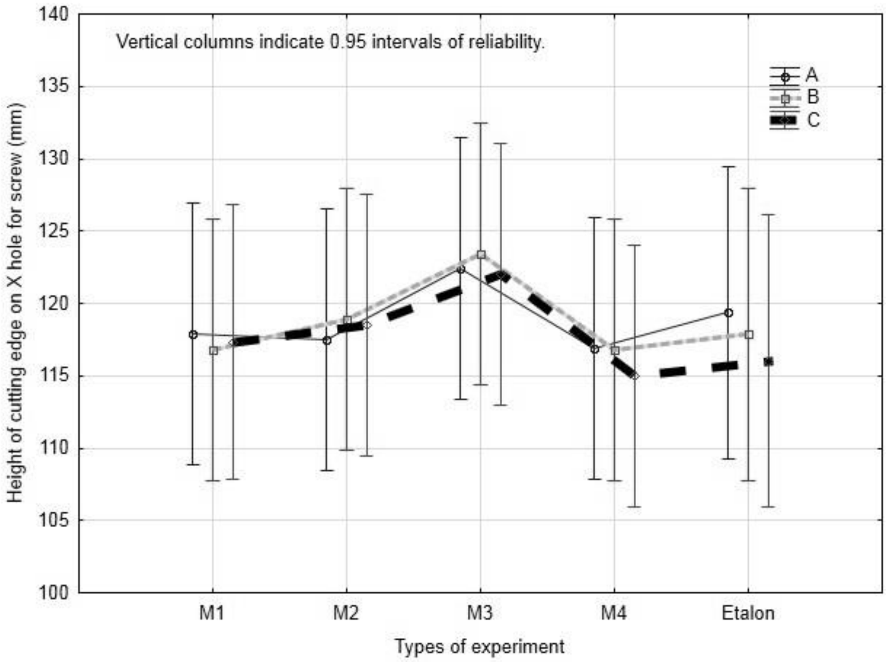

Figure 7. Change of cutting edge height depending on variant of the experiment.

Table 2 shows the particular means of statistically homogeneous groups, i.e. the cutting edge mass, the length of the bottom edge to the peak of the cutting edge and the change of the length of the share face. It is obvious from the results that no statistically significant differences exist between the data sets at the significance level $\alpha = 0.95$ within the evaluated variants of the experiment.

Table 2. Statistical comparison of mean values – Tukey's HSD test (H – homogeneity)

Tested variant of ploughshare	Mass (g)	H	Length of bottom edge to peak of cutting edge (mm)	H	Length of share face (mm)	H
M1	3.46	*	477.00	*	139.67	*
M4	3.60	*	469.50	*	130.70	*
M2	3.68	*	469.50	*	129.00	*
etalon	3.74	*	469.50	*	136.00	*
M3	4.04	*	479.60	*	140.20	*

Figs. 8 to 11 show the wear of the ploughshare.

Figure 8. Wear of ploughshare (M1) after ploughing 12 ha.

Figure 9. Wear of ploughshare (etalon) after ploughing 12 ha.

Figure 10. Wear of ploughshare (M1) after ploughing 14 ha.

Figure 11. Wear of ploughshare (M1) after ploughing 18 ha.

The research results confirmed the conclusions about the necessity of material and structural research in the area of soil processing (Doubek & Filípek, 2011; Chotěborský et al., 2008; Hrabě & Müller, 2013; Kejval & Müller, 2013; Müller et al., 2013; Natis et al., 1999; Natis et al., 2008).

CONCLUSIONS

The research in field conditions was focused on innovations of the ploughshare in the area of the conventional soil processing. The essence of the technical solution consists of using a direction and slope copying the draining off of processed soil; however, keeping the peak of the ploughshare and the possibility of effective production also have to be taken into regard.

It is possible to determine the following conclusions from the research result:

- Ploughing efficiency (that means the speed, fuel consumption, quality, etc.) is the most important from the practical user's perspective. This was definitely confirmed by the efficiency of the creation of the serrated ploughshare owing to the gradual wear. These conclusions can be made on the basis of the cutting conditions of the ´toothed cutting edge´.

- It is possible not only to create a wear resistant surface (overlays, forming) but also to use various geometrical setting of the overlaid layer (the bead) at the same time with the aim to copy the course of draining off of the processed soil. A ploughshare with the functional surface created this way is worn unevenly at ploughing.
- Increasing of the service life owing to the structural solution was proved. The service life increased by more than 20% on average. The ploughshare also preserved a suitable geometrical shape after finishing the field tests.
- The significant benefit is the fact that the suggested structural solution minimized the wear of the share face.

ACKNOWLEDGEMENT. Supported by the Internal Grant Agency of the Faculty of Engineering, Czech University of Life Sciences in Prague.

REFERENCES

Doubek, P. & Filípek, J. 2011. Abrasive and erosive wear of technical materials. *Acta Universitatis Agriculturae et Silviculturae Mendelianae Brunensis* **59**(3), 13–21.

Horvat, Z., Filipovic, D., Kosutic, S. & Emert, R. 2008. Reduction of mouldboard plough share wear by a combination technique of hardfacing. *Tribology International* **41**, 778–782.

Hrabě, P. & Müller, M. 2013. Research of overlays influence on ploughshare lifetime. *Research in Agricultural Engineering*. **59**(4), 147-152.

Chotěborský, R., Hrabě, P., Müller, M., Savková, J. & Jirka, M. 2008. Abrasive wear of high chromium Fe-Cr-C hardfacing alloys. *Research in Agricultural Engineering* **54**(4), 192–198.

Chotěborský, R., Hrabě, P., Müller, M., Savková, J., Jirka, M. & Navrátilová, M. 2009. Effect of abrasive particle size on abrasive wear of hardfacing alloys. *Research in Agricultural Engineering* **55**(3), 101–113.

Kejval, J. & Müller, M. 2013. Mechanical properties of multi-component polymeric composite with particles of Al2O3/SiC. *Scientia Agriculturae Bohemica* **44**(4), 237–242.

Müller, M. & Valášek, P. 2012. Abrasive wear effect on Polyethylene, Polyamide 6 and polymeric particle composites. *Manufacturing Technology* **12**(12), 55–59.

Müller, M. & Hrabě, P. 2013. Overlay materials used for increasing lifetime of machine parts working under conditions of intensive abrasion. *Research in Agricultural Engineering* **59**(1), 16–22.

Müller, M., Chotěborský, R., Valášek, P. & Hloch, S. 2013. Unusual possibility of wear resistance increase research in the sphere of soil cultivation. *Tehnicki Vjesnik-Technical Gazette* **20**(4), 641–646.

Natsis, A., Papadakis, A. & Pitsilis, J. 1999. The influence of soil type, soil water and share sharpness of a mouldboard plough on energy consumption, rate of work and tillage quality. *Journal of Agricultural Engineering Research* **42**(2), 71–176.

Natsis, A., Petropoulos, G. & Pandazaras, C. 2008. Influence of local soil conditions on mouldboard ploughshare abrasive wear. *Tribology International* **41**, 151–157.

Valašek, P. & Müller, M. 2013. Composite based on hard-cast irons utilized on functional parts of tools in agrocomplex. *Scientia Agriculturae Bohemica* **44**(3), 172–177.

Votava, J., Černý, M. & Filípek, J. 2007. Abrasive wear of ploughshare blades made of Austempered Ductile Iron. *Acta Universitatis Agriculturae et Silviculturae Mendelianae Brunensis* **55**(1), 173–182.

Agronomy Research **12**(1), 151–160, 2014

Efficient harvest lines for Short Rotation Coppices (SRC) in Agriculture and Agroforestry

R. Pecenka*, D. Ehlert and H. Lenz

Leibniz Institute for Agricultural Engineering Potsdam-Bornim (ATB), Max-Eyth-Allee 100, 14469 Potsdam, Germany; *Correspondence: rpecenka@atb-potsdam.de

Abstract. Wood from short rotation coppice (SRC) such as poplar, willow and black locust is a promising option for the sustainable production of biofuels and biomaterials. Provided that production technologies, logistic chains and end user structures are well designed in farmers' regional structures, these cropping systems may provide a secure source of income. One of the key problems at present is the lack of knowledge and powerful harvest machinery at practice. Although a lot of machines were developed and tested during the last 30 years, only a few have exceeded the prototype stage. Analysing the process chain for SRC, chip lines seem to be most cost-efficient for harvest, and the modification of forage harvesters for SRC is a promising option. But the high machine weight of forage harvesters is a serious disadvantage due to the limited trafficability of harvest plots in winter. Furthermore, for economic operation of these expensive harvest systems cultivation areas of more than 300 ha are required.
Therefore, ATB has developed a simple and low weight tractor-mounted mower-chipper for medium sized standard tractors (75–150 kW) together with the company JENZ (Germany). The chipper is designed for flexible harvest of wood from SRC and Agroforestry (max. stem diameter 15 cm). The total weight of the harvester (tractor and chipper) is less than 50% of the forage harvester combination resulting in much more flexible field operation and lower harvest costs. The machine has been successfully tested in the last two harvest seasons and is on the market available now.

Key words: Short rotation coppice, poplar, willow, harvest, mower-chipper, wood chips.

INTRODUCTION

Resulting from limited fossil energy resources, global warming, and safety problems in nuclear power stations, the material and energetic use of plant biomass comes more and more in the focus of public interest. Energy wood from farmland is a promising option for sustainable production of biofuels in agriculture and it may help to secure the income of farmers. Therefore, cultivation of fast growing trees (short rotation coppice – SRC), such as poplars (*Populus sp.*), willow (*Salix viminalis*), and black locust (*Robinia pseudoacacia L.*) is of increasing interest. In many European countries SRC plantations are introduced in common agricultural praxis. The cultivation area in Germany has been increased in the last five years from 2,000 ha to approx. 10,000 ha in year 2013 (Schütte, 2010; FNR, 2014). Analysing the current situation in the management of SRCs, several problems in cultivation and mechanization can be observed. In dependence to yield and cropping technology, harvesting cost is estimated to be 35 to 60% of the total costs of biomass production from SRC (Heiß, 2005; Bach, 2007; Scholz, 2007; Spinelli et al., 2009; Schweier & Becker, 2012a; Schweier & Becker, 2012b). Consequently, the optimization of harvest technologies is a prerequisite for the successful expansion of SRC plantations. Despite of more than 30 years of praxis experiences in several European countries, there is a lack of knowledge as well as efficient technical solutions for economic cropping of poplar, willow and black locust. A lot of machines were developed and tested during the last decades, but only a few have exceeded the prototype stage (Scholz et al., 2008).

Current status of harvesting technology

Basically, the existing harvest technology can be classified into the four groups: *Log Lines, Bundle Lines, Chip lines* and Bale Lines (Fig. 1). Numerous publications can be found about all these harvesting technologies in the last decades (Stokes & Hartsough, 1994; Hartsough & Stokes 1997; Scholz et al., 2008; Abrahamson et al., 2010; Schweier & Becker, 2012a; Schweier & Becker, 2012b, Savoie et al., 2012). Advantages and disadvantages, costs and harvest capacities were presented and discussed. Analysing the process chain in SRCs, it can be concluded that the high investment costs for suitable harvest equipment, low flexibility regarding tree variety and cultivation scenario as well as high machine weight accompanied by problems during harvest and low capacities are some of the most important obstructions at present.

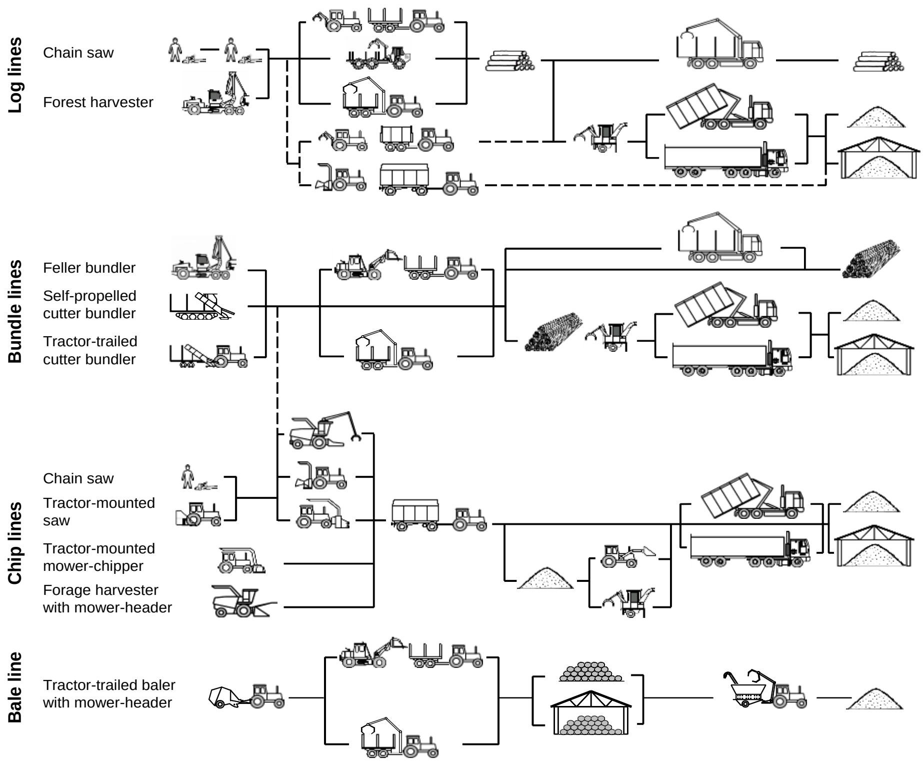

Figure 1. Systematics of harvest and post-harvest technologies for short rotation coppices.

Table 1. Forage harvester-based mower-chippers for SRC

Basic vehicles/ recommended power (KW)	Mower-feeder	Mass (kg) Harvester/ mower	Price (€) Harvester/ mower	Cutting width (mm)	Max. stem diameter (mm)
Class Jaguar 900-830 / 255	Salix HS2	11,000/1,200	337,000/98,000	1000	80
Krone Big X / 380	Woodcut	14,000/2,800	353,000/89,500	1500	< 150
New Holland FR 9000 / 450	130 FB	12,900/2,100	327,000/124,000	Double row with 750 mm distance	150
John Deere 7050 / 350	CRL	14,000/1,500	260,000/95,000	Double row row 750 mm distance	100
Mean value		Mass: 14,870	Price: 420,880		

As shown in Table 1, the mass of basic forage harvester vehicles range from 11 to 14 t. Together with the header units, a forage harvester equipped for SRC averages approximately 15 t in total mass and costs approximately 420,000 €. In addition, for the economic operation of these highly productive harvest systems, cultivation areas of more than 300 ha are required (Scholz et al., 2009), if the harvester is used for SRC cropping alone. The required minimum acreage will be reduced, if the harvester is used for forage during summer. But the reduction will be small taking into account that a high-power forager is necessary to realize satisfying working speeds at harvest of SRC, forest tires are indispensable to avoid damages, a enforced chipping drum is recommended and the cost of the SRC header alone is approximately 100,000 €.

Another group of mower-chippers is based on the use of common agricultural tractors (Table 2). These machines are mounted in front or at the back of the tractor. The required tractor power is up to 400 kW (KWF 2013). Most of these chippers also use a push bar to bend the trees and bring them in a horizontal position before chipping. Only a few developments have focused on harvest and chipping with mower-chippers of trees from SRC in an upright position (Stuart et al., 1983; Wieneke, 1993; Döhrer, 1995). In contrast to forage harvester-based solutions, the cutting unit (drum, cone or disc) is integrated in the tractor-mounted machine. To provide the required power and efficiency, the chipping units are mostly PTO driven. To drive the mowing and feeding units (screws, rollers or rotors), numerous hydraulic components, such as pumps, motors, valves, lines and oil tanks, are necessary. All these mechanical and hydraulic parts add up to machine masses from about 1 to 4 t. Together with the suitable basic tractor the complete harvesting unit can vary in mass and price over a wide range (Table 2). It should be noted that the maximum trunk diameter is very different for the various models. According to the working principle, e.g. the JF harvesters from NY VRAA are limited to 6 cm. Therefore, only willows with an age of 2 or 3 years can be harvested.

Table 2. Tractor-mounted mower-chippers for harvest in SRC

Machine	Mass (kg)	Price (€)	Field layout/ max. stem diameter
JENZ GMHT 140	3,500	85,000	Single or double row (1,400) / 140 mm
NYVRAA JF 192	900	21,000	Single row / 50–60 mm
NYVRAA JF Z20	1,500	28,000	Double row / 30–40 m
EBF Dresden	3,500	> 100,000	170 mm
SPAPPERI model RT	1,800	unknown	Double row / 180 mm
Required standard tractors 75–400 kW	6,000–10,000	75,000–200,000	

A few other prototypes of mower-chippers have been developed using the chassis from self-propelled vehicles or tractors without a standardised three-point linkage. In 1986, a Gandini forage harvester prototype was designed for black locust and poplar plantations, but due to several technical problems the project was terminated in 1994 (Hartsough & Yomogida, 1996). In 1994, Salix Maskiner presented a concept of a special mower-chipper for willow named the Bender (Baldini & Di Fulvio, 2009), and an enhanced version, the Bender 5, has been offered. The Austoft 7700/240 is an Australian harvester for sugar cane adapted for willow harvest (Hartsough & Yomogida, 1996; Kofman, 2012). The BR 600 biomass harvester, based on a self-propelled crawler tractor, has been presented by Plaisance Equipment (PLAISANCE 2013).

Based on the analyses of the current status of harvesting equipment for SRC, the following can be concluded:

- High harvest costs are one of the most limiting factors for increasing SRC acreage in Europe;
- There is no universal low-cost harvester for SRC available at a practical scale. Such harvester should be flexible regarding variety (poplar, willow, and black locust), tree size (stem diameter 2–15 cm), and field conditions (e.g., small fields, difficult soil conditions);
- A new principle for low-cost mower-chippers should be developed to support and increase the production of biomass in SRC.

DEVELOPMENT OF A TRACTOR-MOUNTED MOWER-CHIPPER

Basic requirements

Due to the unsatisfactory situation in SRC harvesting technology, a research project was initiated at the Leibniz Institute for Agricultural Engineering, Potsdam-Bornim, Germany (ATB) to develop a simple and low weight universal mower-chipper for stem diameters at base up to 15 cm. The mass of the unit should be less than 1,000 kg, and it should be mounted in front of medium-sized standard tractors (75–150 kW). To avoid problems with uprooting or breaking of trees while mowing and chipping, the stem should remain in the upright position. Based on own harvest experiences and especially serious problems during harvest of older double row plantations of poplar in Germany it has been decided to develop a unit for harvest of single row plantations only (Ehlert & Pecenka, 2013). For economic and trouble-free harvesting from a long-term perspective, only single-row SRC should be established in the future.

For the systematic development of a new working principle for a tractor-mounted mower-chipper, the following four main features must be realised:

- Simple and robust design of the mower-chipper unit;
- Simple and safe feeding of the mower-chipper with trees of different sizes;
- Avoid felling the trees in a horizontal position before chipping;
- Simple and sure conveying of the chips to the transport units.

Development of a simple and robust mower-chipper unit

The basic idea for the new mower chipper unit is shown in Fig. 2. To minimise the number of powered parts, the functions of mowing, chipping and conveying of chipped material were realised by a compact and simple unit (tool rotor) rotating in a robust housing. For tree mowing, the tool rotor of the prototype is designed as a disc saw with an outer diameter of 1,000 mm. For chipping of the severed stems, knives set on spacer blocks are installed on the upper side of the disk saw. Contrary to most mowing disks in other harvesters, the tool rotor is solid rather than slotted, thus avoiding chips falling on the ground of the field. As a result of this arrangement, the theoretical maximum chip length is limited by the sum of the height of the spacer block and the chipping knife. For an optimal chipping process, a counter bar is installed on the housing. After chipping, the comminuted material is accelerated and moved to the outer edge of the housing at a rotation speed of 1,000 rpm towards the discharge opening.

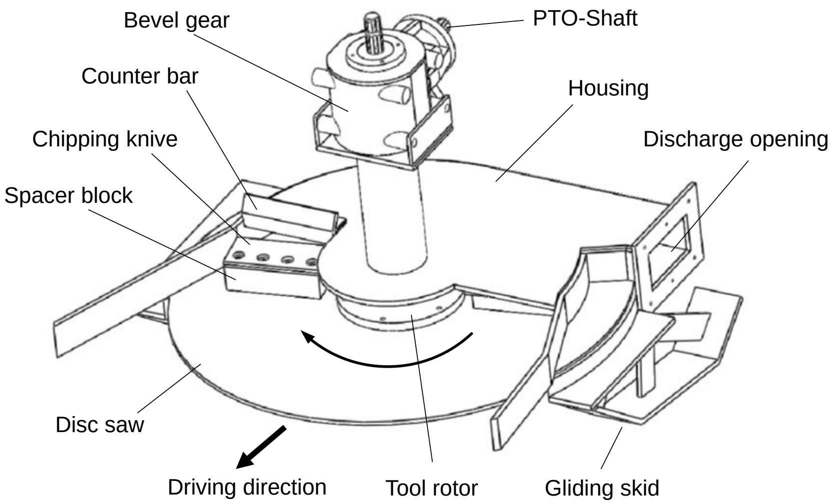

Figure 2. Principle of the ATB mower-chipper unit.

Development of the periphery for safe feeding of trees in upright position and conveying of chips to transport vehicles

The development of a means for failure-free feeding of the mower-chipper unit proved to be the most complicated task. Finally, safe feeding of trees with diameters of up to 150 mm can be realised by a combination of a fixed feeding auger and a spring loaded counter roller (Fig. 3). The field tests showed that trees after mowing sometimes fell ahead and sideways into horizontal positions, resulting in significant yield losses and poor chip quality (over length). To reduce these problems, the trees must be fixed before mowing. SRC trees can grow up to 10 m and more; therefore, they must be supported above their centre of gravity, which can be realised by using a telescoped mast with additional guiding elements. The best guiding and conveying effect was achieved during the tests with the combination of an active hydraulically driven star-wheel and a guiding arm with a barb.

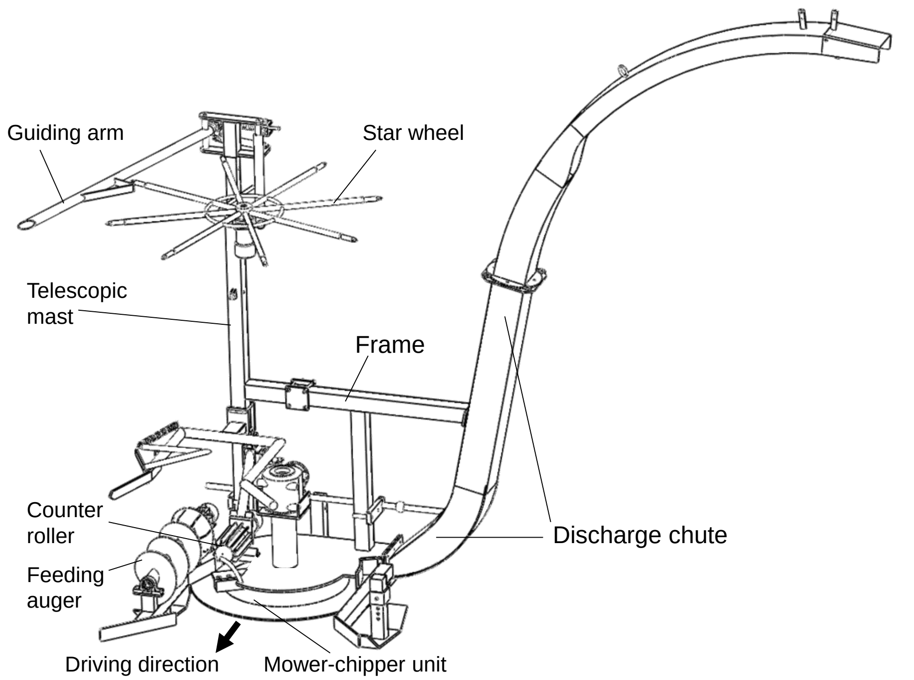

Figure 3. Principle of the ATB mower-chipper unit.

As shown in Fig. 2, the chips of the cutter-chipper unit are thrown off horizontally via the discharge opening. As a result, the material has to be deflected two times for nearby 180°for filling transport units. Tests under real conditions were performed to assess the conveying features of such a discharge shoot with two arcs (Fig. 3). The test results were surprisingly good. In spite of both arcs and a spout cross section area of only 175x175 mm blockages in the discharge shoot were not observed.

RESULTS AND DISCUSSION

The field tests have shown that the basic working principle of mowing and chipping trees in an upright position has significant advantages. The breaking and uprooting of trees during cutting can be completely avoided. The stumps showed a clear cut surface after mowing with the circular saw.

The weight of the complete tractor-mounted mower-chipper, tested until March 2013, was about 600 kg (Fig. 4). Tests performed in SRC with poplars and willows demonstrated the high potential of the new concept as a low cost mower-chipper for practical use on farms. The tool rotor was equipped with only one pair of knives for chipping during the tests. According to the height of the spacer blocks and chipping knives, the theoretical maximum length of the chips was 80 mm. Trees with base diameters of up to 15 cm and a height of 10 m were harvested during the tests. As shown in Fig. 5, the chips had a good quality for later drying during storage and firing in large-scale heating plants. Fig. 6 shows a comparison of coarse chips produced with the novel mower-chipper and typical fine chips produced with a forage harvester. If shorter chips similar to fine chips from forage harvesters have to be produced by the mower-chipper, the height of the spacer blocks can be reduced as well as the number of knifes can be increased.

Figure 4. ATB mower-chipper at harvest of poplar (2013).

Figure 5. Example of wood chips from poplar harvested with the prototype.

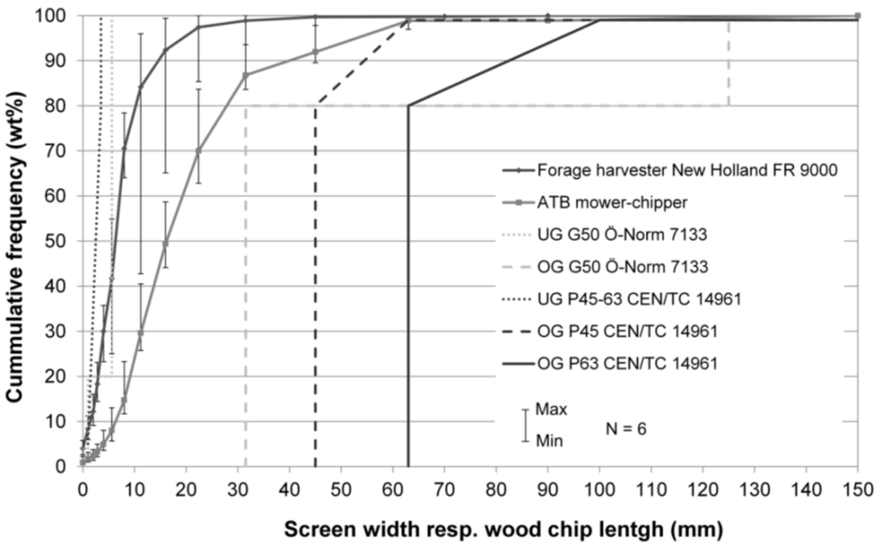

Figure 6. Particle size distributions of wood chips from poplar produced with different harvesters in 2013: Forage harvester New Holland FR 9000 … fine chips P 45/G30; ATB tractor-mounted mower-chipper … coarse chips P 45/G50.

The estimated economic advantages of tractor-mounted mower-chippers in comparison to forage harvesters presented in earlier studies (Ehlert & Pecenka, 2013) were based on effective speeds at harvest of approx. 3 km h^{-1}, versus effective harvest capacities of 0.4 to 0.8 ha h^{-1}. As shown in Table 3, effective speeds of 3 to 5 km h^{-1} were realized with the test unit. The tests were very promising for the future exploitation of the economic advantages of tractor-mounted mower-chippers in practice. Moreover, the full capacity of the mower-chipper unit couldn't be used completely during the field test because of the limited power of the tractor with 110 kW only.

Table 3. Technical data of the mower-chipper (prototype)

Machine parameter	Details
Embodiment	Tractor-mounted at front
Total mass	approx. 600 kg
Mower disk diameter	1020 mm
Tool rotor speed	1000 rev·min^{-1}
Number of teeth of the mower disk	34
Total power requirement	> 75 kW
Max. hydraulic pressure	180 bar
Hydraulic flow rate	45 l min^{-1}
Max. stem diameter	15 cm
Driving speed during chipping*	3–5 km h^{-1}
Specific energy demand*	3–5 kWh $t^{-1}_{d.m.}$

* measured at harvest of two and four years old poplars.

Based on these tests, important conclusions for enhancements of the investigated research machine to a prototype for tests at the practice scale were made. A commercial model of this mower-chipper is available since winter 2013/2014 (company JENZ - Germany, model: GMHS 100, Fig. 7).

Figure 7. JENZ Mower-chipper GMHS 100.

REFERENCES

Abrahamson, L.P., Volk, T.A., Castellano, P., Foster, C. & Posselius, J. 2010. Development of a Harvesting System for Short Rotation Willow & Hybrid Poplar Biomass Crops. *SRWCOWG MEETING*, Syracuse – NY, USA.

Bach, H. 2007. Willow Production and marketing in Denmark. *Bornimer Agrartechnische Berichte* **61**, 152–157.

Baldini, S. & Fulvio, D. 2009. Short Rotation Forestry: Mechanization for the conditions of Italy. *Mondo Macchina* **18**, 36–43 (in Italian).

Döhrer, K. 1995. Harvest technique for wood fields. *Die Holzzucht* **49**, 15–17 (in German).

Ehlert, D. & Pecenka, R. 2013. Harvesters for short rotation coppice: Current status and new solutions. *International Journal of Forest Engineering* **24**, 170–182.

FNR 2014. Fachagentur für Nachwachsende Rohstoffe – Cultivation area of renewable resources 2013. http://mediathek.fnr.de/grafiken/anbauflache-fur-nachwachsende-rohstoffe-2013-grafik.html. 31.01.2014.

Hartsough, B.R. & Stokes, B.J. 1997. Short rotation forestry harvesting–systems and costs. In Proceedings of the *1997 International Energy Agency: Bioenergy task 7, activity 2.1 and activity 4.3 workshop*, Melrose, (GB).

Hartsough, B.R. & Yomogida, D. 1996. Compilation of state-of-the-art mechanisation technologies for short-rotation woody crop production. *Research Report*, University of California, Biological and Agriculture Engineering Department, Davis (US).

Heiß, M. 2005. Auf Achievable gross margins from SRC in Austria. In Proceedings of the *Fachtagung Energieholzbereitstellung*, Wieselburg, AT (in German).

Kofman, P. 2012. Harvesting Short Rotation Coppice Willow. *COFORD Harvesting/Transport* **29**, 1–6.

KWF. 2013. Think first than invest, KWF- market overview for harvest technique for SRC. Groß-Umstadt: Kuratorium für Waldarbeit und Forsttechnik e.V., http://www.kwf-online.org/fileadmin/dokumente/Bioenergie/Dokumente/Kup-Ernter_2011.pdf. 22.05.2013.

PLAISANCE: mulchers, broyeur-récupérateur. Plaisance Equipments. http://www.plaisance-equipements.com. 22.05.2013

Savoie, P., Current, D., Robert, F.S. & Hébert, P.L. 2012. Harvest of natural shrubs with a biobaler in various environments in Québec, Ontario and Minnesota. *Applied Engineering in Agriculture* **28**, 795–801.

Scholz, V. 2007. Mechanization of SRC production. *Bornimer Agrartechnische Berichte* **61**, 130–143.

Scholz, V., Block, A. & Spinelli, R. 2008. Harvesting Technologies for Short Rotation Coppice – State-of-the-Art and Prospects. In Proceedings of the *Agricultural Engineering 2008 Conference and Industry Exhibition,* Crete, (GR).

Scholz, V., Eckel, H. & Hartmann, S. 2009. Processes and costs of SRC cropping on agricultural land. In *Die Landwirtschaft als Energieerzeuger. KTBL-Schrift* **476**, 67–80 (in German).

Schütte, A. 2010. Research and development for cultivation and utilization of wood from agriculture. In Proceedings of the *Symposium Agrarholz 2010*, Fachagentur für Nachwachsende Rohstoffe, Berlin, DE (in German).

Schweier, J. & Becker, G. 2012a. Harvesting of short rotation coppice-harvesting trials with a cut and storage system in Germany. *Silva Fennica* **46**, 287–299.

Schweier, J. & Becker, G. 2012b. New Holland forage harvester's productivity in short rotation coppice: Evaluation of field studies from a German perspective. *International Journal of Forest Engineering* **23**, 82–88.

Spinelli, R., Nati, C. & Magagnotti, N. 2009. Using modified foragers to harvest short-rotation poplar plantations. *Biomass and Bioenergy* **33**, 817–821.

Stokes, B. & Hartsough, B.R. 1994. Mechanization in short rotation intensive culture (SRIC) forestry. In Proceedings of *6th National Bioenergy Conference*, Reno-Sparks, (US).

Stuart, W.B., Marley, D.S. & Teel, J.B. 1983. A prototype short rotation harvester. Proceedings of the *7th International FPRS Industrial Wood Energy Forum* '83, Nashville, (US).

Wieneke, F. 1993. Mower-chipper for energy plantations of poplar and willow. *Landtechnik* **48**, 646–647 (in German).

Continuously adjustable berry sorter

K. Soots[1,*], V. Maksarov[2] and J. Olt[1]

[1]Institute of Technology, Estonian University of Life Sciences, Kreutzwaldi 56, EE51014 Tartu, Estonia; [*]Correspondence: kaarel.soots@emu.ee
[2]Department of mechanical engineering National Mineral Resource University, Vasilevsky island, 21 Line, House 2, 199106 St-Petersburg, Russia;

Abstract. The article has indicated the principle scheme for post-harvest processing of cultural berries according to the possibilities of the developed new berry sorter. The article tackles the constructive features of the post-harvest treatment of berries as well as of the belt sorter that functions on the principle of successive sorting method. The aim of study was to evaluate the technological features of the berry sorter, based on test results, and to determine problematic assemblies in the construction of the device. Continously adjustable gaps between pulleys as new technological solution for belt sorter was tested and initial results are presented in this article with future improvements. Initial results in this article show that novel continuously adjustable berry sorter functioned satisfactorily. The properties of berry fractions produced with novel berry sorter were possible to change with short time. It was also determined that settings to ensure highest berry fraction purity need to be clarify.

Keywords: *agricultural engineering, post-harvest treatment, berry sorter, blueberry*.

INTRODUCTION

The berry mixture, collected with a berry harvesting machine, contains besides berries also leaves, branches, other plant remains, insects and pieces of peat or soil (Fig. 1). Berries indicate here are blueberries, cranberries and dewberries. For cleaning the berry mixture, differences related to the physical-mechanical traits of its components have to be taken into account, such as density, geometric measures, shape, hardness, elasticity, colour and aerodynamic characteristics. In order to remove all extra materials from the berries, one trait is not sufficient, but a set of traits has to be used, in several parallel or successive treatments.

Depending on variety, ripeness, humidity and other factors, the physical-mechanical characteristics of the components of the berry mixture differ in a large extent, whereas the change has a random character (Bosoi et al., 1977). During sorting, the main physical-mechanical features of the berries are their geometric dimensions (Bosoi et al., 1977). There are many berries and varieties of berries. For example, lowbush berries and fruit of the species *Vaccinium corymbosum* are with the diameter of 4 to 12 mm, while the berries of the blueberry '*Northblue*' are with the diameter of up to 20 mm (Starast et al., 2005; Noormets, 2006). The table berries of different varieties have to be preferably at the same diameter, while the minimum for table blueberries is 8 mm (Starast et al., 2005). This presupposes sorting of berries according to their size.

Two sorting methods of bulk are well-known – successive and parallel. In the case of successive sorting method, size groups for sorting of berry set in the order of size are first small, then average and finally big. In case of parallel sorting, the grouping occurs in decreasing order. The book by Grote & Feldhusen (2007) indicates that according to the construction of the working unit, roll, net, line, drum and belt sorters are differentiated.

Figure 1. Berry box filled by the blueberry harvester.

The main disadvantage of belt sorters is the fact that shifting the pulleys of the drum is time-consuming and troublesome, requires great precision and attention. If different varieties of berries have to be sorted, the multiple readjusting of the berry sorter decreases considerably its capacity during the post-harvest primary processing of different berries. The aim of this study was to evaluate the technological features of the berry sorter, based on test results, and to determine problematic assemblies in the construction of the device.

MATERIALS AND METHODS

When developing the post-harvest processing technology of the berries, the technological scheme developed by Lakewood Process Machinery (2014) was adopted as the basis. The technology indicated on Fig. 2 follows the machine harvesting of the berries (Käis & Olt, 2006; Olt & Arak, 2012).

The post-harvest processing of blueberries contains different work procedures. The intake unit for the berries has to ensure a continuous and balanced feed of berries to the processing line. The work operations begin with removal of larger branches from berry mix. Thereafter, light debris (blueberry leaves, pieces of leaves and peat, etc.) is removed from berry mix; this could be best done in an air flow, using the different aerodynamical properties of the berry mixture components. Removing of additives ends with removing of stems from berry mix. This is followed by fractioning of berries into three groups with the help of a novel sorter device. For the separation of berries in fractions by size, belt sorter functioning on the principle of successive sorting method is used in this case (Fig. 2). First fraction is formed by small berries which are moved to litter box. Berries with average diameter form second fraction. Berries of the second fraction are packaged into boxes, deep frozen and then sent to food industry. Third fraction contains only berries of largest diameter and these are used as table berries. After fractioning, bruised and crushed berries are separated from sound berries with the help of an inclined conveyor. Then, the third fraction berries move to the picking table, which is a belt conveyor. Semi-ripe berries, for example, are removed on the picking table. The packaging of table berries, going to the distributive network, is made by an automatic packaging machine. The poor quality berries removed on the inclined conveyor and picking table can be used as industrial berries if necessary. In what follows, one part of the post-harvest processing of berries is described – the construction and working principle of the novel belt sorter.

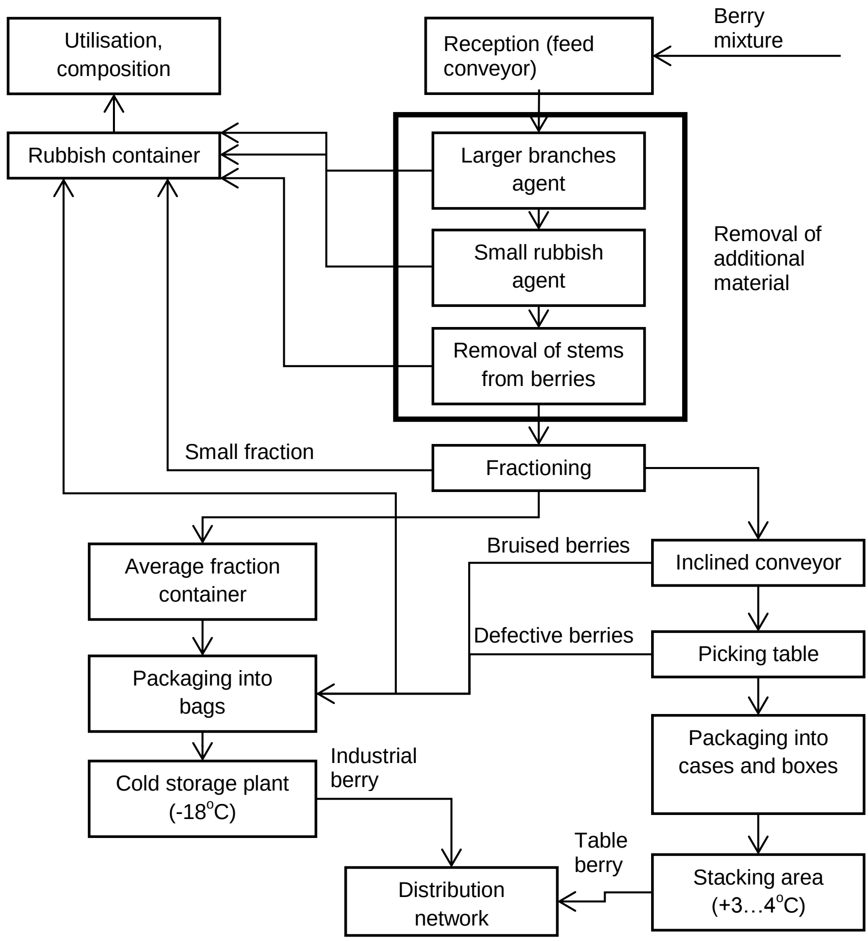

Figure 2. Principle scheme of the post-harvest processing of berries.

The development of the new berry sorter is in its essence solving of a typical product development task (Ulrich & Epinger, 2011). To solve the product development task, TIPS methodology (*Theory of Inventive Problem Solving*) was used (Pahl et al., 2007).

Recesses with a continuous interval for keeping belts are designed for the nonadjustable drum (Fig. 3, position 1), located in the beginning of the sorting area (Fig. 3, position 3) of the berry sorter. The regulated drum (Fig. 3, position 2), located in the end of the sorting area has been compiled from pulleys, the intervals of which can be simultaneously and continuously changed. The adjustable drum (Fig. 4) contains pulleys, a steering shaft, equipped with variable step guiding grooves, steering levers, whereas the tip of each steering lever is connected to a pulley and the other tip is located in the steering shaft groove. The drum contains also a pipe-shaped case for the steering shaft that is equipped with the case's longitudinal opening, which is meant for directing the movement of the steering levers by the axis, a regulating lever with a handle and a fixed disk with a fixator. The steering shaft is equipped with guiding grooves of right and left-hand thread, while at the one side of the circular groove, located at the centre of the steering shaft, there are guiding grooves with right-hand thread, and on the other side, grooves with left-hand thread. Thread handedness is consistent to Fischer et al, 2010. The steering shaft is rigidly connected with a regulating lever, through which the steering shaft can be rotated in relation to the case of the steering wheel. The steering zone of the steering shaft is designed so that the steering rods, attached rigidly to pulleys and positioned through the case opening, the free side of which is in the steering groove, ensures whatever angle of rotation of the pulleys or the same distance in case of position. A disc with split holes is rigidly connected with the case. A fixed disk with a fixator is rigidly attached to the regulating lever. A significant advantage of the innovative sorter is the user friendliness and work efficiency of the constructive solutions of the regulating lever, a good sorting quality, simple handling and readjusting speed. This is the step-free adjustable berry sorter with a fractioning slot (Patent EE05642 B1, 2013).

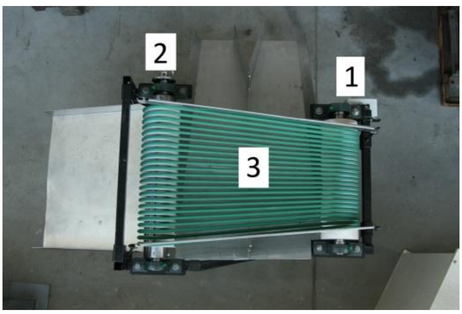

Figure 3. The new berry sorter: 1 – first drum; 2 – smoothly adjustable drum; 3 –sorting area.

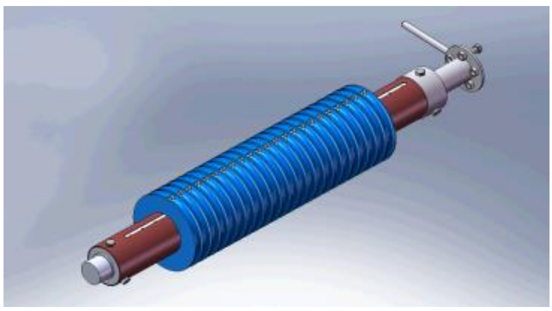

Figure 4. The berry sorter's drum that can be smoothly regulated (Patent EE05642 B1).

Blueberry sorter contains at least three drums with the belts installed on them, which form the sorting area of the blueberries, whereas the regulating drum consists of pulleys, the distance of which can be simultaneously and step-free changed. The regulating drum contains pulleys, a steering shaft equipped with guiding grooves of a changing thread step, steering rods, while the one end of the rod is connected with a pulley and the other end is located in the steering groove of the steering shaft, a pipe-shaped case of the steering shaft that is equipped with the case's longitudinal opening, which in turn is meant for directing the movement of the steering rods by the drum axis, a regulating lever with a handle and a fixed disc with a fixator.

As an explanation, it should be mentioned that screw-shaped guiding grooves have been cut onto the steering shaft, the steps of which correspond to the following conditions:

$$t_{v,n} > \ldots > t_{v,3} > t_{v,2} > t_{v,1} > t_0 < t_{p,1} < t_{p,2} < t_{p,3} < \ldots < t_{p,n}$$

that is, $t_{v,i} > t_0 < t_{p,i}$

where: t_0 – the middle guiding groove of the steering shaft, which is threadless, that is, it is with circular thread, $t_0 = 0$;
t_v – left-sided guiding groove step; $t_v = \Delta \cdot i$;
t_p – right-sided guiding groove step; $t_p = \Delta \cdot i$;
Δ – change of the guiding groove step, mm rotation^{-1}
i – guiding groove serial number, counted from the circular groove located at the centre of the steering shaft;
$i = 1, 2, \ldots, n$.

Each steering groove has a start and end point, while the location of the groove's beginning is determined with the product bi; the location of the groove end is determined with the product $i(b + \Delta)$.

In order to study the functioning of the patented technical solution of the new berry sorter, a prototype of the new berry sorter was manufactured (Fig. 3). The study of the berry sorter sets out determining how and what effect does regulating of the belt distance have on the distribution of the sample mixture between three output fractions received with fractioning. For the research results, the following measurements were implemented:

1. The mass of the berry mixture at the beginning of each experiment.
2. Distribution of output fractions.
3. The average diameters of the berries forming the output fraction.

It was also decided to evaluate the new berry sorter during experiments in a working situation, in order to determine problematic assemblies in the construction of the device.

The tested berry sorter is one part of the post-harvest processing line of berries and this has to be taken into account in planning the laboratory experiments of the prototype. When using post-harvest processing line (Fig. 2), the berry sorter is located relatively at the end part of the line. Before the berries reach the berry sorter the additives are removed from berry mixture.

The novel berry sorter enables to separate berries according to their diameter into 3 fractions. Also, the division of the berry mixture between 1st and 2nd fraction can be adjusted by changing the position of the interim plate. On Fig. 5, the plan of the new berry sorter has been indicated.

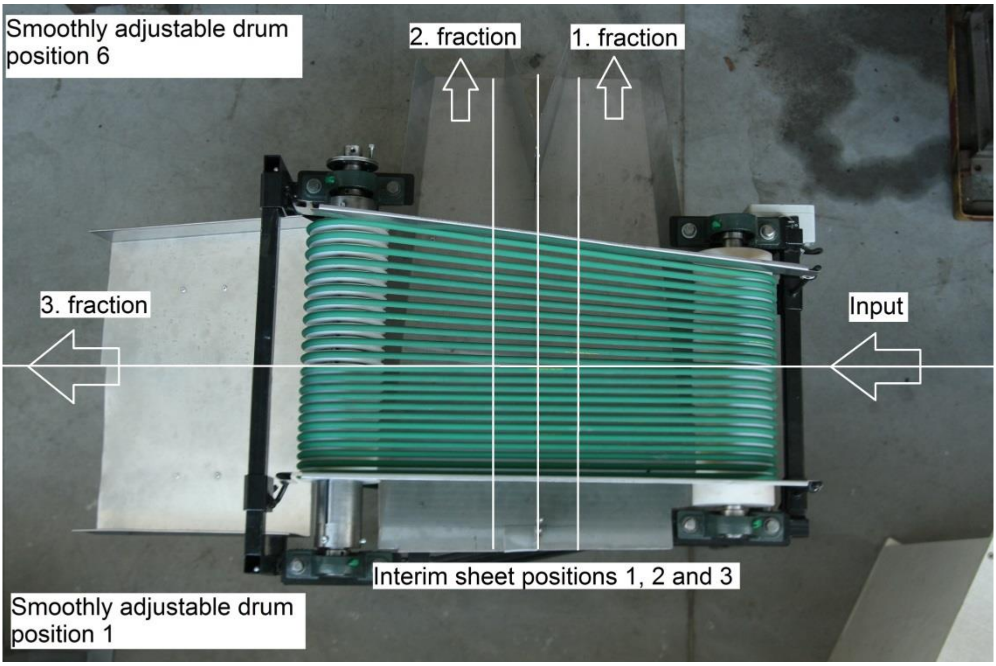

Figure 5. Photo of the berry sorter.

The laboratory experiments of the new berry sorter prototype were conducted in spring 2013 in the agricultural equipment laboratory of the farming and production technology department of the Estonian University of Life Sciences. As adjustable drum did not have fixed regulation steps, then a fixed disc with 6 fixable positions was manufactured for repeating the experiments and limiting the amount of the experiments. The berry mixture included berries with the diameter of d = 1.8–14.5 mm. The total mass of the berry mixture during experiments was m = 4,870 g. To measure mass of fractions, a digital weigh with 10 g precision was used. To determine the diameter of the berries, a gauge block with the precision of 0.05 mm was used. The linear speed of the sorting area, i.e. belts, is $v = 0.12$ m s^{-1} and it was not changed during experiments.

RESULTS AND DISCUSSION

In conducting the first experiments with the new berry sorter, all 18 regulation levels were used. 18 planned experiments were conducted, which formed of six fixed regulating drum positions and three berry deflector nr 2 interim plate positions.

The test results of the new berry sorter have been indicated on Figs 6 to 8 in the case of the interim plate position nr 2, where the division of the sorting area length for fraction 1 and 2 was equal (see Fig. 5). As an explanation, it can be added that the first member of the experiment number indicates the position of the drum that can be regulated and the other member shows the position of the interim plate. The indicated line charts reflect 1/3 of all test results; in this article, test results for the interim plate positions in case of positions 1 and 3 have not been indicated.

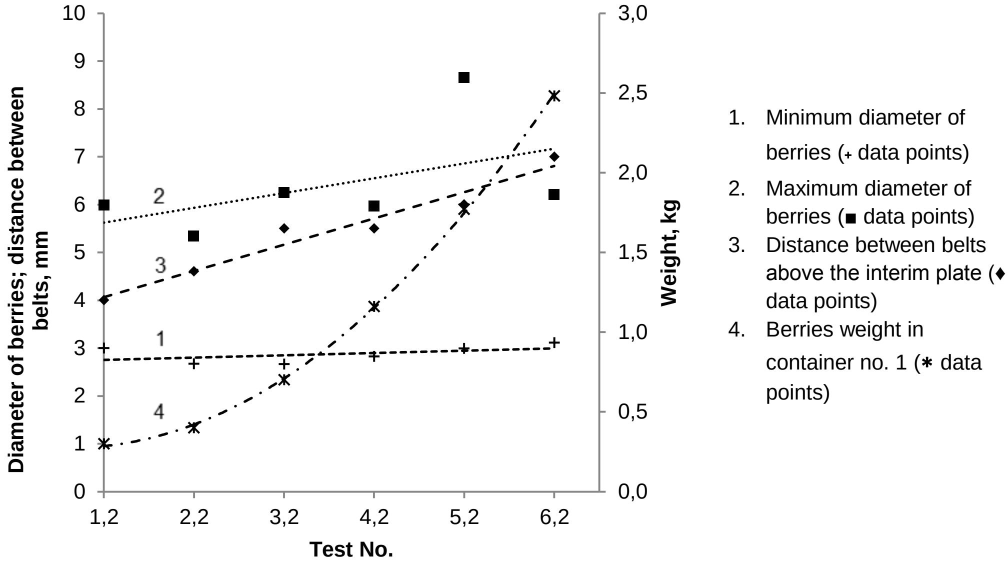

Figure 6. Test results of the first output fraction in case of the interim plate position nr 2. Data points are indicating test results.

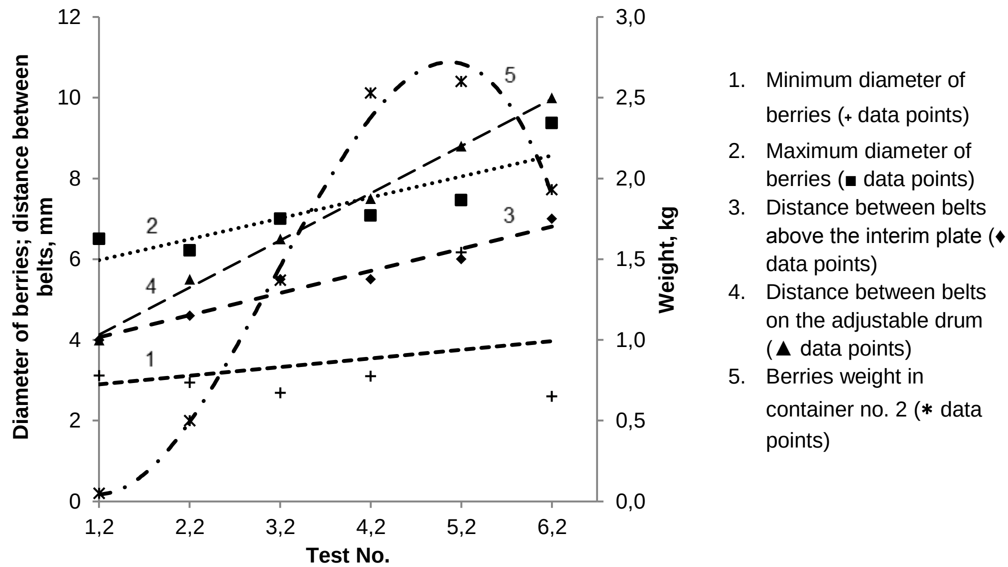

Figure 7. Test results of the second output fraction in case of the interim position nr 2. Data points are indicating test results.

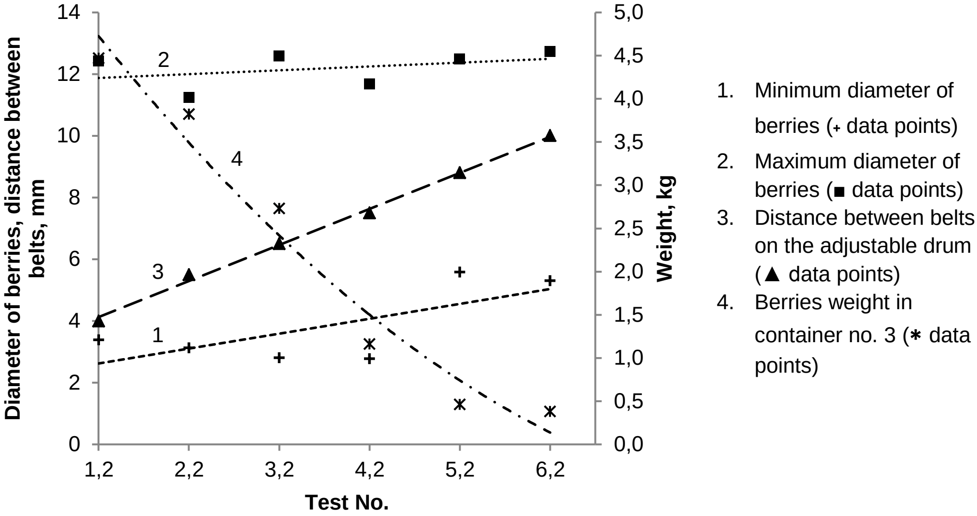

Figure 8. Test results of the third output fraction in case of the interim position nr 2. Data points are indicating test results.

Studying the change of the maximum diameter of berries on Fig. 6 on the basis of the berry mixture that has reached vessel 1, a steep ascent can be seen in experiment 5.2. The line charts indicated on Fig. 7 and 8 indicate that in experiment 5.2 a steep ascent has occurred in the minimum diameter of the berries in vessels 2 and 3. This was probably caused by the back-and-forth movement of the pulleys of the smoothly regulated roller by the drum axis, which is one of the foremost problems at this point.

During tests, there was no indication of the determinate growth or decline of the first fraction berries' diameter, although a certain tendency in the growth of the berries' diameter was sensible. During tests, the first fraction mass increased by increasing the regulatory level of the roller, which was also expected. The bigger sorted area the interim plate of the berry deflector left for the berries going to the first fraction, the bigger was the mass of the berry mixture going into the first fraction. The information indicated on Fig. 6 shows that the maximum diameter of the berries that formed the first fraction is bigger than the distance between belts, except for during experiment 6.2. This was caused by the back-and-forth movement of the belt washers by the drum axis as well as the elasticity of the belts used.

By increasing the distance between pulleys located on the smoothly regulated drum of the berry sorter and thereby also the distance between the belts themselves, the mass and diameter of the berries forming the second fracture increased considerably. Moving the interim plate of the berry deflector nr 2 had an influence also on the second fraction. The bigger sorting area the interim plate of the deflector left for the berries going to the second fraction, the bigger was the mass of the berries forming the second fraction. Fig. 6 indicates that in half experiments, the maximum diameter of berries is bigger than the distance between the belts, and this was caused by the circumstances described in the previous paragraph. Fig. 7 additionally suggests that in case of all experiments (except for experiment 5.2) the minimum diameter of the berries of second fraction is smaller than the distance between the belts above the interim plate. It became evident that this may have been caused by an insufficient length of the sorting surface and the movement technology of not thoroughly developed berries on the sorting surface.

By increasing distances between pulleys, located on the smoothly regulated drum of the berry sorter, the mass of berries of third fraction considerably decreased, while the average diameter of the berries of the third fraction increased. Moving the interim plate did not have an effect on the third fraction. The information indicated on Fig. 8 shows that the minimum diameter of the berries of the third fraction is in case of all tests smaller than the distance between belts on the smoothly regulated roller. Why these berries did not go to the second fraction needs further research.

Based on the test data, it can be said that regulating the distance between the new berry sorter's belts had a significant impact on the division of the berries mixture, and moving the interim plate of the berry deflector nr 2 had an influence on the division between the first and second fraction of the berry mixture. Tests indicate that shifting the pulleys that form the drum was not time-consuming or troublesome, because all pulleys can be moved simultaneously and step-freely. Based on the test results, it can be claimed that when different varieties of berries have to be sorted, then the readjusting of the new berry sorter during the post-harvest initial processing of different berries probably decreases the readjustment time of the berry sorter.

CONCLUSION

The article has presented the methodology for the development of the post-harvest processing devices of the blueberry machine cultivation technology, as well as a description of the test results. During product development work a new berry sorter was developed that is sufficiently flexible for sorting berries of different size. The novel berry sorter with the fractioning slot that can be smoothly regulated functioned satisfactorily. It becomes evident that in berry fractioning, the technology for moving or mixing the berry layer on the belts has to be further improved. Attention has to be also turned to the back-and-forth movement of the pulleys of the smoothly regulated drum by the drum axis in a work situation. The existence of smaller berries in the third fraction that should have been in the second fraction needs further research.

REFERENCES

Bosoi, E., Verniajev, O., Smirnov, I. & Sultan-Shah, E. 1977. Theory, construction and calculation on agricultural machinery. Mechanical Engineering, Moscow, 568 pp.

Fischer, U., Gomeringer, R., Heinzler, M., Kilgus, R., Näher, F., Oesterle, S., Paetzold, H. & Stephan, A. 2010. *Mechanical and Metal Trades Handbook*, (2nd English edition). Verlag Europa Lehrmittel, Germany, 428 pp (in English).

Grote, K.-H. & Feldhusen, J. 2007. *Dubbel Taschenbuch für den Maschinenbau*. Springer DE, 1798 pp.

Käis, L. & Olt, J. 2010. *Low-bush blueberry machine cultivation technology in plantations established on milled peat fields*. Silvio Kosutic (Toim.). Actual Tasks on Agricultural Engineering (271–279). Zagreb, HINUS.

Lakewood Process Machinery. Accessible: http://lakewoodpm.com/ (13.01.2014)

Olt, J. & Arak, M. 2012. *Design and development of the picking reel of motoblock-type harvester*. Agraarteadus: journal of agricultural science: Akadeemilise Põllumajanduse Seltsi väljaanne, XXIII(2), 21–26.

Olt, J., Soots, K. 2013. Patent EE 05642 B1. 2013. *Berry sorter*, B07B13/065.

Pahl, G., Bitz, W., Feldhusen, J. & Grote, K.H. 2007. *Engineering Design. A System Approach*. Third Edition. Springer, Germany, 617 pp.

Starast, M., Karp, K., Paal, T. & Värnik, R. 2005. *Kultuurmustikas ja selle kasvatamine Eestis*. Eesti Põllumajandusülikool. – 65 lk (in Estonian).

Noormets, M. 2006. *Ahtalehise mustika (Vaccinium angustifolium Ait.) ja Kanada mustika (V. Myrttilloides Michx) õie bioloogia mõningaid aspekte; ahtalehise mustika ja hariliku jõhvika (Oxycoccus palustris pers.) kultiveerimine ammendatud freesturbaväljadel.* Väitekiri filosoofiadoktori kraadi taotlemiseks. Juhendajad: Kadri Karp, Taimi Paal, Arthur Randall Olson. Tartu, EMÜ.

Ulrich, T.K. & Eppinger, S.D. 2011. *Product design and development*, Fifth Edition. Irwin McGraw-Hill, USA, 358 pp.

Agronomy Research **12**(1), 171–178, 2014

Impact of the quality of work of fertiliser spreader on nitrous oxide emissions released from soil to the atmosphere

T. Šima[1]*, L. Nozdrovický[1], K. Krištof[1], M. Dubeňová[2] and J. Krupička[3]

[1]Slovak University of Agriculture in Nitra, Faculty of Engineering, Department of Machines and Production Systems, Tr. A. Hlinku 2, 94976 Nitra, Slovak Republic; *Correspondence: tomasko.sima@gmail.com
[2]Slovak University of Agriculture in Nitra, Faculty of Engineering, Department of Production Engineering, Tr. A. Hlinku 2, 94976 Nitra, Slovak Republic
[3]Czech University of Life Sciences Prague, Faculty of Engineering, Department of Agricultural Machines, Kamýcká 129, 16521 Prague, Czech Republic

Abstract. Quality of work of fertiliser spreader is one of the most important factors that affect the nitrous oxide (N_2O) flux from soil to the atmosphere. Calk ammonium nitrate (CAN) with 27% nitrogen content was spread by a fertiliser spreader VICON RS-L connected with a tractor ZETOR 16145 and incorporated into the soil by a power harrow PÖTTINGER LION 301 six hours after its spreading. Application rate of fertiliser was set for 200 kg ha^{-1}. There were selected five monitoring points based on the deviations of application rate for values 172.14, 188.01, 200.68, 213.08 and 227.34 kg ha^{-1}, which means 46.48, 50.76, 54.18, 57.53 and 61.38 kg N ha^{-1}, respectively. Nitrous oxide emissions were measured 7, 14, 21 and 28 days after fertiliser application and incorporation into the soil by a photoacoustic field gas monitor INNOVA 1412 with a multipoint sampler INNOVA 1309. Concentration of N_2O ranged from 0.4264 ppm to 1.2970 ppm. Maximum values were measured 21 days after fertilisation for each variant of the experiment. Based on the data obtained, there were found statistically significant differences among time intervals and among the size of deviations of the application rate at a 95.0% confidence level. Results have shown an impact of the 6% deviation (21 days after fertilisation) and 13.7% deviation (14 and 28 days after fertilisation) from the size of fertiliser application rate on nitrous oxide flux from soil to the atmosphere. There were also found the effects of time interval on nitrous oxide flux from soil to the atmosphere for each of the time intervals 7, 14, 21 and 28 days after fertilisation.

Key words: nitrous oxide, soil emissions, fertiliser, fertiliser spreader, quality of work.

INTRODUCTION

Nitrogen, as an essential element for plant growth (Ambus et al., 2011), is supplied to plants by fertilisers (Kajanovičová et al., 2011). Nitrogen fertilisation is an important factor affecting crop yields (Ložek et al., 1997; Ambus et al., 2011; Kajanovičová et al., 2011). Nitrogen dynamics directly affect a crop growth, soil fertility and potential pollution problems such as NH_3 volatilization, soil acidification, increased NO_3 loads of drinking water, eutrophication of surface water and emissions of the greenhouse gas N_2O (Ludwig et al., 2011). Agriculture contributes to the increase in atmospheric N_2O, accounting for 24% of global annual emissions (IPCC

2007). Nitrous oxide (N_2O) is among the most important greenhouse gases, contributing by 6% to global warming (Loubet et al., 2011; Ranucci et al., 2011), and directly affects the stratospheric ozone layer (Willianms et al., 1992; Ravishankara et al., 2009). Nitrous oxide (N_2O) emissions from agriculture are ranged from 60% (IPCC, 2007) to 75% (Jackson et al., 2009) of the N_2O emissions produced in the world. Agricultural soils are a major source of atmospheric N_2O (Ruser et al., 2001). Global atmospheric concentration of N_2O has increased significantly within the last 150 years and it directly affects the atmospheric environment – increased GHG emissions. In addition, the global warming potential (GWP) of nitrous oxide is 298-times higher in comparison with carbon dioxide (IPCC, 2007). It means that N_2O is one of the major greenhouse gases and contributes to stratospheric O_3 (ozone) depletion (Skiba et al., 2001). Nitrous oxide emitted from soils leads to N loss from the ecosystem and is produced by nitrification and denitrification microbiological activities (Ambus et al., 2006; Jiang-Gang et al., 2007; Senbayram et al., 2012) and chemodenitrification at low pH (< 5.5) (Van Cleemput, Samater 1996). The major N_2O source is denitrification (Ruser et al., 2001). High rate of N fertiliser application increases concern regarding N_2O emissions from intensively farmed fields (He et al., 2009; Pang et al., 2009; Lin et al., 2010; Zhu et al., 2011; Šima et al., 2013g). Although N_2O emissions from the soil increase with the amount of N fertiliser (e.g. Eichner 1990; Bouwman 1996; Verma et al., 2006; Jones et al., 2007; He et al., 2009; Pang et al., 2009; Lin et al., 2010; Mapanda et al., 2011), there is still a lack of data for fertiliser-intensive systems (Pfab et al., 2012). In a compiled data set, N_2O emissions increased significantly with increasing rates of N added (Skiba et al., 2001). The incorrect application rate of fertiliser can result in the increased cost of fertilisers, reduction of crop growth and also negative environmental effects. Quality of work of fertiliser spreader has a positive environmental effect. Therefore for effective application it is necessary to know the transversal uniformity of the fertiliser distribution on the field surface (Šima et al., 2011; 2012a; 2012b; 2013a). The amount of N_2O emissions released from soil into the atmosphere is affected by many factors such as nitrogen application rate, soil properties (pH reaction, humidity, texture, organic matter content and temperature) and weather conditions. Granulometric composition of fertilisers is also very important factor, which must be taken into account (Šima et al., 2013e; 2013f). One of the most important of these factors is the size of the application rate of fertiliser, which depends upon the setting of the fertiliser spreader and quality (uniformity) of the application. Local overdosing causes an increased concentration of nitrogen on the fields (Šima et al., 2012c; 2013b).

The aim of the study was to explore the impact of the quality of work of the fertiliser spreader on the amount of nitrous oxide released from the soil to the atmosphere in different time intervals after fertiliser application.

MATERIAL AND METHODS

The experiment was carried out in Dražovce village, 6 km from Nitra city, Slovakia in May and June 2012. The area is located on long. 48°20′ 56′′ N and lat. 18°4′ 1′′ E and there is a flat land with balanced microrelief after the harvest of perennial forage crops on a field. Temperature during the experiment ranged from

3.4°C to 28.7°C with average value 16.3°C. Air moisture ranged from 29.4 to 98.9% with average 70.1%.

The calk ammonium nitrate (CAN) used is formed by grey and white ammonium nitrate granulates with grounded dolomite decreasing the fertiliser natural acidity. The fertiliser is protected by anticaking surface treatment (www.duslo.sk). The official trade mark of this fertiliser produced by company Duslo, a. s. Šaľa is LAD 27. The chemical composition of LAD 27 consists of 27% of the total nitrogen content, 13.5% of the ammonium nitrogen content and 13.5% of the nitrate nitrogen content; these are important factors that affect the amount of nitrous oxide released from the soil to the atmosphere. The grain size distribution of the fertiliser affects the quality of work the fertiliser spreader. Based on laboratory analysis it was possible to state that there were 90% of particles from 2 to 5 mm in size, maximum 1% was below 1 mm, and no particles were of more than 10 mm. In order to collect fertilisers during measurements of uniformity distribution, there were used collecting trays with a compartment. Their technical parameters meet the Standard ISO 5690/1.

Soil samples were taken for pedological analysis before fertilising and they were analysed at the Department of Soil Science and Geology, the Slovak University of Agriculture in Nitra, Slovakia. The soil type was Haplic Luvisol with a content of clay, silt and sand 37.70, 39.43 and 22.87%, respectively. The humus content was 2.799%, C_{ox} (C_{org}) was 1.624%, and pH was 7.78 and 6.87 for H_2O and KCl, respectively. The soil moisture content of soil samples was measured by a gravimetric method and varied within the ranges 26–28 %, 25–26%, 23–25%, 24–26% and 22–24% during application, 7, 14, 21 and 28 days after application, respectively. During the 16^{th} and 17^{th} days after application of fertiliser there were recorded 3 mm of rainfall.

The double spinning disc fertiliser spreader VICON RS-L was connected with the tractor ZETOR 16145. The fertiliser spreader was set according to manufacturer´s instructions for this type of fertiliser and for the maximum spreading width (for 42 metres in our case). The application rate was 200 kg ha^{-1} (54 kg N ha^{-1}). The machine operating speed was 12 km h^{-1}. The basic requirements for fertiliser application (the maximum wind speed, air moisture, air temperature, filling tray capacity, collecting tray size) given by the Standard ISO 5690/1 and national standards STN EN 13739, Part 1 and Part 2, were met. The spreading pattern was based on our previous research of work quality of fertiliser spreaders (Šima et al., 2011; 2012a; 2012b; 2013a). The application overlap of the working width was set to 50%. Determining the amount of the fertiliser applied to the chosen place requires this fertiliser to be removed for weighing. For this reason, there was not possible to determine the amount of the fertiliser applied to the chosen place where collecting trays with the compartment were placed. Collecting trays with the compartment were placed perpendicularly to the driving direction, in two lines with a 6 m distance. Monitoring points were placed between these lines (3 m from each other), with a calculated (average value) amount of the fertiliser. The position of monitoring points was determined by the amount of the fertiliser applied to the chosen place. The amount of fertiliser decreased with increasing the distance of monitoring points from the driving direction. There were recorded right sides of spreading pattern in both directions with 50% overlap. In this way, it was possible to choose monitoring points with the applied amount of fertiliser 172.14, 188.01, 200.68, 213.08 and 227.34 kg ha^{-1} which means 46.48, 50.76, 54.18, 57.53 and 61.38 kg N ha^{-1}, respectively.

The fertiliser applied on the field surface was incorporated into the soil by tillage (power harrow PÖTTINGER LION 301) during seedbed preparation after six hours in the same day.

Nitrous oxide emissions released from the soil to the atmosphere were measured by the INNOVA measuring devices (LumaSense Technologies, Inc., Denmark), consisting of three main parts (Dubeňová et al., 2013). The photoacoustic field gas monitor INNOVA 1412 with a measurement system based on the photoacoustic infrared detection method is used for the gas analysis; the multipoint sampler INNOVA 1309 serves for gas sampling from 12 sampling points and for the transport of gas samples to INNOVA 1412 for analysis (www.lumasenseinc.com). A notebook with software is the third major component. Software is delivered by the apparatus manufacturer, and it is used for the setup and control of the analysis. Sampling probes were made from a seamless steel pipe with a 114.3 mm outer diameter, 4 mm wall thickness and length 300 mm. Nitrous oxide emissions released from the soil to the atmosphere were measured in selected monitoring points 7, 14, 21 and 28 days after fertilisation. Soil samples were taken to the laboratory within 90 minutes after samples were taken for the gas analysis by a laboratory method. Soil samples were monitored for 24 hours. There was used a 30 min. time interval for the gas analysis. The measuring method and its practical verification were described in our previous studies on N_2O (Šima et al., 2012c; Šima et al., 2013c; Šima et al., 2013d;) and on CO_2 (Šima & Dubeňová, 2013). There were made three replications of the experiment, an average values of nitrous oxide concentration were used for analysis.

The data were analysed by using Kruskal-Wallis test after the normality test using Kolmogorov-Smirnov procedure and the homogeneity of variance by using Levene's test. Kruskal-Wallis test tests the null hypothesis that the medians within each of the samples are the same. Since the P-value is less than 0.05, there is a statistically significant difference occurs between the medians at 95.0% confidence level. The STATGRAPHICS Centurion XVI.I software (Statpoint Technologies, Inc.; Warrenton, Virginia, USA) was used for data analysis. The graphical processing of results was performed using Microsoft Excel 2010.

RESULTS AND DISCUSSION

Spread patterns of the fertiliser were measured, and the position of lines was recorded and saved. Monitoring points were determined based on the calculated average value (Fig. 1) of the amount of applied fertiliser in the first and second spread pattern line. Five monitoring points were chosen with fertiliser application rate 172.14, 188.01, 200.68, 213.08 and 227.34 kg ha^{-1} which means 46.48, 50.76, 54.18, 57.53 and 61.38 kg N ha^{-1}, respectively. Soil samples were taken 7, 14, 21 and 28 days after fertilisation (application and incorporation of the fertiliser).

The basic parameters of measured data are shown in Table 1. An impact of the work quality of fertiliser spreader on nitrous oxide emissions released from soil to the atmosphere 14, 21 and 28 days after fertilisation, however this impact was not found 7 days after fertilisation what could be caused by slower beginning of nitrification and denitrification processes under the given conditions. Fourteen days after fertilisation was found differences in nitrous oxide flux where deviations from set application rate (200 kg ha^{-1}) were above 13.67%. Deviations from set application rate above 6%

(5.995% is difference among the two closes measured application rates) causes statistically significant differences in to nitrous oxide flux. This impact was found 21 days after fertilisation. Decreasing trend and impact of nitrous oxide flux was found 28 days after fertilisation, but still there were significant differences in nitrous oxide flux with deviations from set application rate above 13.67%.

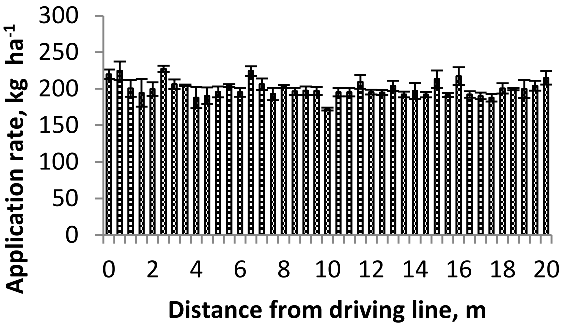

Figure 1. Spread pattern of average values of applied fertiliser with deviations (both replications).

Table 1. Selected parameters of summary statistic and multiple-range test LSD of nitrous oxide emissions released from the soil to the atmosphere, ppm (n = 48)

Time interval, days	Application rate, kg ha^{-1}	Attributes of summary statistics			
		Mean, ppm	Minimum, ppm	Maximum, ppm	Range, ppm
7	172.14	0.4559^{a}_{t}	0.4283	0.4703	0.0420
	188.01	0.4555^{a}_{t}	0.4264	0.4770	0.0506
	200.68	0.4589^{a}_{t}	0.4384	0.4741	0.0357
	213.08	0.4542^{a}_{t}	0.4340	0.4724	0.0384
	227.34	0.4579^{a}_{t}	0.4277	0.4750	0.0473
14	172.14	0.6574^{a}_{u}	0.6081	0.7152	0.1071
	188.01	0.6850^{b}_{u}	0.6186	0.7318	0.1132
	200.68	0.6939^{b}_{u}	0.6169	0.7360	0.1191
	213.08	0.6930^{b}_{u}	0.6142	0.7294	0.1152
	227.34	0.7113^{c}_{u}	0.6593	0.7573	0.0980
21	172.14	0.9893^{a}_{z}	0.8477	1.1340	0.2863
	188.01	1.0318^{b}_{z}	0.8693	1.1708	0.3015
	200.68	1.0907^{c}_{z}	0.9165	1.2162	0.2997
	213.08	1.1384^{d}_{z}	0.9649	1.2555	0.2906
	227.34	1.1795^{e}_{z}	0.9963	1.2970	0.3007
28	172.14	0.7969^{a}_{v}	0.7566	0.9023	0.1457
	188.01	0.8163^{b}_{v}	0.7585	0.9043	0.1458
	200.68	0.8223^{b}_{v}	0.7613	0.9142	0.1529
	213.08	0.8338^{b}_{v}	0.7729	0.9115	0.1386
	227.34	0.8828^{c}_{v}	0.8111	0.9351	0.1240

Different letters as the superscripts ($^{a, b, c, d, e}$) mean the effect of the application rate for selected time and as the subscripts ($_{t, u, v, z}$) mean the effect of the time for selected application rate. It indicates that means are significantly different at $P < 0.05$ according to the LSD multiple-range test at the 95.0 % confidence level.

Result also has shown an effect of time interval after fertilisation to nitrous oxide flux. The peak of nitrous oxide emissions flux was measured 21 days after fertilisation with increasing for 7, 14 and 21 days after fertilisation and decreasing after 28 days, although the measured values after 28 days was higher in comparison with emissions flux 14 days after fertilisation. These results are consistent with our previous study (Šima et al., 2014 in press) where the effects the size of application rates 0, 100, 200 and 300 kg ha^{-1} were analysed. For application rate 200 kg ha^{-1} nitrous oxide concentration ranged from 0.4365 ppm to 1.0397 ppm for 7 and 21 days, respectively.

The amount of nitrous oxide emissions was also highest 21 days after fertilisation. A decrease of nitrous oxide emissions flux was measured on the 28th day. This value of N_2O flux was lower than the max. value measured during the 21st day but still higher than during the 14th day. Lowest N_2O concentration was measured 7 days after fertilisation for both studies. Results are also consistent with another studies where increasing the size of the application rate of fertiliser significantly increased the nitrous oxide flux (e.g. Eichner 1990; Bouwman 1996; Verma et al., 2006; Jones et al., 2007; He et al., 2009; Pang et al., 2009; Lin et al., 2010; Mapanda et al., 2011).

CONCLUSIONS

Based on the results, there were found the effects of the quality of work of fertiliser spreader to nitrous oxide flux from soil to the atmosphere. Irregularity of application of fertiliser resulted in the change of released nitrous oxide emissions. Overdosing of fertiliser increased the amount of emissions. This effect is reflected also in 6% deviation from set application rate of fertiliser and therefore quality of work of fertiliser spreader and correct settings of it implements is even more important, not only from economical point of view but also from environmental aspects.

ACKNOWLEDGEMENTS. The paper reflects the results obtained within the research project NFP No. 26220220014 'Application of information technologies to increase the environmental and economic sustainability of the production agrosystem' (Activity 3.1 Creation of the department of transfer of technology to practice) (OPVaV– 2008/2.2/01-SORO).

REFERENCES

Ambus, P., Zechmeister-Boltenstern, S. & Butterbach-Bahl, K. 2006. Sources of nitrous oxide emitted from European forrest soils. *Biogeosciences* **3**, 135–145.

Ambus, P., Skiba, U., Butterbach-Bahl, K. & Sutton, M. 2011. Reactive nitrogen and greenhouse gas flux interactions in terrestrial ecosystems. *Plant Soil* **343**, 1–3.

Bouwman, A.F. 1996. Direct emissions of nitrous oxide from agricultural soils. *Nutrient Cycling Agroecosystems* **46**, 53–70.

Dubeňová, M., Gálik, R., Mihina, Š. & Šima, T. 2013. Ammonia concentration in farrowing pens with permanent limited range of motion for lactating sows. *Res. Agr. Eng.* **59**, Special Issue, S9–S14.

Eichner, M.J. 1990. Nitrous oxide emissions from fertilized soils: Summary of available data. *J. Environ. Qual* **19**, 272–280.

He, F.F., Jiang, R.F., Chen, Q., Zhang, F.S. & Su, F. 2009. Nitrous oxide emissions from an intensively managed greenhouse vegetable cropping system in Northern China. *Environ. Pollut.* **157**, 1666–1672.

IPCC. 2007. Contribution of Working Groups I, II and III to the Fourth Assessment Report of the Intergovernmental Panel on Climate Change. Eds.: Core Writing Team, Pachauri, R.K. and Reisinger, A. IPCC, 2007, Geneva, Switzerland. pp 104.

Jackson, J., Choudrie, S., Thistlethwaite, G., Passant, N., Murrells, T., Watterson, J., Mobbs, D., Cardenas, L., Thomson, A. & Leech, A., 2009. UK greenhouse gas inventory 1990 to 2007. *Convention on Climate Change*. AEA Technology, 71.

Jiang-Gang, H., Yong-Li, Z., Hong-ying, B., Dong, Q., Jin-yu, C. & Chun-du, W. 2007. N_2O emissions under different moisture and temperature regimes. *Bulletin of Environmental Contamination and Toxicology* **78** 284–287.

Jones, S.K., Rees, R.M., Skiba, U.M. & Ball, B.C. 2007. Influence of organic and mineral N fertiliser on N_2O fluxes from a temperate grassland. *Agric., Ecosyst. Environ.* **121**, 74–83.

Kajanovičová, I., Ložek, O., Slamka, P. & Várady, T. 2011. Bilancia dusíka v integrovanom a ekologickom systéme hospodárenia na pôde. *Agrochémia* **51**, 7–11, (in Slovak, English abstract).

Lin, S., Iqbal, J., Hu, R.G. & Feng, M.L. 2010. N_2O emissions from different land uses in mid-subtropical China. *Agric., Ecosyst. Environ*. **136**, 40–48.

Loubet, B., Laville, P., Lehuger, S., Larmanou, E., Fléchard, C., Mascher, N., Genermont, S., Roche, R., Ferrara, R.M., Stella, P., Personne, E., Durand, B., Decuq, C., Flura, D., Masson, S., Fanucci, O., Rampon, J.N., Siemens, J., Kindler, R., Gabrielle, B., Schrumpf, M., Cellier, P. 2011. Carbon, nitrogen and Greenhouse gases budgets over a four years crop rotation in northern France. *Plant Soil* **343**, 109–137.

Ložek, O., Bizík, J., Fecenko, J., Kováčik, P. & Vnuk, Ľ. 1997. *Výživa a hnojenie rastlín*. Nitra: SUA in Nitra (in Slovak).

Ludwig, B., Jäger, N., Priesack, E. & Flessa, H. 2011. Application of the DNDC model to predict N_2O emissions from sandy arable soils with differing fertilization in a long-term experiment. *Journal of Plant Nutrition and Soil Science* **174**, 350–358.

Mapanda, F., Wuta, M., Nyamangara, J. & Rees, R.M. 2011. Effects of organic and mineral fertilizer nitrogen on greenhouse gas emissions and plant-captured carbon under maize cropping in Zimbabwe. *Plant Soil* **343**, 67–81.

Pang, X.B., Mu, Y.J., Lee, X.Q., Fang, S.X., Yuan, J. & Huang, D.K. 2009. Nitric oxides and nitrous oxide fluxes from typical vegetables cropland in China: Effects of canopy, soil properties and field management. *Atmos. Environ* **43**, 2571–2578.

Pfab, H., Palmer, I., Buegger, F., Fiedler, F., Müller, T. & Ruser, R. 2012. Influence of a nitrification inhibitor and of placed N-fertilization on N_2O fluxes from a vegetable cropped loamy soil. *Agriculture, Ecosystems and Environment* **150**, 91–101.

Ranucci, S., Bertolini, T., Vitale, L., Di Tommasi, P., Ottaiano, L., Oliva, M., Amato, U., Fierro, A., Magliulo, V. 2011. The influence of management and environmental variables on soil N_2O emissions in a crop system in Southern Italy. *Plant Soil* **343**, 83–96.

Ravishankara, A.R., Daniel, J.S. & Portmann, R.W. 2009. Nitrous oxide (N_2O): the dominant ozone-depleting substance emitted in the 21st century. *Science* **326**, 123–125.

Ruser, R., Flessa, H., Schilling, R., Beese, F. & Munch, J.C. 2001. Effect of crop-specific field management and N fertilization on N_2O emissions from a fine-loamy soil. *Nutrient Cycling Agroecosystems* **59**, 177–191.

Senbayram, M., Chen, R., Budai, A., Bakken, L. & Dittert, K. 2012. N_2O emissions and the $N_2O/(N_2O+N_2)$ product ratio of denitrification as controlled by available carbon substrates and nitrate concentrations. *Agriculture, Ecosystems and Environment* **147**, 4–12.

Skiba, U., Sozanska, M., Metcalfe, S. & Fowler, D. 2001. Spatially disaggregated inventories of soil NO and N_2O emissions for Great Britain. *Water, Air, Soil Pollut.* **1**, 109–118.

Šima, T., Nozdrovický, L. & Krištof, K. 2011. Analysis of the work quality of the VICON RS-L fertilizer spreader with regard to application attributes. *Poljoprivredna tehnika* **36**, 1–11.

Šima, T., Nozdrovický, L., Dubeňová, M., Krištof, K. & Krupička, J. 2012a. Effect of satelite navigation on the quality of work of a fertiliser spreader Kuhn Axera 1102 H-EMC. *Acta technologica agriculturae* **4**, 96–99.

Šima, T., Nozdrovický, L., Krištof, K., Jobbágy, J. & Fodora, M. 2012b. The work quality of fertilizer spreader Amazone ZA-M I 12-36 according of the precision agriculture requirements. *Acta facultatis technicae* **17**, 99–108 (in Slovak, English abstract).

Šima, T., Nozdrovický, L., Krištof, K., Dubeňová, M., Krupička, J. & Králik, S. 2012c. Method for measuring of N_2O emissions from fertilized soil after the using of fertilizer. *Poljoprivredna tehnika* **38**, 51–60.

Šima, T., Nozdrovický, L., Dubeňová, M., Krištof, K. & Krupička, J. 2013a. Effect of manual navigation on quality of work of Kuhn Axera 1102 H-EMC fertiliser spreader. In *12th International Scientific Conference on Engineering for Rural Development 2013*. Jelgava, Latvia, pp. 185–189.

Šima, T., Nozdrovický, L., Krištof, K., Dubeňová, M. & Krupička, J. 2013b. Effect of the nitrogen fertiliser rate on the nitrous oxide flux from haplic luvisol soil in the laboratory experiment. *Agronomy Research* **11**(1), 97–102.

Šima, T., Krištof, K., Dubeňová, M., Nozdrovický, L., Krupička, J. & Chyba, J. 2013c. Sonda na polní měření emisí uvolˇňovaných z půdy do atmosféry (Sample probe for field measurement of emissions flux from soil to the atmosphere). Užitný vzor č. 25289 (Utility model no. 25289). Date: 29.4.2013. Praha: Úřad průmyslového vlastnictví (Prague: Industrial Property Office), 2013. In Czech, 2 pages.

Šima, T., Krištof, K., Dubeňová, M., Nozdrovický, L., Krupička, J. & Chyba, J. 2013d. Odběrná sonda na laboratorní měření emisí uvoľňovaných z půdy do atmosféry (Sample probe for laboratory measurement of emissions flux from soil to the atmosphere). Užitný vzor č. 25348 (Utility model no. 25348). Date:13.5.2013. Praha: Úřad průmyslového vlastnictví (Prague: Industrial Property Office), 2013. In Czech, 2 pages.

Šima, T., Krupička, J. & Nozdrovický, L. 2013e. Effect of nitrification inhibitors on fertiliser particle size distribution of the DASA® 26/13 and Ensin® fertilisers. *Agronomy Research* **11**(1), 111–116.

Šima, T., Nozdrovický, L., Krupička, J., Dubeňová, M. & Krištof, K. 2013f. Effect of nitrification inhibitors on electrical conductivity of DASA® 26/13 and Ensin® fertilisers. In *12th International Scientific Conference on Engineering for Rural Development 2013*. Jelgava, Latvia, pp. 185–189

Šima, T., Nozdrovický, L., Krištof, K., Dubeňová, M. & Krupička, J. 2013g. Effect of the vertical and horizontal soil tillage technology to nitrous oxide flux from soil. *Trends in agricultural engineering 2013,* proceeding of CULS in Prague, 586–589.

Šima, T. & Dubeňová, M. 2013. Effect of crop residues on CO_2 flux in the CTF system during soil tillage by a disc harrow Lemken Rubin 9. *Res. Agr. Eng.* **59**, Special Issue, S15–S21.

Šima, T., Nozdrovický, L., Krištof, K. & Krupička, J. 2014 in press. Impact of the size of nitrogen fertiliser application rate on N_2O flux. *Res. Agr. Eng.* At. 15.1.2014 In press. Accepted as 81/2012-RAE.

Van Cleemput, O. & Samater, A.H. 1996. Nitrite in soils: accumulation and role in the formation of gaseous N compounds. *Fertilizer Research* **45**, 81–89.

Verma, A., Tyagi, L., Yadav, S. & Singh, S.N. 2006. Temporal changes in N_2O efflux from cropped and fallow agricultural fields. *Agric., Ecosyst. Environ*. **116**, 209–215.

Williams, E.J., Hutchinson, G.L. & Fehsenfeld, F.C. 1992. NO_x and N_2O emissions from soils. *Global Biogeochem. Cycles* **6**, 351–388.

Zhu, T., Zhang, J. & Cai, Z., 2011. The contribution of nitrogen transformation processes to total N_2O emissions from soils used for intensive vegetable cultivation. *Plant Soil* **343**, 313–327.

Agronomy Research **12**(1), 179–186, 2014

The effect of nitrification inhibitors on nitrous oxide flux from haplic luvisol soil of DASA® 26/13 and ENSIN® fertilisers in a laboratory experiment

T. Šima[1,]*, L. Nozdrovický[1], K. Krištof[1], M. Dubeňová[2] and J. Krupička[3]

[1]Slovak University of Agriculture in Nitra, Faculty of Engineering, Department of Machines and Production Systems, Tr. A. Hlinku 2, 94976 Nitra, Slovak Republic;
*Correspondence: tomasko.sima@gmail.com
[2]Slovak University of Agriculture in Nitra, Faculty of Engineering, Department of Production Engineering, Tr. A. Hlinku 2, 94976 Nitra, Slovak Republic
[3]Czech University of Life Sciences Prague, Faculty of Engineering, Department of Agricultural Machines, Kamýcká 129, 16521 Prague, Czech Republic

Abstract. The aim of the paper was to compare the effects of two very similar fertilisers on nitrous oxide (N_2O) flux from soil to the atmosphere in laboratory conditions. The following fertilisers were used: granulated nitrogenous fertiliser DASA® 26/13 with the nitrogen content of 26%, sulphur content of 13%, and nitrogen fertiliser ENSIN® with the nitrogen content of 26%, sulphur content of 13% and nitrification inhibitors dicyandiamide DCD and 1, 2, 4-triazole (TZ). Both fertilisers are produced by the same manufacturer, DUSLO, Inc., Šala, Slovakia. For both fertilisers, there variants of experiments were carried out for application rates equivalent to 0, 250 and 500 kg ha^{-1}. The amount of the N_2O emissions released from soil to the atmosphere was measured by a photo-acoustic field gas monitor INNOVA 1412 connected to a multipoint sampler INNOVA 1309. The experiments were conducted for 30 days in laboratory conditions. The fertiliser was incorporated into the soil in sampling tubes to a depth of 80 mm after 24 hours of measurement. Subsequently, after every 24 hours of measurement, another 48 hours was carried out, and this measuring cycle was repeated 10 times. The results of our experiment have confirmed that the fertiliser application rate and type of the fertiliser used have a significant effect on N_2O flux and have confirmed the importance of accurate and uniform application of fertilisers in field conditions in order to eliminate the negative environmental effects.

Key words: nitrification inhibitors, nitrous oxide, soil emissions, fertilising, application rate

INTRODUCTION

One of the most important factors affecting crop yields is nitrogen fertilisation (Ložek et al., 1997; Ambus et al., 2011; Kajanovičová et al., 2011). The use of fertilisers has significant effects on intensification of crop production (Šima et al., 2011). Nitrous oxide emissions produced by agriculture in the world range from 60% (IPCC, 2007) to 75% (Jackson et al., 2009). Stratospheric O_3 (ozone) depletion is generally caused by nitrous oxide (Skiba et al., 2001) which is mostly produced by agricultural soils (Ruser et al., 2001). The use of fertilisers is currently connected with the increased flux of N_2O emissions from the soil into the atmosphere (Jones et al., 2007; He et al., 2009; Pang et al., 2009; Lin et al., 2010; Šima et al., 2014 in press). Nitrous oxide is produced in the soil mainly by two biological processes: nitrification and denitrification (Davidson, 1991; Williams et al., 1992; Ložek et al., 1997; Ambus et al., 2006). Inaccurate application of fertiliser causes the local overdosing of fertiliser on the field surface resulting in an increased release of CO_2 and N_2O from the soil into the atmosphere (Šima et al., 2012b; Šima et al., 2012d; Šima et al., 2013d; Šima et al., 2013g). It is apparent than an improved operating quality of a fertiliser spreader has a positive environmental effect. For effective application, it is necessary to know the transversal uniformity of the fertiliser distribution on the field surface, since local overdosing of fertiliser caused by incorrect setup of the fertiliser spreader has negative economical and environmental effects (Šima et al., 2011; 2012b; 2012d; 2013d). The need for using fewer amounts of fertilizers means that it must be applied in a right way, and fertiliser losses are reduced to an absolute minimum. An optimal application of fertilizers, minimisation of spoilage of fertilizers, improvement of existing and development of possible new application techniques - all this requires detailed knowledge of the processes and factors that affect the spreading of fertilisers (Hofstee, 1993). Many factors such as weather conditions, soil properties and mostly nitrogen application rate affect the amount of nitrous oxide emissions flux. Based on this fact, is very important to pay attention to the quality of the work of the fertiliser spreader (Šima et al., 2013a). And, at the same time, an increased amount of nitrogen fertiliser is unusable for plants and in many cases is harmful to the environment. The next factor is the content of nitrification inhibitors in the fertilisers, which may also be considered very important. These inhibit the biological oxidation of ammonium nitrogen into the nitrate nitrogen in the soil. Nitrification inhibitors affect on the granulometric composition (Šima et al., 2013b) of fertilisers and the electrical conductivity (Šima et al., 2013c) of the fertiliser.

The aim of the paper is the study the effects of nitrification inhibitors of two very similar nitrate fertilizers from the same manufacturer on the production of N_2O emissions released from soil to the atmosphere under laboratory conditions – in a laboratory experiment. The fertilizers used were the granulated nitrogen fertilizer with sulphur content, DASA® 26/13, and nitrogen fertilizer ENSIN® containing sulphur and nitrification inhibitors dicyandiamide DCD and 1, 2, 4 triazole – TZ.

MATERIAL AND METHODS

During the experiments, soil samples were collected by five sampling probes from one specific soil location. For collecting the soil samples, sampling probes of own design were used (Šima et al., 2012a; 2012c; Šima & Dubeňová, 2013; Šima et al., 2013e; 2013f). The aim was to obtain soil samples with uniform soil properties and therefore avoid the effect of the natural heterogeneity of soil properties across the arable fields (Šima et al., 2013a). The nitrous oxide released from the soil into the atmosphere was measured in collected non-fertilising sampling probes for 24 hours. Subsequently, equivalent amount of application rates of the fertiliser were incorporated into the soil in the sampling probes under laboratory conditions. Three variants of fertiliser application rate were used: 0 kg ha^{-1}, 250 kg ha^{-1}, 500 kg ha^{-1} and with two repetitions for each variant of non-zero application rate. Measurements were started

48 hours after fertiliser incorporation and were carried out for 24 hours with 48 hours of rest between the measurements, and this measuring cycle was repeated 10 times.

The soil properties (Table 1) were analysed at the Department of Soil Science and Geology at the Slovak University of Agriculture in Nitra, Slovak Republic. The soil moisture content of the soil samples was measured by the gravimetric method. The soil type was identified as haplic luvisol with a slightly alkaline pH reaction and medium humus content.

Table 1. Soil properties

Soil type	Haplic luvisol
Soil moisture content	32–34%
Clay content	37.7%
Silt content	39.43%
Sand content	22.87%
pH H_2O	7.78
pH KCl	6.87
CO_X	1.624%
Hm	2.799%
Bulk density	1.41 g cm^{-3}

During the experiments, we used two very similar fertilizers from the same manufacturer DUSLO, Inc. The granulated nitrogen fertilizer with sulphur content, DASA® 26/13, was used. Nitrogen is in ammonium and nitrate form and sulphur is in water-soluble sulphate form. The granulate has pink to brown colour and the surface is treated with a coating agent. As the second fertilizer, we used the granular nitrogen fertilizer ENSIN® containing sulphur and nitrification inhibitors dicyandiamide DCD and 1, 2, 4 triazole – TZ. The granulate is treated with a coating agent and has green colour. The nitrification inhibitors ensure transformation of ammonium nitrate to nitrogen nitrate in the soil. The advantages of ENSIN® usage compared to DASA® 26/13 are that the fertilizer is applied in 1 dosage and re-application of the fertilizer is not necessary. It allows farmers to save the time and money to increase the crop yields and allows better quality of crops.

The chemical compositions of the DASA® 26/13 and ENSIN® fertilizers are presented in Tables 2 and 3, respectively. The grain-size distribution of the DASA® 26/13 and ENSIN® fertilizers are shown in Table 4.

Table 2. Chemical composition of the DASA® 26/13 fertilizer

Technical specification	Content, %
total nitrogen content (N)	26
ammonium nitrogen content	18.5
nitrate nitrogen content	7.5
sulphur (S) soluble in water	13

Equivalent amounts of application rate of the fertiliser were calculated depending on the diameter of the sampling probes. In our case, the inlet diameter was 106.4 mm and the equivalents of the application rates 250 and 500 kg ha^{-1} were 0.2219 and 0.4437 g of fertiliser, respectively.

Table 3. Chemical composition of the ENSIN® fertilizer

Technical specification	Content, %
total nitrogen content (N)	26
ammonium nitrogen content	18.5
nitrate nitrogen content	7.5
sulphur (S) soluble in water	13
dicyandiamide DCD and 1,2,4 triazole content	0.37–0.74
DCD:TZ ratio	10:1

Table 4. Grain-size distribution of the DASA® 26/13 and ENSIN® fertilizers

	Content of particles, %	
Dimension, mm	DASA® 26/13	ENSIN®
< 1	max. 1	max. 1
2–5	min. 90	min. 90
> 10	0	0

The amount of the N_2O emissions emitting from the soil was measured by INNOVA devices (Lumasense Technologies, Inc.) with the measurement system based on the photo-acoustic infrared detection method. A photo-acoustic field gas monitor INNOVA 1412 and a multipoint sampler INNOVA 1309 were used due to the possibility to analyse a number of samples simultaneously (Dubeňová et al., 2013).

The data obtained were analysed by using the ANOVA test, after a normality test by using the *Kolmogorov-Smirnov* test and a homogeneity of variance by using the *Levene's* test. With ANOVA $P < 0.05$, we continued with the post-hoc LSD multiple range test. We used the software STATGRAPHICs Centurion XVI.I (Statpoint Technologies, Inc.; Warrenton, Virginia, USA). The graphic processing of the results was performed by using the software STATISTICA 7 (Statsoft, Inc.; Tulsa, Oklahoma, USA).

RESULTS AND DISCUSSION

The concentration of N_2O emissions in the sampling probes considerably fluctuated in comparison with the emission concentration before fertilising due to the time period (Fig. 1 and Table 5).

Based on the obtained results, we found the effect of nitrification inhibitors to the intensity and time interval of nitrous oxide emissions released from the soil to the atmosphere in laboratory conditions. The content of nitrification inhibitors in fertilisers slows down the intensity of nitrous oxide emissions releasing. The maximum values, the peak of nitrous oxide flux, after using the 'non inhibitors fertiliser' DASA® 26/13 were measured for 18 and 21 days after application of the fertiliser to the soil for the application rates of 250 and 500 kg ha^{-1}, respectively. The peak of nitrous oxide flux after using the ENSIN® fertiliser was measured 27 days after application of the fertiliser for both application rates. These results correspond with the results obtained by other researchers (e.g., Eichner, 1990; Bouwman, 1996; Verma et al., 2006; Jones et al., 2007; He et al., 2009; Pang et al., 2009; Lin et al., 2010; Mapanda et al., 2011) and also extend the evidence into more detail in this study area concerning the nitrification inhibitors effects on releasing of soil emissions and the properties of fertilisers.

Table 5. The average values of nitrous oxide concentration, ppm

Time,	Application rate of fertiliser, kg ha^{-1}				
days	NF	Dasa250	Dasa500	Ensin250	Ensin500
0	$0.5502_a{}^{s}$	$0.5594_a{}^{s}$	$0.5656_a{}^{s}$	$0.5587_a{}^{st}$	$0.5613_a{}^{s}$
3	$0.5620_{ab}{}^{st}$	$0.5714_{bc}{}^{s}$	$0.5776_c{}^{s}$	$0.5552_a{}^{st}$	$0.5649_{abc}{}^{s}$
6	$0.5651_a{}^{t}$	$0.6095_b{}^{t}$	$0.6178_b{}^{s}$	$0.5509_a{}^{s}$	$0.5540_a{}^{s}$
9	$0.5641_a{}^{t}$	$0.6149_c{}^{tu}$	$0.6997_d{}^{t}$	$0.5830_{ab}{}^{tu}$	$0.6124_{bc}{}^{t}$
12	$0.5601_a{}^{st}$	$0.6433_c{}^{uv}$	$0.8192_e{}^{u}$	$0.6014_b{}^{uv}$	$0.6818_d{}^{u}$
15	$0.5616_a{}^{st}$	$0.6892_c{}^{xy}$	$0.9104_d{}^{v}$	$0.6216_b{}^{v}$	$0.7140_c{}^{u}$
18	$0.5579_a{}^{st}$	$0.7102_c{}^{y}$	$1.0019_e{}^{x}$	$0.6548_b{}^{x}$	$0.7720_d{}^{v}$
21	$0.5553_a{}^{st}$	$0.7109_b{}^{y}$	$1.0726_d{}^{y}$	$0.6794_b{}^{xy}$	$0.8331_c{}^{x}$
24	$0.5581_a{}^{st}$	$0.6993_b{}^{y}$	$0.9983_d{}^{x}$	$0.6931_b{}^{yz}$	$0.8657_c{}^{xy}$
27	$0.5595_a{}^{st}$	$0.6571_b{}^{vx}$	$0.8451_d{}^{u}$	$0.7099_c{}^{yz}$	$0.8778_d{}^{y}$
30	$0.5650_a{}^{t}$	$0.6459_b{}^{uv}$	$0.8055_c{}^{u}$	$0.6905_b{}^{z}$	$0.8571_d{}^{xy}$

Different letters in the rows ($_{a,b,c,d,e}$) mean the effect of the application rate and in the columns (^{s,t,u,v,x,y,z}) mean the effect of the time. It indicates that the means are significantly different at $P < 0.05$ according to the LSD multiple-range test at the 95.0 % confidence level.

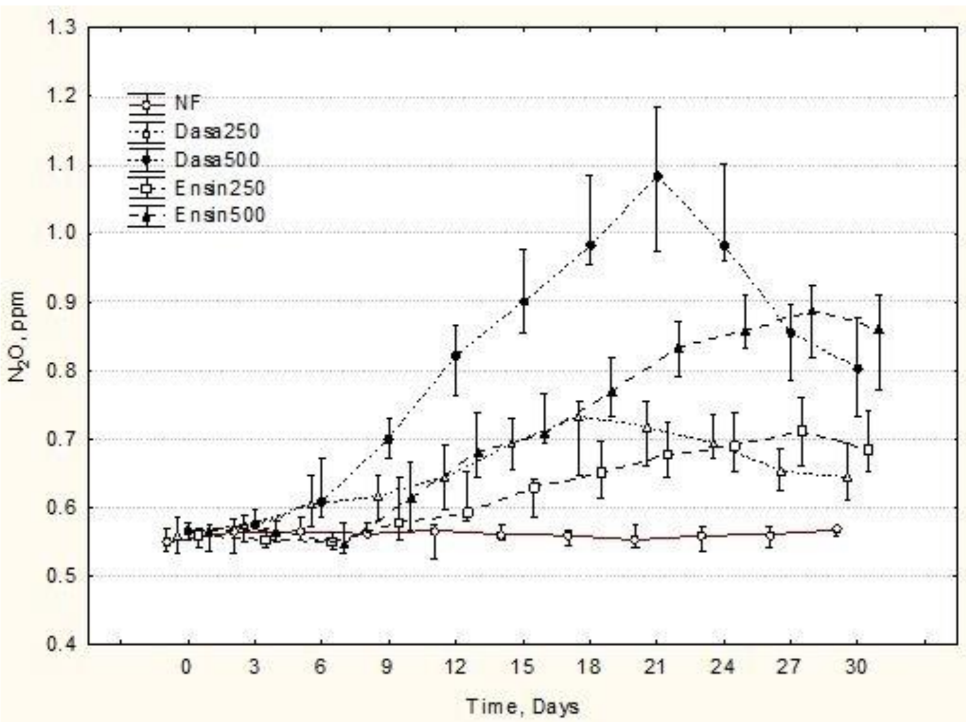

Figure 1. Nitrous oxide concentration in ppm (parts per million), NF – non-fertilizing, point – median, whisker – min.-max. values.

The effect of the size of the application rate to the nitrous oxide emissions released from soil to the atmosphere was also found, and was in agreement with our previous studies (e.g.: Šima et al., 2012c; 2013a; Šima et al., 2014 in press). Nitrification inhibitors slowed the disintegration of fertiliser in the soil and sequentially caused slower nitrogen releasing. It is necessary to include this particular effect in complex research from the perspective of plants and all environmental aspects such as groundwater and leaching of nutrients.

CONCLUSIONS

The aim of the study was to analyse the effects of nitrification inhibitors of two very similar nitrate fertilizers (with and without inhibitors) on the production of N_2O emissions released from the soil to the atmosphere under laboratory conditions – in a laboratory experiment. Increasing the amount of fertiliser results in increasing the amount of nitrous oxide emissions released from soil to the atmosphere. An effect of nitrification inhibitors to nitrous oxide flux was also found. Nitrification inhibitors caused slower disintegration of the fertiliser in the soil and sequentially caused slower nitrogen releasing which allows nutrients to be used by plants rather than to be released as nitrous oxide emissions.

ACKNOWLEDGEMENTS. The paper reflects the results obtained within the research project NFP No. 26220220014 'Application of information technologies to increase the environmental and economic sustainability of the production agrosystem' (Activity 3.1 Creation of the department of transfer of technology to practice) (OPVaV– 2008/2.2/01-SORO).

REFERENCES

Ambus, P., Zechmeister-Boltenstern, S. & Butterbach-Bahl, K. 2006. Sources of nitrous oxide emitted from European forrest soils. *Biogeosciences* **3**, 135–145.

Ambus, P., Skiba, U., Butterbach-Bahl, K. & Sutton, M. 2011. Reactive nitrogen and greenhouse gas flux interactions in terrestrial ecosystems. *Plant Soil*. **343**, 1–3.

Bouwman, A.F. 1996. Direct emissions of nitrous oxide from agricultural soils. *Nutr. Cycling Agroecosyst.* **46**, 53–70.

Davidson, E.A., 1991. Fluxes of nitrous oxide and nitric oxide from terrestial ecosystems. In Rogers & Whitman (eds.): *Microbial production and comsumption of greenhouse gases: Methane, nitrogen oxides and halomethanes*. The American Society for Microbiology, 219–235.

Dubeňová, M., Gálik, R., Mihina, Š. & Šima, T. 2013. Ammonia concentration in farrowing pens with permanent limited range of motion for lactating sows. *Res. Agr. Eng.* **59**, Special Issue, S9–S14.

Eichner, M.J. 1990. Nitrous oxide emissions from fertilized soils: Summary of available data. *J. Environ. Qual.* **19**, 272–280.

He, F.F., Jiang, R.F., Chen, Q., Zhang, F.S. & Su, F. 2009. Nitrous oxide emissions from an intensively managed greenhouse vegetable cropping system in Northern China. *Environ. Pollut.* **157**, 1666-1672.

Hofstee, J.W. 1993. Physical properties of fertilizer in relation to handling and spreading. Thesis Wageningen.

IPCC. 2007. Contribution of Working Groups I, II and III to the Fourth Assessment Report of the Intergovernmental Panel on Climate Change. Eds.: Core Writing Team, Pachauri, R.K. and Reisinger, A. IPCC, 2007, Geneva, Switzerland. pp 104.

Jackson, J., Choudrie, S., Thistlethwaite, G., Passant, N., Murrells, T., Watterson, J., Mobbs, D., Cardenas, L., Thomson, A. & Leech, A., 2009. UK greenhouse gas inventory 1990 to 2007. *Convention on Climate Change*. AEA Technology, 71.

Jones, S.K., Rees, R.M., Skiba, U.M. & Ball, B.C. 2007. Influence of organic and mineral N fertiliser on N_2O fluxes from a temperate grassland. *Agric., Ecosyst. Environ.* **121**, 74–83.

Kajanovičová, I., Ložek, O., Slamka, P. & Várady, T. 2011. Bilancia dusíka v integrovanom a ekologickom systéme hospodárenia na pôde. *Agrochémia* **51**, 7–11, (in Slovak, English abstract).

Lin, S., Iqbal, J., Hu, R.G. & Feng, M.L. 2010. N_2O emissions from different land uses in mid-subtropical China. *Agric., Ecosyst. Environ*. **136**, 40–48.

Ložek, O., Bizík, J., Fecenko, J., Kováčik, P. & Vnuk, Ľ. 1997. *Výživa a hnojenie rastlín*. Nitra: SUA in Nitra (in Slovak).

Mapanda, F., Wuta, M., Nyamangara, J. & Rees, R.M. 2011. Effects of organic and mineral fertilizer nitrogen on greenhouse gas emissions and plant-captured carbon under maize cropping in Zimbabwe. *Plant Soil* **343**, 67–81.

Pang, X.B., Mu, Y.J., Lee, X.Q., Fang, S.X., Yuan, J. & Huang, D.K. 2009. Nitric oxides and nitrous oxide fluxes from typical vegetables cropland in China: Effects of canopy, soil properties and field management. *Atmos. Environ.* **43**, 2571–2578.

Ruser, R., Flessa, H., Schilling, R., Beese, F. & Munch, J.C. 2001. Effect of crop-specific field management and N fertilization on N_2O emissions from a fine-loamy soil. *Nutr. Cycling Agroecosyst*. **59**, 177–191.

Skiba, U., Sozanska, M., Metcalfe, S. & Fowler, D. 2001. Spatially disaggregated inventories of soil NO and N_2O emissions for Great Britain. *Water, Air, Soil Pollut.* **1**, 109–118.

Šima, T., Nozdrovický, L. & Krištof, K. 2011. Analysis of the work quality of the VICON RS-L fertilizer spreader with regard to application attributes. *Poljoprivredna tehnika* **36**, 1–11.

Šima, T., Nozdrovický, L., Krištof, K., Dubeňová, M. & Macák, M. 2012a. A comparison of the field and laboratory methods of measuring CO_2 emissions released from soil to the atmosphere. *Poljoprivredna tehnika* **37**, 63–72.

Šima, T., Nozdrovický, L., Dubeňová, M., Krištof, K. & Krupička, J. 2012b. Effect of satelite navigation on the quality of work of a fertiliser spreader Kuhn Axera 1102 H-EMC. *Acta technologica agriculturae* **4**, 96–99.

Šima, T., Nozdrovický, L., Krištof, K., Dubeňová, M., Krupička, J. & Králik, S. 2012c. Method for measuring of N_2O emissions from fertilized soil after the using of fertilizer. *Poljoprivredna tehnika* **38**, 51–60.

Šima, T., Nozdrovický, L., Krištof, K., Jobbágy, J. & Fodora, M. 2012d. The work quality of fertilizer spreader Amazone ZA-M I 12-36 according of the precision agriculture requirements. *Acta facultatis technicae* **17**, 99–108 (in Slovak, English abstract).

Šima, T., Nozdrovický, L., Krištof, K., Dubeňová, M. & Krupička, J. 2013a. Effect of the nitrogen fertiliser rate on the nitrous oxide flux from haplic luvisol soil in the laboratory experiment. *Agronomy Research* **11**(1), 97–102.

Šima, T., Krupička, J. & Nozdrovický, L. 2013b. Effect of nitrification inhibitors on fertiliser particle size distribution of the DASA® 26/13 and Ensin® fertilisers. *Agronomy Research*. **11**(1), 111–116.

Šima, T., Nozdrovický, L., Krupička, J., Dubeňová, M. & Krištof, K. 2013c. Effect of nitrification inhibitors on electrical conductivity of DASA® 26/13 and Ensin® fertilisers. In *12th International Scientific Conference on Engineering for Rural Development 2013*. Jelgava, Latvia, pp. 185–189.

Šima, T., Nozdrovický, L., Dubeňová, M., Krištof, K. & Krupička, J. 2013d. Effect of manual navigation on quality of work of Kuhn Axera 1102 H-EMC fertiliser spreader. In *12th International Scientific Conference on Engineering for Rural Development 2013*. Jelgava, Latvia, pp. 185–189.

Šima, T., Krištof, K., Dubeňová, M., Nozdrovický, L., Krupička, J. & Chyba, J. 2013e. Sonda na polní měření emisí uvoľňovaných z půdy do atmosféry (Sample probe for field measurement of emissions flux from soil to the atmosphere). Užitný vzor č. 25289 (Utility model no. 25289). Date: 29.4.2013. Praha: Úřad průmyslového vlastnictví (Prague: Industrial Property Office), 2013. In Czech, 2 pages.

Šima, T., Krištof, K., Dubeňová, M., Nozdrovický, L., Krupička, J. & Chyba, J. 2013f. Odběrná sonda na laboratorní měření emisí uvoľňovaných z půdy do atmosféry (Sample probe for laboratory measurement of emissions flux from soil to the atmosphere). Užitný vzor č. 25348 (Utility model no. 25348). Date:13.5.2013. Praha: Úřad průmyslového vlastnictví (Prague: Industrial Property Office), 2013. In Czech, 2 pages.

Šima, T., Nozdrovický, L., Krištof, K., Dubeňová, M. & Krupička, J. 2013g. Effect of the vertical and horizontal soil tillage technology to nitrous oxide flux from soil. *Trends in agricultural engineering 2013,* proceeding of CULS in Prague, 586–589.

Šima, T. & Dubeňová, M. 2013. Effect of crop residues on CO_2 flux in the CTF system during soil tillage by a disc harrow Lemken Rubin 9. *Res. Agr. Eng.* **59**, Special Issue, S15–S21.

Šima, T., Nozdrovický, L., Krištof, K. & Krupička, J. 2014 in press. Impact of the size of nitrogen fertiliser application rate on N_2O flux. *Res. Agr. Eng.* At. 20.12.2013 In press. Accepted as 81/2012-RAE.

Verma, A., Tyagi, L., Yadav, S. & Singh, S.N. 2006. Temporal changes in N_2O efflux from cropped and fallow agricultural fields. *Agric., Ecosyst. Environ*. **116**, 209–215.

Williams, E.J., Hutchinson, G.L. & Fehsenfeld, F.C. 1992. NO_x and N_2O emissions from soils. *Global Biogeochem. Cycles*. **6**, 351–388.

Agronomy Research **12**(1), 187–196, 2014

Measurement of soil resistance by using a horizontal penetrometer working with the two-argument comparative method

F. Varga[1], Z. Tkáč[1], T. Šima[2,*], Ľ. Hujo[1], J. Kosiba[1] and D. Uhrinová[1]

[1]Slovak University of Agriculture in Nitra, Faculty of Engineering, Department of Transport and Handling, Tr. A. Hlinku 2, 949 76 Nitra, Slovak Republic
[2]Slovak University of Agriculture in Nitra, Faculty of Engineering, Department of Machines and Production Systems, Tr. A. Hlinku 2, 94976 Nitra, Slovak Republic;
*Correspondent author: tomasko.sima@gmail.com

Abstract. Currently, the interest in land is high and is increased by in relation to the increasing need for livelihood of the population. Therefore, the need for land use to increase its potential production while ensuring a sustained recovery of agricultural systems still exists. The aim of this publication is to test the measurement of the soil resistance impact at different levels of humidity using a newly designed type of a measuring device – a horizontal penetrometer. The measurements were carried out under field conditions by average soil moisture of 8.47% and 14.24%, on the basis of the two parameters comparative method by using a horizontal penetrometer. The proposed measuring device measured the soil resistance in the tire track and outside of the track after five passages of the tractor. Measuring and recording devices to capture the measured values were also designed. From the results, we can indicate that the soil resistance after each passage increases and we also observed that after the first passage, the soil resistance increased by about 48.1% compared to the initial soil resistance. The average soil bulk density corresponds proportionally with the soil resistance increases in both the absolute and relative terms, depending on the number of tractor passages. It is possible to conclude that the newly designed measuring device is working properly and can be used for all types of tractors equipped with a three-point hitch with the tire tread width of 1,000–2,000 mm. The measurement results will be utilized in mapping of the actual conditions of soil environment.

Key words: soil resistance measurement, soil compaction, bulk resistance.

INTRODUCTION

Soil strength is defined as the resistance which has to be overcome to obtain a given soil deformation. In cultivation operations, high soil strength can be favourable or unfavourable according to the objectives. It is favourable to enable traffic, because it raises the soil bearing capacity, but is unfavourable to soil tillage ,since it increases the draft, making it more difficult to create an optimal soil structure, disturbs seeds germination and root growth (Sirjacobs, et al., 2002). Nowadays, all technological operations in crop production are performed with the use of agricultural machines. This has got plenty of pros such as the low cost per hectare, but one of main cons is the soil compaction side effect. The soil compaction caused by agricultural machinery is an important factor which affects carbon dioxide (Šima & Dubeňová, 2013) and nitrous oxide (Khaledian et al., 2012; Šima et al., 2013) flux from soils and therefore has a significant environmental effect. The machines in use today are larger, and heavier but they also have more power and are more effective (Varga et al., 2009, Varga et al., 2010). They maintain longer contact with soil than ever before. This effects the soil density. Soil compaction results in changes in water and air movement and also affects root growth. Finally, it also affects the yield crop (Savin et al, 2009).

Soil mechanical resistance (SMR) to penetration varies in time and space (Krištof et al, 2010). Soil mechanical resistance is strongly influenced by water content or water potential and the temporal variation in water content through the growing season accounts for part of the temporal variation in SMR (To & Kay, 2005). The functional relation between SMR and soil water content or potential is referred to as the SMR curve. Measurements on soil cores obtained from the depth of 5 to 7.5 cm across a landscape under contrasting tillage practices have shown that the SMR curve varies with soil characteristics such as texture, organic carbon (OC) content and bulk density (D_b) (Da Silva & Kay, 1997).

With reference to the definitions used in soil resistance, it is clear that many of them have focused on soil bulk density. Accordingly, many researchers have used bulk density to measure soil resistance (Kamgar & Minaei, 2001, Chorom & Sadeghzade, 2005, Javadi & Spoor, 2006). The problem is that the developed penetrometers can be used only for local vertical measurements. From a practical point of view, it appears to be the best and the easiest two-argument comparative method to obtain objective results. This method involves continuous measurement of two parameters. On this principle, a measuring device was developed with the two-argument comparative method at the Department of Transport and Handling. The test measuring device was designed according to the works published by Hoffmann et al., (2012), Hoffmann et al. (2013), Chyba et al. (2013) and Šarauskis et al. (2013).

MATERIAL AND METHODS

As a result of soil compaction, the soil resistance increases, therefore it is possible to use this phenomenon to experimentally measure the degree of soil compaction. The penetrometer method is based on this. So, to use a knife jointer to measure soil resistance, we consider it as an experimental method to detect the degree of soil compaction for the traverse mechanism of tractors. As follows, there is a need to theoretically analyze the principle of soil resistance measuring by a knife jointer. Fig. 1 shows the main dimensions of the knife jointer in depth for the particular task.

The total length of the knife jointer L is given by:

$$L = \frac{H + h}{\cos \beta} + \Delta L \qquad \text{[m]} \qquad (1)$$

where: H – frame height from tip of jointer; h – thickness of the longitudinal beam; ΔL – addition to attaching (or wearing / 100 mm); β – angle of jointer.

The length of blade is determined according to:

$$L_1 = \frac{a}{\cos\beta} + \Delta L_1 \qquad [\text{m}] \qquad (2)$$

where: a – working depth; ΔL_1 – addition with respect to the terrain roughness (100 mm).

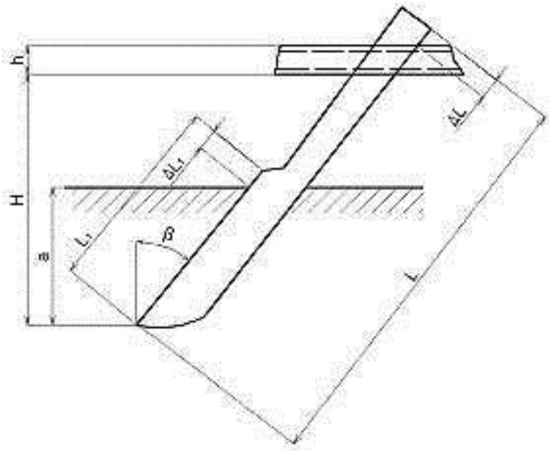

Figure 1. The main dimensions of the knife jointer.

The jointer blade is constructed relative to the vertical axis at an angle β. It depends on the value of this angle whether the slitting plant roots will be sliding along the jointer blade or not. The value of the angle β also determines the recessing ability of jointer (see Fig. 2).

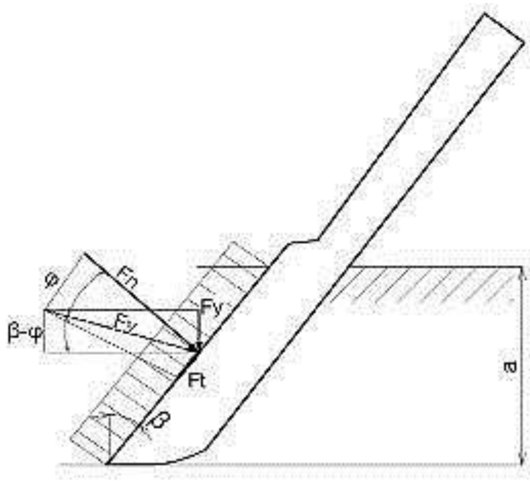

Figure 2. Determining the angle of the jointer blade.

Based on the force relationships solution of the jointer, we assume that the blade of the jointer operates under constant load over the entire length. This load is defined by the centric force F_n, which is calculated by:

$$F_n = \frac{q \cdot a}{\cos\beta} \qquad \text{[N]} \qquad (3)$$

q – specific load on the blade.

The specific load on the coulters q depends on the physical condition of the soil and on the degree of its compaction but also on the state of the blade. The force F_n also causes frictional force F_t, which is given by:

$$F_t = F\ tg\varphi \qquad \text{[N]} \qquad (4)$$

φ – friction angle.

The resultant force of these two forces is the force F_v and is determined according to:

$$F_v = \sqrt{F_n^2 + F^2} = F_n\sqrt{1 + tg^2\varphi} \qquad \text{[N]} \qquad (5)$$

The jointer is pushed into to the land by the vertical component F_y of the resultant force F_v which is calculated according to:

$$F_y = F_v \cdot \sin\left(\beta - \varphi\right) \qquad \text{[N]} \qquad (6)$$

Then it substitutes to:

$$F_y = q \cdot a\left(tg\beta - tg\varphi\right) \qquad (7)$$

It follows from the last formula that the vertical component of the resultant force that causes recessing of the jointer is growing proportionally with the working depth a. For the jointer to recesses into the soil, it must be $F_y > 0$. This will meet the requirement only if:

$$tg\beta - tg\varphi > 0 \qquad (8)$$

Therefore applies to:

$$\beta > \varphi \qquad (9)$$

For the jointer to recess easily, it must be set at greater angle β than the friction angle φ between the steel and the soil. The greatest value of the friction angle is $\varphi = 40°$, which is the value of heavy, wet soil. Therefore, for the jointer to recess under all conditions, there must be $\beta > 40°$. On the basis of this theoretical analysis of force relationships, it applies that soil resistance can be continuously measured on that basis, provided that the force F_n acting on the blade of the jointer will be appropriately registered and measured at work or by moving of the jointer in the soil. On this principle, the measuring device with the two-argument comparative method works.

The methods for measuring soil compaction are based on the principle of measuring the force by inserting an unknown object with a defined geometric shape into the soil. The result shows as the dependency between the force needed to push the object into the soil and the corresponding depth. However, these dependencies have only local significance and cannot be used to establish global soil compaction in a given locality. The developed penetrometers can also only be used for local vertical measurements. From a practical point of view, it appears to be the best and the easiest two-argument comparative method to obtain objective results. This method involves continuous measurement of two parameters. The first parameter characterizes the state of the soil before the negative impact of technology on the soil and the second reflects that negative impact of technology on the soil compaction. Based on this principle, a measuring device was developed with the two-argument comparative method at the Department of Transport and Handling (see Fig. 3), which was really practically tested there.

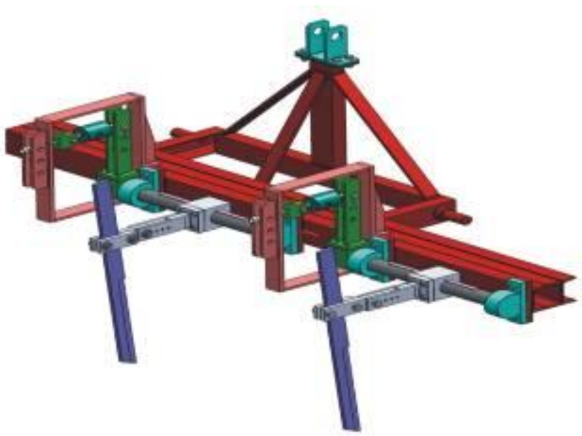

Figure 3. Measuring device with the two-argument comparative method.

The device is attached to the three-point linkage of the tractor with a supporting frame. The beam is welded from three U profiles and it forms the carrying plate of the measuring device. It is fixed to the support frame by two fixing bolts and is adjustable in four positions. This adjustability enables to change the position of the jointers in the wheel track or outside of the wheel track by the tire tread width. There are two shafts pivotally attached to the beam by the bearing housings. On each shaft, there is a jointed blade attached through the hub and shoe. Around the pin, there are pivotally attached shoes with the blade jointer (see Fig. 4).

If the jointer is obstructed, the fuses will be cut so the system is protected against overloading. The principle of the device consists of the fact that in the soil resistance measurement with using jointers, the force applied to the jointers relative to the axis of the shaft causes torque that is transferred through the short arm to the load cells power sensors. The data from the sensors are processed in other measuring and recording devices.

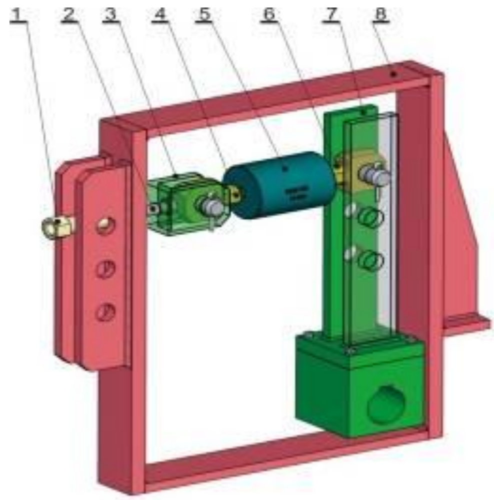

Figure 4. The frame to attach the power sensor: 1 – set screw; 2 – bolt M 12 x 70 STN 02 1101; 3 – sensor bracket; 4, 6 – attachment to the power sensor EMS 150 – 10 kN; 5 – load cells power sensor EMS 150 – 10 kN; 7 – arm, 8 – frame.

The soil resistance was continuously measured in the tire track and outside of the track of a tractor of the type New Holland T6070. The measured parameters – soil resistance (kN) and time (*s*) – were recorded by using the proposed device via load cells power sensors and a handheld digital device HYDAC 2020. The measurements were performed by five passages in the tractor. The soil moisture was 8.47% and 14.24%, the measuring depth 15 cm and tractor speed 3.6 km h^{-1}. The soil bulk density and soil moisture were determined according to the standard norm ISO 11274:1998. All data were processed and graphically illustrated and measurements were performed at two different soil moistures. The land on which the experimental measurements were performed was on school land in Kolíňany, Slovakia. The land was measured after cultivation of winter oilseed rape and spring barley, modified by disks and stubble plough. The type of the soil was brown soil. For measurements, a tractor of the type New Holland T6070 was used, the weight of the tractor with a measuring device: the total of 6,890 kg, 2,860 kg – front axle and rear axle – 4,030 kg. The type of the rear tires used: Firestone 600/65 R38, Radial 9000, pressure 2.5 bar (wheel rim D = 1,000); and the type of front tires: Firestone 480/65 R28, Radial 9000.

RESULTS AND DISCUSION

The results of the soil resistance measurement after multiple passages of a tractor which were recorded by the unit HYDAC 2020 and processed in the PC are shown in the form of a graph in Fig. 5.

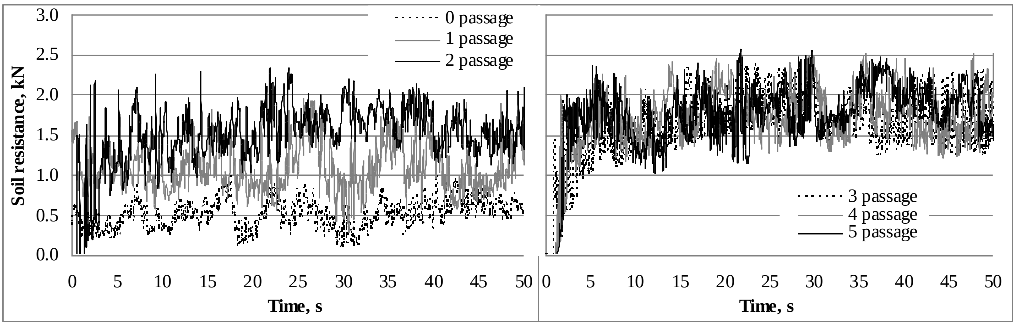

Figure 5. The soil resistance values in the track after each passage (soil moisture 8.47%).

The results of the soil resistance measurement after multiple passages of a tractor at the soil moisture of 14.24% which were recorded and processed in the PC are shown in Fig. 6.

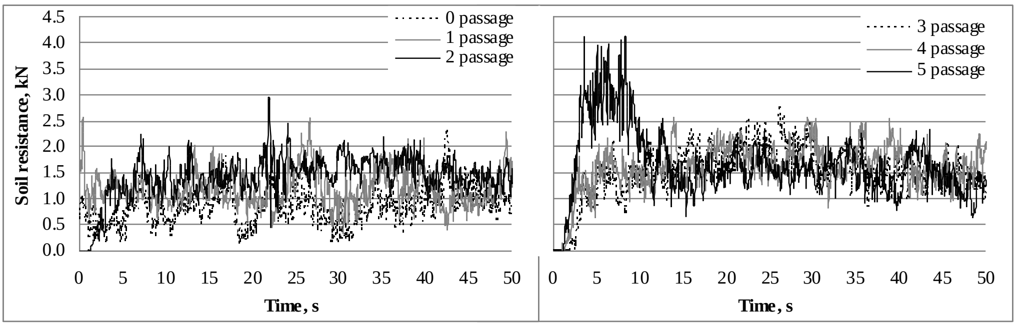

Figure 6. The soil resistance values in the track after each passage (soil moisture 14.24%).

Based on the measurements visible in the graphs, we can compare the values of soil resistance in the track on each passage at different levels of humidity as follows – see Fig. 7. Fig. 8 shows a comparison of the average soil bulk density at different levels of humidity.

The proposed measuring device measured the soil resistance in the tire track and outside of the track after multiple passages at two soil moistures. At the same time, the average soil bulk density and its change after multiple passages of a tractor was measured. As individual graphs show, the soil resistance after each passage increases and it was also observed that after the first passage, the soil resistance increased about 48.1% compared to the initial soil resistance.

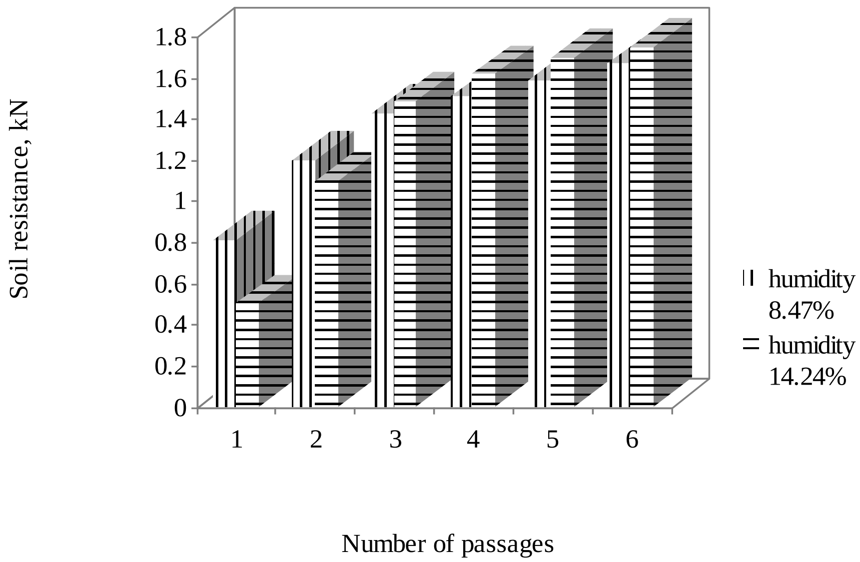

Figure 7. The values of the soil resistance in the track after each passage at different levels of moisture.

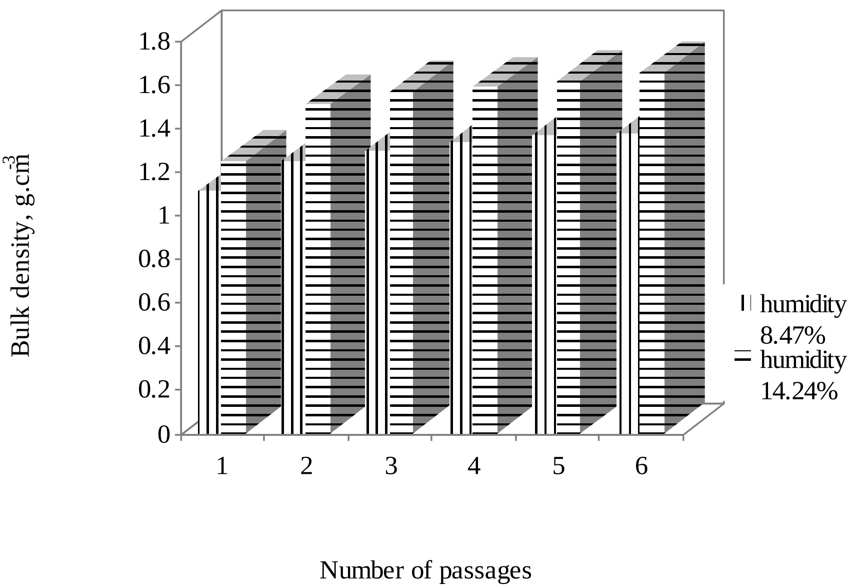

Figure 8. The soil bulk density in the track after each passage at different levels of moisture.

It also increased by about 27.2% after the second passage, about 11.1% after the third passage, about 9.9% after the fourth passage and about 9.9% after the fifth passage compared to the previous soil resistance. The average soil bulk density corresponds to the soil resistance increases proportionally in both absolute and relative terms, depending on the number of tractor passages. The percentage is about 12.6%

after the first passage, about 4.5% after the second passage, about 3.6% after the third passage, about 2.7% after the fourth passage about and about 0.9% after the fifth passage over the previous passage. The second measurements were made under changed humidity conditions from 8.47% to 14.24% and correspond with the results obtained in the first experiment. It is also evident from the graph that the largest increase in soil resistance is after the first passage of the tractor at both values of humidity. Also, the largest increase in the soil bulk density is after the first passage of tractor. In both of these measurements, the higher values of soil bulk density at higher humidity were also measured. If the soil moisture is 8.47%, the land is quite dry which is also reflected in the results of the measurement. Therefore, it can be concluded that since the increase of soil resistance and soil bulk density is influenced by soil moisture and by elevated humidity, the movement of agricultural equipment on the land should be restricted to limit its oppression, thereby reducing its fertility.

CONCLUSIONS

In evaluation of the results, two perspectives are taken into account. First, a measuring device was designed and built for measuring soil resistance with the two-argument comparative method, and simultaneously, measuring and recording devices were designed to capture and record the measured values. The test results showed that the proposed device meets the requirements placed on it and can be used for all types of tractors equipped with a three-point hitch with a tire tread width of 1,000–2,000 mm.

Because of the increasing efforts to accelerate the processing of a large number of measurements, the use of automated penetration systems together with location of the measurements with GPS are increasingly used. This allows us to quickly map the actual conditions of soil environment and to incorporate them into soil maps.

ACKONWLEDGEMENTS. This contribution was realized under the agreement of the solution of the grant project VEGA 1/0857/12 'Reduction of unfavorable impacts of agricultural and transport machinery on environment'.

REFERENCES

Da Silva, A.P. & Kay, B.D. 1997. Estimating the least limiting water range of soils from properties and management. *Soil Science Society of America Journal* **61**, 877–883.

Hoffmann, D., Heřmánek, P., Rybka, A. & Honzík, I. 2012. Evaluation of interaxle carrier and design of mechanical pruner for low trellis system. *Scientia Agriculturae Bohemica* **43**(1), 8–13.

Hoffmann, D., Heřmánek, P., Rybka, A. & Honzík, I. 2013. Design a drive for interaxle mechanical cutter used in low trellises. *Agronomy Research* **11**(1), 39–46.

Chorom, M. & Sadeghzade, F. 2005. The effect of soil compaction on movement, phosphorus and potassium in soil columns. *The Scientific Journal of Agriculture* **27**(2), 139–153.

Chyba, J., Kroulík, M., Lev, J. & Kumhála, F. 2013. Influence of soil cultivation and farm machinery passes on water preferential flow using brilliant blue dye tracer. *Agronomy Research* **11**(1), 25–30.

Javadi, A. & Spoor, G. 2006. The effect of spacing in dual wheel arrangements on surface load support and soil compaction. *Journal of Agricultural Science and Technology* **8**(2), 119–131.

Kamgar, S. & Minaei, S. 2001. Evaluation of the influence of a few effective parameters on soil compaction caused by disk and moaldboard plows. *Agricultural Sciences* **6**(4), 5–19.

Khaledian, M.R., Mailhol, J.C. & Ruelle, P. 2012. Impacts of direct seeding into mulch on the CO_2 mitigation. *Agronomy Research* **10**, 303–310.

Krištof, K., Boďo, T. & Misiewicz, P. 2010. Influence of work implements on selected soil properties. *Technics in agrisector technologies 2010: proceedings of scientific works*, Nitra, november 2010. pp. 86–92.

To, J. & Kay, B.D. 2005. Variation in penetrometer resistance with soil properties: the contribution of effective stress and implications for pedotransfer functions. *Geoderma* **126**(3–4), 261–276.

Savin, L., Nikolić, R., Simikić, M., Furman, T., Tomić, M., Gligorić, R., Jarak, M., Durić, S., Sekulić, P. & Vasin, J. 2009. The influence of soil compaction on changes in soil and sunflower yield. *Savremena poljoprivredna tehnika* **35**(1–2), 26–32.

Sirjacobs, D., Hanquet, B., Lebeau, F. & Destain, M.F. 2002. On-line soil mechanical resistance mapping and correlation with soil physical properties for precision agriculture. *Soil and Tillage Research* **64**(3–4), 231–242.

Šarauskis, E., Romaneckas, K., Sakalaukas, A., Vaiciukevičius, E., Vaitauskiene, K., Karayel, D. & Petrauskas, R. 2013. Theoretical analysis of interaction of disc coulters and straw residues under no-tillage conditions. *Agronomy Research* **11**, 89–96.

Šima, T. & Dubeňová, M. 2013. Effect of crop residues on CO_2 flux in the CTF system during soil tillage by a disc harrow Lemken Rubin 9. *Res. Agr. Eng.* **59**, Special Issue, S15–S21.

Šima, T., Nozdrovický, L., Dubeňová, M., Krištof, K. & Krupička, J. 2013. Effect of crop residues on nitrous oxide flux in the controlled traffic farming system during the soil tillage by LEMKEN Rubin 9 disc harrow. *Agronomy Research* **11**, 103–110.

Varga, F., Jablonický, J., Müllerová, D. & Žikla, A. 2009. Influence of soil resistance on ploughing depth. *Traktori i pogonske mašine* **14**(1), 49–58.

Varga, F., Abrahám, R., Jablonický, J., Boďo, T. & Chrastina, J. 2010. Measurement of soil compaction with horizontal and vertical cone penetrometer. *Savremena poljoprivredna tehnika* **36**(3), 247–255.

Agronomy Research **12**(1), 197–204, 2014

Storage technologies of picked hops during harvest

L. Vent* and A. Rybka

Czech University of Life Sciences Prague, Faculty of Engineering, Kamýcká 129, Praha 6 – Suchdol, Postcode 16521, Czech Republic;
*Correspondence: lvent@tf.czu.cz

Abstract. To prevent interrupting the process of drying or picking due to lack or surplus of hops coming out of picking line, in most cases there is placed a storage container as a capacity equipment. In a container, however, hops are layered, thus temperature and relative humidity increase owing to an increased intensity of hop cones breathing and an insufficient airing, i.e. they mowburn. In the process of breathing a cone loses important substances which results in its worse quality and correspondingly in worse quality of the final product. This work builds on research from 2011. There were monitored changes of physical characteristic of picked hops during storage in container and compared with control variant. This aim of this work is to compare different storage technologies of picked hop in the container. There was a three variants. The control variant was a common stack with a perforated bottom. The second variant was a stack with active ventilation by electric fan. The third variant was a covered stack with passive air circulation. Al stacks had one cubic volume. Data of temperature and relative humidity were continually recorded by MINIKIN TH measuring equipment by EMS Brno company. Another analogue sensors to measure relative humidity and temperature were independently installed for check. The monitoring was each time carried out for 24 hours. Next there were collected a samples for laboratory analysis for product quality. During storage both the temperature and relative humidity of the control variant increased substantially, with temperature values reaching up to 41°C and relative humidity values 100%. The progress of temperatures was almost identical with all the measurements, that is why we present only the average values. The relative humidity of active ventilated variant increased up to 100% but temperature only up to 15°C. The values of humidity of passive ventilated variant were the same (100%) but values of temperature were lower instead of control variant. The highest measured temperature was about 22°C. The conclusion we may draw here says that the best way is passive air circulation. The lowest temperature was measured at variant with fan and it is most important for storage quality of hops but this variant is more expensive due to electric power.

Key words: *hops, storage, alpha and beta acids, hop storage index.*

INTRODUCTION

Nowadays, the most important parameter for trading with hops is content of brewing important substances (alpha and beta bitter acids). Their content is monitored from hop grower to the final processor. The biggest influence on the content of these substances have a climatic condition during the grow season, but we can not control them and the second is postharvest processing, including storaging. Any reduction of the content of these substances have a economic impact for the hop grower. Hop cones, relative humidity of which ranges between 76 and 82% according to Vent et al. (1963), react to separation from the plant in a specific way, primarily by a higher intensity of respiration. The product's relative humidity and temperature will influence and even direct events that occur during storage and may sometimes lead to spoilage and self-heating (Milss, 1989). A higher intensity of respiration results in releasing of relative humidity and energy so that the temperature as well as the surface relative humidity of cones increases. According to Vent (2013) the temperature in the container reaches up to 49°C and the relative humidity up to 100%. This process is described as cone mustiness (Rybáček et al., 1980) and it is intensified by cone damage which is high at mechanical harvest. When the respiration intensity increases, cones lose an important brewery substance which makes the final product less quality. Unlike inert materials such as sand, agricultural products in storage change physically and chemically and need to be managed carefully (Sinha, 1973). Furthermore, consumption of oxygen rises, thus it has to be gained intramolecularly by decomposing the organic substances (Vent et al., 1963). Garetz (1994) states that oxidation processes during storage cause beta acids to become bitter, although they are not bitter in standard conditions compared to α-acids, which get bitter when brewed in the process of isomerization.

MATERIAL AND METHODS

The measurement was carried out in the picking line run by Chmel – Vent Ltd. company in Oploty. For the purpose of the measurement three storage containers had been assembled (Fig. 1). Their volume was 1 m^3 and their bottom was made of perforated sheet steel 1 mm thick, with holes of 8 mm in diameter to allow access of air. The first container served as a check sample. Another container was assembled with the air driven through the perforated bottom. As the source of air flow served MASTER CD 5000 radial ventilator, with power of 2,300 $m^3 h^{-1}$ at a rotational frequency of 1,200 min^{-1}.

Figure 1. Storage container with active ventilation (on the left), with passive ventilation (on the right), and check container (in the middle).

The third variant was represented by a closed container, for which the air outlet was secured by a stack of 0.2 m in diameter and a length of 5 m. Such a concept supposed passive air circulation based on the difference between air intake and air outlet pressures and the air temperature inside the container. The measurement as such included continual (every 3 min) recording of temperature and relative humidity both inside the container and of the surroundings as for all the three variants at the same time. The relative humidity and temperature were measured by special sensors MINIKIN TH with dataloger made by EMS Brno company (Fig. 2). Three repetitions were carried out in the course of the whole measurement, each lasting 24 h. After each repetition the containers were emptied and filled with fresh hops. At the same time, both at the beginning and at the end of each measurement we took a mixed sample of hops to determine the toluene conductometric value according to ČSN 462520-15 as well as the content of alpha and beta bitter acids by spectrophometric method and the aging index (HSI) following the method (ASBC Hops-6) both in the original sample and in the dry matter. The laboratory analyses were provided by Chmelařství, družstvo Žatec laboratory.

Figure 2. Temperature and relative humidity sensors Minikin Th by EMS Brno company.

RESULTS AND DISCCUSION

The first task of the measurement was to determine temperature and relative humidity changes of the picked hops inside the containers. For all the three repetitions the trend of the temperature and relative humidity was very similar. The regular air temperature outside the building ranged from 13°C to 29°C during the three days of measuring. These values do not correspond directly to the air temperature inside the steel warehouse, where the containers with picked hops had been placed. The figure depicting development of the average temperatures (Fig. 3) shows clearly these temperature fluctuations, mostly from 11 a.m. to 2 p.m. The main reasons lie in the position of the sun in the course of the day towards the glass part of the warehouse and the air circulation.

The temperature inside the check container, i.e. without the air circulation, confirmed the expected development. A slight decline in temperature after the container had been filled at the beginning of the measurement was caused by a lower temperature of hop cones than was the air temperature in early morning hours. The temperature increase began as soon as after 20 min of measuring. The average temperature kept on rising continually (Fig. 3), achieving its maximum of 37.8°C at 23:03 which means 15 hours from the container filling. This value could still be recorded for another 18 min and after that started falling slowly (the highest temperature, 41.3°C was recorded during the first repetition), thus confirming Vent's results (2013). The average air temperature at this time ranged from 14.3 up to 14.5°C which is 23.3°C less. The temperature kept on falling until the measurement was finished, when we recorded a temperature of 30.8°C, that is a decrease by 10.1°C during 9 h. A very substantial temperature drop by app. 4°C in the last 20 min was caused by an error in the measurement and is not taken into account.

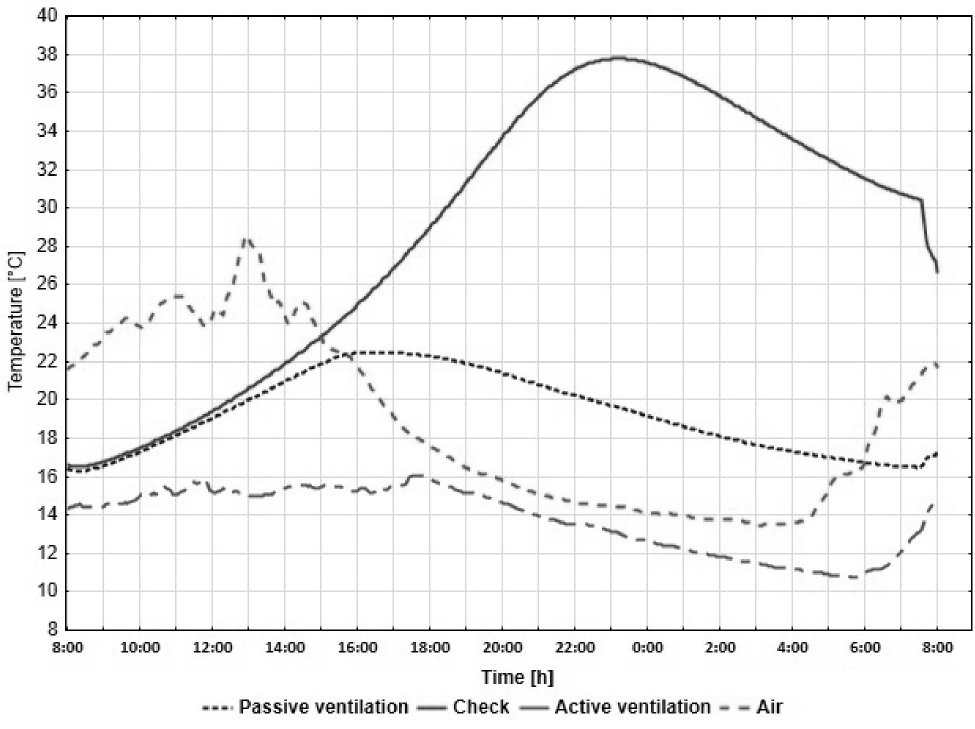

Figure 3. Development of the average temperature of individual variants and the air temperature.

The development of the temperature inside the container with passive air circulation was at the beginning the same as inside the container with no ventilation. However, after four hours of measuring it was evident that warming slowed down compared to the check and reached its maximum of 22.5°C as soon as 8:15 h after filling. At that time the check container temperature was by 2.91°C higher. Already after three minutes, i.e. 8:18 h after filling, the temperature began falling, keeping this trend until the end of the measurement and achieving its final value of 17.0°C. Thus the temperature dropped by 5.5°C during 15 hours which represents a drop by 0.3°C h^{-1}. A substantial temperature drop in the last 20 min was also caused by an error in the measurement and is not taken into account.

The temperature in the container with active air circulation did not show any substantial fluctuation. In the course of the first 10 h of measuring it ranged from 14.3°C up to 16.1°C which at the same time was the maximum value achieved at the time of 9:48 hours from filling. During another 12 h the temperature dropped to the lowest value of the whole measurement, that is 10.8°C at the time of 21:39 hours from filling. In the last two hours of the measurement the temperature inside the container rose by 4.0°C. Fig. 3 illustrates that the temperature inside the container with active air circulation shows with a certain delay a similar trend as the temperature of the surrounding air. This fact can be explained by placing a fan closely to the container, when the air driven into the container had the same temperature as the temperature of the surrounding air. In the contrast, temperature in the container without ventilation does not depend on the temperature of the surrounding air which confirm with results of Vent (2012).

Together with temperature we also measured relative humidity inside the containers. At each measurement of all variants the relative humidity value rose immediately after the measurement had started to the maximum value of 100%, staying unchanged until the end of the measurement. Thus there was no statistically provable difference on the significance level $\alpha = 0.05$ discovered between the relative humidity values which confirm results of Vent & Rybka (2013).

Fig. 4 illustrates that it was the other way round with the measured values of temperature. There were proved significant statistical differences ($\alpha = 0.05$) between individual variants. The highest average temperature was achieved, as it was supposed, by the check variant with no air circulation, namely 28.7°C. The variant with passive air circulation had by 9.46°C or by 33% lower temperature, namely 19.3°C. The lowest average temperature was measured with the variant with active air circulation, 13.8°C, which is by 15.0°C or by 52% lower than with the check variant. In 2011 there was measured by Vent (2012) highest temperature 49°C in the container and they stated that the temperature inside the container depends significantly on the storage time.

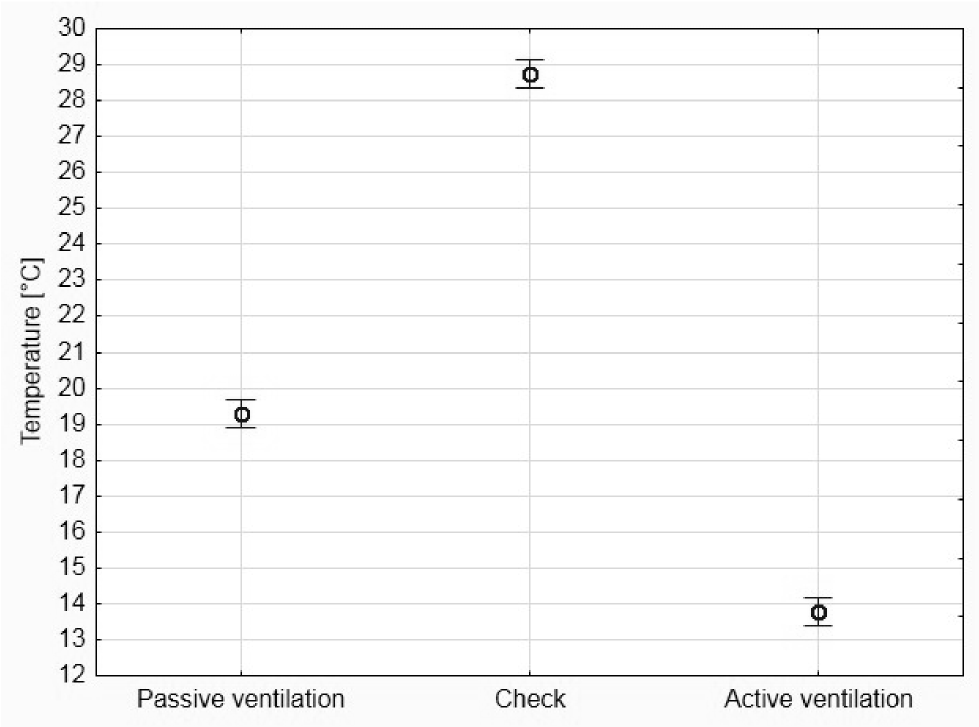

Figure 4. Graphic depiction of compared temperature averages for individual measurement variants with confidence intervals of 0.95.

Another main task of this paper was to verify the influence of technology of picked hops storage on their quality. Four factors were compared, namely the conductometric value, the content of α and β bitter acids by spectrophotometric method, and the aging index value (HSI). The measurement results are shown in Fig. 5, which depicts the average values with confidence intervals 0.95 ($\alpha = 0.05$). The check sample taken before the measurement is termed in the Fig. 5 as 'Start'. The graphic depiction clearly shows that no significant difference between the individual storage variants was proved, thus we may state that regarding the content of important substances, storage technology had no influence on hops quality. However, a closer look shows that the order of individual variants is always the same for all criteria. The best values were achieved by the variant with passive ventilation, followed by the variant with active ventilation, and lastly the check variant (Table 1). The aging index value of the variant with passive ventilation is identical with the starting sample value, that is 0.27.

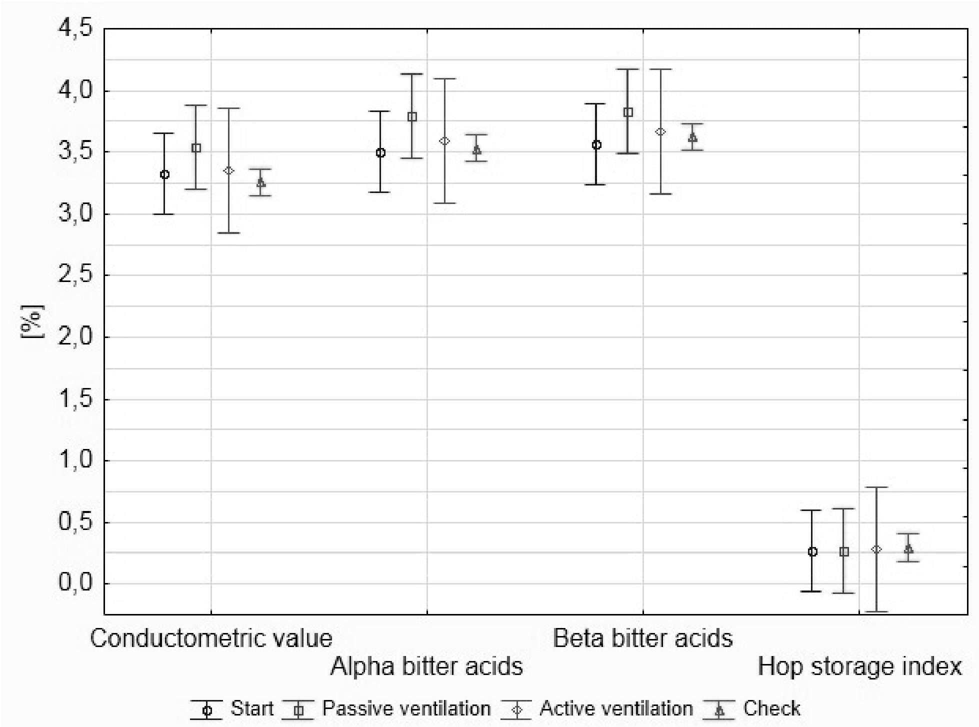

Figure 5. Graphic depiction of compared averages of monitored substances content for individual variants with confidence intervals of 0.95.

Table 1. Compared qualitative parameters of hops

	Conductometric value [%]	α-bitter acids content [%]	β-bitter acids content [%]	Aging index
Passive ventilation	3.54	3.79	3.83	0.27
Active ventilation	3.35	3.59	3.67	0.28
Check	3.26	3.53	3.62	0.29
Start	3.33	3.50	3.57	0.27

CONCLUSION

Given the measured results we may state that of all the tested technologies for hops storage the best results, in all criteria, brought the variant with passive air circulation. The hop cone temperature inside this container did not exceed the value of 22.5°C and the average temperature in the course of 24 hours of storage was 19.3°C (the average air temperature during the measurement was 18.8°C). Laboratory tests proved that from a statistical point of view there is no substantial difference between the verified variants. Even despite these minimal differences, the variant with passive air circulation achieved the best results. The highest conductometric value of 3.54%, the highest content of α-bitter (3.79%) and β-bitter (3.83%) acids determined by spectrophometric method, and together with the original sample the lowest value of storage index 0.27. The check variant with no air circulation achieved the maximum average temperature of 37.8°C (maximum temperature of 41.3°C), thus confirming our measured results from 2011.

ACKNOWLEDGMENTS. This article was written with the support of IGA TF CULS in Prague project number 31160/1312/3115 and NAZV MA CR project number QI101B071.

REFERENCES

Garetz, M. 1994. Hop storage: How to get and keep your hops optimum value. Brewing Techniques, January/February.

Mills, J.T. 1989. Spoilage and heating of stored agricultural products: prevention, detection and control. Research Branch, Agriculture Canada.

Rybáček, V., Fric, V., Havel, J., Libich, V., Kříž, J., Makovec, K., Perlík, Z., Sachl, J., Srp, A., Šnobl, J. & Vančura, M. 1980. Hop production 1, Praha, SZN, 422 (in Czech).

Sinha, R.N. 1973. Interrelations of physical, chemical and biological variables in the deterioration of stored grains. Pages 15–47 in Sinha, R.N.; Muir, W.E., eds. Grain storage: Part of a system. Avi Publishing Co., Westport, Conn.

Vent, L., Antipovič, D., Beránek, F., Blatný, C., Drexler, O., Fiala, V., Fric, V., Gesner, M., Hautke, P., Klapal, I., Kříž, J., Libich, V., Pastyřík, V., Pejml, K., Parlík, Z., Petříček, D., Průša, V., Rybáček, V., Sachl, J., Skládal, V., Stejskal, J., Srp, A., Štys, Z., Vančura, M., Zajíček, E. & Zelenka, V. 1963. Hop production: Organization and technology *1,* Praha, SZN, 409 (in Czech).

Vent, L. 2012. Changes of temperature and humidity parametres of picked hops during storage. *Komunální technika*, roč. 6, č. 5, s. 332–336 (in Czech).

Vent, L. & Rybka, A. 2013. Physical characteristic of picked hops during storage. *Agronomy Research* **11** (1), 125–130.

II LIVESTOCK TECHNOLOGY

Reduction of nitrous oxide and carbon dioxide in the pig barn piggery by different ventilation system intensities

M. Dubeňová[1], T. Šima[2,]*, R. Gálik[1], Š. Mihina[1], G. Vagač[3] and Š. Boďo[1]

[1]Slovak University of Agriculture in Nitra, Faculty of Engineering, Department of Production Engineering, Tr. A. Hlinku 2, 94976 Nitra, Slovak Republic
[2]Slovak University of Agriculture in Nitra, Faculty of Engineering, Department of Machines and Production Systems, Tr. A. Hlinku 2, 94976 Nitra, Slovak Republic;
*Correspondence: tomasko.sima@gmail.com
[3]Slovak University of Agriculture in Nitra, Faculty of Agrobiology and Food Resources, Department of Animal Husbandry, Tr. A. Hlinku 2, 94976 Nitra, Slovak Republic

Abstract. Agriculture, especially animal production, is one of the most important factors influencing greenhouse gases in the atmosphere and causing global warming. The ventilation system in a piggery has a significant impact to carbon dioxide (CO_2) and nitrous oxide (N_2O) concentrations. The concentrations of these gases in pig housing also affect the air quality and welfare of animals. The aim of the paper was to analyze the effect of ventilation system intensity on the concentration of CO_2 and N_2O in a piggery. An experiment was carried out at the Experimental Centre for Livestock at the Department of Animal Husbandry, Faculty of Agrobiology and Food Resources, the Slovak University of Agriculture in Nitra, Slovakia. The concentrations were measured by a photoacoustic field gas monitor INNOVA 1412 connected to a multipoint sampler INNOVA 1309. Three levels of ventilation system intensity were used: low, medium and high. Fattening pigs, the Large White breed were housed in the piggery. For our experiment, three sensors were used inside and two sensors outside the barn. Based on the gathered data, statistically significant differences were found between different ventilation system intensities at a 95.0% confidence level. The concentration of gases fluctuates during day time interval and, based on the results, it is possible to set up a ventilation system intensity to create the best possible air quality in a building for pigs.

Key words: carbon dioxide, concentration, nitrous oxide, pig, ventilator.

INTRODUCTION

Agriculture contributes significantly to polluting gases such as greenhouse gases and ammonia (Kroupa, 2003; Monteny et al., 2006; Aneja et al., 2007; Dubeňová et al., 2011b; Dubeňová et al., 2012). Approximately 20 to 35% of greenhouse gas emissions come from agriculture (IPCC, 2001). Livestock is the source of many pollutants such as gases, odours, dust and microorganisms. 136 gases were found in livestock buildings (Karandušovská et al., 2011). Ventilation systems reduce and control the dust concentration in pig houses (Topisirovic & Radivojevic, 2005; Topisirovic, 2007). According to the European Environment Agency (2010), pig production in Europe represents close to 25% of the livestock emissions. Greenhouse gases like carbon dioxide (CO_2), nitrous oxide (N_2O) and methane (CH_4) participate in global warming and climate change (IPCC, 2007). Agriculture in general, and livestock production in particular, contribute to global warming through emissions of the greenhouse gases: nitrous oxide (N_2O) and carbon dioxide (CO_2). Air pollution is the third largest threat to our planet after biodiversity loss and climate change (most affected by CO_2). The global atmospheric concentrations of these two most important greenhouse gases have increased significantly over the last 150 years (IPCC, 2001) and it affects the atmospheric environment – increased greenhouse emissions (Zavattaro et al., 2012). Nitrous oxide is related to the nitrogen (N) cycle with chemical fertilizers and manures as the most important sources. Nitrous oxide production only takes place under specific conditions since it results from combined aerobic and anaerobic processes nitrification and denitrification, respectively. Normally, conditions in manure are strictly anaerobic and nitrification and denitrification processes will not occur (Monteny et al., 2006). Most of the N_2O is produced in the field conditions by soil tillage (Šima et al., 2013c; Šima & Dubeňová, 2013), from the manure excreted during grazing, animal manure and chemical fertilizers application to land (Šima et al., 2012b; Šima et al., 2013a; Šima et al., 2013b), and also from animal houses where straw of litter is used (Brown et al., 2001; Freibauer & Kaltschmitt, 2001). The nitrous oxide warming potential is 290 to 310 times higher in comparison with the carbon dioxide warming potential (IPCC, 2007). It can usually be estimated that the carbon dioxide produced by livestock is compensated by the photosynthesis of the plants used as feed (Philippe et al., 2011; Šima et al., 2012a). Carbon dioxide emissions differ from one rearing system to another, e.g. weaning and fattening of pigs (Dubeňová et al., 2011a; Dubeňová et al., 2013; Philippe et al., 2007a; Philippe et al., 2007b; Cabaraux et al., 2009). Production of gases, especially CO_2, and wastes by animals are an essential parameter for the ventilation rate estimation using a mass balance method (Pedersen & Ravn, 2008). The methods of manure removal affect the production of harmful gases in the evaluated piggeries for fattening pigs (Mihina et al. 2011). The process of releasing greenhouse gases into the atmosphere depends on the methods of livestock husbandry, nutrition conditions, slurry and manure management and their storage and land application (Palkovičová et al., 2009), number and weight of animals, method and time of manure removal, temperature in the barn, moisture, pH reaction of litter, C:N ratio, etc. The type and power of the ventilation system significantly affect the gas concentration in the pig building (Topisirovic et al., 2010a; Topisirovic et al., 2010b). The gaseous emissions from livestock houses are thus dependent on the housing and the floor systems (Cabaraux et al., 2009).

The aim of the paper was to analyze the effect of the ventilation system intensity on the concentration of CO_2 and N_2O gases in the investigated piggery.

MATERIAL AND METHODS

The experiment was carried out during spring period at the Experimental Centre for Livestock at the Department of Animal Husbandry, Faculty of Agrobiology and Food Resources, the Slovak University of Agriculture in Nitra, Slovakia. A piggery for fattening pigs was investigated, with 2 groups housed in each pen and 1 group of pigs in the last one. Every single pen had a drinking bowl and a feeder. The floor in all of the pens consisted of a bedded system (full floor) and a slatted floor for liquid manure (removed as appropriate). For solid manure removal, conventional technology was used once per day (manually removal). The total capacity of the piggery is 80 fattening pigs. During the experiment, 15 fattening pigs of the Large White breed were used of the average weight of 25.4 kg. Drinking water was provided ad libitum. The fattening pigs were fed ad libitum, all pigs had access to the same feed mixture. The average temperature in the piggery was 27.5°C, the average humidity was 56.2%. The average temperature outside of the piggery was 19.8°C.

During the investigations, 3 sensors were used inside and 2 sensors outside for the gases concentration measurement. The ventilator ran 48 hours for each ventilation system intensity, i.e. Low, Medium and High. The air circulations for Low, Medium and High ventilation system intensities were 0.006, 0.013 and 0.022 $m^3 s^{-1}$ per m^2 of floor surface, respectively. Measurements were always taken in the second half of the measuring time interval. The air circulations values for all ventilation system intensities are shown in Table 1. It means that the first 24 hours was not measured and then the next 24 hours were included in our analysis. Measurement without switching on the ventilator was not performed for the concerns of animal welfare, in order to not unnecessarily stress the animals.

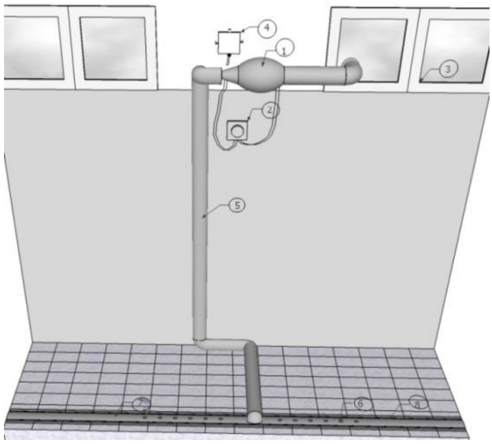

Figure 1. Ventilation system; 1 – ventilator, 2 – control of the intensity of suction (0, I, II, III, IV, V), 3 – window, 4 – electrical supply, 5 – pipe, 6 – holes for the waste air exhaust, 7 – pipe, 8 – grate.

Innova devices (LumaSense Technolgies, Inc., Denmark) were used for the measurement of the concentration of gases. The abovementioned measuring system consists of the following main parts: INNOVA 1412 – a photoacoustic field gas-monitor the measurement system of which is based on the photoacoustic infrared detection method. Gas selectivity is achieved by the use of optical filters and the detection limit is typically in the ppb (part per bilion) region; INNOVA 1309 – a multipoint sampler used for transportation of gas from sampling points to the photoacoustic field gas-monitor INNOVA 1412 for gas analysis. This device includes a 12-channel multiplexer, enabling gas samples to be drawn from up to 12 different sampling locations; the last main part is a computer with software supplied by the manufacturer where the data were saved.

The gathered data were analysed by using the Kruskal-Wallis Test after a normality test by using the Kolmogorov-Smirnov test and a homogeneity of variance by using the Levene's test. We have used the software STATGRAPHICS Centurion XVI.I (Statpoint Technologies, Inc.; Warrenton, Virginia, USA). Graphic presentation of the results was performed using the software STATISTICA 7 (Statsoft, Inc.; Tulsa, Oklahoma, USA).

RESULTS AND DISCUSSIONS

Nitrous oxide

An effect of the ventilation system intensity on the N_2O concentration in the piggery was found. The obtained results are shown in the Table 1 and Fig. 2. Differences were found between the outside concentration, low suction and medium+high ventilation system intensities. There was no statistically significant difference between the medium and high ventilation system intensities.

Table 1. Selected parameters of summarized statistics of N_2O concentration

Intensity of ventilation	Count	Average	Coeff. of variation	Minimum	Maximum	Range
Outside	80	0.4269 $^{\mathbf{a}}$	7.8749%	0.3732	0.5522	0.1789
Low	119	0.7855 $^{\mathbf{c}}$	7.9747%	0.5636	0.9447	0.3811
Medium	119	0.6168 $^{\mathbf{b}}$	11.1326%	0.4617	0.8495	0.3878
High	119	0.6062 $^{\mathbf{b}}$	10.1061%	0.4246	0.7411	0.3165

Note: Different letters in the average value column ($^{a,\ b,\ c}$) indicate that the means are significantly different at $P < 0.05$ according to the LSD multiple-range test at the 95.0% confidence level.

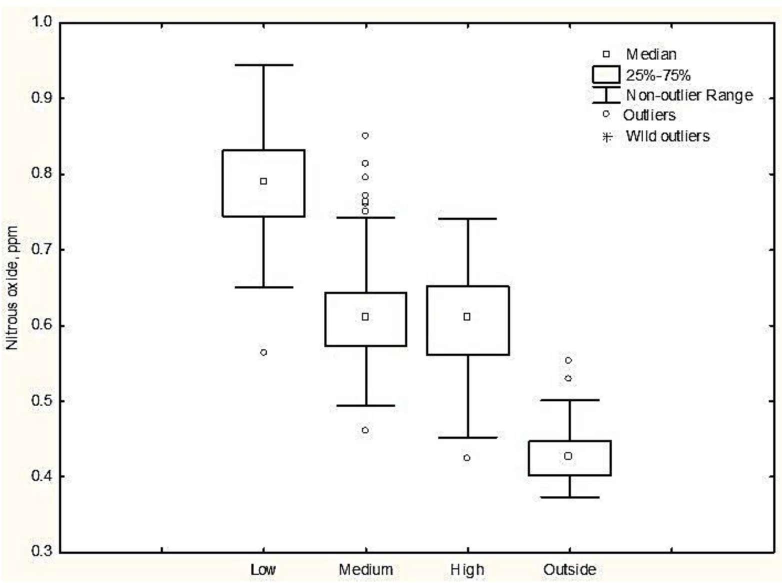

Figure 2. Nitrous oxide concentration in ppm.

Carbon dioxide

An effect of ventilation system intensity on the CO_2 concentration in the piggery was found. The obtained results are shown in the Table 2 and Fig. 3. Some differences were found between outside concentration, low, medium and high ventilation system intensities. Statistically significant differences were found between all ventilation system intensities. Increased ventilation system intensity reduces the carbon dioxide concentration in the pig barn.

Table 2. Selected parameters of summarized statistics of CO_2 concentration

Intensity of ventilation	Count	Average	Coeff. of variation	Minimum	Maximum	Range
Outside	80	549.964 [a]	6.6877%	484.694	628.159	143.465
Low	121	816.341 [b]	9.5548%	709.136	1530.01	820.877
Medium	121	744.042 [c]	9.4594%	648.061	1239.21	591.15
High	121	714.032 [d]	8.2319%	529.032	867.433	338.402

Note: Different letters in the average value column ([a, b, c, d]) indicate that the means are significantly different at $P < 0.05$ according to the LSD multiple-range test at the 95.0% confidence level.

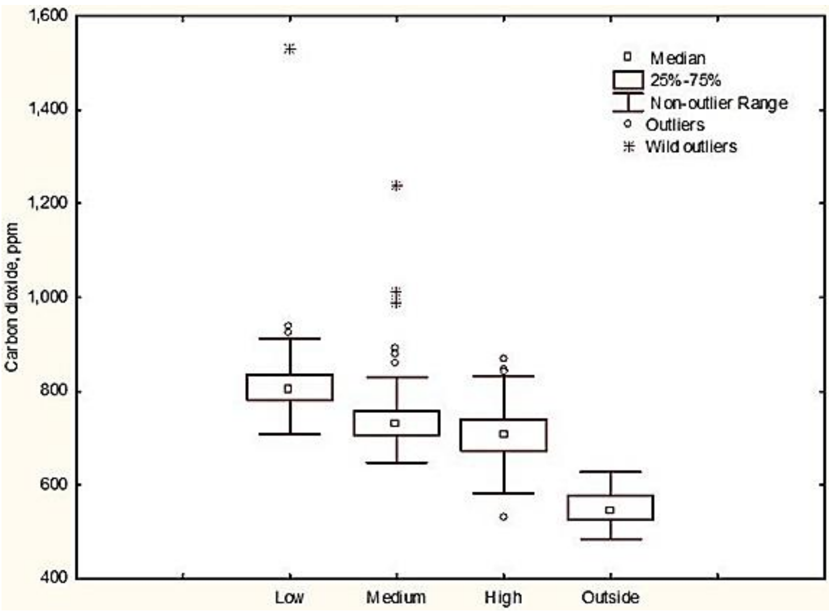

Figure 3. Carbon dioxide concentration in ppm.

Ventilation system intensity had a significant effect on the carbon dioxide and nitrous oxide concentrations in the piggery. Such results confirm our previous results (Dubeňová et al., 2011a; Dubeňová et al., 2011b) and the results obtained by Mihina et al. (2012), where the concentrations of the gases varied depending on the ventilation rate as well as Topisirovic (2007), where the dust concentrations were measured. Carbon dioxide was reduced by increasing the suction rate for all levels of intensity. Nitrous oxide was reduced by increasing the suction, but differences between the medium and high ventilation system intensities were not statistically significant. Similar effects were found (Dubeňová et al., 2013) for the ammonia gas concentration in the piggery for lactating sows with their piglets.

CONCLUSIONS

The paper covered analyses on the effect of ventilation system intensity on the concentrations of CO_2 and N_2O in the piggery for fattening pigs of the Large White breed at the Experimental Centre for Livestock at the Department of Animal Husbandry, Faculty of Agrobiology and Food Resources, the Slovak University of Agriculture in Nitra, Slovakia. A photoacoustic field gas monitor INNOVA 1412 connected to a multipoint sampler INNOVA 1309 were used for measurement of the nitrous oxide and carbon dioxide concentrations. Low, medium and high intensities of the ventilation system was used.

Ventilation system intensity showed a significant effect on the carbon dioxide and nitrous oxide concentrations in the piggery. Carbon dioxide was reduced by increasing the suction rate for all levels of intensity. Nitrous oxide was reduced by increasing the suction rate, but differences between the medium and high ventilation system intensities were not statistically significant. The results of our investigations confirmed that ventilation systems are useful in piggeries including the possibility to optimize gas concentrations and create better welfare for pigs.

ACKNOWLEDGEMENTS. Financed from the project VEGA 1/0609/12 using the INNOVA that was purchased with the support of the project of the EU Structural Funds, 'ITEPAG' no: ITMS 26220220014.

REFERENCES

Aneja, V.P., Blunden, J., James, K., Schlesinger, W.H., Knighton, R., Gilliam, W., Niyogi, D. & Cole, S., 2007. Ammonia assessment from agriculture: status and national needs. In: Monteny, G.-J., Hartung, E. (Eds.), Ammonia Emissions in Agriculture. Wageningen Academic Publishers, Wageningen, pp. 44–51.

Brown, L., Armstrong-Brown, S., Jarvis, S.C., Syed, B., Goulding, K.W.T., Phillips, V.R., Sneath, R.W. & Pain, B.F. 2001. An inventory of nitrous oxide emissions from agriculture in the UK using the IPCC methodology: emission estimate, uncertainly and sensitivity analysis. *Atmospheric Environment* **35**, 1439–1449.

Cabaraux, J.F., Philippe, F.X., Laitat, M., Canart, B., Vandenheede, M. & Nicks, B. 2009. Gaseous emissions from weaned pigs raised on different floor systems. *Agriculture, Ecosystems and Environment* **130**, 86–92 .

Dubeňová, M., Gálik, R., Mihina, Š., Boďo, Š. & Šima, T. 2011a. Vplyv hmotnosti ošípaných na koncentráciu amoniaku vo vybranom objekte počas zimného obdobia. *Technics in Agrisector Technologies 2011: Proceedings of Scientific Works*. FE SUA in Nitra, 20–24.

Dubeňová, M., Gálik, R., Mihina, Š. & Krištof, K. 2011b. Monitorovanie koncentrácie škodlivých plynov v objekte pre výkrm ošípaných. *Rural buildings 2011: Proceedings of Scientific Works*. FE SUA in Nitra. 26–30.

Dubeňová, M., Gálik, R., Mihina, Š. & Šima, T. 2012. Nitrous oxide and carbon dioxide concentration in farrowing pens with permanent limited range of motion for lactating sows. *Poljoprivredna tehnika* **37**, 101–109.

Dubeňová, M., Gálik, R., Mihina, Š. & Šima, T. 2013. Ammonia concentration in farrowing pens with permanent limited range of motion for lactating sows. *Res. Agr. Eng.* **59**, Special Issue, S9–S14.

European Environment Agency, 2010. European community emission inventory report 1990-2008 under the UNECE convention on long-range transbondary air pollution. European Environment Agency, Copenhagen, Denmark.

Freibauer, A. & Kaltschmitt. 2001. *Biogenic Greenhouse Gas Emissions from Agriculture in Europe*. University of Stuttgart, 220.

IPCC, 2001. In: *Houghton, J. T., et al. (Eds.), Climate Change 2001*: The Scientific Background, vol. 94. Cambridge University Press, Cambridge, UK.

IPCC, 2007. Climate Change 2007: The Physical Science Basic. Contribution of Working Group I to the Fourth Assessment Report of the Intergovernmental Panel on Climate Change. Cambridge Univesity Press, Cambridge, United Kingdom/New York, NY, USA.

Karandušovská, I., Mihina, Š., Boďo, Š. & Reichstädterová, T. 2011. Produkcia amoniaku a skleníkových plynov v zmodernizovanom objekte ustajnenia dojíc v letom období. *Rural buildings 2011: Proceedings of Scientific Works*. FE SUA in Nitra. 44–50.

Kroupa, S.V. 2003. Effects of atmospheric ammonia (NH_3) terrestrial vegetation: a review. *Environmental Pollution* **124**, 179–221.

Mihina, Š., Karandušovská, I., Lendelová, J. & Boďo, Š. 2011. Produkcia škodlivých plynov v objektoch pre výkrm ošípaných s rôznym spôsobom odstraňovania hnoja. *Rural buildings 2011: Proceedings of Scientific Works*. FE SUA in Nitra. 84–92.

Mihina, Š., Sauter, M., Palkovičová, Z., Karandušovská, I. & Brouček, J. 2012. Concentration of harmful gases in poultry and pig houses. *Animal Science Papers and Reports* **30**. 395–406.

Monteny, G.J., Bannink, A. & Chadwick, D. 2006. Greenhouse gas abatement strategies for animal husbandry. *Agriculture, Ecosystems and Environment* **112**, 163–170.

Palkovičová, Z., Knížatová, M., Mihina, Š., Brouček, J. & Hanus, A. 2009. Emissions of greenhouse gases and ammonia from intensive pig breeding. *Folia Veterinaria* **53**, 168–170.

Pedersen, B. & Ravn, P. 2008. Characteristics of floors for pig pens: friction, shock absorption, ammonia emission and heat conduction. *Agricultural Engineering International: CIGR Ejournal*, 10.

Philippe, F.X., Laitat, M., Canart, B., Vandenheede, M. & Nicks, B. 2007a. Comparison of ammonia and greenhouse gas emissions during the fattening of pigs, kept either on fully slatted floor or on deep litter. *Livestock Science* **111**, 144–152.

Philippe, F.X., Laitat, M., Canart, B., Vandenheede, M. & Nicks, B. 2007b. Gaseous emissions during the fattening of pigs kept either on fully slatted floors or on straw flow. *Animal* **1**, 1515–1523.

Philippe, F.X., Cabaraux, J.F. & Nicks, B. 2011. Ammonia emissions from pig houses: Influencing factors and mitigation techniques. *Agriculture, Ecosystems and Environment* **141**, 245–260.

Šima, T., Nozdrovický, L., Krištof, K., Dubeňová, M. & Macák, M. 2012a. A comparison of the field and laboratory methods of measuring CO_2 emissions released from soil to the atmosphere. *Poljoprivredna tehnika* **37**, 63–72.

Šima, T., Nozdrovický, L., Krištof, K., Dubeňová, M., Krupička, J. & Králik, S. 2012b. Method for measuring of N_2O emissions from fertilized soil after the using of fertilizer. *Poljoprivredna tehnika* **38**, 51–60.

Šima, T., Nozdrovický, L., Krištof, K., Dubeňová, M. & Krupička, J. 2013a. Effect of the nitrogen fertiliser rate on the nitrous oxide flux from haplic luvisol soil in the laboratory experiment. *Agronomy Research* **11**, 97–102.

Šima, T., Krupička, J. & Nozdrovický, L. 2013b. Effect of nitrification inhibitors on fertiliser particle size distribution of the DASA® 26/13 and Ensin® fertilisers. *Agronomy Research* **11**, 111–116.

Šima, T., Nozdrovický, L., Krištof, K., Dubeňová, M. & Krupička, J. 2013c. Effect of the vertical and horizontal soil tillage technology to nitrous oxide flux from soil. *Trends in agricultural engineering 2013,* proceeding of CULS in Prague, 586–589.

Šima, T. & Dubeňová, M. 2013. Effect of crop residues on CO_2 flux in the CTF system during soil tillage by a disc harrow Lemken Rubin 9. *Res. Agr. Eng.* **59**, Special Issue, S15–S21.

Topisirovic, G. & Radivojevic, D. 2005. Influence of ventilation systems and related energy consumption on inhalable and respirate dust concentrations in fattening pigs confinement buildings. *Energy and Buildings* **37**, 1241–1249.

Topisirovic, G. 2007. Influence of underpressure forced ventilation systems on dust concentration distribution in weaning pigs. *DustConf 2007 How to improve air quality*. International Conference in Maastrich, The Netherlands 23–24 April 2007.

Topisirovic, G., Radojičic, D. & Dražic, M. 2010a. Mogućnosti poboljšanja efektada rada ventilacionog sistema u odeljenjima prasilište i odgajalište na farmi svinja 'Farkaždin'. *Poljoprivredna tehnika* **35**, 5–16.

Topisirovic, G., Radojičic, D. & Radivojevic, D. 2010b. Predlog poboljšanja ambijentalnih uslov u objektima za tov svinja na farmi 'Vizelj'. *Poljoprivredna tehnika* **35**, 17–25.

Zavattaro, L., Grignani, C., Acutis, M. & Rochette, P. 2012. Mitigation of environmental impacts of nitrogen use in agriculture. *Agriculture, Ecosystems and Environment* **147**, 1–3.

Agronomy Research **12** (1), 215–222, 2014

Effect of technical and biological potential on dairy production development

M. Gaworski[1,*] and A. Leola[2]

[1]Department of Production Management and Engineering, Warsaw University of Life Sciences, Nowoursynowska str. 164, 02-787 Warsaw, Poland; [*]Correspondence: marek_gaworski@sggw.pl
[2]Institute of Technology, Estonian University of Life Sciences, Kreutzwaldi 56, EE51014 Tartu, Estonia

Abstract. Dairy production ranks among the most important agricultural activities in many European countries. The general potential of dairy production is created by technical, biological, economic and technological potential. Each unit potential decides about global effectiveness of dairy production including farm as well as national scale. The paper aimed at analyzing importance of some potential in the dairy production development. The significance of technical and biological potential in the dairy production development was indicated, taking into account data coming from Estonian and Polish farms as well as national dairy production systems in two European countries.

Key words: biological potential, dairy production, development, technical potential.

INTRODUCTION

Dairy production is one of the most important agricultural activities in almost all EU countries and in the EU as a whole, both in the previous decades (Viaene & Gellynck, 1997) and at the present time. Every day billions of people around the world consume milk and dairy products.

To provide access to milk and dairy products for consumers it is necessary to create effective dairy system including farms, processing plants, transport means, distribution network and many significant links in the dairy value chain.

Effectiveness of dairy system and its particular parts depends on many factors, including not only assessment of technical and technological solutions but also energy approach (Ahokas et al., 2013). The farm dairy production is an excellent example to show some trends to make dairy production more and more effective.

For the last 50 years, the dairy sector in most developed countries has shifted towards larger herds and greater annual milk production per cow. The driving force in this development has been the need to adopt technologies that require large capital investments and hence depend on larger herds to be profitable. On the other hand, most milk in developing countries is still produced in traditional small-scale systems with little or no mechanization or technological innovations (Gerosa & Skoet, 2013).

The mentioned mechanization, technological solutions, as well as annual milk production per cow and profitability express different kind of potential, which can be recognized in the farm dairy production (Gaworski et al., 2013). Of course it is possible to put some questions concerning significance of technical, technological, biological and economic potential, respectively in the assessment of dairy production development. According to the problem stated, the paper presents results of some analyses, where different kind of the potentials in dairy production were compared.

MATERIALS AND METHODS

To discuss significance of some kind of potential in dairy production, available statistical data edited by Central Statistical Office and organizations responsible for monitoring of dairy production in regional and national scale were collected.

Because the term ‘potential’ is used in relation to some aspects referring to dairy production, so it can be important to give some more deep explanations. We would like to propose the following meaning and scope of research concerning the mentioned term potential in farm dairy production:

- technical potential – set of technical equipment needed to operate herd of cows and milk stream in the farm, including construction complexity;
- technological potential – methods, how dairy cows are kept in the barn, including tie system and loose housing system;
- biological potential – set of data describing dairy cows, i.e. annual milk yield per cow, cows herd size, amount of produced milk;
- economic potential – set of data deciding about economic effectiveness of farm dairy production, e.g. ex-farm milk price, dairy production costs.

The major stage in the undertaken considerations comes down to selection or elaboration of some indices to compare the mentioned potentials in farm dairy production.

The detailed investigations were carried out on the base of data coming from dairy sector in Estonia and Poland. Data concerning two European countries were taken into account to show differences between the regions, where dairy production plays important role in food economy development.

RESULTS AND DISCUSSION

To analyse some relationships between biological potential, economic potential and some aspects of technical potential utilization, the following two indices proposed by Gaworski & Dumas (2012) were used, i.e. index of lost functional benefits (i_f) and index of lost economic benefits (i_e).

The i_f index can be calculated according to the following equation:

$$i_f = \left(1 - \frac{p_i}{p_{\max}}\right) \cdot 100\% \qquad (1)$$

where: i_f – index of lost functional benefits [%]; p_i – milk production in the given month [t·month^{-1}]; p_{max} – maximum milk production per month during 12-months period [t·month^{-1}].

The i_f index expresses effectiveness of milking system utilization defined as relation between amount of milk for milking in the given period and amount of milk, which can be milked in the month with maximum milk production. When the milking installations are used in the months with lower (than maximum) milk production it means that technical potential of the milking installations is not fully utilized. Such situation can be interpreted as lost benefits, when the technical potential is utilized.

However the i_e index can be calculated according to the following equation:

$$i_e = \left(1 - \frac{v_i}{v_{\max}}\right) \cdot 100\% \quad (2)$$

where: i_e – index of lost economic benefits [%]; v_i – pecuniary value of milk produced in the given month [euro]; v_{max} – maximum pecuniary value of milk produced per month during 12-months period [euro].

The proposed indices were calculated for Estonian and Polish conditions of milk production including data for twelve months (January-December) analysed in the period 2011–2013 (Table 1). According to materials published by Statistical Offices in Estonia and Poland, the data concerning amount of milk collected per month were included in the analysis (Table 1). Values of the calculated indices for each month and year were taken to find average values i_f and i_e for particular months (Table 2).

Table 1. Set of data describing biological and economic potential of dairy production in Estonia and Poland for 2011–2013 period

Country	Month	Milk collected [$t \cdot 10^3 \cdot month^{-1}$]			Ex-farm milk price [$euro \cdot t^{-1}$]			Milk pecuniary value [$euro \cdot 10^6 \cdot month^{-1}$]		
		Year			Year			Year		
		2011	2012	2013	2011	2012	2013	2011	2012	2013
Estonia	Jan.	53.8	54.5	57.1	312.6	327.3	321.9	16.82	17.84	18.38
	Feb.	48.4	51.2	52.5	313.2	328.9	327.3	15.16	16.84	17.18
	Mar.	53.5	55.9	59.2	324.0	327.1	329.8	17.33	18.29	19.52
	Apr.	53.0	54.7	58.1	329.5	313.3	325.4	17.46	17.14	18.90
	May	55.9	57.1	61.2	329.1	296.4	326.5	18.40	16.93	19.98
	Jun.	54.2	56.7	60.3	326.9	285.2	327.9	17.72	16.17	19.77
	Jul.	55.3	58.7	61.9	325.8	273.3	330.8	18.02	16.04	20.48
	Aug.	57.0	58.5	61.4	324.9	273.7	333.2	18.52	16.01	20.46
	Sept.	54.3	54.9	58.8	324.6	277.7	344.9	17.62	15.25	20.28
	Oct.	52.6	54.6	58.2	320.4	285.4	352.8	16.85	15.59	20.53
	Nov.	50.9	52.7	56.7	320.4	299.9	361.4	16.31	15.80	20.49
	Dec.	53.4	55.6	60.3	320.0	317.1	375.0	17.09	17.63	22.61
Poland	Jan.	724.2	791.6	782.4	279.0	308.1	300.0	202.04	243.86	234.68
	Feb.	663.8	738.7	724.9	281.9	309.9	301.5	187.15	228.95	218.55
	Mar.	753.3	820.3	813.1	291.0	305.0	304.4	219.19	250.19	247.51
	Apr.	753.0	854.7	816.9	292.3	293.3	305.4	220.10	250.72	249.47
	May	842.5	905.9	891.4	288.8	286.6	305.4	243.36	259.59	272.26
	Jun.	847.7	869.4	859.7	289.6	281.9	308.2	245.50	245.05	264.97
	Jul.	829.7	867.9	892.0	289.5	279.3	315.2	240.20	242.41	281.13
	Aug.	820.7	860.7	867.1	292.1	281.3	321.5	239.76	242.10	278.73
	Sept.	785.5	809.9	822.8	294.3	283.5	337.6	231.13	229.61	277.73
	Oct.	774.1	790.0	816.5	298.7	289.9	348.4	231.27	229.01	284.43
	Nov.	728.2	730.2	768.2	307.9	299.9	373.3	224.25	218.94	286.79
	Dec.	760.2	762.6	810.1	313.8	300.6	378.7	238.55	229.23	306.77

Source: Central Statistical Offices in Poland and Estonia and own calculations

Table 2. Index of lost functional benefits (i_f) and index of lost economic benefits (i_e) calculated for Estonia and Poland including 2011–2013 period

Country	Month	Index of lost functional benefits i_f [%]				Index of lost economic benefits i_e [%]			
		Year			Average	Year			Average
		2011	2012	2013		2011	2012	2013	
Estonia	Jan.	5.6	7.2	7.8	6.8	9.2	2.5	18.7	10.1
	Feb.	15.1	12.8	15.2	14.4	18.2	7.9	24.0	16.7
	Mar.	6.1	4.8	4.4	5.1	6.4	0.0	13.7	6.7
	Apr.	7.0	6.8	6.1	6.7	5.7	6.3	16.4	9.5
	May	1.9	2.7	1.1	1.9	0.7	7.5	11.6	6.6
	Jun.	4.9	3.4	2.6	3.6	4.3	11.6	12.5	9.5
	Jul.	3.0	0.0	0.0	1.0	2.7	12.3	9.4	8.1
	Aug.	0.0	0.3	0.8	0.4	0.0	12.5	9.5	7.3
	Sept.	4.7	6.5	5.0	5.4	4.8	16.6	10.3	10.6
	Oct.	7.7	7.0	6.0	6.9	9.0	14.8	9.2	11.0
	Nov.	10.7	10.2	8.4	9.8	12.0	13.6	9.4	11.6
	Dec.	6.3	5.3	2.6	4.7	7.7	3.6	0.0	3.8
Poland	Jan.	14.6	12.6	12.3	13.2	17.7	6.1	23.5	15.8
	Feb.	21.7	18.5	18.7	19.6	23.8	11.8	28.8	21.4
	Mar.	11.1	9.5	8.8	9.8	10.7	3.6	19.3	11.2
	Apr.	11.2	5.7	8.4	8.4	10.3	3.4	18.7	10.8
	May	0.6	0.0	0.1	0.2	0.9	0.0	11.3	4.0
	Jun.	0.0	4.0	3.6	2.5	0.0	5.6	13.6	6.4
	Jul.	2.1	4.2	0.0	2.1	2.2	6.6	8.4	5.7
	Aug.	3.2	5.0	2.8	3.7	2.3	6.7	9.1	6.1
	Sept.	7.3	10.6	7.8	8.6	5.9	11.5	9.5	9.0
	Oct.	8.7	12.8	8.5	10.0	5.8	11.8	7.3	8.3
	Nov.	14.1	19.4	13.9	15.8	8.7	15.7	6.5	10.3
	Dec.	10.3	15.8	9.2	11.8	2.8	11.7	0.0	4.8

Source: own calculations

The average values of the index of lost functional benefits (i_f) and the index of lost economic benefits (i_e) were presented together including the radar graphs for Estonia (Fig. 1) and Poland (Fig. 2).

For Estonia and Poland the lowest average value of the index of lost functional benefits (i_f) were found in August and May, respectively. However the lowest average value of the index of lost economic benefits (i_e) can be recognized in both countries in May.

When we compare visually the radar graphs on the Figs 1 and 2 as well as detailed values of the discussed indices it is possible to indicate considerable bigger area covered by the graphs for Poland. Such results suggest higher possible losses of functional and economic benefits connected with use of technical potential for milking on the dairy farms. At the same time results of the analyses confirm significance of stability of dairy production and needs to implement proper management practices in dairy production to keep possibly balanced milk flow in the dairy system.

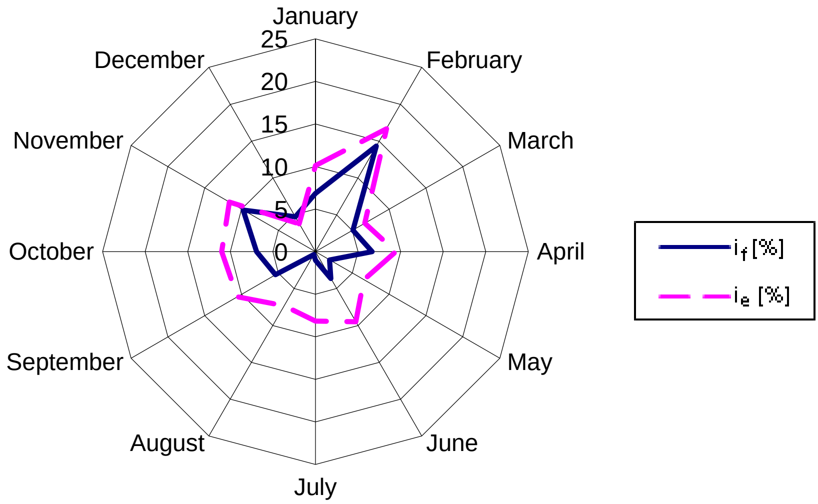

Figure 1. Index of lost functional benefits (i_f) and index of lost economic benefits (i_e) calculated for Estonia (Source: own elaboration).

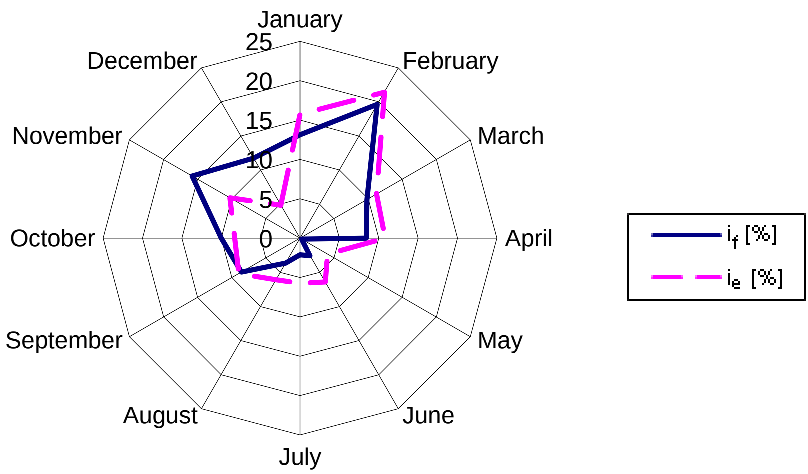

Figure 2. Index of lost functional benefits (i_f) and index of lost economic benefits (i_e) calculated for Poland (Source: own elaboration).

The next step of the investigations included analysis of some factors deciding about differences in biological potential between dairy farm, which can show effect on technical potential, especially milking systems load and capacity. Basing on data coming from Polish dairy system covering 16 regions (voivodeships) with 19,916 herds considered, dairy cows herd size with annual milk yield per cow have been collated. The result of the taken together data for 2012 was presented on the Fig. 3.

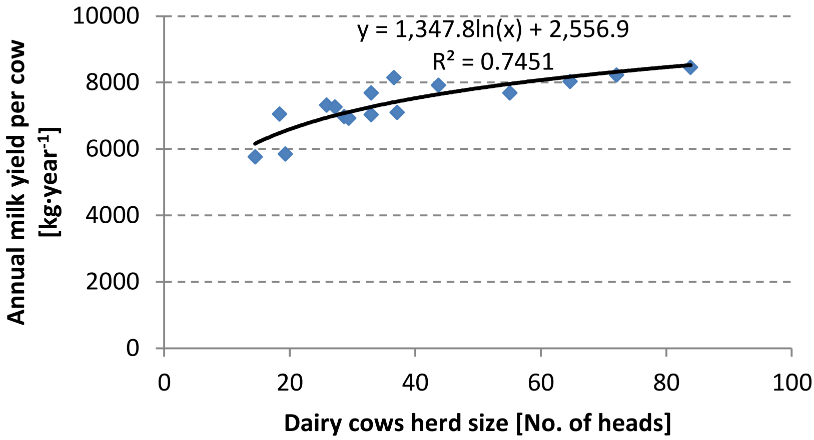

Figure 3. Relationship between annual milk yield per cow and dairy cows herd size for Polish dairy farms under recording system in 2012 (Source: own calculations on the base of data coming from Polish Federation of Cattle Breeders and Dairy Farmers).

It is possible to indicate (Fig. 3) that annual milk yield per cow increases with higher number of dairy cows in the herd. The mentioned relationship can be described by curve with coefficient of determination (R^2) amounted to more than 0.7. Especially for bigger cow herd sizes (more than 40 cows per herd) the increase tendency bases on the points (data) not very distributed around the curve.

Extending discussion concerning the given above relationship there is possible to indicate some additional effects and suggestions. The bigger and bigger size of dairy herds is accompanied by higher annual milk yield per cow and at the same time necessity to use higher capacity milking systems. It means that higher capacity milking systems are used to operate animals characterized by higher annual milk yield. As a result it is possible to indicate that higher technical potential is responsible for operation of higher biological potential. The higher technical potential concerning milking systems is characterized by modern solutions and such modern technical solutions are used on the farms with higher biological potential of cows. The given above considerations confirm importance and advantages coming from simultaneous implement of different kind of progress in agriculture and agricultural activities (Gaworski, 2006).

To develop problem of technical potential modernity in dairy production we have analyzed changes in the number of different kind of milking installations and equipment for farm milk cooling. The data coming from Polish dairy system were included, where each few years detailed statistical monitoring of farms is carried out on the base of questionnaire.

In the field of milking the data concerning the following type of solutions: bucket milking machines and pipeline milking machines were included. However in the field of milk cooling such type of solutions was taken into account: coolers of milk in buckets and tank milk coolers. Including total number of milking installations and cooling systems in Polish dairy farms we have calculated share of more modern solutions (pipelines milking machines and tank milk coolers) in each group of considered technical equipment for 1996, 2002 and 2010.

The results of the carried out calculations (Fig. 4) show considerable differences in the share of modern technical solutions in relation to total number of the given groups of technical equipment. Generally there is possible to note increase in the share of pipelines milking machines and tank milk coolers in the analyzed period. But there can be indicated higher increase in the share of modern equipment for cooling in comparison with increase in the share of pipeline milking machines. We can ask about reason of such tendency. It seems to be important that higher share and changes concerning tank milk coolers result from their lower investment costs (in comparison with milking installation), possibilities to reduce (safe) energy consumption (in comparison with coolers of milk in buckets), needs to meet milk high quality standards and keep raw milk for 2–3 days in the farm, as a result of milk purchase organization.

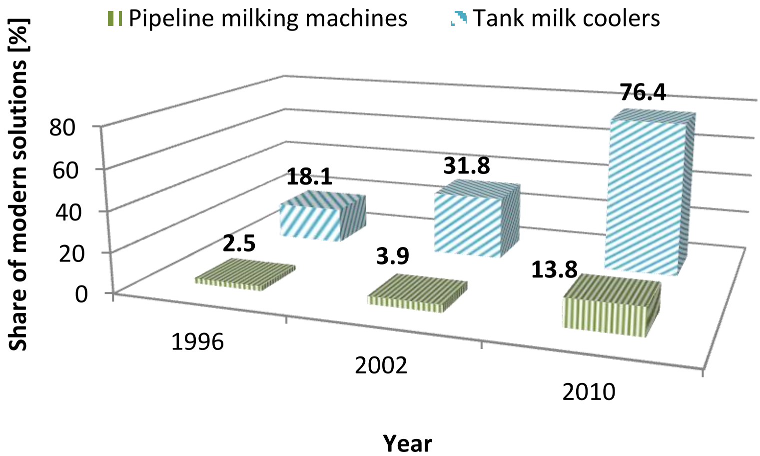

Figure 4. Share of modern technical solutions in relation to total number of milking machines and milk coolers in Poland in the years 1996, 2002 and 2010 (Source: own elaboration on the base of Central Statistical Office data, Poland).

CONCLUSIONS

Dairy production constitutes area, where some indices connected with assessment of different kind of potential can be proposed and used for comparisons between dairy production regions. Results of the carried out analyses show possible losses of functional and economic benefits connected with use of technical potential for milking. Stabile (month by month) dairy production in terms of amount and value of milk collected from the farms is one of the most important factors, which confirm premise for effective use of technical potential (equipment) in dairy production.

The included indices in the analyses show general approach to the important problem of effectiveness of milking systems utilization. At the same time, the indices can be one of the propositions to carry out more deep analyses concerning factors affecting development and assessment of milking systems and their technical potential against a background of biological potential of dairy cow herds.

When dairy farms are implemented with more and more modern technical solutions for milking there is simultaneous improvement of dairy cow herds expressed by annual milk yield per cow and other factors expressing biological advance.

Each part of the dairy system constitutes field of detailed research considerations to assess previous and current development as well as to show premises for further improvement.

REFERENCES

Ahokas, J., Mikkola, H., Jokiniemi, T., Rajaniemi, M., Schäfer, W., Rossner, H., Poikalainen, V., Praks, J., Veermäe, I., Frorip, J. & Kokin, E. 2013. ENPOS – Energy positive farm. *Agronomy Research* **11**(2), 523–527.

Central Statistical Office, 2012. Warsaw, Poland.

Gaworski, M. 2006. Analysis of different forms of advance in dairy production. *Veterinarija ir Zootechnika* **35**(57), 48–52.

Gaworski, M. & Dumas, F. 2012. Assessment of technical potential use in dairy production on an example of comparative analysis covering French and Polish conditions. *Ann. Warsaw Univ. Life Sci. – SGGW, Agricult.* **60**, 89–96.

Gaworski, M., Leola, A. & Priekulis, J. 2013. Comparative analysis on effectiveness of AMS use on an example of three European countries. *Agronomy Research* **11**(1), 231–238.

Gerosa, S. & Skoet, J. 2013. Milk availability: Current production and demand and medium-term outlook. [In:] Milk and dairy products in human nutrition. *FAO*, Rome, 11–40.

Polish Federation of Cattle Breeders and Dairy Farmers, Statistical Office, Warsaw, 2013.

Viaene, J. & Gellynck, X. 1997. Competitiveness of the dairy industry in EU and challenges for new member states. [In:] Integration of the dairy sector with European Union, challenges and chances for Central Europe. Warsaw Agricultural University – SGGW, Warsaw, 11–24.

Agronomy Research **12** (1), 223–230, 2014

IceTag3D™ accelerometric device in cattle lameness detection

E. Kokin[1,*], J. Praks[2], I. Veermäe[2], V. Poikalainen[2] and M. Vallas[2]

[1]Institute of Technology, Estonian University of Life Sciences, Kreutzwaldi 56, EE51014 Tartu, Estonia; *Correspondence: eugen.kokin@emu.ee
[2]Institute of Veterinary Medicine and Animal Sciences, Estonian University of Life Sciences, Kreutzwaldi 1, EE51014 Tartu, Estonia

Abstract. The objective of the pilot study was to evaluate the possibility of using IceTag3D™ accelerometric device for the early detection of lame cows in dairy herd. The measurements were carried out in the experimental cowshed of Estonian University of Life Sciences in the free-stall section with milking parlour. The time the cow spent lying and standing, number of lying bouts, step count and the motion index of 33 dairy cows (14 lame and 19 sound cows) was registered during 15 days period. The measurements confirmed that the lame cows stand and move less than sound animals. As the same trend was in force for older cows it was impossible to differentiate the influence of lameness and age. To clarify the inequality in activity between lame and sound rear legs both legs of lame cows were equipped with loggers (eight cows). Great difference in recordings of diseased and healthy leg lying bouts (ratio 2.47) indicates that this parameter may be one possibility to identify leg disorders. However, further investigations are needed to synchronize video- and IceTag recordings and identify threshold values.

Key words: dairy cow, lameness, accelerometer.

INTRODUCTION

Lameness of dairy cows has been classified as very important welfare problem at loose housing. With increasing herd size the need for an objective, automatic lameness scoring grows considerably (Anonymous, 2001; Berckmans, 2004; Poikalainen et al., 2004, 2013; Kokin et al., 2007).

For cows' gait registration and analysis four basic approaches are suggested – using walk-through scales, systems with pressure sensitive walk-over mats, automatic analysis of video-signals, and activity monitoring using accelerometric systems.

Walk-through scales, based on vertical ground reaction force measurements of individual limbs were elaborated and are available commercially. Vertical forces measured over time with two parallel force plates are used to calculate a number of limb movement variables. To separate the results of individual animal within a group walking through the system special algorithm was developed (Rajkondawar et al., 2006).

The preliminary research of using mats with sensors responding to the foot pressure has been carried out by different groups (Maertens et al., 2007). At the University of Helsinki and Estonian University of Life Sciences a walk-over mat with quasipiezoelectric sensors was tested for automatic cows' gait registration (Poikalainen et al., 2010).

Research has proved that automatic use of video signals has great potential to be used for continuous monitoring of lameness. The automatic lameness detection methods by vision analysis of feet movement and back curve were elaborated. A strong linear regression exists between locomotion score given by automatic system and by experts (Maertens et al., 2007; Pluk et al., 2009).

Accelerometric systems monitoring locomotion activity, lying and standing behaviour can be used also for lameness estimation. However, their accuracy is not as good as in case of gait registration systems described above. It can be improved using three-dimensional accelerometers especially when attached to a leg (Chapinal et al., 2010).

Detailed information about the gait and activity gives valuable information about the leg health status of dairy cows. Moreover, by Nielsen et al. (2010) the activity data may provide important input to algorithms for automatic detection of lameness. Assessing walking peculiarities in cows by visual or video-based observations is very time consuming. It is the reason why sensitivity and specificity of automated recording devices for lameness detection have become a focus of recent research. Several commercially available data loggers record lying and walking behaviour in cattle. Loggers are attached around the neck (Martiskainen et al., 2009), body (Champion et al., 1997), or leg (Müller & Schrader, 2003; O'Driscoll et al., 2008; Pastell et al., 2009; Robert et al., 2009; Trénel et al., 2009). Loggers used on the leg are more common than those attached around the neck or the body and are able to measure lying and standing time quite precisely. These are less accurate when assessing other behaviours such as activity (Müller & Schrader, 2003; Robert et al., 2009; Trénel et al., 2009), unless the sampling interval is extremely short (every 10 ms; Scheibe & Gromann, 2006).

Loggers attached to the leg use mainly the accelerometers as the information source. In our experiments IceTag3D™ loggers were used. The objective of our pilot study was to evaluate the possibility of using this type of loggers for the early detection of lame cows in dairy herd.

MATERIAL AND METHODS

IceTag3D™ is a logger with accelerometric sensors that measures animal activity with sampling rate 16 Hz, and has data granularity up to 1 second. The logger is programmed to record the g-force in three dimensions. The waterproof loggers are usually attached to the lateral side of the cow's hind leg above the metatarsophalangeal joint by means of a special strap. The device memory is sufficient to store the results of 60 days measurements. For wireless download of data from the on-board memory of the IceTag logger to a personal computer (PC), where the dedicated IceTagAnalyser software is installed, a desktop unit IceReader is used.

The IceReader is connected to a PC via standard USB connection. By swiping the logger over the IceReader, the user can activate or deactivate logger and download data from the IceTag to PC on a per-second basis. Data are exported to an Excel spreadsheet. For each recording the IceTagAnalyser computes:

1) the time the cow spent lying and standing, determined by the sensor passing a specific threshold between horizontal/vertical position;

2) lying bouts count determined by start and end time of each lying bout;

3) step count determined on the number of times the cow lifts her tagged leg, based on the acceleration of the animal leg;

4) the motion index which reflects the average magnitude of acceleration on each of the 3 axes (IceRobotics Ltd, Product Guide 2010).

Our measurements were carried out in the experimental cowshed of Estonian University of Life Sciences in the free-stall section with milking parlour. This section has 70 laying cubicles, 35 automatic feeders for mixed rations, 2 water troughs. Cows had *ad libitum* access to the feeders and water troughs. Cows were milked twice per day. A week before the experiments a professional hoof trimmer inspected the hooves, recorded the presence of injuries and trimmed the hooves. Cows' gait was assessed by using 5 numerical rating score system: 1–2 sound, 3–5 lame (Sprecher et al., 1997).

Two experimental groups of animals were formed:

1) to clarify the difference in moving activity in connection with leg health status one rear leg of each of 33 cows was equipped with a logger (14 cows lame – injured one rear leg, 19 cows sound, 15 days period);

2) to clarify the inequality in activity between lame and sound rear legs both legs of lame cows were equipped with loggers (subsample of first experimental group with eight cows, 10 days period).

In the first experimental group eight lame cows had hooves lesions diagnosis (digital dermatitis, lesion in the sole and white line disease), six lame cows were found out in addition by visual inspection. Five of them had rating score 4, nine animals had rating score 3.

In the second experimental group three cows had hooves lesion diagnosis and five cows were defined as lame by visual inspection. One cow had rating score 4 and seven cows had rating score 3.

The loggers were attached in sound animals mainly on the lateral side of the right hind leg. In cases of injury caused by the logger rubbing against the leg, the device has to be transferred to the left hind leg. In the first experiment in lame animals the loggers were attached to the healthy rear leg. The data from the IceTags were collected in April, 2013 with six days delay after fitting the loggers. Data were downloaded at the barn (Fig. 1).

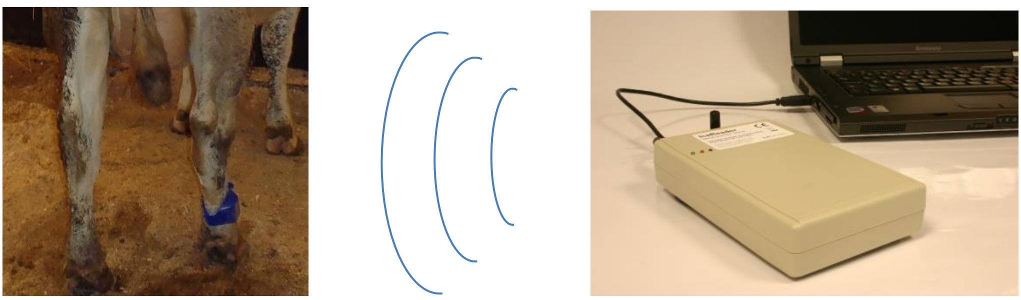

Figure 1. Eksperiment layout: IceTag sensor is attached to cow's right hind leg (left) and reading device (right) is communicating with it by radiolink.

After attaching the loggers five animals tried to get rid of them, shaking the loaded leg. By MacKay et al. (2012) cows showed an increase in time spent standing and decrease in time spent lying over the first two tagged days. Authors recommend that data may not be reliable until two days after the attachment of the device. In our experiments we analysed recorded data starting with the seventh day, allowing animals to adjust with the loggers for longer period.

In case of four sound animals the legs equipped with the logger were changed during the experiment as signs of rubbing developed. Nielsen et al. (2010) also report that injuries will develop within a few days if the device is attached so tight that it cannot move up and down and around the leg.

Total of 481 and 80 measurements were collected for the first and second experimental group of animals, respectively.

The data registered by the IceTags were prepared for the analysis in MS Excel and processed using SAS software version 9.2 (SAS Inst. Inc., Cary, NC, USA). Least-square means were estimated from linear mixed models or generalized linear mixed model (for not normally distributed motion index) with fixed effect of lameness, lactation, experimental day and random effect of cow.

RESULTS AND DISCUSSION

Descriptive statistics of IceTags records for 33 cows are presented in Table 1.

The data in table describes variations in mean values of cows' standing and lying time in sec, number of steps, motion index and lying bouts calculated from axcelerometric parameters. The other main statistical parameters are also described.The variability of recorded activity of cows between the experimental days is great. The reason may be the changing environment in the experimental cowshed because of different tests going on simultaneously that disturbs the animals.

Table 1. Descriptive statistics of recorded activity data per day of 33 cows (481 measurements)

Variable	Mean	Standard dev.	Mini-mum	Lower quartile	Median	Upper quartile	Maxi-mum
Standing, s	45,216	8,363	23,377	40,228	45,317	50,250	71,539
Lying, s	41,181	8,365	14,861	36,150	41,068	46,172	63,023
Steps	2,311	897	809	1,633	2,206	2,864	6,398
Motion index	6,682	3,029	1,844	4,596	6,156	8,314	21,248
Lying bouts	72	89	10	24	38	85	656

The values of the least-square means of the parameters recorded by the IceTags are presented in Table 2 depending on lameness and age of cows.

The age of cows is reflected by the lactation number (1, 2, and 3). The difference of mean lying time for sound and lame cows is about 29 min, the difference of mean lying time between first and second lactation is about 28 min and between second and third lactation – about 6 min per day.

Table 2. Least-square means with standard errors (SE) of recorded activity data per day of 33 cows

Item	Lying, sec		Standing, sec		Motion Index		Lying bouts		Steps	
	Mean	SE	Mean	SE	Mean	SE	Mean	SE	Mean	SE
Sound	40,446	1,843	45,952	1,843	6,788	634	54	11	2,335	196
Lame	42,167	2,110	44,228	2,111	5,423	581	46	11	1,905	183
Lactation 1	40,058	2,464	46,334	2,463	6,547	818	56	15	2,224	249
Lactation 2	41,748	2,028	44,651	2,027	6,102	628	41	9	2,260	209
Lactation 3	42,114	2,706	44,284	2,705	5,590	767	54	16	1,867	230

Thomsen et al. (2012) used IceTags to evaluate the relationship between gait rating scores (GRS 1–5), lying behaviour and indicators of hoof lesions in dairy cows. They concluded that gait rating scoring and duration of lying bouts may be used as tools in the management of hoof health in dairy herds. Blackie et al. (2011) found that the lame cows (GRS–3) spent significantly longer lying down compared to non-lame (GRS–1 or GRS–2) cows (13 h day^{-1} vs. 10.9 h day^{-1}, respectively). But the differences in lying times between lame and non-lame cows only differed significantly in the evening period (16:01–23:00). By Chapinal et al. (2010) lame cows tended to spend more time lying down because of longer lying bouts. There was no effect of lameness on frequency of lying bouts or the number of steps taken.

The results of our statistical analysis show also that there is the trend that the lame cows stand and move less than sound animals. We found also that the age of cows has clear effect to the activity: older cows' activity was lower. However, considering daily variations of cows' data the number of experimental animals was insufficient to identify the possible influence of lameness to activity data based on one sensor per cow measurements.

Descriptive statistics of IceTags records for lame and sound rear leg of lame cows are presented in Table 3.

Standing and lying time measured by diseased and healthy legs are similar, quite similar are also motion index and number of steps. Great difference is in recordings of lying bouts (Fig. 2): average ratio 2.47 (duration of each bout by diseased leg 5 min. 15 sec., by healthy leg 9 min. 44 sec.).

Table 3. Descriptive statistics of lame cow activity per day by lame and sound rear legs recordings (eight cows with total of 80 measurements)

Characteristic	Leg	Motion Index	Standing, h	Lying, h	Steps	Lying bouts
Average	diseased	5,281	11:50:11	12:09:49	1,998	139
	healthy	5,170	11:59:55	12:00:10	2,061	74
Min	diseased	4,257	10:09:33	10:16:02	1,642	65
	healthy	4,600	10:16:29	10:03:57	1,701	34
Max	diseased	7,004	13:43:58	13:50:27	2,554	217
	healthy	7,415	13:56:03	13:44:23	2,639	111
Standard dev.	diseased	821	1:03:40	1:03:40	274	45
	healthy	856	1:06:24	1:06:34	282	22
Ratio diseased/healthy (average)		1.07	0.99	1.02	0.96	2.47

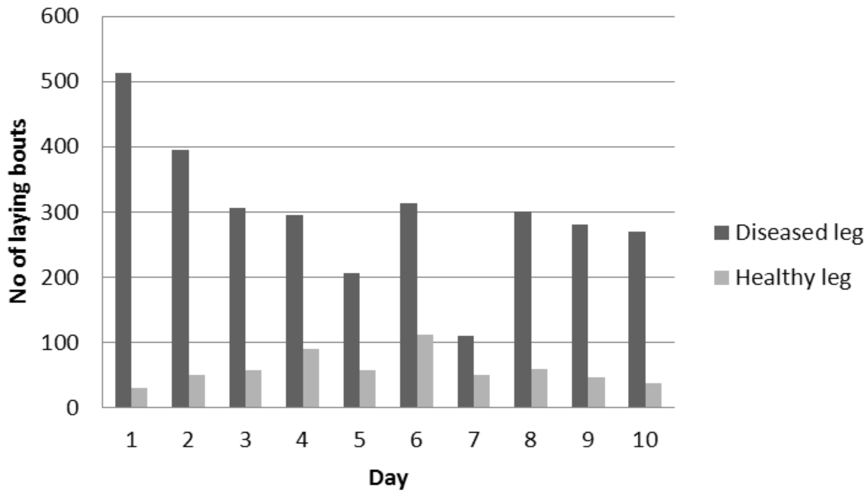

Figure 2. The difference of number of laying bouts between the lame and sound legs.

The number of lying bouts is abnormally great. By Higginson et al. (2010) the difference in data of lying bouts between legs in the alternate leg device placement was caused by the movement of the upper leg while the lower leg was immobile. Trénel et al. (2009) recommended to use filtering procedures in studying the number and duration of lying and upright periods obtained from the IceTag device as the data may contain minor movements; for example, shifts in lying position or grooming while lying.

Tolkamp et al. (2010) used IceTag sensors with indicated minimum lying bout criterion of 4 min. If short 'lying' episodes (i.e. < 4 min) are recorded in standing cows, such episodes should not be considered to separate standing episodes. Standing episodes were, therefore, re-calculated. All lying episodes of less than 4 min. were ignored. This reduced the number of lying episodes up to 88%, but had only minor effects on total estimated lying and standing time (between 0.5 and 3.2%). By Ito et al. (2009) standing and lying bouts of < 2 min were ignored because these readings were likely associated with leg movements at the time of recording. They used HOBO Pendant G Data Logger.

Obviously lame cows lay down on a side so that healthy leg stays below, allowing the painful lame leg to move freely. According to our measurements this parameter may be one possible indicator by which to identify the diseased leg.

CONCLUSION

Taking into account the great variation of cow data (number of steps, motion index, lying bouts, time for standing and lying) between experimental days, the total number of measurements for our experimental animals was not sufficient to identify the influence of lameness by these parameters based on one sensor per cow measurements. By the results of statistical analysis there is trend that the lame cows stand and move less than sound animals. However, as the same trend was in force for older cows it was impossible to differentiate the influence of lameness and age.

Great difference in recordings of diseased and healthy leg lying bouts (ratio 2.47) indicates that this parameter may be one possibility to identify leg disorders. However, further investigations are needed to synchronize video- and IceTag recordings and identify threshold values.

Our experiments gave us the valuable information for planning the measurement series in future studies.

ACKNOWLEDGEMENTS. This research was supported by the IUT8-1. The authors are most grateful for the collaboration with staff of the Märja experimental farm, who kindly permitted us to carry out the experiments for this study.

REFERENCES

Anonymous. 2001. Scientists' Assessment of the Impact of Housing and Management on Animal Welfare. *Journal of Applied Animal Welfare Science* **4(1),** 3–52.

Berckmans, D. 2004. Automatic on-line monitoring of animals by precision livestock farming. In: Madec F. and Clement G. (eds.). *Animal Production in Europe: The way forward in a changing world.* In between Congress of the ISAH Proceedings 1. Saint-Malo – France, October 11–13, 27–30.

Blackie, N., Amory, J., Bleach, E. & Scaife, J. 2011. The effect of lameness on lying behaviour of zero grazed Holstein dairy cattle. *Applied Animal behaviour Science* **134**, 85–91.

Champion, R.A., Rutter, S.M. & Penning, P.D. 1997. An automatic system to monitor lying, standing and walking behaviour of grazing animals. *Applied Animal behaviour Science* **54**, 291–305.

Chapinal, N., de Passille, A.M. & Rushen, J. 2010. Correlated changes in behaviour indicators of lameness in dairy cows following hoof trimming. *J. Dairy Sci.* **93**, 5758–5763.

Higginson, J.H., Millman, S.T., Leslie, K.E. & Kelton, D.F. 2010. Validation of a new pedometry system for use in behavioural research and lameness detection in dairy cattle. *The First North American Conference on Precision Dairy Management.* http://www.precisiondairy2010.com/proceedings/s6higginson.pdf (assessed January, 2014).

IceRobotics Ltd, Product Guide 2010.

Ito, K., Weary, D.M. & von Keyserlingk, M.A.G. 2009. Lying behavior: assessing within- and between-herd variation in free-stall-housed dairy cows. *J Dairy Sci.* **92**(9), 4412–4420.

Kokin, E., Veermäe, I., Poikalainen, V., Praks, J., Pastell, M., Ahokas, J. & Hautala, M. 2007. Environment, health and welfare monitoring in precision livestock farming of dairy cattle. In: Cox, S. (ed.) *Precision Livestock Farming '07.* Wageningen Academic Publishers, 171–177.

MacKay, J.R.D., Deag, J.M. & Haskell, M.J. 2012. Establishing the extent of behavioural reactions in dairy cattle to a leg mounted activity monitor. *Applied Animal Behaviour Science* **136**, 35–41.

Maertens, W., Baert, J., Vangayte, J., Vranken, E., Berckmans, D. & Sonck, B. 2007. Acquisition techniques for Dairy Cow Gait Analysis. In: Cox, S. (ed.) *Precision Livestock Farming '07.* Wageningen Academic Publishers, 133–140.

Martiskainen, P., Järvinen, M., Skön, J-P., Tiirikainen, J., Kolehmainen, M. & Mononen, J. 2009. Cow behaviour pattern recognition using a three-dimensional accelerometer and support vector machines. *Applied Animal Behaviour Science* **119**, 32–38.

Müller, R. & Schrader, L. 2003. A new method to measure behavioural activity levels in dairy cows. *Applied Animal Behaviour Science* **83**, 247–258.

Nielsen, L.R., Pedersen, A.R., Herskin, M.S. & Munksgaard, L. 2010. Quantifying walking and standing behaviour of dairy cows using a moving average based on output from an accelerometer. *Applied Animal Behaviour Science* **127**, 12–19.

O'Driscoll, K., Boyle, L. & Hanlon, A. 2008. A brief note on the validation of a system for recording lying behaviour in dairy cattle. *Applied Animal Behaviour Science* **111**, 195–200.

Pastell, M., Tiusanen, J., Hakojärvi, M. & Hänninen, L. 2009. A wireless accelerometer system with wavelet analysis for assessing lameness in cattle. *Biosystems Engineering* **104**, 545–551.

Pluk, A., Bahr, C., Maernets, W., Veermäe, I., Kokin, E., Praks, J., Poikalainen, V., Pastell, M., Ahokas, J., van Nuffel, A., Vangeyte, J., Snock, B. & Berckmans, D. 2009. Approach to model based motion scoring for lameness detection in dairy cattle. In: Lokhorst, C. and Groot Koerkamp P.W.G (eds.) *Precision livestock farming'09.* Wageningen Academic Publishers, 357–362.

Poikalainen, V., Ahokas, J., Praks, J., Hautala, M., Aland, A. & Veermäe, I. 2004. Automatic Measurement System for Cows Leg Disorder Determination. In: Madec F. and Clement G. (eds.) *Animal Production in Europe: The way forward in a changing world.* In between Congress of the ISAH: Proceedings 1. Saint-Malo – France, October 11–13, 2004, 123–124.

Poikalainen, V., Praks, J., Kokin, E., Aland, A., Veermäe, I., Peets, S., Ahokas, J., Pastell, M., Hautala, M., Berckmans, D., Bahr, C. & Miljkovic, D. 2010. Elaboration of basic methods for automatic analysis of cows' gait. *Agronomy Research* **8(1)**, 216–225.

Poikalainen, V., Kokin, E., Veermäe, I., & Praks, J. 2013. Towards an automatic dairy cattle welfare monitoring. Aland, A., Banhazi, T. (Toim.). *'Livestock housing: Modern management to ensure optimal health and welfare of farm animals.* Wagenigen, Netherlands: Wageningen Academic Publishers, 393–406.

Poursaberi, A., Bahr, C., Pluk, A., Van Nuffel, A. & Berckmans, D. 2010. Real-time automatic lameness detection based on back posture extraction in dairy cattle: Shape analysis of cow with image processing techniques. *Computers and Electronics in Agriculture* **74**, 110–119.

Rajkondawar, P., Liu, M., Dyer, R., Neerchal, N., Tasch, U., Lefcourt, A., Erez, B. & Varner M. 2006. Comparison of Models to Identify Lame Cows Based on Gait and Lesion Scores, and Limb Movement Variables. *Journal of Dairy Science* **89**, 4267–4275.

Robert, B., White, B.J., Renter, D.G. & Larson, R.L. 2009. Evaluation of three-dimensional accelerometers to monitor and classify behavior patterns in cattle. *Computers and Electronics in Agriculture* **67**, 80–84.

Scheibe, K.M. & Gromann, C. 2006. Application testing of a new three-dimensional acceleration measuring system with wireless data transfer. *Behav. Res. Methods* **38**, 427–433.

Sprecher, D.J., Hostetler, D.E. & Kaneene, J.B. 1997. A lameness scoring system that uses posture and gait to predict dairy cattle reproductive performance. *Theriogenology* **47**, 1179–1187.

Thomsen, P.T., Munksgaard, L. & Sørensen, J.T. 2012. Locomotion scores and lying behaviour are indicators of hoof lesions in dairy cows. *The veterinary Journal* **193**(3), 644–647.

Tolkamp, B.J., Haskell, M.J., Langford, F.M., Roberts, D.J. & Morgan, C.A. 2010. Are cows more likely to lie down the longer they stand? *Applied Animal behaviour Science* **124**, 1–10.

Trénel, P., Jensen, M.B., Decker, E.L. & Skjøth, F. 2009. Technical note: Quantifying and characterizing behavior in dairy calves using the Icetag automatic recording device. *J Dairy Sci.* 92(7), 3397–401.

Agronomy Research **12**(1), 231–236, 2014

Fodder feeding peculiarities when introducing the VMS automatized cow milking system

A. Saliņš[*], J. Priekulis and A. Laurs

Faculty of Engineering, Latvia University of Agriculture, J. Čakstes bulv.5, LV-3001 Jelgava, Latvia; [*]Correspondence: ansis.salins@gmail.com

Abstract. The research concerns fodder distribution solutions for cows which are milked using the VMS robotised equipment produced by the company *DeLaval*. The research is conducted at the milking cow farm 'Līgotnes' of the Latvia University of Agriculture study and research farm 'Vecauce'. In the research, cattle-shed cows receive fodder in three different places: together with the basic feed mixture while eating at the feeding table, in the robotised milking stand and at the fodder feeding stations.

The research has stated that this feeding system is rational. Adding fodder to feed mixture (about 10% of its mass) is necessary as it improves the feed mixture taste qualities. Hence, it increases the consumption of this mixture and also the cow yield. If fodder is not added to the mixture, the productivity of highly productive cows deteriorates and can decrease by 10%. Moreover, we can add to basic feed mixture fodder prepared at the farm using the grains grown there. Usually, such fodder is cheaper than the bought one, and therefore decreases the prime cost of the milk.

Fodder is also fed also in the robotised cow milking stands as such an approach stimulates cows to visit the milking stands more frequently. But during the research we found that highly productive cows with the yield exceeding 30 kg per day do not manage to eat all the due fodder amount during milking. Therefore, fodder feeding stations are necessary for feeding of highly productive cows. They shall be placed after the sorting gates so that the cows that are not directed to milking by the automatic sorting system could visit the fodder stations. Moreover, the number of fodder feeding stations per one cow milking group should not be less than two.

Key words: feeding cows, fodder, AMS, fodder stations.

INTRODUCTION

Fodder is an important means of feeding with high energy concentration and good digestibility of nutritive stuffs. As a result, it is widely used for feeding of milking cows. But with introduction of automatic milking (AMS), fodder is also used as a peculiar stimulus for visiting milking stands. It is necessary as in the case of automatic milking cows must visit the milking stand themselves. But in any herd there are also 'lazy' cows that like to spend much time in the recreation area and not visit the AMS even if the interval till the next milking time is significantly exceeded (Laurs et al., 2008). Therefore, in case of robotised milking, a part of the total fodder amount is fed in the milking stand in order to stimulate cows to visit the AMS regularly (Latvietis et al., 2008).

Cows can receive the rest of the fodder amount with the basic feed mixture fed at the feeding table, but sometimes fodder is also served at specially organized fodder feeding stations. But the usage of such stations is connected to the necessity of an additional area and also costs (Latvietis & Priekulis, 2011).

Currently, literature does not specially describe the necessity of feeding fodder as a part of the feed mixture and at the fodder stations, therefore, the aim of our research was to find out the practical necessity of such feeding places (Nydegger & Bolli, 2009).

MATERIALS AND METHODS

For research, we used the data from the milking cow farm ‘Līgotnes’ of the LLU study and research farm ‘Vecauce’, where in a separate section automatized milking is introduced using two VMS milking stands produced by the company *DeLaval* (Fig 1).

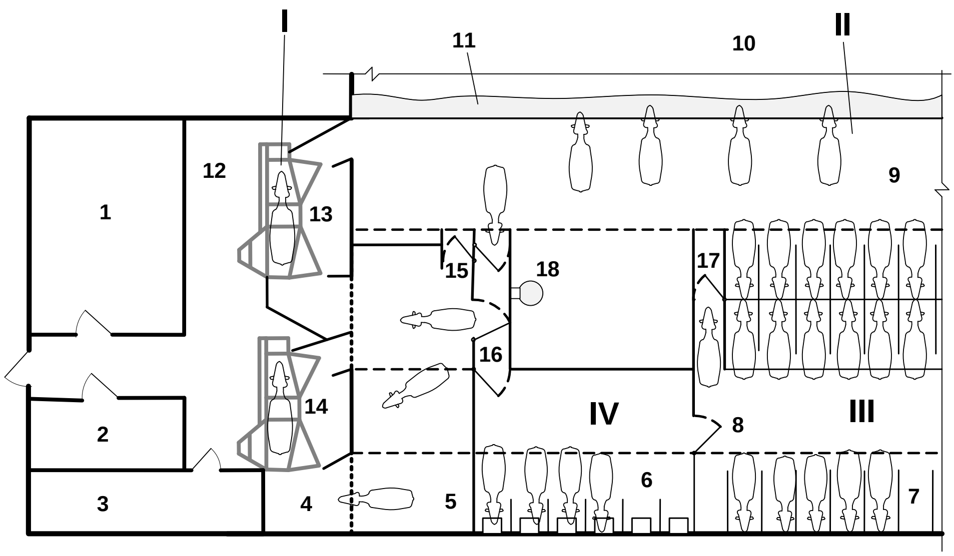

Figure 1. Cattle-shed section plan at the LLU study and research farm Vecauce, where the AMS cow milking is introduced: I – milking area; II – feed mixture feeding area; III – recreation area; IV – combined fodder feeding area; 1 – milk room; 2 – computer room; 3 – technical corridor; 4 – milking anteroom; 5 – pre-milking area; 6 – combined fodder feeding stands; 7 – recreation boxes; 8 – one-way gates; 9 – manure passage; 10 – feed table; 11 – fed basic feed mixture; 12 – corridor; 13, 14 – AMS; 15 – cow after-sorting gates; 16 – cows before-sorting gates; 17 – transition corridor with one-way gates; 18 – rotating combs for treatment of cows bodies.

In this case, cows were fed in three places – at the feed table, during milking and at the fodder feeding stations. The basic feed mixture fed at the feed table included medicine and maize silage, perennial herbs hay and the fodder produced at the farm (rolled barley grains, common salt and different admixtures), and cows could eat an unlimited amount of this mixture. In turn, during milking and at the feed stations, cows were fed bought fodder the distribution of which was conducted with a herd management system.

Research was conducted in two cycles. During the first cycle, we clarified the necessity of including fodder into feed mixture, as there was the hypothesis that the fodder amount necessary for cows could be fed in milking stands and at feed stations not including it into the mixture as this could improve the frequency of visiting the AMS.

During the second cycle, we clarified the possibility of cows feeding at the feed table and during milking refusing to use the feed stations.

The length of the first research cycle was 10 weeks. Changes in feeding took place from the 5th week but the necessary data were summarized about the first and the last four weeks of the research cycle, including into the interval of two other weeks. Information on yields and visiting the AMS was obtained from the data accumulated in the herd management system. In addition, cows were grouped according to their yield per day, separately grouping animals with the yield below 15, 15–25, 25–35, 35–45 and above 45 kg per day. Additionally, feed cost were calculated per one kilo of milk using for the calculated cost of the feed produced at the farm and the bought fodder prices (Brade et al., 2008).

The second research cycle was conducted one year later and its duration was 2 weeks. During that, cows were fed like in the first period of the first research cycle and were also divided into analogical yield groups. Using the herd management system, we found the time spent by the cows with different productivity in the robotised milking stand, and also the average number of milking times per day.

The maximum fodder amount that can be received by each animal of a separate productivity group was calculated using formula

$$M_{s.i} = M_{m.i} + v_s \cdot n_{s.i} \cdot t_{s.i}, \quad (1)$$

where: $M_{s.i}$ – maximum fodder amount that can be received by each cow of i productivity group, kg day^{-1}; $M_{m.i}$ – fodder amount eaten by i-group cow with feed mixture, kg day^{-1}; v_s – average fodder consumption speed, kg min^{-1}. According to the literature data (Latvietis et al., 2008), the average fodder consumption speed for a cow is 0.33 kg min^{-1}; $n_{s.i}$ – average number of milking times for i cow group animals, times per day; $t_{s.i}$ – average length of one milking time for i-group cows, min.

For the cows of a corresponding yield group to be able to eat the necessary fodder amount, the following inequality shall be in force

$$M_{s.i} \geq M_o, \quad (2)$$

where M_o – normative fodder amount for one cow of i yield group, kg day^{-1}.

RESULTS AND DISCUSSION

Information on the frequency of visiting the AMS and on the yield for the cows of different productivity depending on fodder adding to the mixture is summarized in Table 1.

Table 1. The effect of the cow feeding solution on the frequency of visiting the AMS and changes in the yield (Validity 95%)

Trial period	Productivity group, kg day^{-1}	Average frequency of visits to AMS, times day^{-1}	Average yield, kg day^{-1}
Before exclusion of fodder from basic feed mixture	below 15	2.05	13.01
	16–25	2.45	21.04
	26–35	3.04	30.05
	above 36	3.10	39.89
After exclusion of fodder from basic feed mixture	below 15	2.10	13.22
	16–25	2.68	20.86
	26–35	3.12	28.88
	above 36	4.00	38.25

The information received when processing the data accumulated in the cow herd management system is seen in Table 2.

Table 2. The average duration of milking one cow and the number of milking times per day depending on the yield (Validity 95%)

Productivity group, kg day^{-1}	Average duration of one milking time, min	Average number of milking times for one cow, per day
below 15	8.20	1.60
16–25	8.36	2.32
26–35	8.52	2.62
36–45	8.90	3.20
above 46	9.12	3.63

In order to obtain the data with the validity of 95% that is depicted in Table 1 and Table 2, a statistical analysis was carried out (Arhipova, 2003). From the table we can see that the time spent by cows in the milking stand is within 8.2 to 9.12 minutes and it depends on the yield. The higher the yield of the cow per day, the longer is the duration of one milking time. Moreover, more productive cows also visit the milking stand more frequently. For example, if the average yield is only 10 kg day^{-1}, these cows are milked 1.6 times per day, but the cows with the average yield of 50 kg day^{-1} visit the milking stand 3.63 times per day.

Information on the amount of fodder necessary for cows depending on the yield and the practically available fodder amount that the animals can receive with the feed mixture and visiting the milking stand is summarized on Fig. 2.

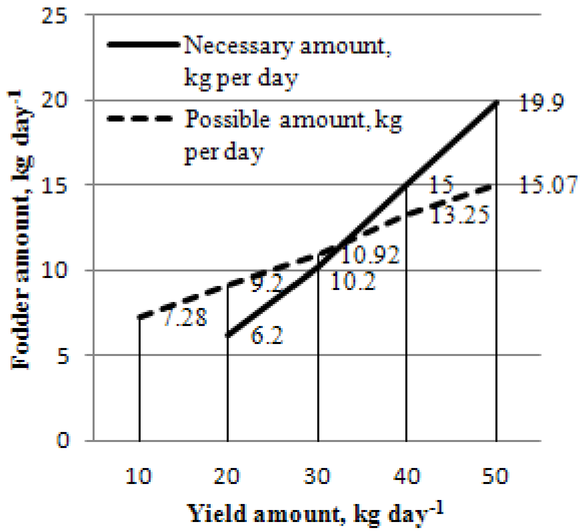

Figure 2. Fodder amount necessary for cows of different productivity and the practically received fodder amount if fodder is included into the feed mixture (~10% of its mass) (Osītis, 2005) and additionally fed in the milking stands, but fodder stations are not used.

From the figure, we can see that the cows with the bigger yield receive the bigger fodder amount. It happens because these cows spend more time in the milking stand and also visits it more often. Moreover, they eat a larger amount of the feed mixture, which includes fodder. But this fodder amount increase is not sufficient for highly productive cows, the yield of which exceeds 30 kg per day (7,000–8,000 kg year^{-1}), as they need 15 and more kg of fodder per day. Hence, it is expedient to also use fodder feeding stations for feeding of these cows, as they can receive the lacking fodder amount there.

In addition, there is also another solution to the problem – to increase the fodder amount added to the feed mixture. But then obesity of less productive cows is possible. Therefore, in this case, all cows milked by robotised milking equipment shall be grouped according to the yield level, not allowing the difference of more than 20 kg a day in the yield of the cows included in one group.

CONCLUSIONS

1. If cows are milked using the VMS robotised milking equipment produced by the *DeLaval* Company, the duration of one milking time and the number of visits to milking stands per day depends on the yield. The milking duration of the cows with the average yield of 10 kg a day is 8.2 minutes, but the milking duration of the cows with the average yield of 50 kg day^{-1} – 9.12 minutes. Moreover, the numbers of visits to milking stands for the cows of corresponding yields are 1.6 and 3.6 times per day. Therefore, for more productive cows it is possible to eat a larger amount fodder during milking per one day.

2. The most productive cows also consume the greatest amount of feed mixture, which contains fodder, and therefore can receive the largest total amount of fodder via this feed mixture.

3. If the average cow yield does not exceed 30 kg day^{-1}, cows can receive the necessary amount of fodder with the basic feed mixture, and also during milking, but if the yield is more than 30 kg day^{-1}, the fodder amount received in the abovementioned ways is not sufficient and additional cow feeding is desirable using fodder feeding stations.

ACKNOWLEDGEMENTS: This work was developed thanks to the project 'Support for Implementation of Master Studies at the LUA' financed by the European Social Fund. Agreement No. 2011/0020/1DP/1.1.2.1.1/11/IPIA/VIAA/011.

REFERENCES

Arhipova, I. 2003. Bāliņa S. Statistika ekonomikā. Riga. Datorzinību centrs, 352 pp. (in Latvian).

Brade, E. & Brade, W. 2008. Wie Viel Korn braucht die Milch? *Neue Landwirtschaft* **5**, 58–59 (In German).

Latvietis, J., Priekulis, J. & Eihvalde, I. 2008 Problems of cow feeding in robotic milking and loose handling conditions. *7th International Scientific Conference 'Engineering for rural development'*. Jelgava, May 29–30, pp. 270–274.

Latvietis, J. & Priekulis, J. 2011. Consumption of concentrated feed for milk cows in conditions of robotized technology. *10th International Scientific Conference 'Engineering for rural development'*. Proceedings, Vol. 10. Jelgava, pp. 55–58.

Laurs, A., Priekulis, J., Zujs, V. & Saliņš, A. 2008. Milking frequency in milking robots with feed first cow traffic. *7th International Scientific Conference 'Engineering for rural development'*. Jelgava, May 29–30, pp. 275–278.

Nydegger, F. & Bolli, S. 2009. Strukturproblematik bei Mischrationen für Hochleistungsherden. Ergebnisse einer Erhebung auf Milchviebetrieben. In: ART-Berichte, Tänikon 719. p. 8. (In German).

Osītis, U. 2005. Dzīvnieku ēdināšana kompleksā skatījumā. Jelgava: LLU, 320 pp. (in Latvian).

Agronomy Research **12**(1), 237–244, 2014

Heating of large agricultural and industrial buildings

M. Zajicek[1,*] and P. Kic[2]

[1]Institute of Information Theory and Automation, The Academy of Science of The Czech Republic, v.v.i.; [*]Correspondence: zajicek@utia.cas.cz
[2]Czech University of Life Sciences Prague, Faculty of Engineering, Czech Republic

Abstract. This paper presents the results of the simulation calculations used in the selection and design of an appropriate method of heating of large buildings for agricultural or industrial purposes. These halls are characterized by a large built-up area, large room height and high consumption of energy for heating. The aim of the simulation calculation was to find a way of heating, which leads to a reduction in energy consumption while maintaining the required thermal comfort of indoor environment.

The calculations were performed using the CFD software ANSYS-Fluent. For comparison of variants, a 3D model was used, including a heat source, natural convection and heat transfer through surrounding structures. The results of the thermal comfort of the working environment in the level of people or the growing zone of plants or the storage space for goods were mainly studied. The second area of interior space, especially important in terms of heat losses, is the level of the ceiling.

The results of the calculations provide a detailed analysis of the vertical temperature profiles and the effect of the surrounding walls surface temperature on the thermal state of an indoor environment.

The created model was verified according to the results of experiments in large buildings equipped with different heating systems. Based on the results of the simulation calculations and according to the results of experimental measurements, radiant heating method seems to be the suitable heating system solution for studied types of buildings.

Key words: energy, radiation, thermal comfort, simulation.

INTRODUCTION

Heating of large buildings together with ventilation or air conditioning represents a very important issue, which significantly affects the operation of these facilities. This article is aimed at the buildings used in industry, agriculture or as different repair shops and service centres. These buildings are used year-round and must be kept at the required air temperature, corresponding to the requirements of workers or technological processes. These buildings are characterized by a large surface area, high height, and large overall volume. This creates a need for substantial inputs for heating, which together with the high cost of energy can manifest itself quite significantly in the efficiency of production, or in the satisfaction and functional reliability of these buildings. Energy consumption, indoor climate and sophisticated regulation systems take a great deal for well-constructed buildings (Rajaniemi & Ahokas, 2012; Reinvee et al., 2012).

There is different information in literature concerning the heating and ventilation of these buildings. Recommendations of several authors are focused on radiant heating by different types of heating panels (Cihelka, 1961; Kotrbaty & Kovarova, 2002; Basta, 2010; Vio, 2011.)

The following article briefly summarizes some of the results of the measurements in the practical operation of an industrial open-plan hall and at the same time it is shown how they can use modern simulation methods to verify the assumptions in the pre-design phase.

MATERIALS AND METHODS

For the research work presented in this paper, the measurement of a large-area industrial hall of the total interior height of 8 m was used, which was equipped with several different types of heating. This building was selected for this research as there are not so many large halls, where is possible to study two completely different heating systems of indoor sections in one single-storey building (200 x 150 m) with the same thermal properties of the surrounding walls.

The greater part of the hall was heated by hot air; few sections were heated by hot-water radiant panels mounted below the ceiling. It was possible to examine and compare the two different concepts of heating under actual operating conditions. The thermal state of the environment was measured in the working zone in three different sections of the hall heated by hot air and in one section heated by radiant heating panels. The height temperature profile was measured both in the hall section heated by hot air as well as in one section heated by radiant panels.

As the studied large industrial building was equipped with very sophisticated technological equipment operating in three work shifts under extremely hard control of all activities, it was necessary to choose representative places suitable both for studying different heating systems and as regards the placement of measurement instruments between the installed machinery with operators very carefully. It was also very important from the perspective of measurement to choose a place, which is not influence by the other heating system, only by the studied one.

For measurements of the thermal environment, a sensor measuring the global spherical thermometer of diameter D = 150 mm FPA805GTS was used with centrally-located Pt100 sensor for measuring the globe temperature T_g (°C), with a measuring range of -50 to +200°C, the temperature of the surrounding air T_a (°C) was measured by the sensor FH A646-2 including the temperature sensor NTC type N with and operative range from -30 to +100°C, with accuracy ± 0.1 K, and the relative air humidity Rh (%) by a capacitive sensor with an operative range from 5 to 98%, with accuracy ± 2%. For an indicative control of the thermal comfort of the indoor environment in the hall, Kata-thermometer 24/66, F 567 was used. The sensors were connected to the instrument ALMEMO 2590-9. The temperature profiles inside the hall were measured using an ALMEMO 2690-8 instrument with a thermocouple Ni-NiCr. All measured data were subsequently recorded.

From the measured values (ten values of each parameter were measured at the level of 1.1 m above the floor, regularly distributed in the area of roughly 25 m^2 in each measured section of the hall), the average globe temperature T_g (°C) and air temperature T_a (°C) were calculated, which were used according to the equation (1) for calculation of the mean radiant temperature T_r (°C) and according to the relation (2) for the operative temperature T_o (°C), an important parameter for evaluation of thermal environment, particularly in terms of the influence of radiation. The heat transfer coefficient h_{kg} ($W \cdot m^{-2} \cdot K^{-1}$) was calculated according to the equation (3). From the measured cooling time τ (s) of Kata-thermometer and the calibration constant Q ($J\ m^{-2}$), the average values of the so-called cooling rates Kata-values K ($W\ m^{-2}$) were calculated according to the equation (4).

$$T_r = \left\{ \sqrt[4]{\left[\left(T_g + 273 \right)^4 \right] + \left[1{,}855 \cdot 10^7 \cdot h_{kg} \cdot \left(T_g - T_a \right) \right]} \right\} - 273, \tag{1}$$

$$T_o = 0.5 \cdot T_a + 0.5 \cdot T_r, \tag{2}$$

$$h_{kg} = 1.4 \cdot \left(\frac{\left| T_a - T_g \right|}{D} \right)^{0.25}, \tag{3}$$

$$K = \frac{Q}{\tau}, \tag{4}$$

where: T_r – mean radiant temperature (°C); T_g – globe temperature (°C); h_{kg} – heat transfer coefficient ($W\ m^{-2}\ K^{-1}$); T_a – air temperature (°C); T_o – operative temperature (°C); K – cooling rate Kata-value ($W \cdot m^{-2}$); Q – calibration constant ($J\ m^{-2}$); τ – cooling time (s).

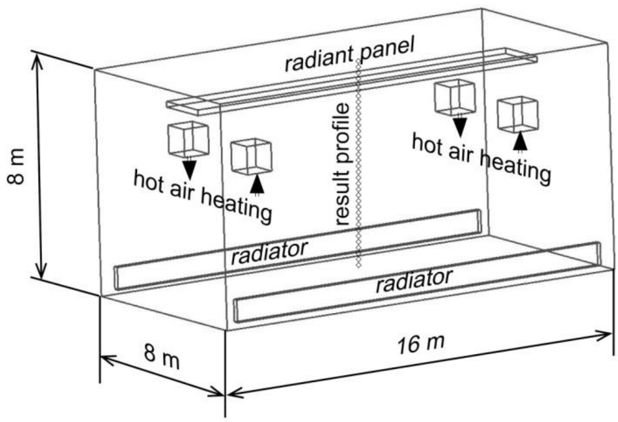

Figure 1. The geometrical model of the computational domain with zones used for simulation of different heating system concepts.

The simulation of conditions in the hall was carried out using the CFD (computational fluid dynamics) program Ansys Fluent. Fig. 1 shows the geometrical model. The computational domain is a rectangular block of width 8 m, height 8 m, and length of 16 m. The ceiling radiant panel is located at the height of 15 m and the dimensions of the panel are 2 x 14 m. Four input/output openings of the hot air heating system are located at a distance of 2 m from the front/back walls and 1.2 m from the side walls. Classic hot water radiators, each with dimension 15 x 0.8 x 0.2 m, are located on both long sides of the hall at the height of 1 m above the floor. The computational domain consists of about 1 million tetrahedral cells with the characteristic dimension of about 15 cm.

RESULTS AND DISCUSSION

The results of the measurements in the hall

The results of the measurement of the thermal environment in the hall are summarized in Table 1. The results are obtained by measurement of the thermal environmental state. Monitoring points HA 1, HA 2 and HA 3 were measured in sections with hot air heating. Measuring point RP was in a section with radiant heating.

Table 1. Average values of the thermal state of the environment in 3 sections of the hall with hot air heating and in one section with radiant heating panels (HA 1, HA 2, HA 3 – measuring points in sections with hot air heating; RP – measuring point in a section with radiant heating panels)

Section	T_a	T_g	Rh	v	K	T_r	T_o
	°C	°C	%	m s^{-1}	W m^{-2}	°C	°C
HA 1	21.97	22.62	25.2	0.21	279.3	22.9	22.4
HA 2	24.65	25.22	22.2	0.09	171.7	25.4	25.0
HA 3	25.05	25.66	20.8	0.10	166.5	25.9	25.5
RP	24.45	25.67	21.0	0.10	183.6	26.2	25.3

The measurement results in Table 1 indicate that there are considerable differences in air temperature between the sections with hot air heating. The lowest air temperature was measured in section HA 1, farther away from the inlet of warm air. Contrarily, the air temperature in section HA 3 was too high. In terms of comfort, there is a recommended optimum environment for working activity in a hall where people are working on machine tools or in light assembly (Act No. 262/2006 Coll., labour class II b) with average body energy production, M = 106–130 W m^{-2}, the recommended air temperature of 14–32°C, relative humidity of 30–70%, and air velocity from 0.05 to 0.3 ms^{-1}. Generally, the inside air T_a temperature was too high and the relative humidity Rh of the whole building too low, as there are no sufficient sources of vapour inside. In the section with radiant panels, the globe temperature T_g is higher than the average air temperature T_a. The air-speed was at an acceptable level.

The optimum cooling rate Kata-value K should be between 170 and 250 W m^{-2}. If it is less than 170 W m^{-2}, people feel warm, if it is more than 250 W m^{-2}, people feel cold. The thermal comfort from this point of view was too cold in the measuring point HA 1 and too warm in the place of measurement HA 3.

The comparison of the vertical profiles in the hall shown in Fig. 2, where the mean values of the set of 20 measurements are presented, is very interesting. The vertical temperature profiles measured in the section heated by hot air and in the section heated by radiant panels are completely different. It is obvious that hot air heating causes lower air temperature in the zone near the floor where people move and significantly higher temperature near the ceiling. This increases heat losses through the top of the walls and the ceiling. Contrarily, radiant heating panels heat the floor and the floor environment where people work by radiation; the upper part of the hall is cooler. This is very beneficial in terms of reduction of energy consumption for heating.

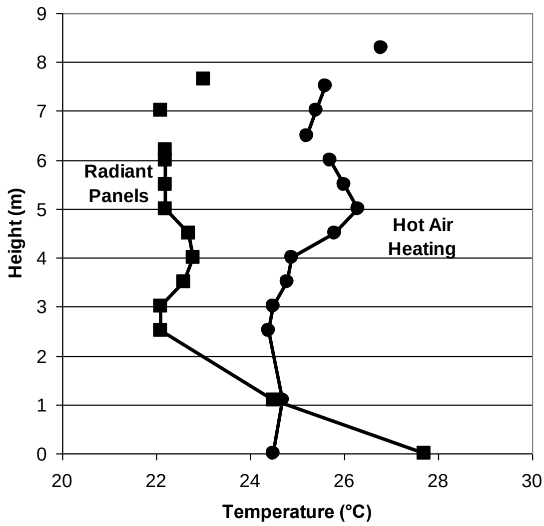

Figure 2. Comparison of the mean values of the vertical temperature profiles measured in the section heated by hot air and in the section heated by radiant panels.

The results of the simulations of heating in the hall

All solved cases assume the same initial conditions, namely, the initial temperature inside and outside of the building is 7°C, the total heat transfer coefficient through the side walls is 12 W m^{-2} K^{-1}, through the ceiling 18 W m^{-2} K^{-1}, and through the floor 10 W m^{-2} K^{-1}. The surface-to-surface Fluent's radiation model can be used to account for the radiation exchange in an enclosure of grey-diffuse surfaces. The energy exchange between two surfaces depends on their size, separation distance, and orientation. These parameters are accounted for by a geometric function called a view factor, which is the prescription of the fact of how the total radiation flux is distributed to surfaces other than the source surfaces.

Three basic variants are solved as shown in Fig. 3 − hot air heating with classical warm water radiators (A), using a forced ventilation system, which brings pre-heated air into the domain (B), and radiant panels located under the ceiling (C). All these cases consider the same input thermal power of 35 kW supplied into the building. Fig. 3 shows the typical contours of the temperature profile shapes for the solved variants. The difference between the whirl shape of forced air movement (A) and the stratification of radiator heating (B) can be seen nicely. The main advantage of forced convection is the fast heating of the whole space. While the time needed to heat the whole indoor space by radiant panel heating or hot water radiator heating is about 2 hours for the presented boundary conditions, hot air heating can achieve the similar effect in about 20−30 minutes.

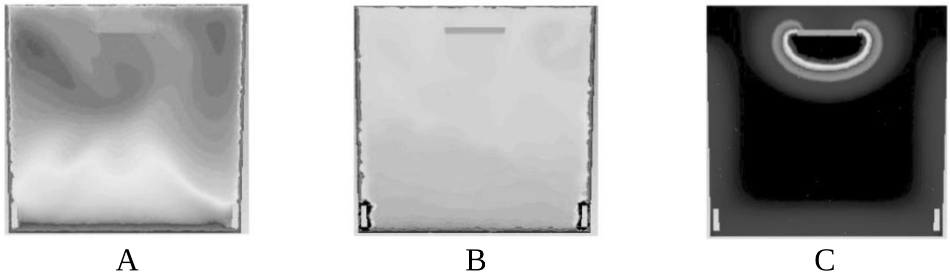

Figure 3. The character of the temperature profiles during (A) - hot air heating, (B) - hot water radiator heating and (C) - radiant panel heating.

This fact is shown in Fig. 4. It compares the vertical temperature profile in the central vertical axis of the domain for radiant heating panels on the left side and heating with conventional hot water radiators on the right. It is evident that after two hours from turning the heating system on, the central area of the domain achieved the temperature of about 24°C, but in the case of radiant heating panels significantly higher gradients towards higher temperatures can be seen, caused by direct heat transfer onto the heated surface. The classical hot water radiator heating, however, leaves the bottom of the domain cooler, because of the heat transfer through the floor. Those numerical results correspond well with the dependence obtained from the measurements shown in Fig. 2.

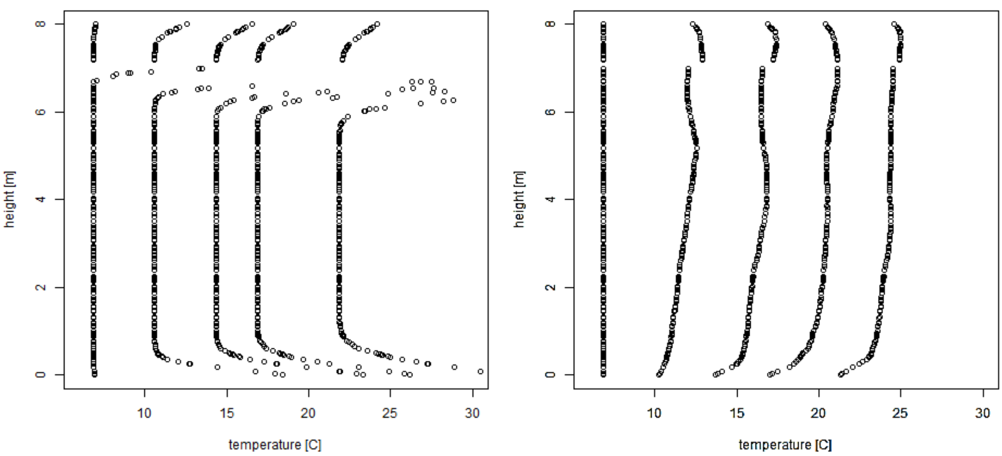

Figure 4. Temperature profile development for radiant panel and hot water radiator heating, the time step is 30 minutes.

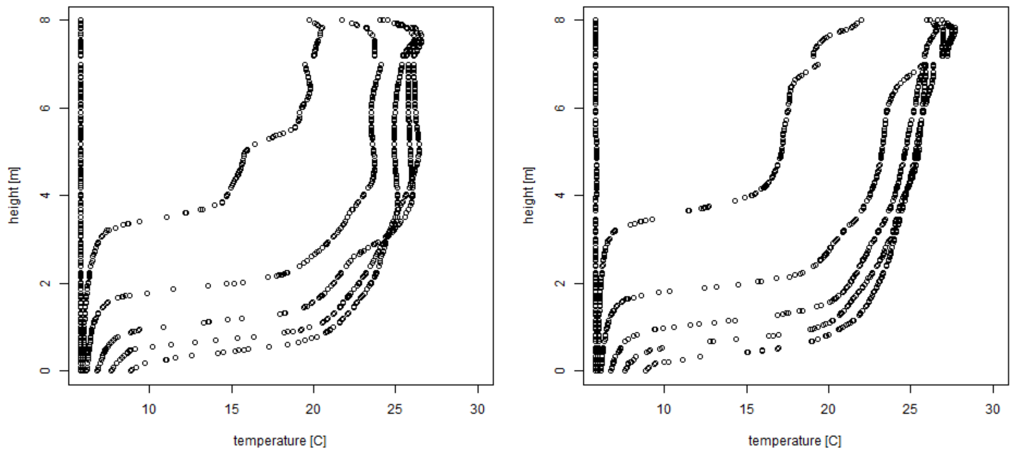

Figure 5. Temperature profile for hot air heating in the plane of ventilators and in the central plane of the hall, the time step is 5 minutes.

The situation during hot air heating is illustrated in Fig. 5, where the time step between the curves is shorter. The two graphs show the profiles in the central vertical axis and in the middle between the inlet and outlet opening. It is clearly seen that the effect of natural convection together with ventilation make the upper part of the domain heated very quickly, but forced ventilation leads to quick mixing of cold and hot air.

CONCLUSIONS

Heating the large industrial and agricultural buildings with radiant heating panels looks advantageous. The thermal comfort of the people who are moving in such areas is guaranteed by the increase in the surface temperature due to the radiation heat transfer and the results of measurements and simulations confirm that the temperature on heated surface can be up to six times greater than in the surrounding environment. Hot air heating is mainly usable mainly when there is a need for quick compensation of temperature fluctuations caused by operational needs. Conventional hot water radiators are shown as particularly disadvantageous because of the long heating time which goes together with temperature stratification and therefore increases the heating costs due to the need to overheat the upper parts of the building space to achieve the required conditions just above the floor.

ACKNOWLEDGEMENTS. Access to the computing and storage facilities owned by the parties and projects contributing to the National Grid Infrastructure MetaCentrum, provided under the programme ‘Projects of Large Infrastructure for Research, Development, and Innovations’ (LM2010005) is highly acknowledged.

REFERENCES

Act No. 262/2006 Coll. Government Regulation No. 361/2007 Coll. Laying down the conditions for the protection of health at work. Changes: 9/2013 Coll., 48 pp. (in Czech).

Basta, J. 2010. *Large Radian Heating*. Grada Publishing, Praha, 128 pp. (in Czech).

Cihelka, J. 1961. *Radian Heating*. SNTL, Praha, 373 pp. (in Czech).

Kotrbaty, M. & Kovarova, Z. 2002. Heating by suspended radiant panels. *Vytapeni, vetrani, instalace* **4**, 134–138 (in Czech).

Rajaniemi, M. & Ahokas, J.), 2012. A case study of energy consumption measurement system in broiler production. *Agronomy Research* **10**(1), 195–204.

Reinvee, M., Uiga, J., Tärgla, T., Pikk, P. & Annuk, A. 2013. Exploring the effect of carbon dioxide demand controlled ventilation system on air humidity. *Agronomy Research* **11**(2), 463–470.

Vio, M. 2011. *Climatization with Radiant Systems.* Editoriale Delfino, Milano, 264 pp. (in Italian).

III PRODUCTION ENGINEERING

Agronomy Research **12**(1), 247–254, 2014

Evaluation of friction force using a rubber wheel instrument

R. Chotěborský[1,*] and M. Linda[2]

[1]Department of Material Science and Manufacturing Technology, Faculty of Engineering, Czech University of Life Sciences, Kamýcká 129, 6521 Prague 6, Czech Republic; [*]Correspondence: choteborsky@tf.czu.cz
[2] Department of Electrical Engineering and Automation, Faculty of Engineering, Czech University of Life Sciences, Kamýcká 129, 16521 Prague 6, Czech Republic

Abstract. Abrasive wear is the most important process for innovation of new materials in agriculture. The method depends on the internal (the microstructure of the abraded material) and external (characteristic of the abrasive particle, force, etc.) conditions. A modified rubber wheel instrument based on the ASTM G65 procedure was used to obtain the study results. The results showed that the friction between an abrasive particle and abraded material was influenced by the microstructure of the abraded material and this relationship can be used for abrasive wear evaluation. The study result also showed that the limitation of using the rubber wheel method was the natural frequency of the system. In this study, the natural frequency was found to be 200 Hz, which is useful for elimination of the algorithm for frequency and amplitude during wear analysis.

Key words: abrasive wear, intensity of wear, dry rubber wheel test, microstructure.

INTRODUCTION

Friction as an important physical effect required a lot of theoretical and experimental work to be understood (Qi et al., 2011; Cozza, 2014).

To understand the physical effect of friction in any process, it is necessary to consider in detail both the theoretical and experimental study of the process (Ceschini et al., 2006). The friction mechanism between abrasive particles and abraded material is more complicated than the mechanism between one particle and abraded material. The random process between a rubber wheel and sand particles can cause a linear motion of the particles if their interaction maintains the rotation. Applying a rotational movement linearly and with the interaction between the particle and the material could cause sliding of the material and one of the aspects of the sliding process is friction and friction coefficient.

If the frictional force acts at a distance, it causes energy loss which converts to heat and in practice, for example, the friction between a chisel and soil increases fuel consumption (Radziszewski et al., 2005; Jokiniemi et al., 2012; Korres et al., 2013; Kučera & Chotěborský, 2013).

The value of the friction coefficient depends on the boundary conditions of the particles and sliding material. If the size of the particle is small, the microstructure phase and adhesion phase influence the boundary conditions. For instance, there is the assumption that the microstructure of a metal with two very different phases such as solid solution and intermetallic has a different friction coefficient than a microstructure with a solid solution. The total friction energy consumption as well as other indicators were determined based on the size of the frictional force. The density of friction energy represents the amount of friction energy in relation to a friction stressed amount of mass. The density of friction energy, the intensity of wear, and the mean shear stress are the indicators that determine the critical energy level which characterizes the friction process (Ceschini et al., 2006; Kučera & Chotěborský, 2013). Although there are publications focused on the abrasive wear of a multiphase material, the authors only described the relationship between the microstructure and volume loss of the materials (Chotěborský et al., 2009a; Chotěborský et al., 2009b; Kazemipour et al., 2010; Petrica et al., 2013a; Wang & Li, 2010; Sabet et al., 2011) as well as the test condition and the volume loss of the materials (Jankauskas & Skirkus, 2012; Chotěborský, 2013; Petrica et al, 2013b).

The goal of this article is the evaluation of an abraded material with respect to the influence of microstructure characteristics on the friction force (Fig. 1) and friction coefficient.

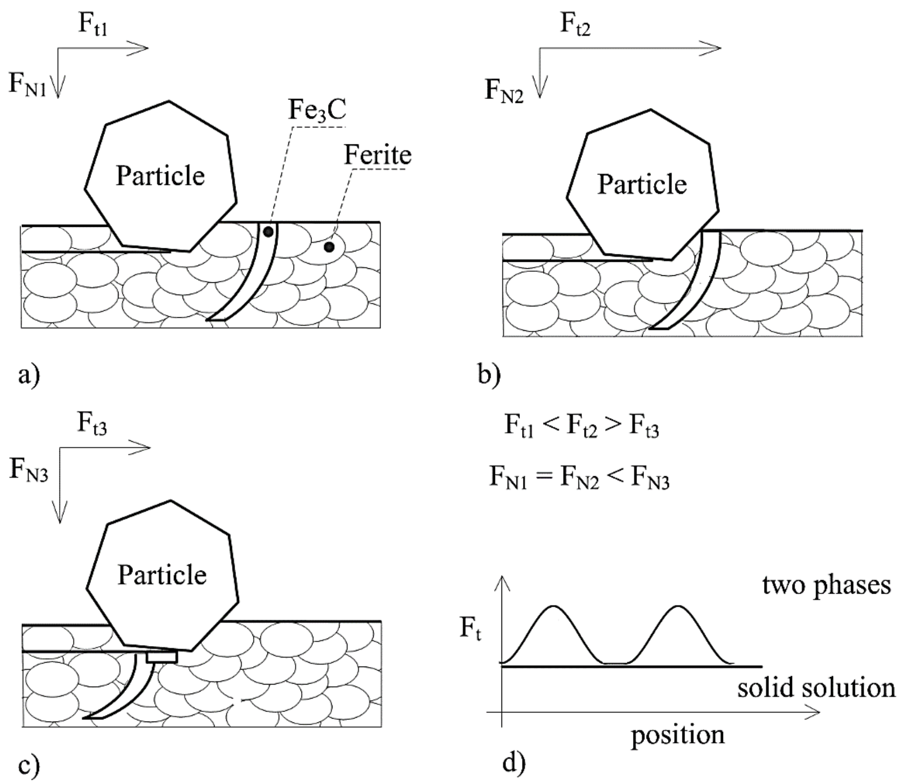

Figure 1. Scheme of abrasive particle and abraded material interactions.

MATERIALS AND METHODS

A dry rubber wheel tester (DRWT; Stevenson, 2005) was used for evaluation of abrasive wear. The lever was placed in the deformation member with a strain gauge as shown in Fig. 2. A calibrated strain gauge was joint into the converter and DAQ Advantech USB4716 (200 kSa s^{-1}) and the data was moved to a PC as is shown in the schema in Fig. 3. The data (more than 500 MB files) was evaluated by SciLab 5.4.0 where the scripts for frequency, amplitude and mean of friction force analyses were respectively examined.

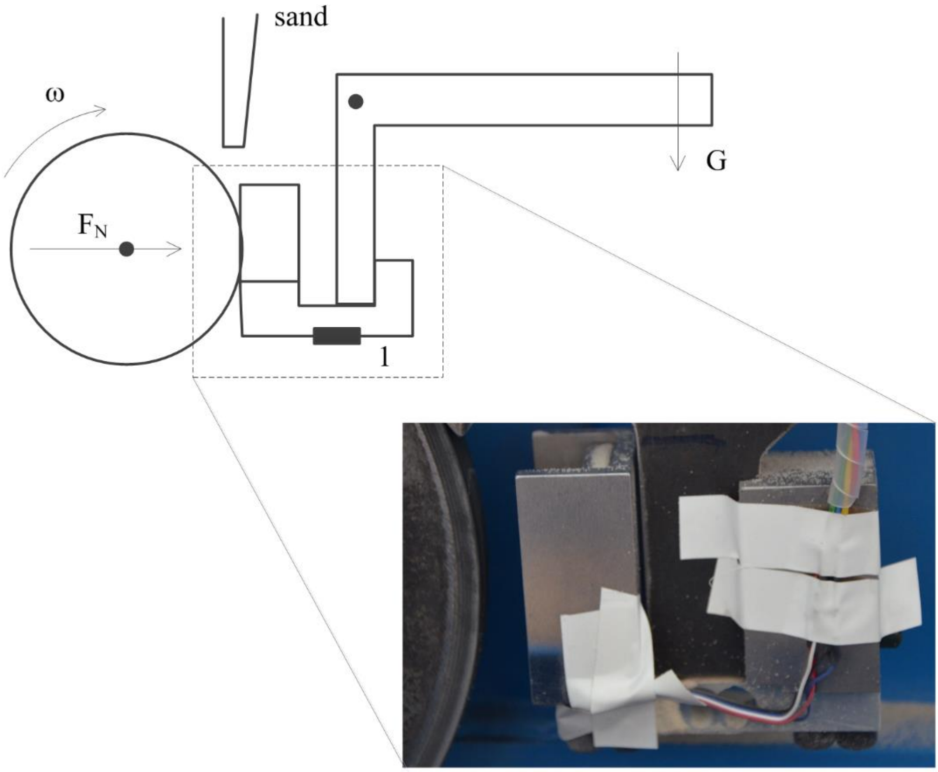

Figure 2. Scheme of instrumentation DRWT.

In Table 1, the materials used for the abrasive wear test are shown. These materials were grouped by their typical structure characteristics. The first group of tested materials was coated with very hard particles in structure. HVOF coating tungsten carbides in cobalt matrices (sample no. 1) where the ratio of hard particles was higher than 90 volume percentage. Plasma spray coating alumina oxide (sample no. 2) and plasma spray coating alumina oxide particles in metal matrix (sample no. 3) content particles > 90 volume percentage. Both alumina oxide ceramics materials were hard but very brittle and in this case there is the presumption that the adhesive strength is small between the phases in composite. Material Eucor (sample no. 4) is a mixed ceramics material with particles of alumina oxide and zirconia dioxide vitrified with silicon dioxide. The second group were materials without large hard phases, Creusabro 8000 (sample no. 5) is abrasive wear steel with martensitic structure and a small ratio of retained austenite, Sverker 21 is tool steel with martensitic structure and small chromium carbides in martensitic matrices, Fluxofil 58 (sample no. 7) which is a hardfacing material with martensitic matrices after weld depositing. The third group of tested materials were high chromium hardfacing deposits, Tubrodur 14.70 (sample no. 8) which is a hardfacing deposit with large chromium-rich carbides in eutectics matrices, SK 256-O (sample no. 9) is hardfacing similar to sample no. 8 with higher amount of large chromium-rich carbides in matrices, SK 45-O (sample no. 10) is hardfacing material similar to the previous and the microstructure amount of chromium-rich carbides and particles of niobium carbides, the ratio of chromium-rich carbides are also similar to sample no. 8. The samples were cleaned in ultrasonic bath after the test and mass loss was measured with the accuracy of 0.1 mg. The volume losses were determined from the density of tested material by the hydrostatic method.

Table 1. Tested materials

Sample no.	Characterizations of the tested material
1	HVOF coating WC+Co – nature
2	Plasma Al_2O_3 – nature
3	Plasma Al_2O_3 in 316L matrix – nature
4	Eucor (ZrO_2 + Al_2O_3 + 15% SiO_2) – nature
5	Creusabro 8000 (0.25C; 1.4Mn; 1.5Cr) – polished
6	Sverker 21 (1.5C; 11.8Cr; 0.8Mo; 0.8V) 65 – polished
7	Fluxofil 58 (0.45C; 0.6Si; 1.6Mn; 5.5Cr; 0.6Mo) – polished
8	Tubrodur 14.70 (3.5C; 22Cr; 3.5Mo; 0.4V) – polished
9	SK 256-O (5.5C; 1.2Mn; 1.2Si; 25 Cr) – polished
10	SK A45-O (5.3C; 21Cr; 6.3Mo; 6Nb; 1.9W; 1V) – polished

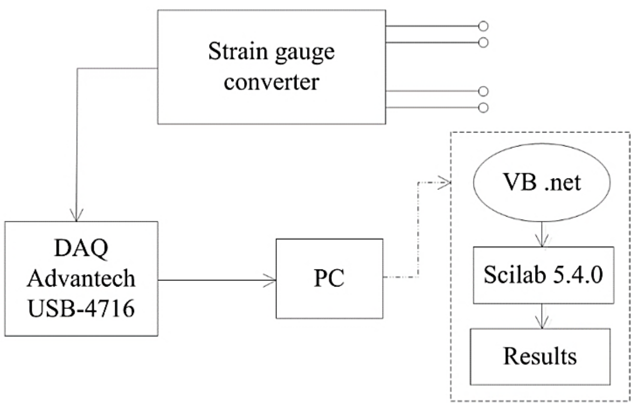

Figure 3. Scheme of the measurement setup.

RESULTS AND DISCUSSION

The experimental results are presented in Table 2. The values of volume loss represent how many cubic millimeters are given out per one meter of test distance. Friction force and its standard deviation were calculated from all measurements. The standard deviation values showed a change in friction force at varying measurements. The hardness of the tested material was determined by a standard Rockwell tester at a 150 kg load. Ceramic materials were very brittle and it was not possible to use the measurement using the Rockwell's method (Type C).

In Fig. 4, the effect of friction force on the first cycle measurement of the different materials is illustrated. Ceramic materials such as alumina oxide plasma spray coating achieved the lowest friction force. In this case, the cohesion of the structure spray coating was small and cracking with abrasive particles was possible (Sarikaza, 2005; Gok, 2011). The resistance passing through the particles was small and the kinetic energy of abrasive particles was transferred to cohesive failure. The wear rate was stable as a result of the dependency between friction force and distance (Fig. 4) for the total test time. The amplitude of the dependency between friction force and distance was small indicating that cohesion failure needs small energy. The volume loss of alumina oxide plasma spray coating was very high, but metallic matrices can increase wear resistance. It seems that alumina oxide in metallic matrices showed higher cohesive strength. The comparison of the ceramic materials showed a correlation between volume loss and friction force. The last material in this group, WC + Co composite, obtained small volume loss and friction force due to the higher fracture toughness of a HVOF composite. Indentation of abrasive particle into material was small corresponding to the small friction force. A higher number of passage particles is needed for the wear mechanism. Analyses of abrasive particles indicate that sand particles were broken. Comparing the volume loss and friction force at the same test time, the volume loss decreased with increasing friction force. It seems that a higher worn surface led to a higher area. For sand crashing, friction force increased intensively because crashing process requires high energy consumption. The amplitude of the dependency between friction force and distance was high, which could be due to sand crashing.

The results of the second group of materials showed that single-phase microstructure (without minority phases) partly indicated some correlation between friction force, hardness and volume loss. The worn surfaces were grooved with a different roughness. The roughness value depended on hardness because the ploughing mechanism depends on the indentation depth of the abrasive particle. The dependency between friction force and distance was stable while the amplitude was small, indicating that the abrasive particle thus shifts rather than the combination of rotating and shifting. This also indicates that sand particles had no influence due to lack of failure. Important behavior has been found as it was observed that the friction force on sample no. 5, decreased with the test distance (Fig. 5). This material showed a small amount of retained austenite, due to the wear mechanism and loading, with strengthened surface. On the other hand, the samples no. 6 and 7 had strengthened surfaces before the test because they were polished and this strengthened layer was worn before the test (Fig. 5).

The results of the third group of materials showed multiphase microstructure with high toughness although it had small volume loss but high friction force. The dependency between friction force and distance was not stable and the amplitude was high, indicating that sand obtained higher fracture toughness than chromium-rich carbides into matrices. Hardfacing and carbides also showed failure rather than sand. The analysis of the used sand after the test showed no failure.

Table 2. Measured values of the tested materials

Sample no.	Volume loss [$mm^3 \times m \times 10^{-3}$]	Friction force [N]	Hardness HRC
1	2.8 ± 0.3	14.72 ± 1.22	56 ± 1.5
2	292 ± 38	13.56 ± 0.32	N/A
3	166 ± 15	14.61 ± 0.42	N/A
4	43.6 ± 3.5	15.75 ± 0.52	N/A
5	14.7 ± 0.9	16.72 ± 0.44	40 ± 2.2
6	4.1 ± 0.6	15.98 ± 0.32	58 ± 1.4
7	16.2 ± 1.1	17.09 ± 0.35	38 ± 2.5
8	5.2 ± 0.4	16.3 ± 0.36	47 ± 1.7
9	3.7 ± 0.25	15.72 ± 0.22	56 ± 1.3
10	2.6 ± 0.07	16.09 ± 0.51	59 ± 1.3

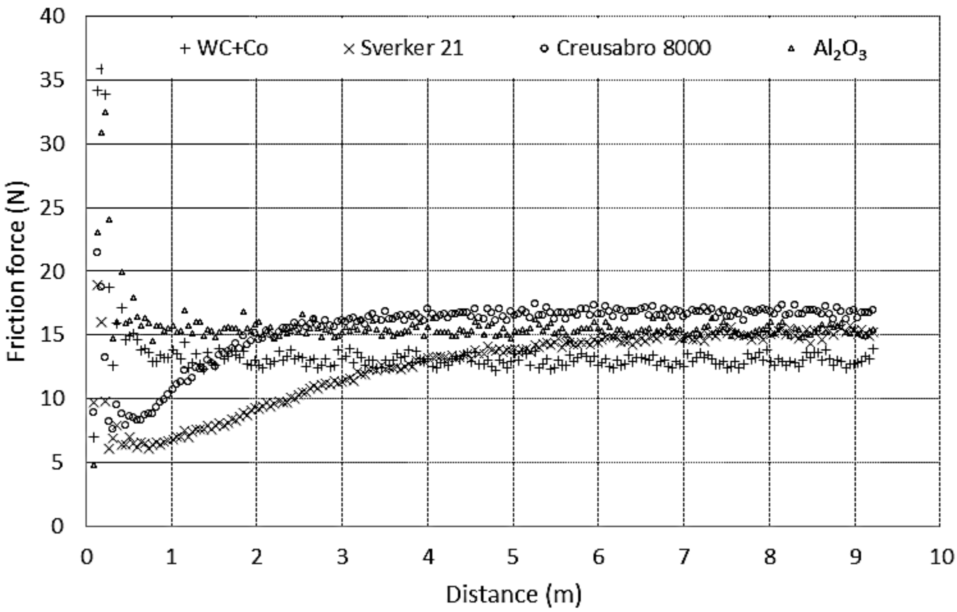

Figure 4. Measured data in the first cycle (for clarity, only the mean value from 4kSa).

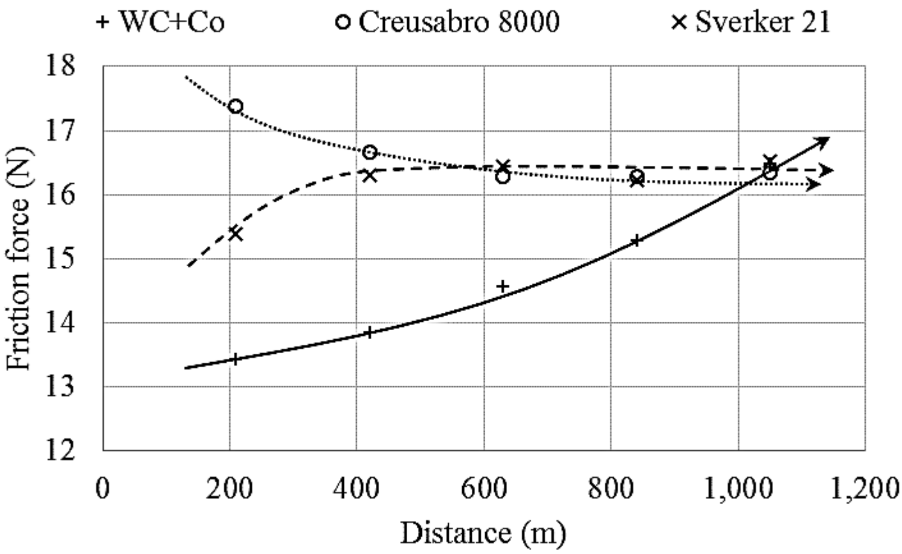

Figure 5. Dependency between mean friction force and distance for each cycle DRWT.

CONCLUSION

Evaluation of the abrasive wear process by a modified rubber wheel instrument revealed the following results:

- For single phase materials like steel, the friction force can represent wear since the friction force is proportional to the volume loss. Also, strengthening can be analyzed during the wear process.
- For multiphase materials like cast iron or metal matrix composite, the friction force, frequency and amplitude can represent cohesive strength between the hard phase and matrices. With a material with high cohesive strength, the abrasive particle can also break.
- The limitation of using the rubber wheel method is the natural frequency of the system. In this study, the natural frequency was found to be 200 Hz and this frequency is necessary to eliminate the algorithm for frequency and amplitude during wear analysis. Additionally, this phenomenon increases the requirement for the computation or hardware component such as memory capacity.

ACKNOWLEDGEMENT. The study was supported by the project TA CR no. TA01010192.

REFERENCES

Ceschini, L., Palombarini, G., Sambogna, G., Firrao, D. & Scavino, G. 2006. Friction and wear behaviour of sintered steels submitted to sliding and abrasion tests. *Tribology International* **39**, 748–755.

Chotěborský, R. 2013. Effect of heat treatment on the microstructure, hardness and abrasive wear resistance of high chromium hardfacing. *Research in Agricultural Engineering* **59**, 23–28.

Chotěborský, R., Hrabě, P., Müller, M., Válek, R., Savková, J. & Jirka, M. 2009a. Effect of carbide size in hardfacing on abrasive wear. *Research in Agricultural Engineering* **55**, 149–158.

Chotěborský, R., Hrabě, P., Müller, M., Savková, J., Jirka, M. & Navrátilová, M. 2009b. Effect of abrasive particle size on abrasive wear of hardfacing alloys. *Research in Agricultural Engineering* **55**, 101–113.

Cozza, R.C. 2014. Influence of the normal force, abrasive slurry concentration and abrasive wear modes on the coefficient of friction in ball-cratering wear tests. *Tribology International* **70**, 52–62.

Gok, M.S., Gencel, O., Koc, V., Kuchuk, Z. & Cay, V.V. 2011. Effect of abrasive particle sizes on abrasive wear of ceramic coatings sprayed by plasma process. *Powder Metallurgy and Metal Ceramics* **50**, 95–104.

Jankauskas, V. & Skirkus, R. 2012. Development and testing of materials with reduced wear by fixed abrasive. *Key Engineering Materials* **527**, 229–234.

Jokiniemi, T., Rossner, H. & Ahokas, J. 2012. Simple and cost effective method for fuel consumption measurements of agricultural machinery. *Agronomy Research* **10**, 97–107.

Kazemipour, M., Shokrollahi, H. & Sharafi, S. 2010. The Influence of the Matrix Microstructure on Abrasive Wear Resistance of Heat-Treated Fe–32Cr–4.5C wt% Hardfacing Alloy. *Tribology Letters* **39**, 181–192.

Korres, S., Feser, T. & Dienwiebel, M. 2013. A new approach to link the friction coefficient with topography measurements during plowing. *Wear* **303**, 202–2010.

Kučera, M., & Chotěborský, R. 2013. Analysis of the process of abrasive wear under experimental conditions. *Scientia Agriculturae Bohemica* **44**, 102–106.

Radziszewski, P., Varadi, R., Chenje, T., Santella, L. & Sciannamblo, A. 2005. Tumbling mill steel media abrasion wear test development. *Minerals Engineering* **18**, 333–341.

Petrica, M., Katsich, C., Badisch, E. & Kremsner, F. 2013a. Study of abrasive wear phenomena in dry and slurry 3-body conditions. *Tribology International* **64**, 196–203.

Petrica, M., Badisch, E. & Peinsitt, T. 2013b. Abrasive wear mechanisms and their relation to rock properties. *Wear* **308**, 86–94.

Sabet, H., Khierandish, Sh., Mirdamadi, Sh. & Goodarzi, M. 2011. The Microstructure and Abrasive Wear Resistance of Fe–Cr–C Hardfacing Alloys with the Composition of Hypoeutectic, Eutectic, and Hypereutectic at Cr/C = 6. *Tribology Letters* **44**, 237–245.

Sarikaya, O. 2005. Effect of some parameters on microstructure and hardness of alumina coatings prepared by the air plasma spraying process. *Surface & Coatings Technology* **190**, 388–393.

Stevenson, A.N.J. & Hutchings, I.M. 1996. Development of the dry sand/rubber wheel abrasion test. *Wear* **195**, 232–240.

Qi, J., Wang, L., Wang, Y., Pu, J., Yan, F. & Xue, Q. 2011. The tribological performance of selected solid lubricant films in sand-dust environments. *Wear* **271**, 899–910.

Wang, Q. & Li, X. 2010. Effects of Nb, V, and W on microstructure and abrasion resistance of Fe-Cr-C hardfacing alloys. *Welding Journal* **89**, 133–139.

Agronomy Research **12**(1), 255–262, 2014

ISO/TS 16949 among Latvian production companies focused on automotive industry

G. Civcisa[1*] and A. Grislis[2]

[1]Riga Technical University, Institute of Mechanical Engineering, Ezermalas 6k, LV 1006, Riga, Latvia; *Correspondence: guna.civcisa@rtu.lv
[2]Riga Technical University, Institute of Road Transport, Ezermalas 6k, LV 1006, Riga, Latvia

Abstract. Nowadays vehicle spare parts and materials manufacturers more than ever need a system approach which makes it possible to become a part of global supply-chain in the automotive industry. Such system approach could be implemented by developing a quality management system. The ISO/TS 16949 is particular requirements for the application of ISO 9001:2008 for automotive and automotive–related products production. The aim of this study is to analyze the diffusion of certified quality management systems ISO/TS 16949 and ISO 9001. The ISO survey of certifications has been a source for the analysis conducted for the data within a four–year period. Three main topics are discussed in this paper: the ISO 9001 and ISO/TS 16949 certificates diffusion in the world and in Latvia; the fundamental requirements in the ISO/TS 16949; an applicable tool for reviewing customer complaints in automotive production. This study has been focused on automotive industry therefore it highlights issues relating to industry–specific standard.

Key words: automotive, standard, quality management systems.

INTRODUCTION

The automotive industry is the biggest industry in the world (Hoyle, 2005) and there are few industries more global than the automotive sector (ISO, 2012). The total number of produced vehicles tends to increase year by year. The world motor vehicle production statistics shows that there were over 61 million vehicles in 2009, but there were 84 million vehicles in 2012 in the world (OICA, 2013).

The International Standardization Organization (ISO) developed the ISO 9000 family of quality management systems (QMS) standards more than 25 years ago, so enterprises might apply a quality management approach. The ISO 9001 is the most well–known standard of certification to ISO management systems. Application of ISO 9001 is not limited as regards the type of economic activity, industrial sector or the size of organization. ISO 9001 requirements should be regarded as additional complementary to requirements for products (ISO, 2008). The ISO 9001 standard is widely recognized throughout the world up to now more than one million and one hundred thousand organizations certificates were issued (ISO, 2013).

The ISO/TS 16949 is particular requirements for the application of ISO 9001:2008 for automotive and automotive related products production; it has interpreted them and added specific requirements (Nicolson, 2007). The actual version of the ISO/TS 16949 was published in 2009 and this is the third edition of this standard. This edition cancels and replaces the second edition (2002), but the first edition was published in 1999. The ISO/TS 16949:2009 was prepared by the International Automotive Task Force (IATF), with support from ISO/TC 176, Quality management and quality assurance (ISO, 2009) for the automotive sector. The ISO/TS 16949 includes all requirements of ISO 9001:2008 which are appear within closed boxes, but does not replace ISO 9001. To understand ISO/TS 16949 fully, the ISO 9001 requirements shall be understood (Kymal, 2004). ISO/TS 16949 certificate of conformity is often required of suppliers by the automobile manufacturers (ISO, 2011) and it could be explained by the fact that in many cases over 70% of the vehicles' contents from supply organizations (Bransky, 2008).

Despite the fact that Latvia is not a country of vehicle manufacturing (road vehicle assembling), thus at first it seems that it has nothing common with the ISO/TS 16949 standard. However, if we look closer, it becomes clear that there are companies which manufacture components for the automotive industry. The most used standards are ISO 9001, ISO 14001 (environmental management system) and ISO 18001 (occupational health and safety management system) in Latvian production industries (Lazdiņa, 2012). Among the observed trends, there is a growing interest in sector–specific standards, for instance ISO/TS 16949:2009 (Mežinska, 2011; Lazdiņa, 2012).

Taking into account amount of automotive industry, it is very important to satisfy the needs of customers and other stakeholders (Hoyle, 2005). Customers play a significant role in QMS and there is emphasis on customer satisfaction by meeting customer requirements. Although customer satisfaction is included in ISO 9001 but ISO/TS 16949 is more customer–focused and goes beyond (Kymal, 2004), additional requirements are aimed at strengthening the customer (Nicoloso, 2007).

MATERIALS AND METHODS

This study is focused on an automotive industry standard implementation. Both quantitative and qualitative research methods are used in this study: analysis of statistical data, analysis of absolute and relative statistical quantities, literature review, document (standard) analysis, comparative analysis as well as Cause–and–Effect diagram. A comparative analysis has been applied to determine the implementation of certified QMS in the world and Latvia. This study presents the implementation of QMS during a four–year (2009–2012) period. Statistical data are obtained from ISO management system standard certification surveys and International Organization of Motor Vehicle Manufacturers (OICA) database. The Cause–and–Effect diagram is designed in MS Visio.

The Cause–and–Effect diagram also called Ishikawa diagram and the fishbone diagram was developed by Japanese Professor Kaoru Ishikawa (Juran & Blanton Godfrey, 1998; Charantimath, 2003; Hoyle, 2005) in the last century, 1950–ies years. This diagram is considered as one of seven basic tools of quality (Targue, 2004; Hoyle, 2005). The Cause–and–Effect diagram is a graphical method to list cause of particular problems (Charantimath, 2003) and to show the relationship between cause and effect

(Hoyle, 2005). Ishikawa diagrams were first applied to manufacturing problems (Juran & Blanton Godfrey, 1998) and are still often used in quality management in the manufacturing firms (Rajkumar et al., 2013). In this study, the Cause–and–Effect diagram was used to demonstrate how it is applied to solving the problem of customer complaints in particular industry.

The Technical Specification ISO/TS 16949 defines the quality management system requirements for the design and development, production and, when relevant, installation and service of automotive–related products (ISO, 2009). The requirements in the ISO/TS 16949 are covered within Clause 4 through Clause 8:

- Clause 4 contains an overall general and documentation requirements for establishing QMS;
- Clause 5 contains requirements regarding the commitment of top management to the development and implementation of the QMS and continually improving its effectiveness through management reviews and for the fulfilment of customer satisfaction;
- Clause 6 contains resource management issues and for the ones all requirements related with resources;
- Clause 7 (the largest clause with most of the sub–clauses) contains all aspects of product realization, starting from the planning of product realization, customer–related processes, design and development, as well as covers purchasing process, production and service provision and control of monitoring and measuring devices;
- Clause 8 contains monitoring and measurement, data analysis and continual improvement requirements.

In this study, the clauses of ISO/TS 16949 were explored to determine the requirements related to the customer complaints.

RESULTS AND DISCUSSION

This section of the article describes the results of an analysis that was carried out to compere the number of certificates issued to ISO 9001 and ISO/TS 16949 in the world and in the Latvia. An explanation of requirements particularly related to the customer complaints is also given according to the requirements of ISO/TS 16949. An example of practical application, the one of quality tools: Cause–and–Effect diagram is presented by analyzing customer complains.

According to the data of ISO survey, at least 50,071 ISO/TS 16949:2009 certificates had been issued in 83 countries/ economies up to the end of 2012 (ISO, 2013). When average number of ISO 9001 certificates issued during the period 2009–2012 worldwide total have been compared to yearly issued ISO/TS 16949 certificates (Fig. 1), it can be concluded that ISO/TS 16949 certificates had been issued about 24 times less.

Despite this fact, certification to ISO/TS 16949 shows increased tendency in the four–year period. In 2009 there had been issued 41,240 certificates of ISO/TS 16949, but up to the end 2012, the number of issued certificates has increased up to 21%.

According to the latest survey of ISO (ISO, 2013) and calculations made by the authors (Fig. 2), at the end of 2009 there were 708 ISO 9001:2008 certificates issued, while at the end of 2012, there were 791 certificates issued in Latvia. In 2012, the number of issued ISO 9001certificates has grown by 12% (+ 83) compering to 2009.The number of ISO/TS 16949:2009 certificates were nearly unchanged during 2009–2012, only 7 enterprises in Latvia had this certificate. After evaluating the statistical data one can conclude that the first three companies received ISO/TS 16949 (automotive sector) certificates in Latvia in 2007.

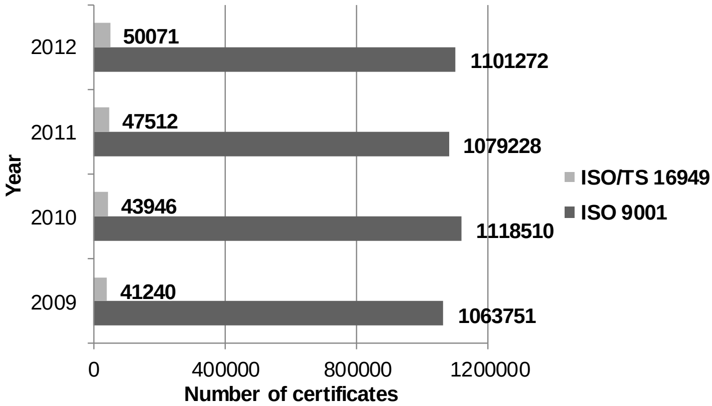

Figure 1. Number of QMS certificates worldwide during 2009–2012. Source: authors' calculation from ISO data, 2013.

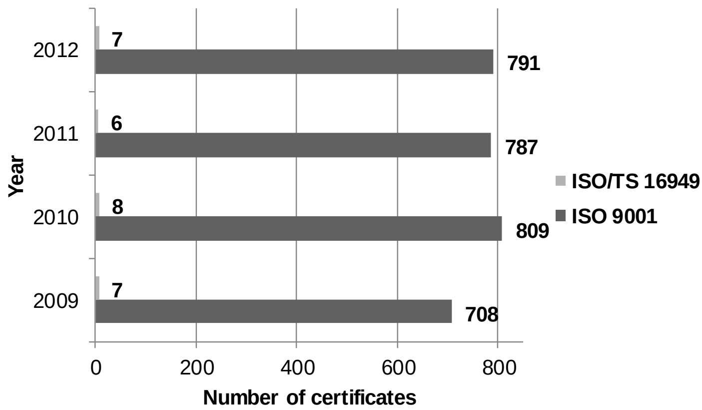

Figure 2. Number of QMS certificates in Latvia during 2009–2012. Source: authors' calculation from ISO data, 2013.

According to the latest survey of ISO (ISO, 2013) and calculations made by the authors (Fig. 2), at the end of 2009 there were 708 ISO 9001:2008 certificates issued, while at the end of 2012, there were 791 certificates issued in Latvia. In 2012, the number of issued ISO 9001certificates has grown by 12% (+ 83) compering to

2009.The number of ISO/TS 16949:2009 certificates were nearly unchanged during 2009–2012, only 7 enterprises in Latvia had this certificate. After evaluating the statistical data one can conclude that the first three companies received ISO/TS 16949 (automotive sector) certificates in Latvia in 2007.

The analysis of ISO/TS 16949 standard diffusion reveals some common conclusions. The largest number of certificates of conformity to ISO/TS 16949 in the end of 2012 has been issued in the East Asian and Pacific (26,985) and European (11,017) regions. Germany (3,184) and Italy (1,147) are the leading industry players in Europe and takes 5th and 8th position respectively in the world's top ten countries for certificates; while the absolute leader of the issued certificates is China (17,975) (ISO, 2013).

ISO 9001 also ISO/TS 16949 specify requirements to enhance customer satisfaction. From literature review it has been revealed that ISO/TS 16949 is more customers driven if compared to ISO 9001:2008. Sub–clauses related to customer satisfaction have been compared to analyze correspondences and differences in both ISO 9001:2008 and ISO/TS 16949:2009. The results of analysis are presented in Table 1.

Table 1. Clauses related to the customer satisfaction within ISO 9001:2008 and ISO/TS 16949:2009

ISO 9001:2008	Sub–clause	Sub–clause	ISO/TS 16949:2009
Process approach	0.2	0.2	Process approach
General	1.1	1.1	General
		4.2.4.1	Records retention
Customer focus	5.2	5.2	Customer focus
		5.6.1.1	Quality management system performance
Provision of resources	6.1	6.1	Provision of resources
		6.2.2.2	Training
		6.3.2	Contingency plans
Determination of requirements related to the product	7.2.1	7.2.1	Determination of requirements related to the product
Customer satisfaction	8.2.1	8.2.1	Customer satisfaction
		8.2.1.1	Customer satisfaction — Supplemental
Analysis of data	8.4	8.4	Analysis of data

The analysis of ISO 9001:2008 standard has shown that customer satisfaction has been mentioned in seven sub– clauses. As ISO/TS 16949 is written consistent to the ISO 9001:2008 standard, the same seven sub–clauses plus five supplemental specific requirements related to customer satisfaction are included. All these supplemental requirements of the automotive standard specified in the column ISO/TS 16949 of Table 1 are discussed further. Sub–clause 4.2.4.1, records retention, requires control of records regarding regulatory and customer requirements. Sub–clause 5.6.1.1 requires that management reviews should reflect how satisfaction of customers is reached regarding with supplied product. Sub–clause 6.2.2.2, training, puts extra emphasis on competent personnel to satisfy requirements of customer. In sub–clause 6.3.2 the standard requires preparation of contingency plans for emergency situations. Plus one extra sub–clause is added for gaining supplemental customer satisfaction. It is the 8.2.1.1 sub-clause, where indicators of performance are required for evaluation realization processes.

Customer complaints are indicator of low customer satisfaction, although requirements have been agreed by customer, this does not constantly ensure high customer satisfaction. Both standards contain requirements relating to review of customer complaints. Sub–clause 7.2.3 c), customer feedback, including customer complains, requires that an organization should introduce activities and communication with customers for obtaining feedback information and customer complaints. Sub–clause 8.5.2 a), reviewing nonconformities (including customer complaints), requires that an organization should establish a documented procedure to define requirements for reviewing customer complaints. One additional requirement relating customer complaints is in ISO/TS 16949. Sub–clause 8.2.2.4, requires that internal audit frequency should be increased if customer complaints occur.

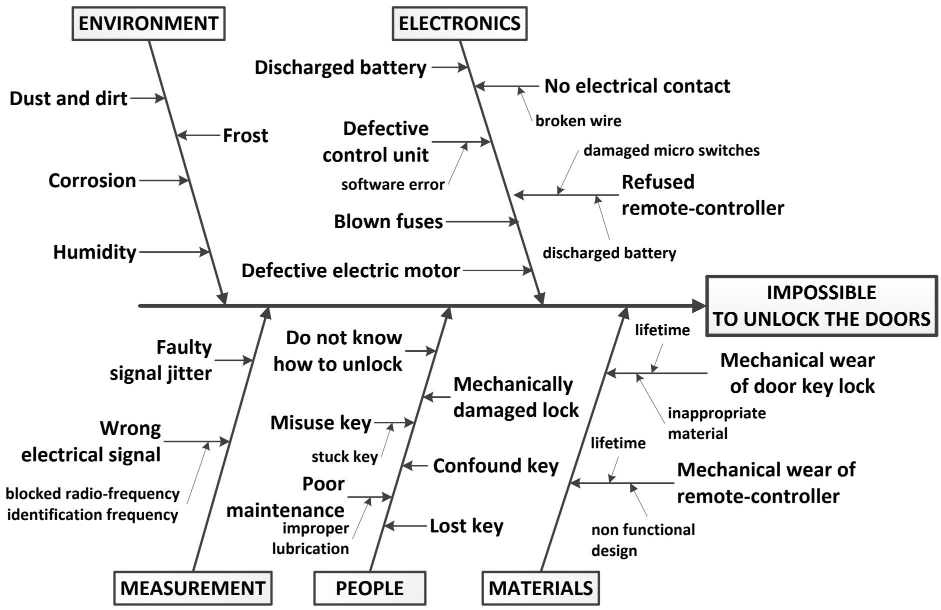

Figure 3. An example of Cause–and–Effect diagram in automotive industry.

In the example shown above, the constriction and possible application of Cause–and–Effect diagram has been demonstrated. This method is good with the graphical visibility of the relationship between cause and effect. A Cause-and-effect diagram is a well-known tool for identifying possible causes for an effect or problem. As it is shown in the Fig. 3, it could be used in automotive industry as a quality control tool at manufacturing processes in accordance with ISO/TS 16949. Since automotive production is multi step technological process involving many operations in several technological plants, a cause-and-effect diagram could provide easy and fast solution and be very useful tool for identifying and organizing the known or possible causes of the specific defect.

CONCLUSIONS

This study is valuable for providing information about the diffusion of ISO/TS 16949 certificates in automotive industry worldwide and in Latvia during the four–year period. Additionally, the implementation of standards ISO 9001 and ISO/TS 16949 are also compared. The main objective for the analysis of the standard ISO/TS 16949 was to found requirements where customer complaints are emphasized. With the specific example from the automotive sector, the potential solution for analyzing customer complaints is presented.

The first conclusion is that, obtained results show that the certification to ISO/TS 16949 in automotive industry in the world is widely diffused and should be characterized by a growing trend, while it should be characterized as unchanged in Latvia.

The second conclusion to be drawn from this study is that there are three particular requirements regarding customer complaints in the requirements of ISO/TS 16949 and the whole system should be characterized as customer–focused. At first, the customer is emphasized in one of the eight quality management principles and then through the whole system in order to monitor its satisfaction.

The third conclusion is regarding to one requirement (8.5.2.1) in the standard ISO/TS 16949 where is stated that an organization should define process for problem solving. Certainly, there many tools have been used to determine the root cause with the aim to implement corrective and preventive actions. The potential causes can be collected either by speaking with customers or from complaints recorded by customers (Hoyle, 2005). The use of Cause–and–Effect diagram is one of possible technique in the field of quality management for analyzing customer complaints or any others nonconformities.

REFERENCES

Bransky, J. 2008. Ensuring vehicle performance. *ISO Focus* 5(3), 17–19.

Charantimath, P.M. 2003. *Total Quality Management*. Pearson Education, Delhi, 272 pp.

Hoyle, D. 2005. *Automotive Quality Systems Handbook*. 2nd ed. Elsevier Ltd., Oxford, 712 pp.

ISO. 2008. *ISO 9001:2008 Quality management systems – Requirements*. ISO copyright office, Geneva, 27 pp.

ISO. 2009. *Quality management systems – Particular requirements for the application of ISO 9001:2000 for automotive production and relevant service part organizations*. ISO copyright office, Geneva, 39 pp.

ISO. 2011. *ISO & Road vehicles*. ISO Central Secretariat, Geneva, 4 pp.

ISO. 2012. *How ISO standards support global car industry*. ISO Central Secretariat, Geneva, 56 pp.

ISO. 2013. ISO Survey of Certification – 2012. International Organization for Standardization.Link: http://www.iso.org/iso/home/news_index/news_archive/news.htm?refid=Ref1788 (accessed on: 04.10.2013.)

Juran, Joseph, M. & Blanton Godfrey, A. 1998. Juran's quality handbook. 5th ed. McGraw-Hill Professional, New York, 1872 pp.

Kymal, C. 2004. *The ISO/TS 16949 Implementation Guide: Gaining Value from Your ISO/TS 16949 Implementation*. Paton Press LLC, Chico, 130 pp.

Lazdiņa, I. 2012. BVLatvia certification. Presentation materials at seminar: *Quality management and ISO certification for Latvian companies – do I need it and how it can help the promotion of the company's export promotion*. 14 March 2012, Riga, Latvia, 20 pp (in Latvian).

Mežinska, I. 2011. *Improvement methodologies of integrated management systems for production industry enterprises in Latvia*. Doctoral Dissertation Summary. Riga Technical University, Riga, 40 pp.

Nicoloso, E. 2007. Bridging the gap between quality management systems and product quality. *ISO Management Systems*, 7(1), 7–11.

OICA. 2013. The International Organization of Motor Vehicle Manufacturers. World Motor Vehicle Production. Link: http://www.oica.net/category/production-statistics/ (accessed on: 28.12.2013.)

Anbu, A., Rajkumar, M.D., Srikumar, V., Kumar, P.S., Asha, P.J. & Renukadevi, K. 2013. An Application of Fish Bone Diagram for Quality Improvement Measure and to Reduce the Scraps While Manufacturing. In Global Institutes Amritsar and University of Mauritius (eds): *International Conference on Sustainable Manufacturing and Operations Management ISOM–2013*. Thane, India, pp. 357–360.

Tague, N.R. 2004. *The Quality Toolbox.* 2nd ed., ASQ Quality Press, Milwaukee, 584 pp.

Agronomy Research **12**(1), 263–268, 2014

Testing a method for evaluating the performance of coatings on end mills in semi-industrial conditions

T. Leemet[1,*], J. Allas[1], M. Madissoo[1], E. Adoberg[2] and R. Saar[3]

[1]Institute of Technology, Estonian University of Life Sciences, Kreutzwaldi 56, EE51014 Tartu, Estonia; [*]Correspondence: Tonu.Leemet@emu.ee
[2] Institute of Physics, University of Tartu, Riia 142, EE51014 Tartu, Estonia
[3]Department of Materials Engineering, Faculty of Mechanical Engineering, Tallinn University of Technology, Ehitajate tee 5, EE19086 Tallinn, Estonia

Abstract. Milling remains as one of the most versatile machining operation in manufacturing. Machine tools with several axis of movement and precise numerical controls are able to manufacture complex geometries for medical implants, parts needed in space technology etc. The quality of the workpiece and the cost of manufacturing are influenced by many factors, tool selection being one with considerable impact. Depending on the specific type of milling operation and the material of the billet, the coating of the cutting tool can have a significant influence to quality and cost of the process.
In this study an attempt is made to develop a methodology for relatively simple but effective means for evaluating the suitability of a coating for a particular milling operation. Flank wear width is generally recognized as the key indicator for tool life criteria. Relatively complex geometry of the end mill makes the flank wear measurements somewhat difficult. In practice several other indication of tool wear are used: changes in the spectra and volume level of the sound emitted from the cutting process, shape and color of the chips, quality of the manufactured surface and the presence of the burrs. In this work the flank wear measurements by optical measurements are analyzed and reasoned, additional information is found by scanning electron microscopy. Three industrial PVD coatings – TiAlN, naCo and nACro were tested.

Key words: PVD coatings, milling, tool life, cutting tool wear phenomenon.

INTRODUCTION

Depending of the particular manufacturing situations several choices for the cutting tool selection can be made. Finding the optimal, i.e. most cost-effective solution is not a straightforward task. Machining is a complex phenomenon consisting of many potentially influential parameters. For instance, the overall stiffness of the machine tool is the first parameter to consider when choosing between high speed steel or carbide tools, the former having higher toughness should be the preferred choice for machine tools with lower stiffness. Carbide tools, although harder and therefore having superior wear resistance, are more fragile, thus more prone to fracturing when used on machine tools with low stiffness. Leaving other factors constant on acceptable level carbide tools are known to have higher material removal rate at the same tool life. Implementation of dedicated hard coating on the tool amplifies it even further. Tool geometry and machining parameters are additionally among the key factors to be considered in the machining process.

There are numerous different coatings available on the market today. The industry segment is constantly in search and development of new coatings with enhanced properties. Tool manufactures give general recommendations about coating selection and usage conditions depending on the material to be machined. Still in many practical cases the choice of the cutting tool and coating remains as a matter of subjective preference based on limited experience. One purpose of the current research is an attempt to develop method suitable for evaluating the suitability of specific coatings for milling of chosen material.

The essential task of the coating is to modify the contact conditions in the cutting region between the different wear surfaces reducing wear intensity, prolonging tool life and assuring the quality of the finished surface. Benefits of the coating arise from its higher hardness and wear resistance at elevated temperature, accompanied with lower friction coefficient between contacting surfaces and good chemical and thermal stability (Sarwara et al., 2008). Reports have been published about tool life of coated tools being three times higher than the one for uncoated tools (Trent, 1996). Coatings are usually up to 5 microns in thickness and deposited either via physical or chemical vapor depositions technology.

Considerable amount of scientific papers have been published in the field of tool life or tool quality investigations in general. It can be seen from literature that great number of coating – workpiece material combinations with in depth analyses of wear mechanism have been studied and published (Filice et al., 2007). In this work, an alternative approach is taken with focus on manufacturing aspect instead of tribology.

The emphasis of the current work is on two key concepts of interest to the scientific community today (Odelros 2012): 1. Developing and implementing the methodology for fast and reliable evaluation of cutting tool quality in industry like situation. To fulfil this aim the testing routine based on ISO 8688 International Standard has been developed. Coating choice for particular coating – workpiece material combination has been investigated and discussed; 2. Determining the best choice from three coatings (TiAlN, nACro and nACo) qualitatively for milling HYDAX 25 steel.

MATERIALS AND METHODS

HYDAX 25 was chosen as test material due to its widespread usage and relatively good machinability characteristics. In principle it is a derivative of the S355 construction steel with higher manganese content for achieving elevated machinability due to the relatively hard manganese particles in the matrix leading to extended chip breakage, thus elevating automated cutting operation capabilities. Material was used in as-received state, hot-rolled bars with rectangular cross-section of 105 mm in side length, test billets were cut into pieces of 300 mm in length. The nominal chemical composition and values of mechanical properties are given in Table 1.

Three coatings were chosen to be tested, all of which were deposited on end mills with exactly the same geometry. Platit π 80 arc ion plating PVD unit at Tallinn University of Technology, Estonia, was used for deposition of hard coatings (Gregor, 2010). Substrate material was the same at all instances – solid carbide, WC/Co. All cutting edges were inspected prior to testing. An average acceptable level of coating quality was verified and assured. The cutting edges of all instruments tested looked sharp with no burrs or coating flaking. Summary with cutting tool overview and information about used coatings is presented in Table 2.

Table 1. Nominal workpiece composition and mechanical properties, HYDAX 25

Cast analyses		Tensile test	
MPa	wt. %	Parameter	MPa
340	0.21	$R_{p0.2}$	340
552	0.20	R_m	552
26.4	1.04	A_5, %	26.4
56	0.012	Z, %	56
144.7	0.106	HBW	144.7

Table 2. Cutting tool parameters and properties of coatings

Type of mill	Shank form	Coating	Diameter	Flute angle	Coating thickness	Adhesion*
HPC endmill	cylinder	nACo	8 mm	35°/38°	1.40 μm	HF 3
HPC endmill	cylinder	TiAlN	8 mm	35°/38°	1.71 μm	HF 3
HPC endmill	cylinder	nACro	8 mm	35°/38°	2.01 μm	HF 3

*Daimler–Benz adhesion method

Milling experiment was designed in a way which ensured and retained constant cutting conditions throughout testing. HAAS SMM-HE vertical CNC machining center was used. Material was cut by layers with thickness of 4 mm, toolpath with climb-milling passage moving along spiral cutting path was programmed by MasterCam X6 CAM software. As high speed machining is becoming more and more popular in everyday machining practice, the cutting parameters for testing were chosen according to guidelines suggested for high speed machining with dry air blast cooling as machining environment. Cutting parameters are presented in Table 3.

Table 3. Cutting parameters used in milling experiments

Cutting speed v_C , m min^{-1}	238
Width of cut, a_E , mm	1.6
Depth of cut, a_P , mm	4
Feed per tooth, mm Z^{-1}	0.08
Material removal rate, cm^3 min^{-1}	19.2
Coolant	Dry air blast

Tested tools were periodically observed and tool wear recorded after cutting two layers of material. The volume of the material removed by cutting one layer was 113.5 cm^3, the tool wear was recorded periodically after cutting of 227 cm^3 of material, which corresponds to 36 m of cutting length. For the estimation of the tool wear, i.e. system composed of cutter and its coating, an optical ZEISS Discovery V12 stereomicroscope with software ZEN was utilized. For performing the flank wear quantitative measurements the near vicinity of the region between worn and un-worn segments of the flank face was used for observations. Every end mill was tested for 252 m of cutting length (1,589 cm^3 of removed material).

Focusing on flank wear and notch wear on the flank face has been justified following numerous research papers published on the subject (Lim et al, 1999; Ezugwu et al, 2001; Ezugwu et al, 2005).

RESULTS AND DISCUSSION

Experimental results are summarized on micrographs by stereomicroscopy at Fig. 1 where flank faces of different end-mills with different coatings are aligned in a row.

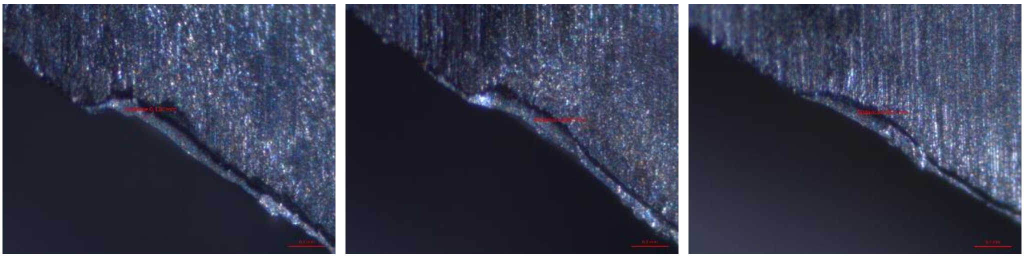

a) b) c)

Figure 1. Flank wear on clearance face on three end mills, x63: a) nACo; b) TiAlN and c) nACro.

It is evident from the figures that tools with different coatings bare non-similar resistance to wear. This can be concluded visually from the micrographs of Fig. 1. Adhesive wear composed on abrasive wear results in notch wear mark at the depth of cut line, 4 mm from the tip of the end mill along the shank centerline. Quantitative measurements of overall flank wear lead to results concluded in Table 4, from where it is justified to state that nACro coating has the highest wear resistance in the studied machining situation.

Table 4. Flank wear width values after cutting 252 m

Specific coating on end mill	Flank wear land width, mm
nACo	0.120
TiAlN	0.087
nACro	0.067

For additional information about the current state of features on tested end mills, SEM micrographs were taken, Fig. 2. Same spot as with optical microscopy was under inspection. Angle of view has been tilted to reveal rake face, flank face and the cutting edge in between. From here it is seen that nACo and TiAlN coatings have developed a degree of adhered debris on the rake face. Whereas the planes on nACro coated end mill are relatively clean.

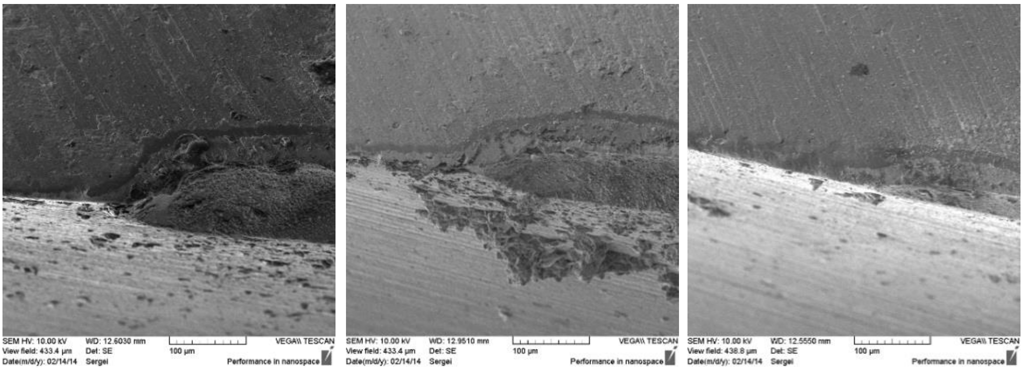

a) b) c)

Figure 2. SEM micrographs of the end mill cutting edge: a) nACo; b) TiAlN and c) nACro.

CONCLUSIONS

1. Methodology for cutting wear determinations has been proposed and tested. Three coatings, nACo, TiAlN and nACro on end mills were used to machine HYDAX 25 construction steel. Within constant conditions end mill with nACro coating has the least amount of wearing.

2. Major wear mechanism in action is abrasion. Notch wear due to adhesive wear is also clearly evident. No mentionable signs of built up edge, thermal cracking, edge chipping or plastic deformation was reported.

3. Following the outcome of the performed research it suffices to say that the proposed method as such has some potential shortcomings. Suitability of a particular coating based only on the estimation of the overall flank wear value is potentially overlooking other important and influential parameters. Quality of the finished surface and actual dimensions of the feature being machined together with in-situ cutting force measurements are considered for inclusion for future investigations.

4. Wear on rake face of the tool i.e. crater wear was left out from considerations. Future work should also include chemical wear mechanism as a component affecting tool life.

ACKNOWLEDGEMENTS. This work has been supported by the Estonian Ministry of Education and Research within the Project No. 3.2.1101.12-0013 'Advanced Thin Hard Coatings in tooling'.

REFERENCES

Astakhov, V.P. 2006. *Tribology of Metal Cutting*. Elsevier, 425 pp.

Sarwara, M., Haider, J., Perssonb, M. & Hellberghb, H. 2008. Evaluating the performance of TiN coating on a PM HSS milling cutter used in manufacturing of bandsaws. Available at: Open Access repositories (http://core.kmi.open.ac.uk)

Lim, C.Y.H., Lim, S.C. & Lee, K.S. 1999. Evaluation of the performance of CBN tools when turning Ti–6Al–4V alloy with high pressure coolant supplies. *Tribology International* **32**, 393–398.

Ezugwu, E.O., Da Silva, R.B., Bonney J. & Machado, Á.R. 2005. The performance of TiN-coated high speed steel tool inserts in turning. *Int. J. Mach. Tool Manu.* **45**, 1009–1014.

Ezugwu, E.O. & Okeke, C.I. 2001. Tool life and wear mechanisms of TiN coated tools in an intermittent cutting operation. *J. Mat. Process. Tech.* **116**, 10–15.

Trent, E.M. 1996. *Metal Cutting, 3rd Edition*, Butterworth/Heinman.

Odelros, S. 2012. *Tool wear in titanium machining*, Uppsala Universitet, 63 pp.

Filice, L., Micari, F., Settineri, L. & Umbrello, D. 2007. Wear modelling in mild steel orthogonal cutting when using uncoated carbide tools. *Wear* **262**, 545–554.

Gregor, A. 2010. *Hard PVD Coatings for Tooling*. Tallinn University of Technology, 140 pp.

Davim, J.P. *ed.:* 2007. *Machining*, Springer, 358 pp.

Agronomy Research **12**(1), 269–278, 2014

Machining quality when lathing blanks with ceramic cutting tools

V. Maksarov*, A. Khalimonenko and D. Timofeev

Department of mechanical engineering National Mineral Resource University, Vasilevsky island, 21 Line, House 2, 199106 St-Petersburg, Russia;
*Correspondent: maks78.54@mail.ru

Abstract. The article deals with the problems of improving quality of parts machined on lathe type machine tools. Improvements are suggested by predicting the operability (tool life parameter) of cutting tools equipped with replaceable ceramic inserts. It is proposed to forecast the operability of ceramic tools on the ground of relation between operational characteristics of the ceramic and microstructural parameters of the ceramic material. Microstructural parameters of ceramic inserts are determined by non-destructive testing method, evaluating them by estimating the specific electric resistance of the material.
As a result of research, a relation has been detected between operability of the inserts and the specific electric resistance of the insert material.
Obtained results permit one to determine the stability range borders for lathing blanks with tools equipped by ceramic cutting inserts and to predict flawless work.

Key words: metals cutting, ceramic cutting inserts, machining precision.

INTRODUCTION

Advancement of production engineering is one of the significant factors in state-of-the-art mechanical engineering. Feature of the present-day production includes the use of new tool materials having high cutting properties. Cutting ceramics belong to those materials.

High efficiency of machining, tool-life gain, reduction of costs at the expense of replacement of grinding procedures with cutting, and reduction of processing time at the expense of significant cutting speed increase are the main reasons of cutting ceramics use on production of exact elements of machine parts. Moreover, using cutting tools equipped with ceramic inserts, one can process hardened steels and other hard-to-cut materials.

At present, the amount of cutting ceramics on the whole of used tool materials does not exceed 5–8%. According to forecasts, the rate of ceramics will increase up to 15% in near future (Bandony & Buljan, 1988). It could occur due to the fact that known hard alloys will be replaced by cutting ceramics from straight forward economic considerations.

Moreover, using cutting tools equipped with ceramics one can process not only cast iron and structural steel, but also heat-resistant and hardened steels and other hard-to-cut materials.

All the types of cutting ceramics combine the properties of ceramic and metal constituents. They differ from other materials in higher strength characteristics, lower toughness and tendency to crack initiation, having high cutting properties. Ceramics use is bounded in the practice of metal cutting as yet since it is considered as too «high-speed» for standard conditions of processing and brittle for wide use.

Investigation of one of the main components of processing system – a cutting tool – is the main task on control of turning process quality. Control of handling process quality is directly connected with information on the ability of tool to carry out processing with specified accuracy parameters in the specified time period, i.e. with information on the working ability of cutting tool (Margules, 1980).

Different behavior of cutting plates made of ceramics of the same type was observed on their use under the same conditions of processing. Half-finished products processed with tools equipped with same cutting plates made of ceramics of the same type at the constant parameters of cutting modes had various indices of dimensional accuracy, surface roughness, and geometrical deviations. Life period of the tool equipped with identical cutting plates also varied on the preservation of constant parameters of cutting modes. Above-mentioned circumstances dictate the necessity to find parameters influencing the distinction of behavior on cutting with ceramics, which is an urgent question since, in particular, the problem of control of treatment process quality and working ability of tool equipped with cutting ceramics is in a formative stage.

At present, the methods of control of the working ability of cutting tool equipped with ceramics are in the stage of study and therefore require further development and improvement. To develop such methods it is necessary to have verified, reliable information on the structural parameters of cutting ceramics, detection and validation of which can give the clear idea of the most rational use of cutting tool for the definite processing conditions, which enables us to realize the control of working ability of ceramic cutting tool. Problems arising on the investigation of such objects as cutting tools determine the reasonability of experimental techniques use.

MATERIALS AND METHODS

Structural composition of tool material qualitatively influences its mechanical properties and wear during cutting. The better the structure is, the better the cutting properties. This dependence is true also for cutting ceramics; therefore it is required to determine the relationship between ceramic structure and the working ability of tool which is equipped with it. It is known (Margules, 1980), that cutting ceramics is a conducting material and being structurally inhomogeneous material it has a definite value of resistivity. Investigations showed (Maksarov et al., 2008a; 2010) that ceramic plates with resistivity value approaching $R = 100\ \Omega$ have the best cutting properties. Ceramic plates with resistivity value approaching $R = 10\ \Omega$ have the poorest cutting properties. From this one can conclude that ceramic plates with $R = 100\ \Omega$ have the microstructure of higher quality in comparison with ceramic plates with $R = 10\ \Omega$.

Several ceramic plates of grade VOK63 with various values of resistivity were selected to confirm the theory.

Plates of cutting ceramics were prepared in special way to carry out the structural investigations of material using microscope. The samples were subjected to microgrinding according to the specially developed technique (Maksarov et al., 2008b). Up-to-date ceramics of grade VOK63 taken for the investigation consists of 75% of Al_2O_3 + 25% of (Ti, W) C, which is proved out on computing of image obtained using metallographic microscope (Fig. 1).

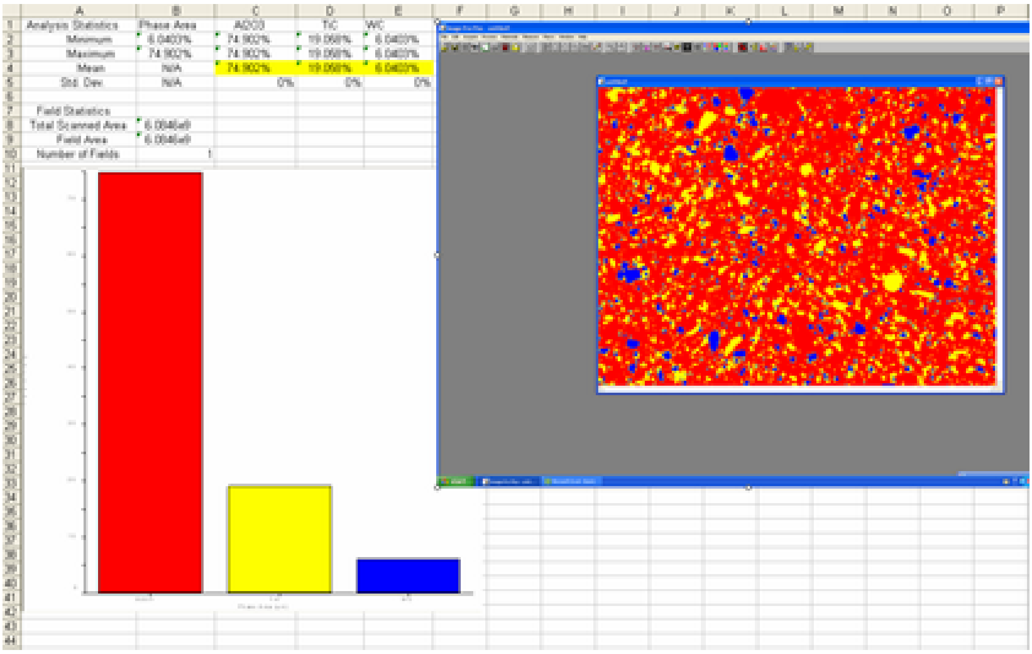

Figure 1. Percent distribution of Al_2O_3, TiC, and WC in VOK63 ceramics.

Photographs obtained using microscope (Fig. 2) show that microstructural parameters of the samples with different resistivity differ from each other.

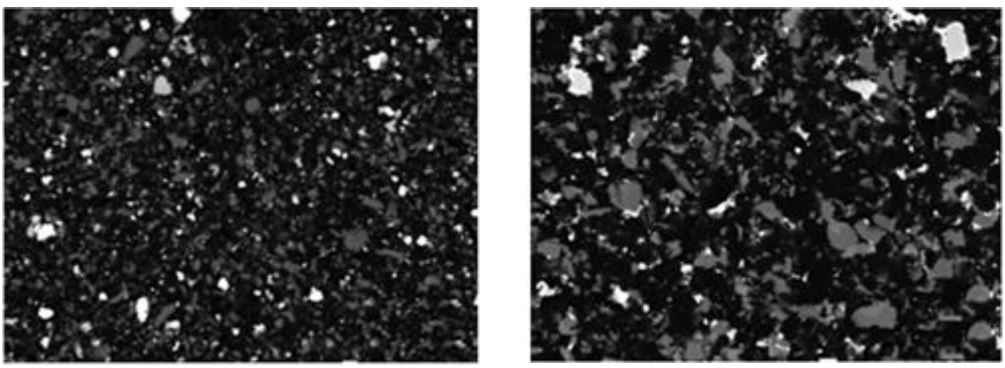

a b

Figure 2. Structure of ceramics of grade VOK63: a – $R \approx 100\ \Omega$, b – $R \approx 10\ \Omega$.

Samples with resistance close to R = 100 Ω have better structural parameters than others. As computing showed (Fig. 3), the samples of ceramic plates with relatively low resistivity ($R = 10\ \Omega$) are characterized by large diameter of grains ($D_{CP} = 2.21$ μm), high percentage of porosity ($\Pi = 14\%$), low value of cumulative line of grain boundary extension ($C = 7.76 \cdot 1\ \text{mm}^{-2} \cdot 10^2$), and small quantity of grains ($H = 21.5$). The samples of ceramic plates with relatively high resistivity ($R = 100\ \Omega$) are characterized by the following parameters: $D_{CP} = 1.51$ μm, $\Pi = 8\%$, $C = 5.186 \cdot 1\ \text{mm}^{-2}\ 10^2$, $H = 46.76$.

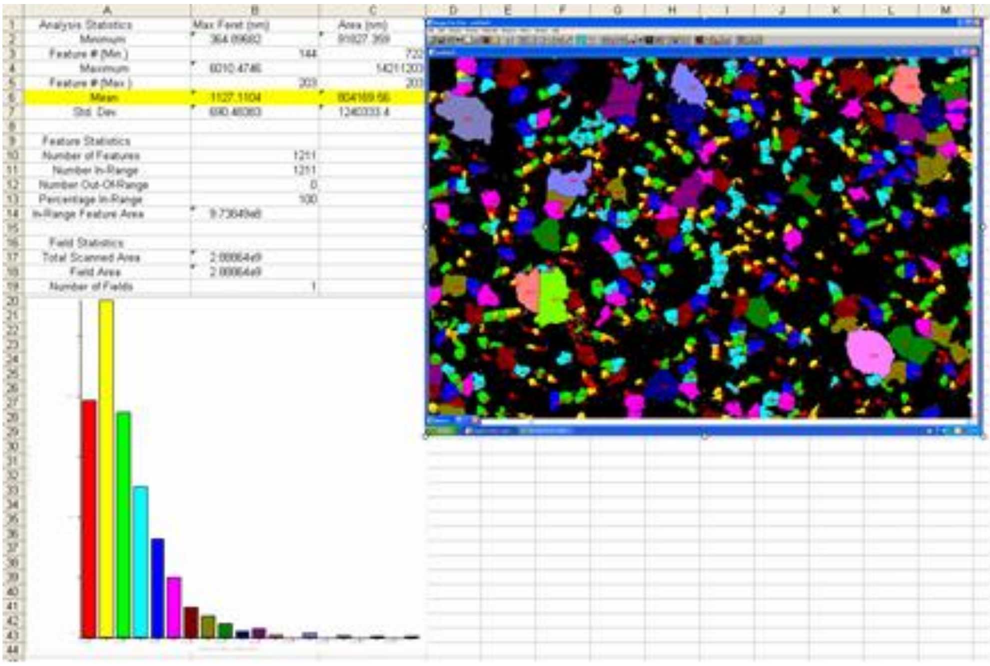

Figure 3. Structural parameters of ceramics of grade VOK63.

Treatment of experimental data enabled us to establish relationship between resistivity and structural parameters of ceramics, as a result of which we obtained the following dependence:

$$R = 542.9 \frac{H^{2.35}}{C^{1.14} \cdot D_{\mathrm{SR}}^{3.029}},\ \Omega \qquad (1)$$

This points to the fact that the better the microstructure of cutting ceramic plates (relatively small-sized grains, small their quantity, high values of cumulative line of grain boundary extension, and low porosity of material), the more the value of their resistivity. The data obtained is the base to determine the cutting properties of ceramics depending on the structural parameters of material, data about which one can obtain by determination of the resistivity of each plate before its use.

RESULTS AND DISCUSSION

A number of experiments, in which the final treatment of identical half-finished products was carried out with running values of cutting modes, were carried out to determine the cutting properties of ceramics of grade VOK63 with different values of resistivity (Maksarov et al., 2008a; 2008b). According to the results, we have found the connection between the wear of cutting plate and cutting modes, based on the parameters of plate wear on rear face $h_Z = f(t, S, V)$, where t is cutting depth, S is tool feed, and V is cutting speed. Ceramics wear mechanism turned out to be peculiar. Plate bluntness occur mainly on clearance face in the form of typical strokes of wear located at right angle to main cutting edge in the region contacting with cutting surface. Wear of the rake face is negligible in comparison with wear of clearance face (Maksarov et al., 2010).

Dependence of wear of clearance face on the duration of cutting path showed significant difference in reaching of wear equal to 0.5 mm. Correlation of traversed path lengths for VOK63 with $R = 100\ \Omega$ and VOK63 with $R = 10\ \Omega$ turned out to be 8/6 and the functional dependences of wear on cutting modes look as follows:

- for BOK63 with $R = 100\ \Omega$:

$$h_Z = 0.08\frac{V^{0.38} \cdot S^{0.17}}{t^{0.66}}, \text{ mm,} \tag{3}$$

- for BOK63 with $R = 10\ \Omega$:

$$h_Z = 0.04\frac{V^{0.22} \cdot S^{0.023}}{t^{0.11}}, \text{ mm.} \tag{4}$$

The next important step in the investigations was to determine accuracy margin Ψ on the processing of half-finished articles with VOK63 ceramics with different values of resistivity and to determine the relationship between accuracy margin and mode parameters (Maksarov et al., 2010). To determine this relationship we used the results of previous experiences, on treatment of the results of which we derive the dependences $\Psi = f(t, S, V)$ which enabled us not only to determine accuracy margin on processing (Fig. 4), but also to predict the tool work without defective products at the expense of use of optimal processing modes and rational selection of cutting ceramic plates.

Thus, the question of ceramic tool working ability control and the question of turning process quality control in whole reduce to the determination of optimal working characteristics of the tool used (Maksarov et al., 2008). Knowing of these characteristics and starting from the definite accuracy margin of material enables us to calculate the optimal parameters of processing modes and, accordingly, to predict the work without defective products. These dependencies were proved using out-of-round gage (Fig. 5) which is a measuring device for determination of roundness, i.e. the largest distance from the points of real profile of cylindrical surfaces in cross-section up to abutting (female) circle.

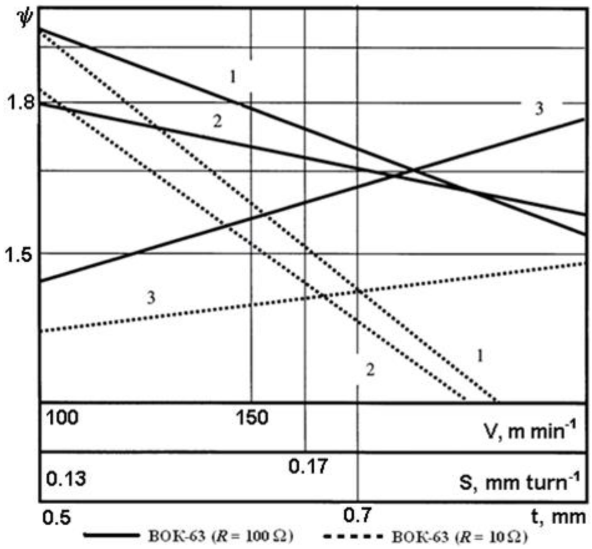

Figure 4. Graphical dependence $\Psi = f(V, S, t)$: 1 – $\Psi = f(V)$, 2 – $\Psi = f(S)$, 3 – $\Psi = f(t)$.

Figure 5. Roundness tester, Roundtest RA–120.

Results of measurements presented as a cross-section of the part were obtained using Roundness tester Roundtest RA–120 with device to extract the harmonic components of roundness (out-of-roundness profiles) and with devices to exclude the inaccuracy of initial centering of the part from the measurement results. It is determined on the analysis of images obtained that deviations of the parameter of nonroundness of the processed part on processing using tool equipped with cutting ceramics with resistivity $R = 100\ \Omega$ (Fig. 6) are less than on processing using tool with $R = 10\ \Omega$ (Fig. 7).

Thus, one can finally conclude that the half-finished product processing accuracy under the same cutting modes with VOK63 ceramics with the parameters of resistivity $R = 100\ \Omega$ is higher than on processing using ceramics with $R = 10\ \Omega$, which is proved by the analysis of investigations carried out and calculated dependencies obtained on their treatment and testing carried out using out-of-round gage (Maksarov et al., 2010).

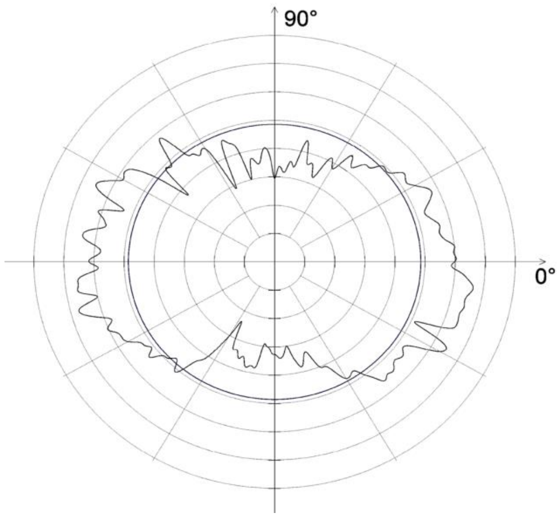

Figure 6. Out-of-roundness profile obtained on processing a part with VOK63 ceramics with $R = 100\ \Omega$.

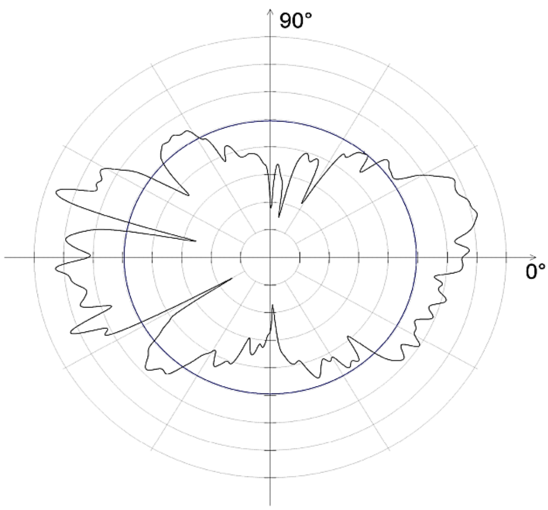

Figure 7. Out-of-roundness profile obtained on processing a part with VOK63 ceramics with $R = 10\ \Omega$.

On control of turning process quality it is necessary to ensure the stability of technological system of mechanical operation. Stability is a necessary criterion of operational integrity and the principal dynamic criterion of processing quality. Boundaries of stability region of cutting tool equipped with plates made of cutting ceramics of grade VOK63 with different values of electrical resistance depending on cutting speed and the depth of cut layer of half-finished workpiece were determined on the basis of data obtained.

Fig. 8 shows the calculated boundaries of stability region corresponding to various states of parameters of the system: R_1 for cutting ceramics of grade VOK63 with parameters of resistivity $R = 10\ \Omega$ and R_2 for cutting ceramics of grade VOK63 with $R = 100\ \Omega$.

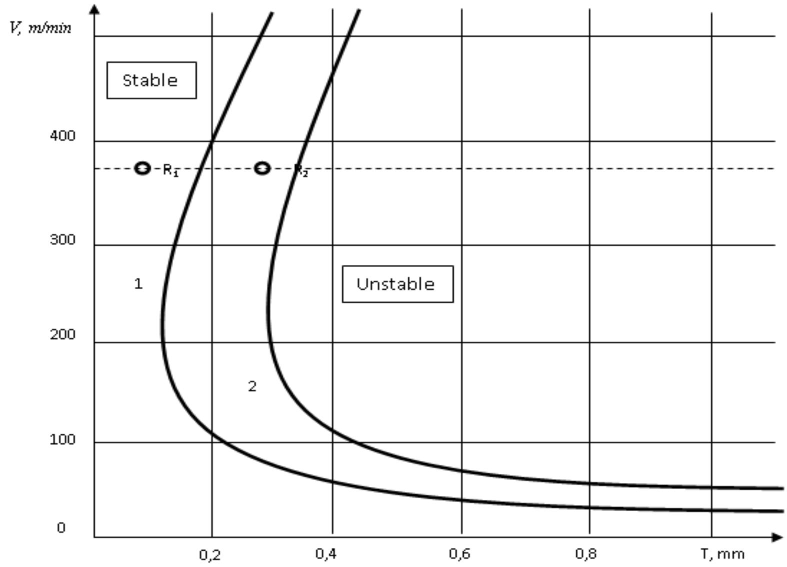

Figure 8. Boundaries of stability region of cutting tool equipped with plates made of cutting ceramics with various values of resistivity.

Significant displacement of stability region boundary found for cutting ceramic plates with low value of electric resistance is clear visible in comparison with multi-ohm ceramic plates.

It is suggested to control the working ability of cutting tool equipped with cutting ceramics starting from data obtained on the previous stages of the work, according to the following model (Fig. 9). This model is based on the dependence of working ability on the value of electrical resistance of each ceramic cutting plate and the parameters of processing quality, including *T* (tool life period), *IT* (dimensional tolerance), and *Ra* (surface roughness class).

Ceramic plates of the same grade have different values of electrical resistance *R* which depend on material porosity (*П*), cumulative line of carbide grain boundary extension (*C*), diameters of carbide grains (D_{CP}), and quantity of carbide grains (*H*). Relationship between the value of electrical resistance and structural parameters manifests itself as follows: plates with electrical resistance close to $R = 100\ \Omega$ have microstructural parameters of more quality as compared with others. They have smaller average diameter of carbide grains, the largest length of boundary line of carbide grains, greater quantity of carbide grains, and at the same time low percentage of surface porosity. Structural parameters of ceramic plates have a great influence on the working ability of cutting tool equipped with them and the processing quality in whole. The smaller the carbide grain size, larger the cumulative line of carbide grain boundary extension, lower the percentage of material porosity, and more the quantity of carbide grain in the definite bulk of material, the higher the wear-resistance of the cutting tool.

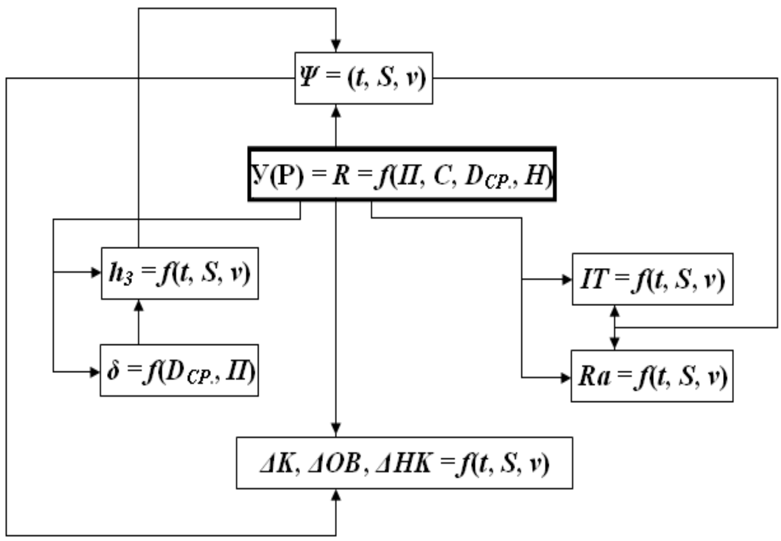

Figure 9. Working capacity control model for tool equipped with cutting ceramics.

All other things being equal such a tool will have larger life period (*T*), it can be used to process the more critical surfaces of half-finished articles with high-performance dimensional accuracy (dimensional tolerance *IT*), surface roughness class (*Ra*) and the accuracy of form and location of surfaces (cone shape *ΔK*, ovality *ΔOB*, nonroundness *ΔHK*).

Influence of the value of electrical resistance on the wear of clearance face of ceramic plate (h_3) and thus on the working ability of tool is also specified by the structural parameters of the sample. The more the value of the electrical resistance of ceramic plate is, the better microstructural parameters are. According to them, the tool performance time under the constant processing modes (*t*, *S*, *v*) rises considerably, that is the tool life period (*T*) increases, which enables us to correct essentially the processing speed increasingly and thus to increase the working ability of tool on the preservation of standard wear value.

CONCLUSIONS

Plates made of cutting ceramics have definite resistivity, ceramics structure is characterized by the following main parameters: grain quantity, average diameter of carbide grains, cumulative line of carbide grain boundary extension, and material porosity.

Ceramic plates with relatively low electrical resistance have larger grain diameter, higher percentage of porosity, low value of cumulative line of grain boundary extension, and small grain quantity; and vice versa, structural parameters have inverse values in samples with high value of electrical resistance.

Comparison test showed that the wear-resistance of ceramics of grade VOK63 with R = 100 Ω is 1.56 times high in comparison with VOK63 ceramics with R = 10 Ω on steel cutting under the same parameters of cutting modes *v*, *S*, *t*.

Dimensional wear of cutter with cutting ceramics has a significance influence on the accuracy and geometry of parts processed. Analysis of graphical dependences obtained enables us to conclude that ceramics with R = 100 Ω ensures higher accuracy and better geometric shape of the finished piece surface in comparison with ceramics with R = 10 Ω. Derivation of that dependence enables us not only to determine the accuracy margin of the part, but also to predict work without defective products.

Capability to control the working ability of cutting tool equipped with cutting ceramics at the expense of selection of parameters of cutting modes on the processing using the tools with different electroconductivity is determined.

REFERENCES

Baldony, J.K. & Buljan, S.T. 1988. Ceramics for machining. *J. Am. Ceram. Soc. Bull.* **67**(2), 381–38. (in Russian).

Maksarov, V.V., Olt, J. & Khalimonenko, A.D. 2010. *The quality management of the process of turning the instrument of the cutting ceramics.* NWTU, SPb. 172 pp. (in Russian).

Maksarov, V.V., Olt, J., Laatsit, T. & Khalimonenko, A.D. 2008a. Control of working capacity of the cutting tool, equipped with removable inserts of the cutting ceramics. SPb. Polytechnika. *Metal-working* **6**(48), 50–58 (in Russian).

Maksarov, V.V., Olt, J., Laatsit, T. & Khalimonenko, A.D. 2008b. A study of tools, equipped with removable inserts of the cutting ceramics. SPb. *Tools and technology* **30–31**, 132–136. (in Russian).

Margules, A.U. 1980. *Cutting metals cermets*. Mechanical Engineering, Moscow, 160 pp. (in Russian).

Agronomy Research **12**(1), 279–284, 2014

Cellular structures from perforated metallic tape and its application for electromagnetic shielding solutions

V. Mironovs[1], M. Lisicins[1], I. Boiko[2,*], T. Koppel[3], V. Zemchenkovs[1], V. Lapkovskis[1,*] and A. Shishkin[1]

[1]Riga Technical University, Laboratory of Powder Materials, Azenes 16/20, LV-1048, Riga, Latvia
[2]Riga Technical University, Institute of Mechanical Engineering, Ezermalas 6k, LV-1006, Riga, Latvia; *Correspondence: irina.boiko@rtu.lv
[3]Tallinn University of Technology, Chair of Working Environment and Protection, Ehitajate tee 5, EE19086, Tallinn, Estonia

Abstract. The current study is devoted to the manufacturing of cellular structures from perforated steel tapes, which are obtained as a waste during stamping of fine-sized details. Obtained cellular structures can be used for electromagnetic shielding solutions. The relevance of the current study can be characterized as in modern working and living environments there is an increasing need for electromagnetic shielding solutions. This need can be based on several points of view: 1) a need to protect workers from electromagnetic fields (EMFs) generated by working machinery, 2) a need to protect sensitive electronic devices from the surrounding EMFs, 3) minimizing health risk from EMFs in the living areas (high tension power lines, power transformers etc), 4) counter-espionage applications (preventing electronic surveillance). Besides, the recycling of metal wastes is one of the significant modern tasks of the industry.
The different methods of manufacturing of protective shield from perforated materials by profiling and welding are studied. The methodology for manufacturing of lightweight and reliable (including strength and corrosion resistance) protective shield is elaborated and offered. The main directions for using of such protective shield are the following: protection from electromagnetic fields, solar radiation and noise.
This study undertook shielding efficiency measurements in a controlled environment. Test materials were irradiated with various electromagnetic fields: 1) low frequency magnetic field, 2) low frequency electric field and 3) high frequency electromagnetic field. The results showed great differences in between different test samples. The best shielding factor was obtained with the samples where the electromagnetic absorbing material was thickest.

Key words: perforated metallic waste, cellular structures, profiling, welding, electromagnetic fields, shielding.

INTRODUCTION

World Health Organization electromagnetic fields (EMF) are recognized as one of the most widespread adverse factors of environment (Bonner, 2002). In industrial production and construction the various industrial processing equipment and devices for the scientific purposes, creating EMF of average frequencies is used (Borner et al., 2011). In environment intensive EMF of ultralow frequencies are created electrified vehicles and by railway transports (Muc, 2001). Electric and magnetic fields of industrial frequency are created also by electricity transmission air-lines, panel board to substations, including built in buildings (Coll et al., 2010). Sources of electromagnetic fields are also personal computers and various household devices. Electromagnetic fields may interact with electronic and electrical equipment, magnetic systems and also living spaces and workplaces (Koppel et al., 2013).

It should be mentioned that in a context with our research activities the range of frequencies of electromagnetic radiation of the magnetic-pulsed technological processes is of importance due to powerful EMF sources used (Table. 1).

Table 1. Range of frequencies of EMF of some technological processes and operations

Maximum energy of EMF, kJ	Frequency range, kHz	Technological processes and operations
0.5–10	0.5–3	DC welding, application of tiristors, and impulse welding.
1.0–200	5–100	Magnetic-pulse processing, electro-hydraulic cleaning, electric discharge equipment.
30–3,000	0.1–50	High-frequency processes of magnetic-pulse processing, plasma physics equipment, electric discharge systems etc.

There are several approaches for weakening of EMF influence:

- passive, active, collective, or individual shielding,
- control to exposure to EMF by reduction of time of contact with EMF sources,
- distance control between EMF source and protected objects,
- structural improvement of the equipment decreasing a level of the EMF influence.

Shielding is the most effective way of protection against EMF influence. EMF damping or shielding effectiveness (SE) depends on depth of penetration of high-frequency current in a shield wall, and can be expressed in form of simple relationship (1) or in decibels. It can be characterized the relationship of EMF strength in the absence of the shield (H_0) and in the presence of the shield (H).

$$SE = \frac{H_0}{H}. \tag{1}$$

Magnetic permeability influences on shielding effectiveness of steel sheet materials (Fujita et al., 2005). High magnetic permeability of shield material along with high frequency of a shielded field decrease depth of penetration and therefore minimising a thickness of shielding screens. Moreover, the shielding screens not only weakens, but also distort and dissipate magnetic field influence for the protected area. Schelkunoff's theory (Schelkunoff, 1943) characterize the shielding effectiveness as a combination of following effects (2):

$$SE = A + R + B \tag{2}$$

where: A is a shield material's absorption; R is a reflection loss, and B is a component of multiple reflection loss inside the shield (Morari et al., 2011).

The shielding effectiveness determined by varies for electric and magnetic fields and depends on coordinates of a point of measurement. This circumstance complicates its quantitative assessment. It is possible to shield both a source of radiations, and a workplace of the operator.

There are plenty of EMF shielding materials for commercial applications (Chomerics Inc., 2013). Special attention is paid to metallized fabrics, protective paints or films or other special materials (Dixon & Masi, 1998) which can be used as shielding materials. The Laboratory of Powder Materials of Riga Technical University is carrying out a research on possible application of sputtered iron powder materials for EMF shielding design is suggested (Mironovs & Polakovs, 2011).

This paper covers an inexpensive solution for electromagnetic processing equipment shielding against EMF. For protection against pulsed electromagnetic fields (PMF) shielding screens fabricated from perforated sheet metal materials, grids, or ferromagnetic plates located outside of the cylindrical coil or the casing closing a working zone can be applied.

MATERIALS AND METHODS

Laboratory of powder materials of Riga Technical University is carrying out research activities on development of cellular structures made of punched metal tapes (Fig. 1) (Mironovs et al., 2012; Mironovs et al., 2013).

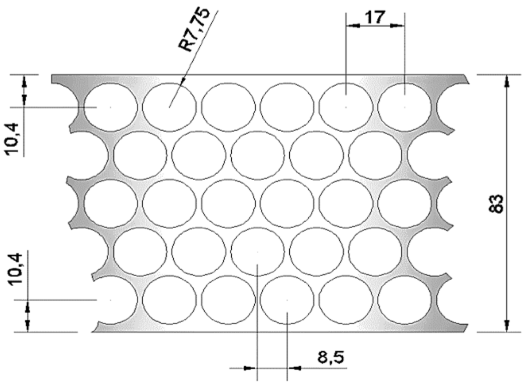

Figure 1. Punched steel tape (sheet thickness 1.2 mm) as a source material for shielding screens.

EMF shielding capability of screens made of the steel punched tape by welding (Fig. 2a) and an interlacing (Fig. 2b) was estimated.

Investigation presented in current paper was conducted with use of a permanent magnet (Fig. 3). Evaluation of magnetif field strength was carried out by means of laboratory gauss-meter FH-55.

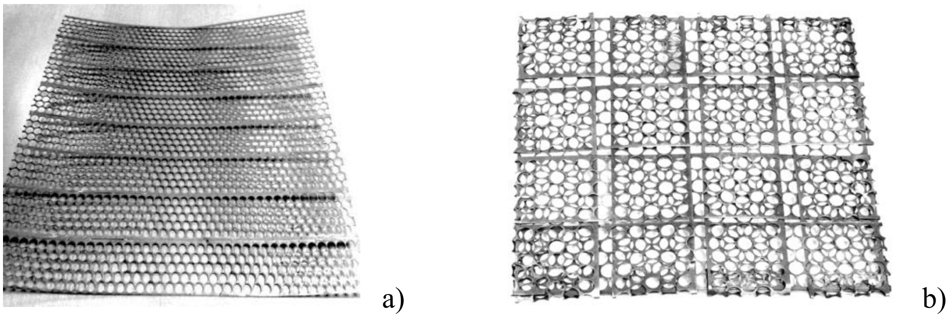

Figure 2. Shilding screens of 500 x 500 mm made of punched steel tape (Fig. 1.) thickness 1.2 mm. a) welded, b) interlaced.

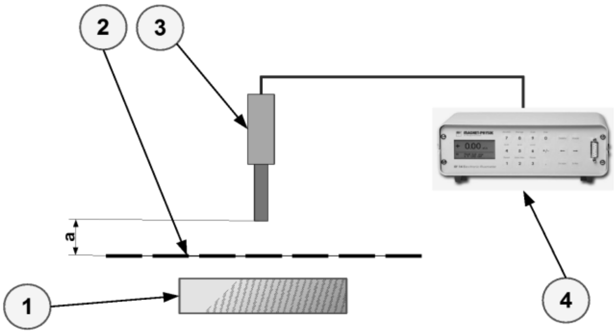

Figuer 3. Installation schematics for determination of intensity of EMF of permanent magnet, where: 1 – permanent magnet Fe-Nd-B, 2 – perforated steel shield, 3 – hall probe, 4 – Gauss-/teslameter FH-55).

For evaluating shielding effectiveness for the EMF the electromagnetic coil installation has been used (Figs 4, 5).

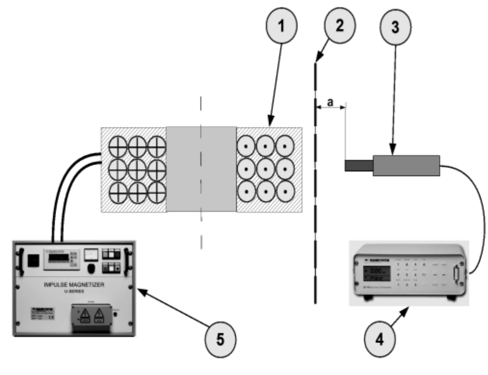

Figure 4. Measurement of EMF on a lateral coil surface (transversally to magnetic flux).

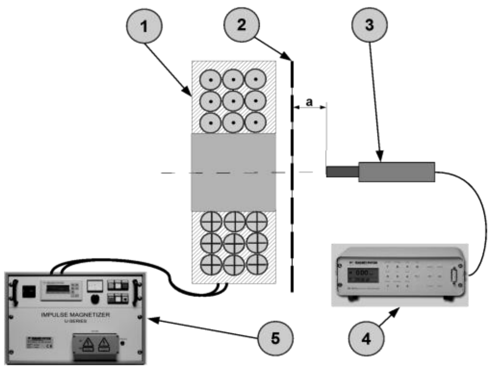

Figure 5. Measurement of EMF on coil axially to magnetic flux.

where: 1 – coil; 2 – perforated steel shield; 3 – hall probe; 4 – Gauss-/teslameter FH-55; 5 – Impulse currents source (2,800 J, Impulse currents up to 60,000 A).

RESULTS AND DISCUSSION

Change of magnetic field strength of a permanent magnet depending on distance to the measuring instrument probe without screen and with application of two types of screens (Fig. 7) was investigated. The maximum field intensity on the magnet's surface was measured (2.4 MA m^{-1}). Relationship between distance *a* and magnetic field strength of a permanent magnet (according to the scheme in Fig. 3) is shown in Fig. 6.

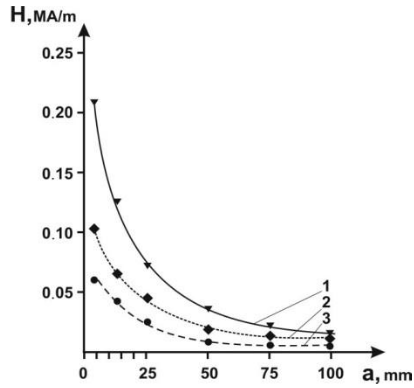

Figure 6. Damping curve of magnetic field strength with distance *a:* 1 – without shielding screen; 2 – with single layer welded shield; 3 – with dual layer interlaced shield.

Results of measurement of pulse EMF at various arrangement of the coil and mesh screens from the shielding screens made of steel punched tapes is presented in Fig. 7.

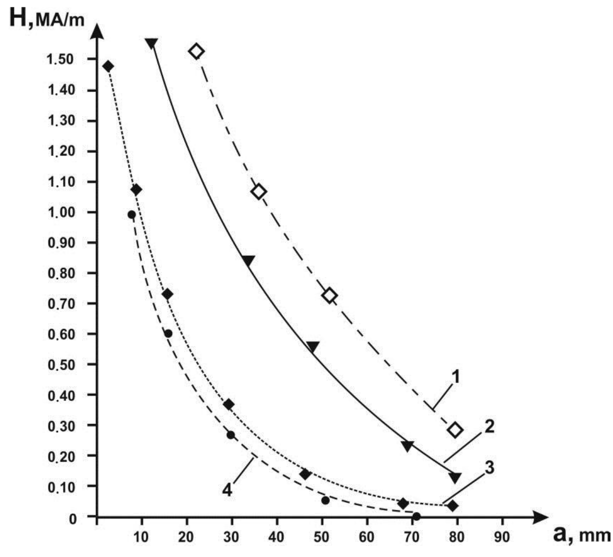

Figure 7. Damping of pulsed EMF in axial and transversal position of the screen shielding: 1 –axially to magnetic flux without shielding screen; 2 – axially to magnetic flux shielding screen; 3 – transversally to magnetic flux without shielding screen, 4 – transversally to magnetic flux shielding screen.

CONCLUSIONS

1) An experimental analysis of shielding effectiveness of shielding screens made of perforated (punched) steel tapes is done. It was found that perforated shielding screens may decrease magnetic field strength in both cases: a static magnetic field of the permanent magnet and in case of electromagnetic field generated by coil.

2) The shielding effectiveness of presented shielding materials depends on variety of parameters and have to be evaluated for each specific application e.g. interlaced shielding screen has demonstrated a better performance for electromagnetic field damping.

ACKNOWLEDGEMENTS. This work has been supported by the Latvian Council of Science within the Project Nr. 110/2012 'Titanium compound wear-resistant nano-coatings in mechanical engineering'.
We would like to thank students M. Lisicins and K. Zitans (Riga Technical University) for active participation.

REFERENCES

Bonner, P. 2002. *Establishing a dialogue on risks from electromagnetic fields,* 66 pp.

Borner, F., Bruggermeyer, H., Eggert, S., Fisher, M., Heinrich, H., Hentschel, K. & Neuschulz, H. 2011. *Elektromagnetische Felder am Arbeitsplatz / Electromagnetic fields at workplaces: A new scientific approach to occupational health and safety*, 46 pp.

Chomerics Inc. 2013. *EMI Shielding Engineering Handbook*, 225 pp.

Coll, J., Ängskog, P., Karlsson, C., Chilo, J. & Stenumgaard, P. 2010. Simulation and measurement of electromagnetic radiation absorption in a finished-product warehouse. *Electromagnetic …*, pp.881–884.

Dixon, D. & Masi, J. 1998. Thin coatings can provide significant shielding against low frequency EMF/magnetic fields. *Electromagnetic Compatibility, 1998. 1998 …*, 2, pp. 1035–1040.

Fujita, K., Inoue, T. & Emoto, H. 2005. Improvement of permeability and magnetic shielding effect of pure iron magnetic shield materials. JFE Tech Rep **6**, 24–28.

Koppel, T., Tasa, T. & Tint, P. 2013. Electromagnetic fields in contemporary office workplaces. *Agronomy Research* **11**(2), pp.421–434.

Mironovs, V., Lisicins, M., Boiko, I & Zemchenkovs, V. 2013. Manufacturing of cellular structures from perforated metallic materials. *Agronomy Research* **11**(1), 139–146.

Mironovs, V., Lisicins, M. & Lapkovskis, V. 2012. Formation of Cellular Structures Made from Perforated Metal Tape. In *Cellular Materials – CELLMAT 2012*.

Mironovs, V. & Polakovs, A. 2011. The screen to protect against electromagnetic radiation. LR patent LV 14320 B.

Morari, C., Balan, I. & Pintea, J. 2011. Electrical conductivity and electromagnetic shielding effectiveness of silicone rubber filled with ferrite and graphite powders. *Progress In …*, 21, pp. 93–104.

Muc, A., 2001. *Electromagnetic fields associated with transportation systems*, Available at: http://www.rhsc.ca/TransEMF.pdf [Accessed January 2, 2014].

Schelkunoff, S. 1943. *Electromagnetic waves*, 530 pp.

Agronomy Research **12**(1), 285–290, 2014

The logistics aspects influencing the resultant strength of adhesives at practical application

M. Müller* and P. Valášek

Department of Material Science and Manufacturing Technology, Faculty of Engineering, Czech University of Life Science, Kamýcká 129, 16521 Prague, Czech Republic; *Correspondence: muller@tf.czu.cz

Abstract. Practical application of construction adhesives is required under various climatic conditions and in various environments. The temperature of an environment alone is regarded a limiting factor from the logistics point of view influencing the effectiveness of subsequent application, namely in winter months. The aim of the experimental part is to define the influence of temperature as an essential logistics factor subsequently influencing the resultant strength of the adhesive bond at its application. Further, redress of adhesives properties after extreme temperatures of storing, transit, etc. was investigated. Higher temperatures reached during the logistics flows negatively influence the adhesive bond strength. The temperature also influences change in the failure area.

Key words: adhesive bond creation, bonding technology, climatic conditions, temperature.

INTRODUCTION

Practical application of construction adhesives is required under various climatic conditions and in various environments (Müller 2013; Müller et al., 2013). Each environment has its specific properties, which basically influence the entire strength and reliability of an adhesive bond (Doyle & Pethrick, 2009; Liljedahl at al., 2009; Müller 2013).

Successful use of adhesives in practice is limited by two basic groups of factors. The first group is adhesive properties and the conditions of an adhesive bond creation. Adhesive properties can be influenced, e.g. by unsuitable storing. The second group is the factors exerted by the environment, namely by changes in temperature, humidity, prospective direct contacts with degradation agents. Although both abovementioned groups of influences affect the mechanical properties of adhesive bonds (above all their strength) together, it is important to separately review each particular factor in a form of laboratory experiments, as well as with respect to a particular type of adhesive (Josbi et al., 1997; Müller, 2009; Müller & Herák, 2013; Müller et al., 2013).

Under certain extreme conditions, it is better to use other bonding technologies, e.g. soldering, welding, riveting, etc. In the cases where the bonding method is prescribed, e.g. in a quality manual, it is necessary to follow it.

In various climatic zones, extreme temperatures fluctuations often occur outside in summer and winter months. However, in practice, adhesives can meet much higher or, in contrary, lower temperatures than is recommended by the producer from the logistics flows point of view (sun radiation, sun radiation through glass, transit in a car, storing in an unheated warehouse, etc.). The temperature of the environment alone is regarded as a limiting factor from the logistics point of view influencing the effectiveness of subsequent application, namely in winter months. The storage and working temperature of most adhesives is between 10 and 20°C.

Messler (2004) ascertained the causes of adhesive bond failure by analyzing which unsuitable storage conditions also belong here. It is necessary to consider the climatic conditions in the world at application of adhesives owing to the globalized society (Müller, 2009; Müller, 2013). A considerable fluctuation of the environment temperature is related to it, which can be regarded as extreme for application of adhesives.

The aim of the experimental part is to define the temperature influence as the essential logistics factor influencing subsequently resultant strength of the adhesive bond at its application. Two-component construction adhesives with working temperatures around 20°C were used for the experiments. The interval of tested temperatures ranged from -20 to 100°C. The possibility of applying adhesives the packaging of which was exposed to temperatures from -20 to 100°C was investigated. Further, restoring of the properties of adhesives (the adhesive bond strength) after extreme temperatures of the storage, transit, etc. was investigated. Adhesive bonds were created 24 hours after exposing to specific temperatures. Statistical methods were used for making conclusions.

MATERIALS AND METHODS

The basis of the adhesive bonds laboratory testing was determination of the tensile lap-shear strength of rigid-to-rigid bonded assemblies according to the standard CSN EN 1465. Laboratory tests were performed using standardized test specimens made from constructional plain carbon steel S235J0 according to the standard CSN EN 1465 (dimensions $100 \pm 0.25 \times 25 \pm 0.25 \times 1.6 \pm 0.1$ mm and lapped length of 12.5 ± 0.25 mm).

Ahead of bonding, the surfaces of the bonded specimens were blasted using the Al_2O_3 of F80 grain size (Müller 2011). Using the profilograph Surftest 301, the following values were determined: Ra 1.29 ± 0.07 μm, Rz 6.39 ± 0.33 μm. The surface was chemically cleaned by Acethone P6401 before own adhesive bonding process.

The following list presents identification of the tested adhesives (two-component epoxy adhesives) which are used in text for better, clear arrangement: Bison epoxy metal (BME), Lepox 1200 and hardened P11 (L1200P11), Loctite Nordbak 7256 (LN7256), 3 – TON Epoxy adhesive 30 min (A3T30), 3 – TON Epoxy adhesive 4 min (A3T4). The adhesives are recommended to be applied at the ´room´ temperature, 22 ± 2°C.

Two series on tests were performed. The environment which the adhesives in packaging were exposed to was common for both series. The adhesives (the resin and the hardener) in the packaging were exposed to the surrounding temperatures -20, 22 (the laboratory-comparison standard), 60, and 100°C for the duration of 24 h.

Particular variants of the test are described in the results as xx/yy (e.g. -20/22). ´xx´ means the temperature of the environment which the adhesive was exposed to for 24 hours. ´yy´ (-20, 60, and 100) means the temperature of the orientation of putting the adhesive. The adhesive bonding procedure for the first series was as follows: The adhesive was mixed and applied on prepared bonded surface after removal of the adhesive from the packaging. Own adhesive bonding process was performed at the laboratory temperature (22 ± 2°C). The temperatures of the packaging of all adhesive were measured by means of a contactless infra-thermometer Testo 845 after removing the adhesive from the given environment. Further, temperature was measured during the test that means the temperature of applying the adhesive.

The following adhesive bonding procedure was used for the second series: The adhesive in the packing was removed from an air-conditioner chamber and was left at the laboratory temperature for tempering for 24 h. The subsequent procedure was the same as for the first series. The created adhesive bonds were left to harden for 48 hours under laboratory conditions (22.7 ± 0.5°C). Then, destructive testing on the universal testing machine LabTest 5.50ST followed.

RESULTS AND DISCUSSION

Fig. 1 shows the results of the adhesive bond strength created by means of ANOVA by the lowest squares method. The failure area changed owing to the storage temperature. This change occurred only for some adhesives. Storage temperatures ranging below the freezing point showed up negatively with respect to the possibility of working with the adhesive. Handling the adhesives, i.e. mixing parts A and B exposed to the temperature – 20°C, was possible after 250 ± 120 seconds.

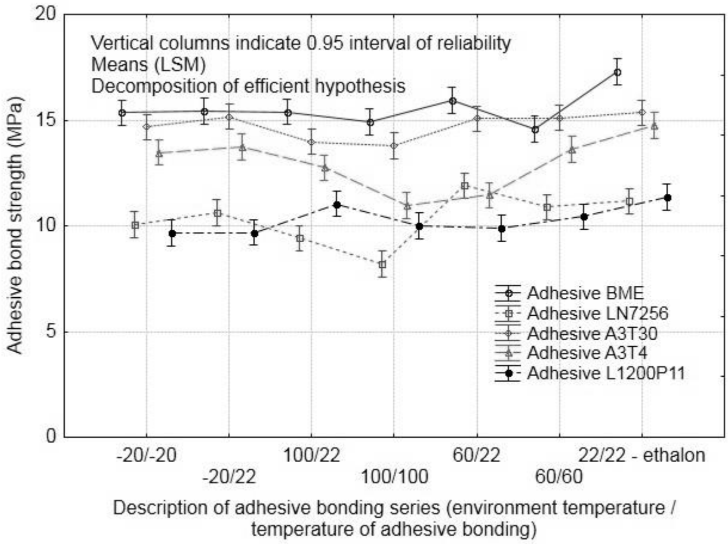

Figure 1. Influence of temperature on adhesive bond strength.

Comparison of series 1 and 2 was performed due to the influence of temperature. T-test was used for the comparison. The state where there is no statistically significant difference between the compared sets from the mean values point of view ($p > 0.05$)

was described as the zero hypothesis H_0. Table 1 shows the conclusions of the performed statistical evaluation.

The statistical evaluation (Table 1) proved that the zero hypothesis was confirmed with all adhesives when comparing the data sets between temperatures -20/-20 and -20/22 ($p > 0.28$). Agreement among particular temperatures in all three cases was only proved with the adhesive A3T30 ($p > 0.11$). Agreement in all cases ($p > 0.09$) was proved among the sets of temperatures data 100/100 and 100/22, except for the adhesives A3T4 ($p = 0.00$) and LN7256 ($p = 0.04$). Arguably, different values were measured at temperatures 100/100 and 22/22 with all tested adhesives ($p < 0.01$). The zero hypothesis was confirmed only with the adhesive L1200P11 ($p > 0.55$) between temperatures 100/22 and 22/22. The dependence always follows the properties of particular adhesives among the sets of temperature data of 60/60, 60/22 and 22/22. No agreement was proved among the compared data sets with the adhesives BME and A3T4. On the contrary, the zero hypothesis was proved in all cases of the comparison with the adhesive A3T30.

Table 1. Statistical comparison of the measured data – T-test; H_0: $p > 0.05$

Adhesive	Comparison	p	Comparison	p	Comparison	p
BME	-20/-20 : -20/22	0.77	100/100 : 100/22	0.57	60/60 : 60/22	0.00
	-20/-20 : 22/22	0.00	100/100 : 22/22	0.01	60/60 : 22/22	0.00
	-20/22 : 22/22	0.00	100/22 : 22/22	0.00	60/22 : 22/22	0.01
LN7256	-20/-20 : -20/22	0.37	100/100 : 100/22	0.04	60/60 : 60/22	0.00
	-20/-20 : 22/22	0.05	100/100 : 22/22	0.00	60/60 : 22/22	0.44
	-20/22 : 22/22	0.40	100/22 : 22/22	0.00	60/22 : 22/22	0.10
A3T30	-20/-20 : -20/22	0.28	100/100 : 100/22	0.55	60/60 : 60/22	0.86
	-20/-20 : 22/22	0.11	100/100 : 22/22	0.00	60/60 : 22/22	0.46
	-20/22 : 22/22	0.69	100/22 : 22/22	0.00	60/22 : 22/22	0.41
A3T4	-20/-20 : -20/22	0.54	100/100 : 100/22	0.00	60/60 : 60/22	0.00
	-20/-20 : 22/22	0.00	100/100 : 22/22	0.00	60/60 : 22/22	0.00
	-20/22 : 22/22	0.00	100/22 : 22/22	0.00	60/22 : 22/22	0.00
L1200P11	-20/-20 : -20/22	0.98	100/100 : 100/22	0.09	60/60 : 60/22	0.21
	-20/-20 : 22/22	0.00	100/100 : 22/22	0.00	60/60 : 22/22	0.00
	-20/22 : 22/22	0.00	100/22 : 22/22	0.55	60/22 : 22/22	0.01

It is optimal to harden the adhesive BME at laboratory temperature. It can be stated that the bonds created at 60/60, 60/22, and -20/22 with the adhesive LN7256 reach statistically comparable values of adhesive bond strength. Higher strength value was reached in the series 60/22. The adhesive A3T30 did not show statistically significant differences in particular test series, except for the series 100/100 and 100/22. The adhesive A3T4 showed statistically significant differences in particular test series, i.e. the adhesive showed lower values of the adhesive bond strength. The adhesive L1200P11 showed values comparable with the laboratory ones in testing at 100/22.

The adhesive A3T30 can be recommended in cases where constant temperature (the laboratory one, 22°C) is not guaranteed due to practical application in the logistics area, i.e. transit, storage, etc. The adhesive LN7256 is suitable for use till the maximum temperature of 60°C. Negative storage values not exceeding the tested – 20°C do not decrease the adhesive bond strength.

Significant differences are visible (Fig. 2) from evaluation of the results of the temperature of put adhesive (series 1). The graph in Fig. 2 was created by means of ANOVA by the lowest square method. The temperature of put adhesive in series 2 did not significantly differ from the laboratory one. The temperature change among particular types of adhesives occurred due to a chemical reaction at mixing the resin and the hardener.

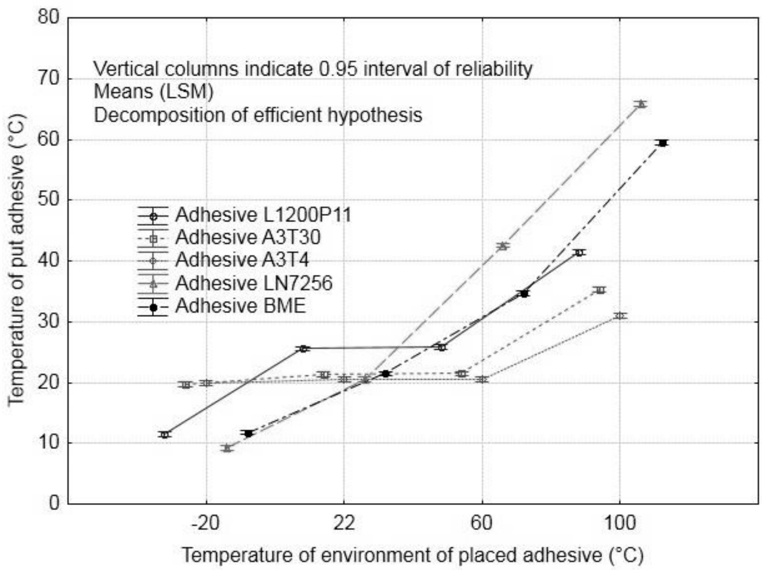

Figure 2. The influence of the environmental temperature of placed adhesive on the total temperature of put adhesive (during the hardening process).

Experimental results confirm the statement of authors about the negative and harmful effects which the environment can have on the adhesive bond (Crocombe 1997; Court et al., 2001; Messler, 2004; Frigione et al., 2006).

CONCLUSIONS

The results of the performed experiments proved the essential influence of storage management (logistic) in the area of adhesive bonding technology. The results suggest a necessity to keep the technologic discipline in the area of the storage temperature guaranteed by a producer.

The adhesive A3T30 can be recommended in cases where constant temperature (the laboratory one, 22°C) is not guaranteed due to practical application in the logistics area, i.e. transit, storage, etc. The adhesive LN7256 is suitable for using till the maximum temperature of 60°C. Negative storage values not exceeding the tested – 20°C do not decrease the utility properties.

The following points were ascertained by comparing the ascertained values with the comparison standard 22/22:

- There was a considerable fall in the adhesive bond strength values with all adhesives in series 1. This was at the temperatures – 20°C and 100°C (variants -20/- 20 and 100/100). The average fall of the adhesive bond strength was 9.78 % for the variant – 20/- 20 and 17.66% for the variant 100/100.
- A lower fall of the strength occurred at the temperatures – 20 and 100°C in series 2, i.e. at the adhesives which were left for tempering at laboratory temperature for 24 h after exposal to increased/decreased temperature. The average increase of the adhesive bond strength in series 2 compared to series 1 was as follows: 2.5 % for the variant – 20/20 and 7.5% for the variant 100/22.
- At the temperature of 60°C, the adhesive bond strength fell as well as increased. The difference between series 1 and 2 was also not unambiguous.

ACKNOWLEDGEMENT. Supported by the Internal grant agency of the Faculty of Engineering, the Czech University of Life Sciences in Prague.

REFERENCES

Court, R.S., Sutcliffe, M.P.F. & Tavakoli, S.M. 2001. Ageing of adhesively bonded joints – fracture and failure analysis using video imaging techniques. *International Journal of Adhesion & Adhesive* **21**(6), 455–463.

Crocombe, A.D. 1997. Durability modelling concepts and tools for the cohesive environmental degradation of bonded structures. *International Journal of Adhesion & Adhesives* **17**(3), 229–238.

Doyle, G. & Pethrick, R.A. 2009. Environmental effects on the ageing of epoxy adhesive joints. *International Journal of Adhesion & Adhesives* **29**(1), 77–90.

Frigione, M., Aiello, M.A. & Naddeo, C. 2006. Water effects on the bond strength of concrete/concrete adhesive joints. *Construction and Building Materials* **20**(10), 957–970.

Josbi, S.B. Gray, T.F., Banks, W.M., Hayward, D., Gilmore, R., Yates, L.W. & Pethrick, R.A. 1997. Environmental ageing of adhesively-bonded joints II. Mechanical studies. *Journal of adhesion* **62**(1–4), 317–335.

Liljedahl, C.D.M., Crocombe, A.D., Wahab, M.A & Ashcroft, I.A. 2007. Modelling the environmental degradation of adhesively bonded aluminium and composite joints using a CZM approach. *International Journal of Adhesion & Adhesives* **27**(6), 505–518.

Messler, R. W. 2004. *Joining of materials and structures from pragmatic process to enabling technology*. Burlington: Elsevier, 790 pp.

Müller, M., Chotěborský, R. & Hrabě, P. 2009. Degradation processes influencing bonded joints. *Research in Agricultural Engineering* **55**(1), 29–34.

Müller, M. 2011. Influence of surface integrity on bonding process. *Research in Agricultural Engineering* **57**(4), 153–162.

Müller, M. & Valášek, P. 2013. Degradation limits of bonding technology depending on destinations Europe, Indonesia. *Tehnicki Vjesnik-Technical Gazette* **20**(4), 571–575.

Müller, M. 2013. Research of liquid contaminants influence on adhesive bond strength applied in agricultural machine construction. *Agronomy Research*. **11**(1), 147–154.

Müller, M. & Herák, D. 2013. Application possibilities of adhesive bonds – Europe, Indonesia. Scientia Agriculturae Bohemica. **44**(3), 167–171.

Agronomy Research **12**(1), 291–298, 2014

EPDM rubber material utilization in epoxy composite systems

P. Valášek* and M. Müller

[1]Department of Material Science and Manufacturing Technology, Faculty of Engineering, Czech University of Life Sciences Prague, Kamýcká 129, Prague; *Correspondence: valasekp@tf.czu.cz

Abstract. Observing of possibilities for secondary raw materials utilization should rank among the key interests of the society. Nowadays, there are a lot of modern workplaces which are devoted to the possibilities of collecting, processing and using rubber materials. EPDM waste rubber in the form of particles is one of the many products of these workplaces. One of the possibilities for recycling this waste particles material is their interaction with another polymeric material. A reactoplastic which is filled with these particles comes into consideration. This way of utilization of the material is inexpensive and simple. The paper focuses on chosen mechanical qualities of the Epoxy/EPDM waste rubber composite. The waste rubber was gained as one of the outputs of a recycling line of the firm Gumoeko, Ltd., the reactoplastic was represented by a two-component epoxy resin. Distraction of rubber particles in the epoxy matrix was achieved by mechanical mixing without using the technology of vacuum. In the paper, the porosity, tensile strength and shear strength of the composites with various concentrations of EPDM are described. The resulting composite systems may find their application in the field of agriculture - especially during joining and sealing materials of larger units where high quality connections are not required.

Key words: agriculture, mechanical properties, reactoplastic, waste.

INTRODUCTION

EPDM rubber (ethylene propylene diene monomer (M-class) rubber) is an example of a synthetic elastomer. EPDM rubber finds application in a number of industrial branches owing to its properties (high resistance to weather influences, etc.), it is used for production of washers and tubes which are applied in the area of the automotive industry. It can be also found in a number of various machines which are applied in agriculture (tractors, hardvestors, etc.). Waste EPDM rubber can be processed on modern lines whose outcomes are EPDM particles or powder. One of the possibilities for using waste inorganic particles is their inclusion into plastics – this is material utilization. Waste material recycling in the form of plastics filler is common. Materials with hard inorganic particles (SiC, Corundum) which are abrasive wear resistant can be mentioned in the agriculture (Valasek & Muller, 2012; Muller & Valasek, 2013b). Interaction of waste fillers with epoxy resins can lead to an increase in materials suitable for adhesive bonding as well as cementing (Valasek & Muller, 2013a). For example, Ku et al. (2010) used glass powder (5–12.5 wt %) with the dimension of 2–32 μm for increasing the values of a tensile strength. It is necessary to realize that adhesive bonding is a method of joining which is used in agriculture – see the cooperation between the companies Henkel and New Holland (Muller and Valasek, 2013a). Only the possibility of filling epoxy resins with waste particles and the possible application of these materials in agriculture are the topics of this paper.

Many authors have dealt with the possibilities of filling polymeric materials with waste rubber. For example, Subramaniyan et al. (2012) used waste rubber particles for improving the mechanical properties of a polyurethane foam filled with Kenaf fibres. Using waste rubber together with fibers is also described by Cerbu and Curtu (2011) who increased the impact strength of a composite on a basis of an epoxy resin, glass fibers, and waste rubber particles. Valasek et al. (2013) describe the comparable values of the shear strength of the bonds created by an unfilled epoxy resin and by a resin filled with waste rubber particles of the size of 27.6 ± 14.2 μm. The properties of epoxy resin can be changed by adding of appropriate types of fillers. Dadfar and Ghadami (2013) used carboxyl-terminated butadiene acrylonitrile for optimizing the failure properties of an epoxy resin reinforced by glass fibres. Xu et al. (2013) present an example of the modification of epoxy resins by means of a liquid rubber (CTBN liquid rubber).

The aim of the performed experiment is to describe the influence of EPDM waste rubber on a change in the mechanical properties of two-component epoxy resins which are commonly used for joining materials in agriculture and are easily fillable with inorganic fillers. The paper defines the change in the tensile strength and lap-shear tensile strength and describes the porosity and hardness of the achieved materials. The performed experiment defines potential application areas of the achieved material, not only in the area of agricultural machines – it defines the cohesive strength of the material and its adhesive strength in the boundary of a steel adherent and an adhesive.

MATERIALS AND METHODS

Preparation of test samples

Rubber EPDM granulate was gained from the company Gumoeko, Ltd. The granulate is produced by mechanical shattering of the waste from the production of washers and tubes for the automotive industry, above all. The mixture of the granulate is disposed of impurities during processing. The producer states a possibility for using the granulate for sports surfaces, isolations and paddings. This type of granulate is not dangerous waste. A particular size of particles was measured by using a stereoscopic microscope.

The rubber EPDM granulate was added to epoxy resins Eco Epoxy 1200/324 (EE) and Glue Epox rapid (GR). They are two-component resins which are suitable for filling with inorganic types of fillers. The filler concentration in the epoxy resins was expressed by volume percentages: 5–20 vol.%. Dispersion of the rubber particles was achieved by mechanical mixing. The test samples were prepared by casting (into forms made from a silicone rubber) according to relevant standards and were hardened according to the technological requirements of the resins producer.

Laboratory tests

The test samples determined for specification of the cohesive strength by means of the tensile strength were prepared according to the requirements of the standard CSN EN ISO 3167. The test samples were tested on a universal testing machine. The speed of the cross beam motion was 6 mm min^{-1}. The setting of the tensile characteristics was performed in accordance with the standard CSN EN ISO 527 (see Fig. 1).

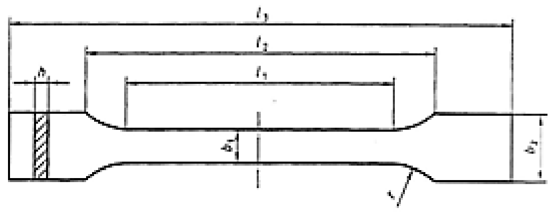

Figure 1. Multipurpose-made test sample – Tensile strength (CSN EN ISO 3167, 2004).

For the lap-shear strength description in the boundary of the adherent and the filled system, overlapped assemblies were made (CSN EN 1465, see Fig. 2). Surface preparation is important (Novak, 2011). The surface of 1.5 mm thick steel sheets (S235J0) onto which the composite system was applied was at first blasted using the synthetic corundum of the fraction F80 under the angle of 90°. In this way, the average surface roughness of Ra = 1.39 ± 0.36 μm, Rz = 9.9 ± 0.31 μm was reached. Then the surface was cleaned and degreased using perchlorethylene and prepared for the composite mixture application.

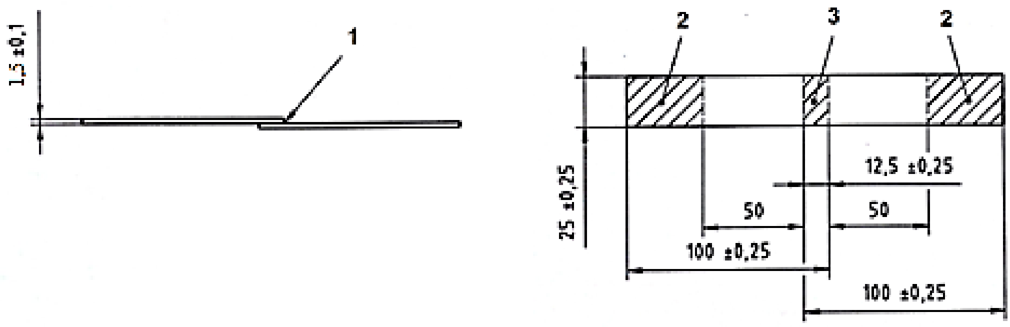

Figure 2. Test sample – Lap-shear tensile strength (CSN EN 1465, 1997).

The evaluation of the failure of the test sample surface and adhesive layers was performed using a stereoscopic microscope. A statistical evaluation of the results was performed by means of the programme Statistica – one-factor ANOVA, reliability level $\alpha = 0.05$. For the statistical comparison, the T-test was used when the zero hypothesis H_0 ($p > 0.05$) states an agreement of the statistical sets of data.

RESULTS DISCUSSION

The density of the EPDM rubber waste particles corresponded to 1.12 g cm^{-3}, the density of Eco Epoxy 1200/324 was 1.15 g cm^{-3} and the density of Glue Epox Rapid 1.15 g cm^{-3}. The mutual interaction between the resin and the particles is influenced by their morphology. Only the interphase interaction is the key in filled materials. The

EPDM waste particles were subjected on the stereoscopic microscope. The average value of particle size was 1,092 ± 403 µm. Fig. 3 presents the distribution of particle sizes and their morphology.

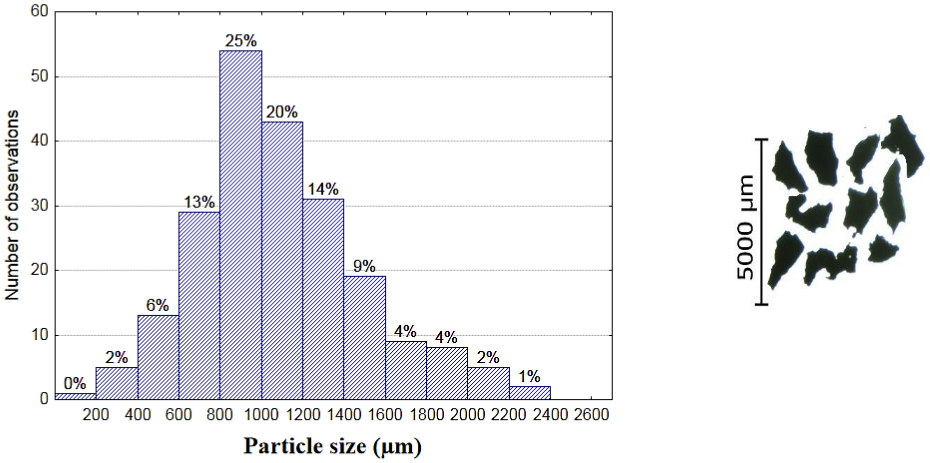

Figure 3. Histogram – size of the EPDM waste rubber particles and their morphology.

The strength of the filled epoxy resins in the boundary of the steel adherent and the adhesive was found by the methodology of testing the adhesive bonds shear-strength (CSN EN 1465). The failure always occurred in the adhesive bond, it was the adhesive failure in all cases – so the weak place of the bond was situated directly in the boundary of the steel adherent and the filled epoxy resin. All filled systems showed considerably lower shear strength compared to unfilled epoxy resin (see Fig. 4).

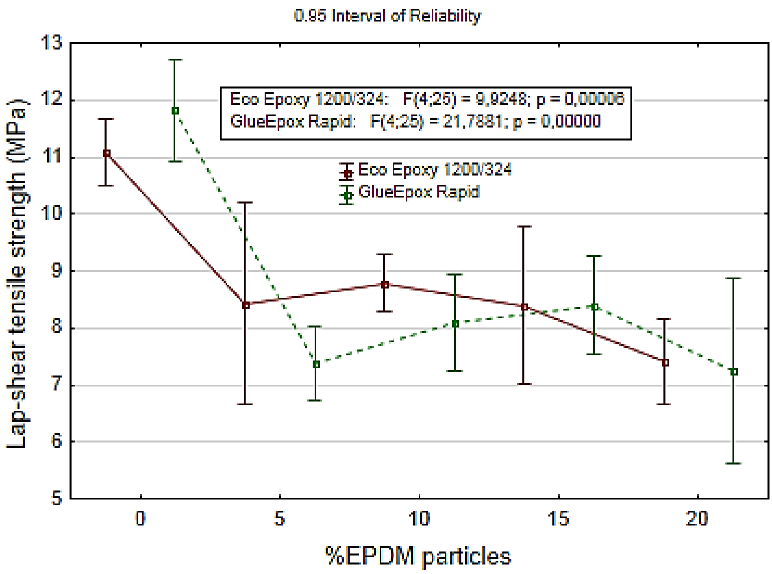

Figure 4. Lap-shear tensile strength.

The statistical tests of the data were tested by the F-test, where an agreement of dispersion variances was confirmed in all cases. Consequently, the T-test was used for comparison of the data sets for particular types of filled epoxy resins (see Table 1). The zero hypothesis H_0 describes confirmation of the hypothesis – there is no statistically significant difference among the compared sets of data.

Table 1. T-test – Lap-shear tensile strength

	T-test	Eco Epoxy 1200/324				
	H_0:(p > 0.05)	0	5	10	15	20
GlueEpox	0		0.00	0.00	0.00	0.00
	5	0.00		0.62	0.97	0.20
	10	0.00	0.12		0.50	0.00
	15	0.00	0.03	0.53		0.14
	20	0.00	0.85	0.26	0.13	

The cohesive strength of filled epoxy resins was evaluated by the means of the tensile strength (CSN EN ISO 3167, see Fig. 5). These values were considerably lower compared to unfilled resin.

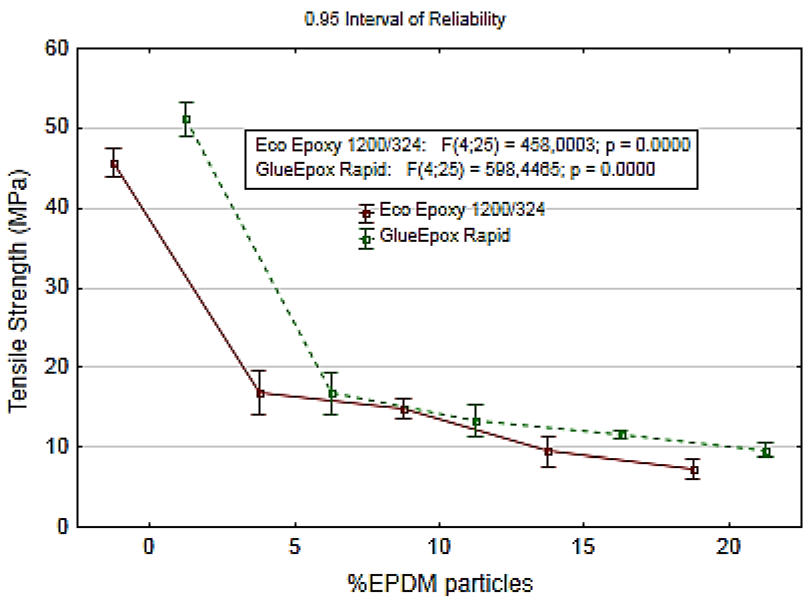

Figure 5. Tensile strength.

The statistical sets of data were compared again (see Table 2). The F-test did not confirm the agreement of dispersion variances in some cases, in this case, a two-selective T-test with dispersion variances inequality was used.

Table 2. T-test –Tensile strength

T-test		Eco Epoxy 1200/324				
H_0:(p > 0.05)		0	5	10	15	20
GlueEpox	0		0.00	0.00	0.00	0.00
	5	0.00		0.12	0.00	0.00
	10	0.00	0.02		0.00	0.00
	15	0.00	0.00	0.06		0.03
	20	0.00	0.00	0.00	0.00	

Fig. 6 shows a typical failure area of filled epoxy resins. The epoxy matrix is brittle – the failure starts directly in the matrix. EPDM rubber particles are tenacious and they are capable of considerable elastic deformation (as is usual for elastomers). At the moment of maximum carrying capacity of the test sample, it comes to the failure of the matrix at first and consequently to the failure of elastic particles. However, it is obvious from the experiment that increasing the concentration of EPDM rubber particles considerably decreases the tensile strength of the material – it decreases the cohesive strength of the system.

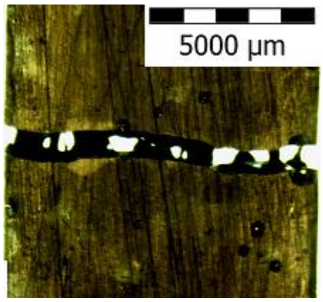

Figure 6. Failure of a brittle matrix with filler (Glue Epox with 20% of EPDM rubber particles).

The inclusion of EPDM rubber particles led to the rapid fall of the lap-shear tensile strength and the tensile strength of both reviewed epoxy resins. The lap-shear tensile strength of the Eco Epoxy resin decreased from the value 11.08 ± 0.47 MPa to the value 7.41 ± 0.64 MPa (at Glue Epox from 11.82 ± 0.72 MPa to 7.24 ± 1.41 MPa). High standard deviations are worth noticing too – the variation coefficient of 19.5%. The sheer fall of the tensile strength was proportional to the filler concentration in the matrix. The tensile strength decreased from the value 45.75 ± 1.48 MPa to the value 7.32 ± 1.16 MPa for Eco Epoxy (for Glue Epox, from 51.17 ± 1.87 MPa to 9.67 ± 0.75 MPa). The variation coefficient did not exceed 15%. The abovementioned confirms the fact that the presence of particles considerably decreases the observed characteristics. Air pores were easily identified under the stereoscopic microscope when evaluating the failure areas by a picture analysis. The presence of pores is related to the preparation technology of the test samples when no special technology (e.g. vacuum) was used and this was owing to the effort to minimize costs. The air pores can lead to a decrease of mechanical properties.

The presence of waste particles decreases the final price. So long as we consider zero price of the waste raw material, the particles used decrease the price of epoxide at the concentration 20% up to 24% (this can be up to € 3.38 at the considered retail price of the epoxy resin Glue Epox Rapid, see Fig. 7). The lines handling the waste material utilization do not offer these products at zero prices, however, the offered price per 1 kg is considerably lower than the price of the epoxide.

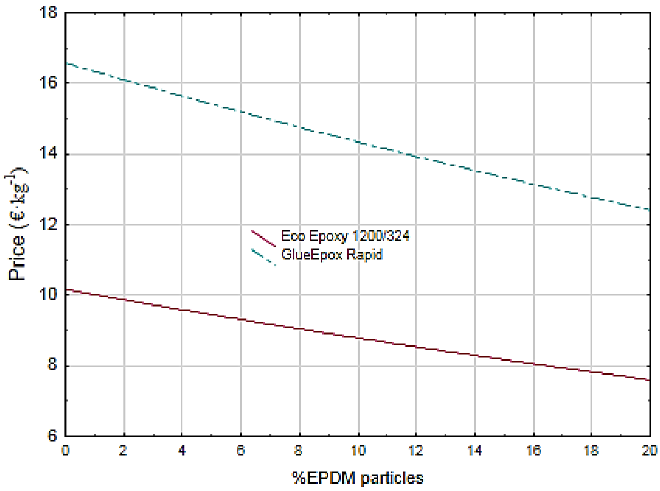

Figure 7. Description of the price of filled systems.

CONCLUSIONS

The results stated above narrow the spectrum of utilization of these materials. It is not possible to use these materials for the bonds and applications requiring high strength and reliability owing to their properties. In the area of agriculture, these materials can, above all, prospectively be used for cementing the adhesive bonding of larger units where high strength of the bond is not required. An example can be utilization of the material for floors where the resistance of epoxides is an advantage (Mleziva, 1993). The material can also be used for filling larger cracks and for shaping of imbalances. The performed experiments confirmed the assumption of authors Xue Qunji and Wang Qihua (1997) that filler application in epoxy resins considerably influences the final properties. The rubber particles used considerably decreased the shear strength of the overlapped adherents compared to the experiment of Valasek et al. (2013) who used particles of the size 27.6 μm. According to Ku et al. (2010), inorganic microparticles can improve the tensile strength in some cases, however, this is not the case in this experiment, where the boundary of the particles and the resin was prone to creation of cracks and it came to decreasing the strength. Optimization of mechanical properties would be possible in combination with another filler (e.g. with fibres), as Subramaniyan et al. (2012) state. It is true, the mechanical properties are low, but the described way of utilization is material utilization of the waste also generated in the production and liquidation of agricultural machines. The limits of the material with EPDM waste rubber of the middle particle size higher than 1,000 μm can be summed up in the following way:

- the inclusion of 20% of EPDM particles led to the decrease of the lap-shear strength of 33% for Eco Epoxy and of 39% for Glue Epox Rapid,
- the inclusion of 20% of EPDM particles led to the decrease of the tensile strength of 84% for Eco Epoxy and of 81% for Glue Epox Rapid.

ACKNOWLEDGEMENT. This paper was written with the assistance of the grant IGA TF CZU.

REFERENCES

Cerbu, C. & Curtu, I. 2011. Mechanical characterization of the glass fibres/rubber/resin composite material. *Materiale Plastice* **48**(1), 93–97.

CSN EN ISO 3167. 2004. Plastics – Multipurpose test specimens. Czech Standards Institute.

CSN EN ISO 527-1. 1997. Plastics – Determination of tensile properties – Part 1: General principes. Czech Standards Institute.

CSN EN 1465. 1997. Adhesives – Determination of tensile lap-shear strength of rigid-to-rigid bonded assemblies. Czech Standards Institute.

Dadfar, M.R & F. Ghadami. 2013. Effect of rubber modification on fracture toughness properties of glass reinforced hot cured epoxy. *Materials and Design* **47**, 16–20.

Ku, H., Trada, M., Cecil, T & Wong, T. 2010. Tensile Tests of Phenol Formaldehyde Glass-Powder Reinforced Composites: Pilot Study. *Journal of applied polymer science* **116**, 10–17.

Mleziva, J. 1993. Polymery: výroba, struktura, vlastnosti a použití.(Polymers: manufacture, structure, properties and applications). Prague –Sobotáles.

Muller, M. & Valasek, P. 2013. Assesment of bonding quality for several commercially available adhesives. *Agronomy Research* **11**(1), 155–162.

Novak, M. 2011. Surface duality hardened steels after grinding. *Manufacturing technology* **11**, 55–59.

Valasek, P. & Muller, M. 2013a. Polymeric composite based on glass powder – usage possibilities in agrocomplex. *Scientia Agriculturae Bohemica* **3,** 107–112.

Valasek, P. & Müller, M. 2013b. Composite based on hard-cast irons utilized on functional parts of tools in agrocomplex. *Scientia Agriculturae Bohemica* **3,** 172–177.

Valasek, P., Zarnovsky, J. & Muller, M. 2013. Thermoset composite on basis of recycled rubber. *Advanced materials research* **801**, 67–73.

Valasek, P. & Muller, M. 2012. Polymeric particle composites with filler saturated matrix *Manufacturing technology* **12**, 272–276.

Subramaniyan, S.K., Mahzan, S., Ghazali, M.I., Ismon, M. & Zaidi, A.M.A. 2012. Mechanical behavior of polyurethane composite foams from kenaf fiber and recycled tirerubber particles. *Applied Mechanics and Materials 3rd International Conference on Mechanical and Manufacturing Engineering*, ICME 2012; November, 861–866.

Xu Shi Ai & Wang Gong Tao, Mai J. Yiu Wing. 2013. Effect of hybridization of liquid rubber and nanosilica particles on the morphology, mechanical properties, and fracture toughness of epoxy composites. *Material Science* **48**, 3546–3556.

Xue Qunji & Wang Quiha. 1997. Wear mechanisms of polyetheretherketone composites filled with various kinds of SiC. *Wear* **213,** 54–58.

INSTRUCTIONS TO AUTHORS

Papers must be in English (British spelling). English will be revised by a proofreader, but authors are strongly urged to have their manuscripts reviewed linguistically prior to submission. Contributions should be sent electronically. Papers are considered by referees before acceptance. The manuscript should follow the instructions below.

Structure: Title, Authors (initials & surname; an asterisk indicates the corresponding author), Authors' affiliation with postal address (each on a separate line) and e-mail of the corresponding author, Abstract (up to 250 words), Key words (not repeating words in the title), Introduction, Materials and methods, Results and discussion, Conclusions, Acknowledgements (optional), References.

Layout, page size and font

- Use preferably the latest version of **Microsoft Word**, doc., docx. or rtf. format.
- Set page size to **B5 Envelope or ISO B5 (17.6 x 25 cm)**, all margins at 2 cm.
- Use single line spacing and justify the text. Do not use page numbering. Use indent 0.8 cm (do not use tab or spaces instead).
- Use font Times New Roman, point size for the title of article **14 (Bold)**, author's names 12, core text 11; Abstract, Key words, Acknowledgements, References, tables and figure captions 10.
- Use *italics* for Latin biological names, mathematical variables and statistical terms.
- Use single ('…') instead of double quotation marks ("…").

Tables

- All tables must be referred to in the text (Table 1; Tables 1, 3; Tables 2–3).
- Use font Times New Roman, regular, 10 pt. Insert tables by Word's 'Insert' menu.
- Do not use vertical lines as dividers; only horizontal lines (1/2 pt) are allowed. Primary column and row headings should start with an initial capital.

Figures

- All figures must be referred to in the text (Fig. 1; Fig. 1 A; Figs 1, 3; Figs 1–3). Use only black and white or greyscale for figures. Avoid 3D charts, background shading, gridlines and excessive symbols. Use font **Arial** within the figures. Make sure that thickness of the lines is greater than 0.3 pt.
- Do not put caption in the frame of the figure.
- The preferred graphic format is EPS; for half-tones please use TIFF. MS Office files are also acceptable. Please include these files in your submission.
- Check and double-check spelling in figures and graphs. Proof-readers may not be able to change mistakes in a different program.

References

- **Within the text**

In case of two authors, use '&', if more than two authors, provide first author 'et al.':

Smith & Jones (1996); (Smith & Jones, 1996);
Brown et al. (1997); (Brown et al., 1997)

When referring to more than one publication, arrange them by following keys: 1. year of publication (ascending), 2. alphabetical order for the same year of publication:

(Smith & Jones, 1996; Brown et al., 1997; Adams, 1998; Smith, 1998)

- **For whole books**

Name(s) and initials of the author(s). Year of publication. *Title of the book* (*in italics*). Publisher, place of publication, number of pages.

Shiyatov, S.G. 1986. *Dendrochronology of the upper timberline in the Urals*. Nauka, Moscow, 350 pp. (in Russian).

- **For articles in a journal**

Name(s) and initials of the author(s). Year of publication. Title of the article. *Abbreviated journal title* (*in italic*) volume (in bold), page numbers.

Titles of papers published in languages other than English, German, French, Italian, Spanish, and Portuguese should be replaced by an English translation, with an explanatory note at the end, e.g., (in Russian, English abstr.).

Karube, I. & Tamiyra, M.Y. 1987. Biosensors for environmental control. *Pure Appl. Chem.* **59**, 545–554.

Frey, R. 1958. Zur Kenntnis der Diptera brachycera p.p. der Kapverdischen Inseln. *Commentat.Biol.* **18**(4), 1–61.

Danielyan, S.G. & Nabaldiyan, K.M. 1971. The causal agents of meloids in bees. *Veterinariya* **8**, 64–65 (in Russian).

- **For articles in collections:**

Name(s) and initials of the author(s). Year of publication. Title of the article. Name(s) and initials of the editor(s) (preceded by In:) *Title of the collection (in italics)*, publisher, place of publication, page numbers.

Yurtsev, B.A., Tolmachev, A.I. & Rebristaya, O.V. 1978. The floristic delimitation and subdivisions of the Arctic. In: Yurtsev, B. A. (ed.) *The Arctic Floristic Region*. Nauka, Leningrad, pp. 9–104 (in Russian).

- **For conference proceedings:**

Name(s) and initials of the author(s). Year of publication. Name(s) and initials of the editor(s) (preceded by In:) *Proceedings name (in italics)*, publisher, place of publishing, page numbers.

Ritchie, M.E. & Olff, H. 1999. Herbivore diversity and plant dynamics: compensatory and additive effects. In: Olff, H., Brown, V.K. & Drent R.H. (eds) *Herbivores between plants and predators. Proc. Int. Conf. The 38th Symposium of the British Ecological Society*, Blackwell Science, Oxford, UK, pp. 175–204.

....………

Please note

- Use '.' (not ',') for decimal point: 0.6 ± 0.2; Use ',' for thousands – 1,230.4;
- Use '–' (not '-') and without space: pp. 27–36, 1998–2000, 4–6 min, 3–5 kg
- With spaces: 5 h, 5 kg, 5 m, 5°C, C : D = 0.6 ± 0.2; p < 0.001
- Without space: 55°, 5% (not 55 °, 5 %)
- Use 'kg ha$^{–1}$' (not 'kg/ha');
- Use degree sign ' ° ' : 5°C (not 5 ^{O} C).